BONE MORPHOGENETIC PROTEINS AND THEIR RECEPTORS IN THE DEVELOPMENT OF BONE METASTASIS IN PROSTATE CANCER

by

Lin Ye

Metastasis & Angiogenesis Research Group
Cardiff University School of Medicine
Cardiff

March 2008

Thesis submitted to Cardiff University for the degree of Doctor of Philosophy

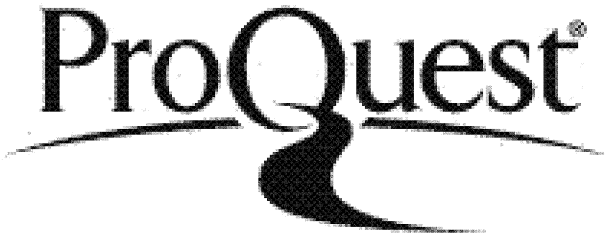

ProQuest LLC
789 East Eisenhower Parkway
P.O. Box 1346
Ann Arbor, MI 48106-1346

DECLARATION

This work has not previously been accepted in substance for any degree and is not concurrently submitted in candidature for any degree.

Signed ..... (candidate) Date .....

STATEMENT 1

This thesis is being submitted in partial fulfillment of the requirements for the degree of PhD.

Signed .....(candidate) Date .....

STATEMENT 2

This thesis is the result of my own independent work/investigation, except where otherwise stated.Other sources are acknowledged by explicit references.

Signed.....(candidate) Date .....

STATEMENT 3

I hereby give consent for my thesis, if accepted, to be available for photocopying and for inter-library loan, and for the title and summary to be made available to outside organisations.

Signed.....(candidate) Date .....

STATEMENT 4 - BAR ON ACCESS APPROVED

I hereby give consent for my thesis, if accepted, to be available for photocopying and for inter-library loans **after expiry of a bar on access** approved by the Graduate Development Committee.

Signed.....(candidate) Date .....

Acknowledgements

First of all, I would like to thank Professor Wen G. Jiang and Professor Howard Kynaston deeply for their supervision and support throughout the two and half years of my Ph.D. study. I am grateful to Professor Robert Mansel for the kind permission to working in the Metastasis & Angiogenesis Research Group based at the Department of Surgery. It was a great honour for me to pursue higher degree at a world-class laboratory, from which I will benefit in my future career.

I am also grateful to Mr. Jonathan M. Lewis-Russell, Dr. Gaynor Davies, Dr. Tracey Martin, Dr. Christian Parr, Mr. Mansel L. Davies and Mr. Andrew J Sanders for their helpful suggestions and encouragement. I would also like to thank Mr. Gareth Watkins for his technical help and assistance.

I am also very grateful to my family for their unwavering support. Without their patience and kindness this work would not have succeeded. Special thanks go to my wife Haiyan Mao and my lovely angel Xinyu, and also to my parents Xiangrong Ye and Sufen Zhang who have cherished and encouraged my passion in scientific research since I was still a little boy.

This work was kindly supported by the Desna Robins Jones Charitable Trust and Cancer Research Wales.

PUBLICATIONS:

Full PAPERS (published or accepted):

Ye L, Lewis-Russell JM, Sanders AJ, Kynaston H and Jiang WG. (2007) HGF/SF upregulates the expression of Bone Morphogenetic Protein 7 in prostate cancer cells. Urol Oncol, in press

Ye, L., J. M. Lewis-Russell, H. Kynaston and W. G. Jiang (2007). Endogenous Bone Morphogenetic Protein-7 Controls the Motility of Prostate Cancer Cells Through Regulation of Bone Morphogenetic Protein Antagonists. J Urol. 178(9):1086-1091.

Ye, L., J. M. Lewis-Russell, H. G. Kyanaston and W. G. Jiang (2007). Bone morphogenetic proteins and their receptor signaling in prostate cancer. Histol Histopathol. 22(10):1129-1147.

Ye, L., H. G. Kynaston and W. G. Jiang (2007). Bone metastasis in prostate cancer: Molecular and cellular mechanisms (Review). Int J Mol Med. 20(1):103-111.

Ye L, Lewis-Russell JM, Davies G, Sanders AJ, Kynaston H and Jiang WG. (2007). Hepatocyte growth factor up-regulates the expression of the bone morphogenetic protein (BMP) receptors, BMPR-IB and BMPR-II, in human prostate cancer cells. Int J Oncol. 30(2):521-529.

Full papers submitted and in preparation:

Ye L, Kynaston H and Jiang WG. BMP-9 induces apoptosis in prostate cancer cells through upregualtion of PAR-4. (submitted in July, 2007 to Cancer Research)

Ye L, Kyaston H and Jiang WG. BMP-10 prevents cell growth of prostate cancer cells by triggering apoptosis. (manuscript in preparation)

Ye L, Kynaston H and Jiang WG. The expression of PAR-4 in prostate cancer and its relation to the clinical outcome. (manuscript in preparation)

Ye L and Jiang WG. Overexpression BMP-9 inhibits cell growth and motility of the breast cancer cell. (manuscript in preparation)

Ye L and Jiang WG. Reduced BMP-10 expression associates with long term survival of patients with breast cancer (manuscript in preparation)

ABSTRACTS & CONFERENCE PRESENTATIONS:

L Ye, JM Lewis-Russell, H Kynaston and WG Jiang. ENDOGENOUS BMP-7 SUSTAINS THE EXPRESSION OF BMP ANTAGONISTS, NOGGIN AND FOLLISTATIN IN PROSTATE CANCER CELLS. ASCO Prostate Cancer Symposium, Orlando, February 2007

L Ye, JM Lewis-Russell, H Kynaston and WG Jiang. HGF/SF REGULATES THE EXPRESSION OF BONE MORPHOGENETIC PROTEIN ANTAGONIST, NOGGIN IN PROSTATE CANCER CELLS. ASCO Prostate Cancer Symposium, Orlando, February 2007

L Ye, H Kynaston and WG Jiang. 17-β-ESTRODIAL REGULATES THE EXPRESSION OF BONE MORPHOGENETIC PROTEIN RECEPTOR, BMPR-II IN PROSTATE CANCER CELLS. ASCO Prostate Cancer Symposium, Orlando, February 2007

L Ye, JM Lewis-Russell, MD Mason, H Kynaston and WG Jiang. Hepatocyte Growth Factor Regulates The Expression Of Noggin In Prostate Cancer Cells. British Prostate Group (BPG) meeting, Cardiff, September 2006

Russel-Lewis J, Davies G, **Ye L**, Jiang WG, Kynaston H. Growth and Differentiation Factor-9 is a putative responsive molecule to HGF, in vitro and in vivo, in human prostate cancer cells. American Urology Association (AUA), May 2006.

Ye L, Russel-Lewis J, Davies G, Mason MD, Kynaston H, Jiang WG. Expression of BMP7 and its impact on the motility and invasion of prostate cancer cells. Collaboration in Cancer Research Conference, Cardiff, March 2006

Russel-Lewis J, **Ye L**, Mason MD, Jiang WG, Kynaston H. GDF-9 in the motility and invasion of prostate cancer cells. Collaboration in Cancer Research Conference, Cardiff, March 2006

Davies G, **Ye L**, Lewis-Russell J, Mason MD, Jiang WG. Targeting PLC-gamma reduces HGF/SF induced in vitro in vasion and migration in prostate cancer cells. Collaboration in Cancer Research Conference, Cardiff, March 2006

Ye L, Russel-Lewis J, Davies G, Mason MD, Kynaston H, Jiang WG. Expression of BMP7

is regulated by hepatocyte growth factor. ASCO Prostate Cancer Symposium, San Francisco, Feburary 2006

Ye L, Russel-Lewis J, Davies G, Mason MD, Kynaston H, Jiang WG. Genetic manipulation of Expression of BMP7 and its impact on the motility and invasion of prostate cancer cells. ASCO Prostate Cancer Symposium, San Francisco, February 2006

Russel-Lewis J, **Ye L**, Mason MD, Jiang WG, Kynaston H. Expression of GDF-9 on the motility and invasion of prostate cancer cells. ASCO Prostate Cancer Symposium, San Francisco, February 2006

Davies G, **Ye L**, Lewis-Russell J, Mason MD, Jiang WG. A hammerhead ribozyme transgene targeted to PLC-gamma reduces HGF/SF induced in vitro invasion and migration in prostate cancer cells. ASCO Prostate Cancer Symposium, San Francisco, February 2006

Russel-Lewis J, Davies G, **Ye L**, Kynaston H, Jiang WG. Hepatocyte growth factor increased the expression of osteoprotegrin in human prostate cancer cells. ASCO Prostate Cancer Symposium, San Francisco, February 2006

Ye L, Russel-Lewis J, Davies G, Mason MD, Kynaston H, Jiang WG. Expression of BMP7 is regulated by hepatocyte growth factor. British Prostate Group, London, December 2005

Ye L, Russel-Lewis J, Davies G, Mason MD, Kynaston H, Jiang WG. Genetic manipulation of Expression of BMP7 and its impact on the motility and invasion of prostate cancer cells. British Prostate Group, London, December 2005 (**oral presentation**)

Russel-Lewis J, **Ye L**, Mason MD, Jiang WG, Kynaston H. Expression of GDF-9 on the motility and invasion of prostate cancer cells. British Prostate Group, London, December 2005

Davies G, **Ye L**, Lewis-Russell J, Mason MD, Jiang WG. A hammerhead ribozyme transgene targeted to PLC-gamma reduces HGF/SF induced in vitro invasion and migration in prostate cancer cells. British Prostate Group, London, December 2005

Lewis-Russell J M, **Ye L**, Kynaston H and Jiang W. The Role of Bone Morphogenic Proteins in Prostate Cancer. Welsh Urological Society, April 2005

Ye L, Lewis-Russell JM, Davies G, Mason MD, Kynaston H and Jiang WG. Upregulation of expressions of the bone morphogenetic protein (BMP) receptors, BMP-RIB and BMP-RII in prostate cancer cells by HGF/SF. National Cancer Research Institute (NCRI) Cancer Conference, 2005, Birmingham, UK

AWARDS:

A study from this thesis, 'Genetic manipulation of Expression of BMP7 and its impact on the motility and invasion of prostate cancer cells, by **Ye L**, Russel-Lewis J, Davies G, Mason MD, Kynaston H, Jiang WG', has been awarded the ASCO (American Society of Clinical Oncology) Foundation Merit Award in February 2006

Summary

Bone morphogenetic proteins (BMPs) are key factors in bone formation. Selective BMPs have been implicated in the progression and in particular the bone metastasis of prostate cancer. However, the exact role of the BMPs and the signaling pathways initiated by BMP in cancer including prostate cancer are poorly understood. This study aims to investigate the role of a panel of newly discovered BMPs in prostate cancer and the possible signal transduction pathways in prostate cancer.

In the current study, we examined the expression of certain BMPs, the BMP receptors and putative intracellular signaling molecules in prostate cell lines using RT-PCR, which allowed us to design the strategy of *in vitro* experiments. Reduced/loss of expression of both BMP-9 and BMP-10 was seen in high grade foci in prostate cancer specimens using immunohistochemical staining. Aberration of BMP receptors and certain antagonists were also seen. This suggests that these BMPs and the receptors may play profound roles in the development and progression of prostate cancer. A panel of prostate cancer cell lines were subsequently established, with which either a specific BMP or BMP receptor were genetically manipulated. Firstly, knock-down of BMP receptor-IB (BMPR-IB) and BMP receptor-II (BMPR-II) using ribozyme transgenes, resulted in an increase of cellular proliferation, which suggested that both receptors are responsible in mediating the inhibitory effects of BMPs on cell growth in prostate cancer cells. Secondly, the reduction of endogenous BMP-7 using a hammerhead ribozyme transgene led to stimulation of cellular motility and adhesion of prostate cancer cells. This was found to be the result of a feedback down-regulation of both Noggin and Follistatin, antagonists of BMPs, after loss of BMP-7. Thus, a novel mechanism underlying the action of BMP-7 was established: the endogenous antagonist dependent action of BMP-7.

The study went on to demonstrate that BMP-9 and BMP-10 can inhibit cellular growth, invasion and migration using *in vitro* function assays. Recombinant human BMP-9 and BMP-10 were also generated using affinity chromatography and will be utilised in the future investigation.

In conclusion, endogenous BMP antagonist is an important mechanism in the action of BMPs in cancer cells. Furthermore, BMP-9 and BMP-10 function as potential tumour suppressors in prostate cancer. BMPs and BMP receptors signaling play profound roles in prostate cancer. These molecules and their antagonist may have important therapeutic implications in disease specific bone metastasis.

CONTENTS

List of Figures

Chapter 4

Chapter 5

Chapter 6

Chapter 7

List of Tables

Abbreviations

aa	amino acid
Ab	antibody
ACVR1	activin A receptor, type I
ACVR1B	activin A receptor, type IB
ACVR1C	activin A receptor, type IC
ACVR2A	activin A receptor, type IIA
ACVR2B	activin A receptor, type IIB
ACVRL1	activin A receptor type II-like 1
ADT	Androgen-deprivation therapy
Ag	antigen
ALK	Activin receptor-like kinase
ALP	alkaline phosphatase
AMH	Anti-Mullerian hormone
AMSH	associated molecule with the SH3 domain of STAM
ATCC	American Type Culture Collection
BAMBI	BMP and activin membrane bound inhibitor
b-FGF	basic fibroblast growth factor
BGP	bone gla protein
BISC	BMP-induced signaling complexes
BMP	Bone morphogenetic protein
BMP6P1	bone morphogenetic protein 6 pseudogene 1
BMPR1A	bone morphogenetic protein receptor, type IA
BMPR1B	bone morphogenetic protein receptor, type IB
BMPR2	bone morphogenetic protein receptor, type II
bp	base pair
BPH	benign prostatic hypertrophy
BSA	bovine serum albumin
BSP	bone sialoprotein
BSS	Balanced salt solution
CDK2	cyclin-dependent kinase 2
CDMP	cartilage-derived morphogenetic protein
CIP1/WAF1	cyclin-dependent kinase inhibitor (CDKI) p21
cm	centimetre
CO_2	carbon dioxide
Co-Smad	common mediator Smad
DD3/PCA3	dihydrodiol dehydrogenase 3 also known as prostate cancer antigen 3
ddH_2O	double-distilled water
DEPC	diethyl pyrocarbonate
DHT	dihydrotestosterone
DMEM	Dulbecco's modified eagles medium
DMP	dentin matrix protein

DMSO	dimethyl sulphoxide
DNA	deoxyribonucleic acid
dNTP	deoxyribonucleoside triphosphate
DRE	digital rectal examination
DSPP	dentin sialophosphoprotein
E. coli	Esherichia coli
ECACC	European Collection of Animal Cell Culture
ECL	enhanced chemiluminescence
ECM	extracellular matrix
EDTA	ethylene diaminetetraacetic acid
EGF	epidermal growth factor
ELISA	enzyme-linked immunoabsorbant assay
EMT	Epithelial-mesenchymal transdifferentiation/transformation
ET-1	endothelin-1
ET_AR	endothelin receptor type A
Fab	antibody binding site fragment
FCS	foetal calf serum
FGF	fibroblast growth factor
FITC	fluorescein isothiocyanate
G	gravity's (unit of relative centrifugal force)
G418	geneticin
GalNAC-T3	UDP-N-Acetyl-α-D-galactosamine transferase
GDF	growth differentiation factor
GFP	green fluorescent protein
H_2O_2	hydrogen peroxide
HBSS	Hanks Balanced Salt Solution
HCl	hydrogen acid
HEPES	N-hydroxyethylpiperazine-N'-2-ethansulphoxide
HGF/SF	hepatocyte growth factor/scatter factor
hr	hour
HRP	horseradish peroxidase
ID-1/2/3	Inhibitor of differentiation factor
IF	immunofluorescence
Ig	immunoglobulin
IGF	insulin-like growth factor
IGF	insulin-like growth factor
IGFBP	IGF binding protein
IL	interleukin
I-Smad	inhibitory Smad
JNK	Jun N-terminal kinases
Kb	kilo-base
kDa	kilo-dalton
KGF	keratinocyte growth factor
LA-PCR	high fidelity long and accurate PCR

LB	Luria-Bertani
LHRH	Leutenising hormone releasing hormone
m	metre
M	Molar
mA	milli-amp
mAb	monoclonal antibody
MAD	mothers against decapentaplegic homolog
MAPK	mitogen-activated protein kinase
M-CSF	macrophage colony-stimulating factor
ME	mercaptoethanol
MEPE	matrix extracellular protein
mg	milligram
MGP	matrix gla protein
MH1	Mad homology 1
MH2	Mad homology 2
MIC	macrophage inhibitory cytokine
min	minute
ml	milli litre
mM	milli molar
MMP	matrix metalloproteinase
mRNA	messenger ribonucleic acid
MW	molecular weight
NaCl	sodium chloride
NAG-1	NSAID activated gene-1
NaN3	sodium azide
NaOH	sodium hydroxide
NCPs	non-collagenous proteins
NEDD4-2	neural precursor cell expressed, developmentally down-regulated 4-2
NF-kB	Nuclear factor kappa B
ng	nano-gram
$NiSO_4$	Nickel Sulphate Heptahydrate
NLK	Nemo-like kinase
nM	nano molar
nm	nanometre
NO	nitric oxide
NSAID	nonsteroidal anti-inflammatory drug
OP	osteogenic protein
OPG	osteoprotegerin
OPN	osteopontin
PAGE	polyacrylamide gel electrophoresis
PAR1	protease-activated receptor
Par-4	Prostate apoptosis response-4
PBS	phosphate buffered saline
PBS	phosphate-buffered saline

PCR	polymerase chain reaction
PCs	proprotein convertases
PCSK5	proprotein convertase subtilisin/kexin type 5
PCSK6	proprotein convertase subtilisin/kexin type 6
PDF	prostate derived factor
PDGF	platelet-derived growth factor
PFC	preformed hetero-oligomeric complexes
PI	Propidium iodide
PI3K	phosphoinositide 3-kinase
PKC	protein kinase C
PLAB	placental bone morphogenetic protein
PSA	prostate specific antigen
PSMA	prostate specific membrane antigen
PTGFB	placental transforming growth factor-beta
PTHrP	parathyroid hormone related protein
PTPN3	protein tyrosine phosphatase, non-receptor type 3
RANKL	receptor activator of nuclear factor-κB ligand
Rb	retinoblastoma
rh-BMP	recombinant human BMP
RNA	ribonucleic acid
RNAse	ribonuclease
rpm	revolutions per minute
RPMI	Roswell Park Memorial Institue
R-Smad	receptor-regulated Smad
RT	reverse transcription
SD	standard deviation
SDS	sodium dodecyl sulfate
sec	second
SIBLINGS	Small Integrin-Binding Ligand N-linked Glycoproteins
Ski	Sloan-Kettering retrovirus
SLRPs	Small Leucine-Rich Proteoglyans
Sma	small family member
Smad	Sma and MAD
Smurf	Smad ubiquitin regulatory factor
TAB1/2/3	TGF-ß activated binding protein
TAE	Tris/acetate/EDTA electrophoresis buffer
TAK1	MAPKKK TGF-ß activated tyrosine kinase 1
TBE	Tris/Borate/EDTA electrophoresis buffer
TBS	Tris-buffered saline
TE	Tris/EDTA buffer
TEMED	N,N,N',N'-tetramethylethylenediamine
TGFBR1	transforming growth factor, beta receptor I
TGFBR2	transforming growth factor, beta receptor II
TGFBR3	transforming growth factor, beta receptor III

TGF-β	Transforming growth factor-β
THPO	thrombopoietin
TIMP	tissue specific inhibitor of matrix metalloproteinase
TNF-a	tumour necrosis factor-alpha
TNM	tumour, node and metastasis
Tob	transducer of ErbB-2
tPA	tissue plasminogen activator
Tris	Tris-(hydoxymethyl)-aminomethane
TRITC	Tetra-Rhodamine Isothiocyanate
U	unit
UCH37	ubiquitin: C-terminal hydrolase
μg	microgram
UICC	American Joint Committee on Cancer and International Union Against Cancer
μl	microlitre
μM	micro molar
uPA	urokinase plasminogen activator
UV	ultraviolet
V	volt
VEGF	vascular endothelial growth factor
VGR	Vegetal-related
Wnt	wingless-type
Wnt1	Wingless and /NT-1
WT	wild type
XIAP	X-linked inhibitor of apoptosis protein

Chapter 1

General Introduction

1.1 Prostate cancer

Prostate cancer is the most commonly diagnosed cancer in men in the UK and US, and is the second or third leading cause of death from cancer in men in these countries (CancerStats, 2005; Jemal *et al.*, 2006). One in six men in the US will be diagnosed with the prostate cancer within their lifetime (Jemal *et al.*, 2006).

1.1.1 Epidemiology and risk factors

1.1.1.1 Age

Increasing age is the most important risk factor for prostate cancer. The clinical diagnosis of prostate cancer increases directly with age(Scott *et al.*, 1969), although nine percent of men in their twenties have histological evidence of prostatic intraepithelial neoplasia (Sakr *et al.*, 1993). Before the age of 50, the diagnosis of prostate cancer is rare. The probability of developing an invasive prostate cancer by age: from birth to 39 years-0.01%, for age group of 40-59 years-2.66%, for age 60-69years-7.19%, and above 70 years old-14.51% (Jemal *et al.*, 2006).

1.1.1.2 Race

The highest incidence of prostate cancer is found in African Americans, for whom the age-adjusted incidence rate is 272 per 100,000. In contrast, the incidence is only 50.3 for the American Indian/Alaska Native (Jemal *et al.*, 2006). The risk of developing prostate cancer begins to increase at the age of 50 years in white men, who have no family history of the disease, and at the age of 40 years in black men (Richard Pazdur, 2005).

1.1.1.3 Family history

Several studies have shown a higher risk of developing the disease in male relatives of men with prostate cancer (Steinberg *et al.*, 1990; Lesko *et al.*, 1996). First-degree relatives of men with prostate cancer have a two or three-fold increased risk compared to the general population. This risk may be tenfold if three or more relatives in the family are affected (Steinberg *et al.*, 1990). Family history and hereditary factors are estimated to be important in 5% to 10% of all prostate cancers, and 40% of those cancers diagnosed below the age of 55 (Walsh and Partin, 1997). Walsh and Partin suggested that the hereditary prostate carcinoma should be suspected in families with an early age at onset and/or multiple affected family members (Walsh and Partin, 1997).

1.1.1.4 Diet

It has been demonstrated that a positive association exists between prostate cancer and fat intake in most case-control studies, and that a higher fat intake is also associated with the incidence of advanced disease (Yip *et al.*, 1999). There are two significant differences between Asian and Western diet, lower fat intake and higher soy protein consumption in Asia. It has also been demonstrated that micronutrients in the diet, including Vitamin A, lycopene, selenium and Vitamin E have a potential of preventing prostate cancer (Hirayama, 1979; BCCPSG, 1994; Clark *et al.*, 1996; Giovannucci and Clinton, 1998; Yoshizawa *et al.*, 1998).

1.1.1.5 Geography

The incidence rates for prostate cancer are the highest in Northern America (119.9 per 100,000), Australia/New Zealand (79.9 per 100,000) and Western Europe (61.6 per 100,000), whereas it is lowest in Asia (4.4 per 100,000 in South central Asia, 1.6 per 100,000 in China) (Figure 1.1) (Parkin *et al.*, 2005). The geographical variation is probably due to multiple factors including -racial, dietary, environmental factors and cancer detection programmes in the population.

An addition to the above, there are some other potential risk factors for the development of prostate cancer. Radiation exposure has been implicated in the development of prostatic cancer particularly in young men (Beral *et al.*, 1985). A meta-analysis has also suggested that high level of serum testosterone is related to an increased risk of developing prostate cancer (Shaneyfelt *et al.*, 2000).

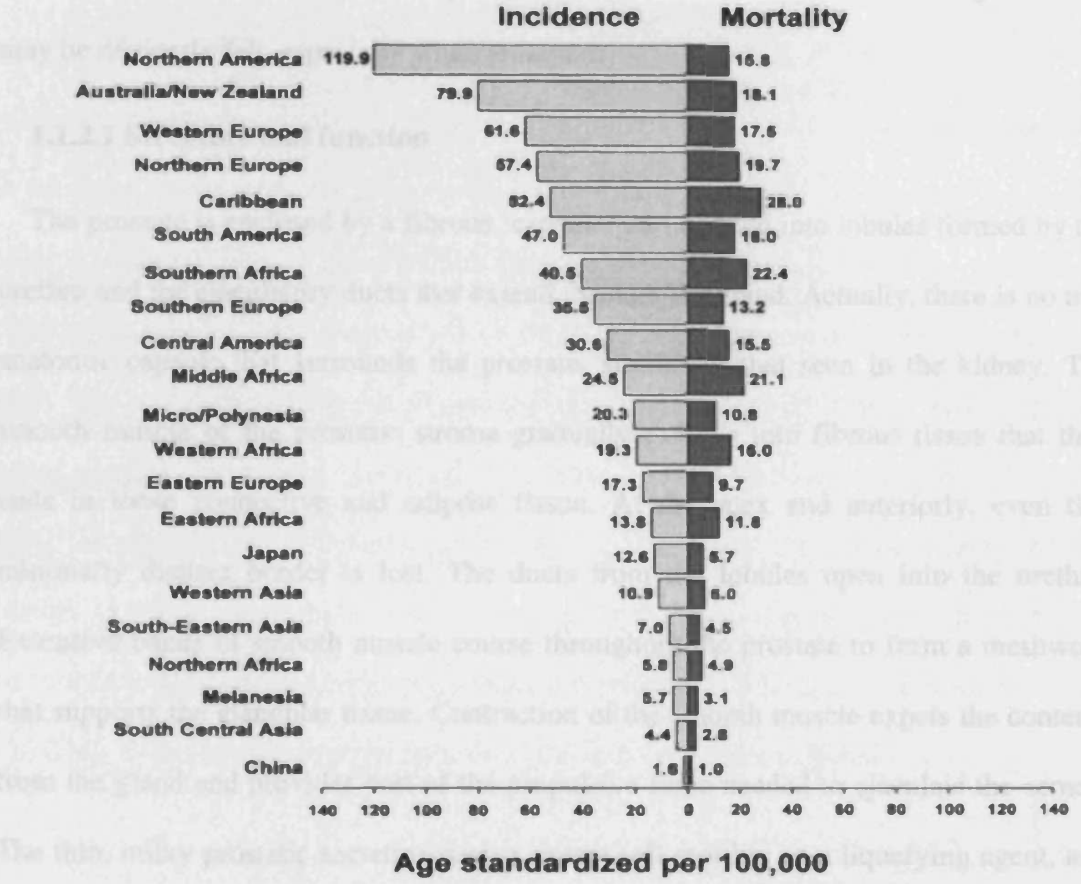

Figure 1.1 Age-standardized Incidence and Mortality Rates for Prostate Cancer. Data shown per 100,000 (Parkin *et al.*, 2005).

1.1.2 Anatomy and histology of prostate

The prostate is a firm, partially glandular and partially muscular gland, which is the size and shape of a chestnut. It is situated in the pelvis, below the bladder, above the superior fascia of the urogenital diaphragm, and in front of the rectum, through which it may be distinctly felt, especially when enlarged.

1.1.2.1 Structure and function

The prostate is enclosed by a fibrous 'capsule' and divided into lobules formed by the urethra and the ejaculatory ducts that extend through the gland. Actually, there is no true anatomic capsule that surrounds the prostate, similar to that seen in the kidney. The smooth muscle of the prostatic stroma gradually extends into fibrous tissue that then ends in loose connective and adipose tissue. At the apex and anteriorly, even this minimally distinct border is lost. The ducts from the lobules open into the urethra. Extensive bands of smooth muscle course throughout the prostate to form a meshwork that supports the glandular tissue. Contraction of the smooth muscle expels the contents from the gland and provides part of the propulsive force needed to ejaculate the semen. The thin, milky prostatic secretion assists sperm cell motility as a liquefying agent, and its alkalinity protects the sperm in their passage through the acidic environment of the female vagina. The prostate also secretes the enzyme acid phosphatase, which is often measured clinically to assess prostate function. The discharge from the prostate makes up about 40% of the volume of the semen.

1.1.2.2 Zonal anatomy

In 1981, Dr. McNeal defined the concept of anatomic zones (McNeal, 1981). There are four anatomic regions within the normal prostate: the peripheral zone, the central zone, the transition zone, and the anterior fibromuscular stroma (Figure 1.2). The peripheral zone constitutes over 70% of the glandular prostate. It forms a disc of tissue whose ducts radiate laterally from the urethra, lateral and distal to the verumontanum. It is the most common site in the prostate for developing prostate carcinoma. The central zone constitutes 25% of the glandular prostate. Its ducts arise close to the ejaculatory duct orifices and follow these ducts proximally, branching laterally near the prostate base. The significant difference in histological structure between central and peripheral zones suggests important biological differences. The transition zone constitutes two small lobules that abut the prostatic urethra and represent the region where nodular benign prostatic hypertrophy (BPH) primarily originates. The anterior fibromuscular stroma forms the entire anterior surface of the prostate as a thick, non-glandular apron, shielding from view the anterior surface of the three glandular regions.

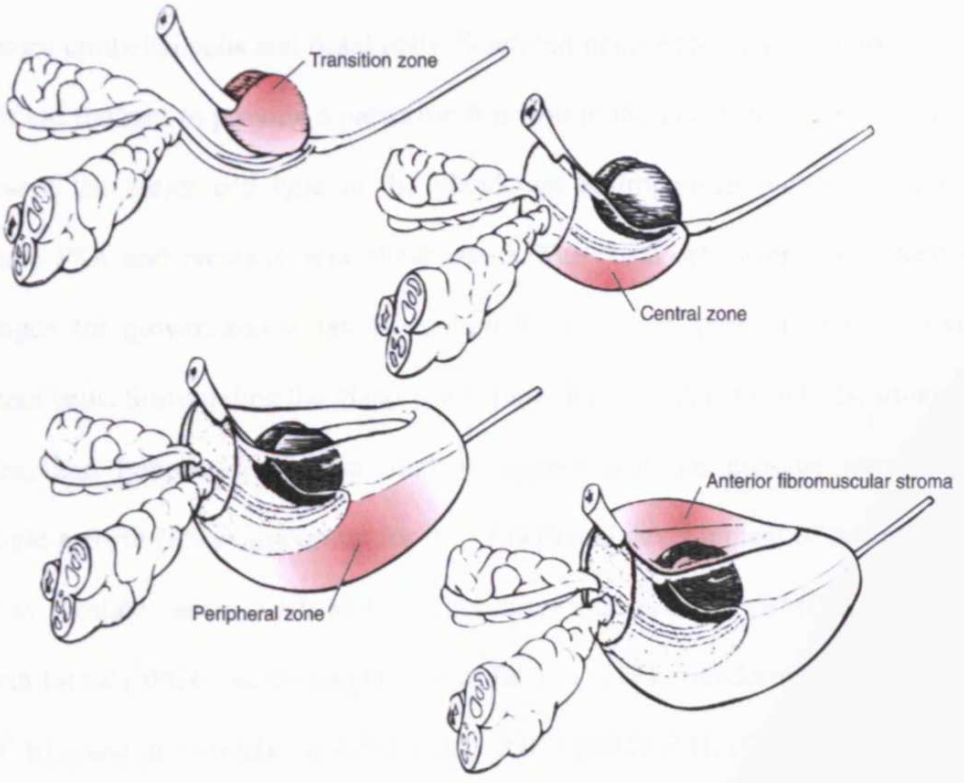

Figure 1.2 Zonal anatomy of the prostate. The prostate consists of three glandular zones and an anterior fibromuscular stroma (Oh *et al.*, 2003).

1.1.2.3 Basic histology of prostate

The prostate is comprised of branching glands, with numerous follicular pouches the lining of which, frequently shows papillary elevations. The follicles open into elongated ducts, which join to form twelve to twenty small excretory ducts. Small colloid masses, known as amyloid bodies are often found in the gland tubes. The ducts are lined by secretory epithelial cells and basal cells. Scattered neuroendocrine cells are also present, which are thought to provide a paracrine function in the gland. Secretory epithelial cells represent the major cell type in the gland, are androgen-dependent for growth, and produce PSA and prostatic acid phosphatase. The basal cell layer is not dependent on androgen for growth and is felt to contain the stem cell population for the epithelial prostate cells. Surrounding the gland is a stroma that includes fibroblasts, smooth muscle, nerves, and lymphatics. Recent studies suggest that the prostate stroma produces multiple growth factors important for the growth and development of normal prostate as well as prostate cancer, such as bone morphogenetic proteins (BMPs), basic fibroblast growth factor (bFGF), keratinocyte growth factor (KGF), transforming growth factor- β1 (TGF-β1), and insulin-like growth factors (IGF-I and IGF-II) (Chung, 1995; Matsubara, 1995; Byrne *et al.*, 1996; Cooper *et al.*, 2003; Condon, 2005; Kleinberg *et al.*, 2006).

1.1.3 Screening and early detection

Men with early prostate cancer have no specific symptoms. In some cases, prostate cancer has been found coincidently during histological examination in patients undergoing surgery for benign prostatic hyperplasia (Di Silverio *et al.*, 2003).

1.1.3.1 American Cancer Society guideline for screening and early detection

Both the prostate-specific antigen (PSA) blood test and digital rectal examination (DRE) are suggested as screening tests for prostate cancer in men over 50 years old who have at least a 10-year life expectancy. Men at high risk, which includes African-American men and men with a strong family of one or more first-degree relatives diagnosed of prostate cancer before age 65, should begin testing as early as age 45. Men at even higher risk, due to multiple first-degree relatives affected at an early age, could begin testing at age 40. Depending on the results of this initial test, no further testing might be needed until age 45 (Smith *et al.*, 2006).

Information with regard to what is known and what is uncertain about the benefits, limitations, and harms of early detection and treatment of prostate cancer, should be provided to all men so that they can make an informed decision about testing.

1.1.3.2 PSA test

Prostate specific antigen (PSA) is a prostatic secretory glycoprotein, and is a serine esterase with trapsin-like and chymotrypsin-like activity. Its biological function is to lyse ejaculate clot in semen. Beginning in 1988, a marked increase in detection of prostate cancer occurred owing to the widened application of a test for PSA. The detection rate began to decline in 1997 but began to increase again in 2000 (Hsing *et al.*, 2000). However, there are still controversies and intense debates exist about the true value of PSA for routine screening, as it may not contribute to the reduction of mortality due to its lead and length time biases and overdetection (Cookson, 2001). PSA is prostate specific, but not prostate cancer specific. Although screening with PSA for prostate cancer has not been adopted in the United Kingdom, this test remains an

important diagnostic and predictive tool. Various molecular forms of PSA can be found in the circulation: free PSA, PSA complexed with α1-antichymotrypsin, and PSA complexed with α2-macroglobulin. The 95th percentile of PSA among "healthy" populations of men more carefully screened to exclude prostate cancer (95% specificity) has been used to establish age- and race-specific PSA ranges (Table 1.1). It has been demonstrated that the annual PSA increasing velocity has a prognostic potential. PSA test is essentially useful in prognosis and diagnosing recurrence after treatment and the development of hormone refractory prostate cancer.

Table 1.1 PSA thresholds based on age and race (Walsh *et al.*, 2002a).

Age Decade (Years)	"Normal" PSA Ranges (ng/mL)			
	Based on 95% Specificity*		Based on 95% Sensitivity†	
	White Males‡	*Black Males§*	*White Males§*	*Black Males§*
40	0–2.5	0–2.4	0–2.5	0–2.0
50	0–3.5	0–6.5	0–3.5	0–4.0
60	0–4.5	0–11.3	0–3.5	0–4.5
70	0–6.5	0–12.5	0–3.5	0–5.5

*Upper limit of normal PSA determined from 95th percentile of PSA among men without prostate cancer.
†Upper limit of normal PSA required to maintain 95% sensitivity for cancer detection.

1.1.3.3 Other tumour markers

The requirements of a new prostate cancer marker are clear. The eagerly anticipated 'supermarker(s)' should distinguish benign disease from malignant disease; it should have a high sensitivity, specificity, and positive and negative predictive value; it should

diagnose potentially life-threatening tumours rather than slow-growing ones; and it should be inexpensive and easy to use (Chodak, 2006). Recent studies on the molecular biology of prostate cancer have led to a rapid rise in the number of putative prostate tumour markers. Some of the promising tumour markers include prostate specific membrane antigen (PSMA), dihydrodiol dehydrogenase 3 also known as prostate cancer antigen 3 (DD3/PCA3, which is a non-coding mRNA), protein tyrosine phosphatase, non-receptor type 3 (PTPN3, which codes a protein tyrosine phosphatase), and Hepsin (Yang and Tonks, 1991; Bussemakers *et al.*, 1999; Luo *et al.*, 2001; Burger *et al.*, 2002). However, according to the limited genetic information of each marker, none of these tumour markers has adequate sensitivity and specificity for screening and for early detection of prostate cancer. A recent study suggests that a combination of multiple markers, by way of molecular profiling, may provide a more powerful approach in diagnosing prostate cancer than any single marker alone. The combination of UDP-N-Acetyl-α-D-galactosamine transferase (GalNAC-T3), PSMA, Hepsin and DD3/PCA3 has clearly shown such an advantage (Landers *et al.*, 2005).

1.1.4 Grading and staging system

Before a decision can be made about treatment, the prostate cancer would have to be classified with the TNM (tumour, node and metastasis) staging system and given a Gleason score.

1.1.4.1 The Gleason grading system

The Gleason system is the most widely accepted grading scheme for prostate cancer, and is based on glandular differentiation (Gleason and Mellinger, 1974). A prostate tumour usually exhibits multiple histological patterns. The commonest pattern is referred to as the primary and the second most common pattern the secondary. The primary and secondary patterns are recorded separately and given a Gleason grade of 1 to 5 which signify that grade of 1 is a near-normal pattern, and grade 5, the absence of any glandular pattern and therefore more poorly differentiated. The sum of these two patterns produces the Gleason score which ranges therefore from 2 to 10. Gleason score is used to assess the aggressiveness: a score of 2-4 is considered low grade or well differentiated; a score of 5-7 is considered moderate grade or moderately differentiated; a score of 8-10 is considered high grade or poorly differentiated.

1.1.4.2 TNM staging system

In 2002, American Joint Committee on Cancer and International Union Against Cancer (UICC) published an updated TNM system (Table 1.2) (Greene FL, 2002). The staging of prostate cancer is based on digital rectal examination, laboratory tests, plain radiographs, and radioisotope bone scan. Computed tomography and magnetic resonance imaging are also used for staging in order to determine the presence of extracapsular spread or distant metastasis. Pathological staging may follow prostatectomy and/or node sampling or dissection.

Table 1.2 TNM Staging System.

Stage	Definition
Primary Tumour, Clinical (T)	
TX	Primary tumour cannot be assessed
T0	No evidence of primary tumour
T1	Clinically in apparent tumour not palpable or visible by imaging
T1a	Tumour incidental histological finding in 5% or less of tissue resected
T1b	Tumour incidental histological finding in more than 5% of tissue resected
T1c	Tumour identified by needle biopsy (e.g. because of elevated PSA) Tumo7r found in one or both lobes by needle biopsy, but not palpable or Reliably visible by imaging, is classified as T1c.
T2	Palpable tumour confined within prostate Invasion into the prostatic apex or into (but not beyond) the prostatic Capsule is not classified as T3, but as T2.
T2a	Tumour involves less than or equal to half a lobe
T2b	Tumor involves more than half a lobe but not more than 1 lobe
T2c	Tumour involves both lobes
T3	Tumour extends through the prostatic capsule
T3a	Extracapsular extension (unilateral or bilateral)
T3b	Tumour invades seminal vesicle(s)
T4	Tumour is fixed or invades adjacent structures other than seminal vesicles: bladder neck, external sphincter, rectum, levator muscles, and/or pelvic wall
Primary Tumour, Pathologic (pT)	
pT2	Organ confined
pT2a	Unilateral
pT2b	Bilateral
pT3	Extra-prostatic extension
pT3a	Extra-prostatic extension
pT3b	Seminal vesicle invasion
pT4	Invasion of bladder, rectum
Regional Lymph Nodes (N)	
NX	Regional lymph nodes cannot be assessed
N0	No regional lymph node metastasis
N1	Metastasis in regional lymph node or nodes
Distant Metastasis (M)	
MX	Distant metastasis cannot be assessed
M0	No distant metastasis
M1	Distant metastasis
M1a	Non-regional lymph nodes
M1b	Bone(s)
M1c	Other site(s)

There is no pathologic T1 classification. When more than one site of metastasis is present, the most advanced category is used. pM1c is most advanced (AJCC Cancer Staging Manual. 6th ed. New York, NY: Springer-Verlag; 2002).

1.1.5 Management

The treatment of prostate cancer particularly when it is localised requires a thorough analysis by the patient of the risks and benefits of each option, enabling him to choose the right therapy. The biopsy grade, clinical stage, and prostate-specific antigen (PSA) level provide prognostic information that helps to choose individually suitable treatments, which include watchful waiting, surgery, radiotherapy, hormonal therapy and cryotherapy.

1.1.5.1 Early localised prostate cancer

Early localised prostate cancer includes clinical stage T1 and T2 without involvement of lymph node and metastasis. Standard treatments for localized prostate cancer include watchful waiting (or active surveillance), radical prostatectomy, and radiotherapy (external beam or brachytherapy with or without androgen ablation). Three essential factors are helpful in decision making when considers selection of therapies: the overall life expectancy of patients as determined by age and comorbidity; the biological characteristics and the predicted aggressiveness and behaviour of the tumour and, finally the preferences of the patient for the various treatment options, with consideration of complications, adverse effects, relative efficacy, and quality-of-life issues.

1.1.5.2 Locally advanced prostate cancer

Locally advanced prostate cancer refers to tumours at stage T3 or T4 but without evidence of distant metastasis. In general, radiotherapy or hormone therapy, or a combination of both is recommended for patients in this category. Watchful waiting is

also suitable for the older patients and for those with significant comorbidity and reduced life expectancy.

1.1.5.3 Metastatic prostate cancer

Patients with metastatic prostate cancer are incurable. The aim of treatment for this category of patients is to control the extent and activity of the tumour by suppressing the levels of testosterone, such as castration or using androgen receptor blocking agents. In hormone refractory prostate cancer palliative chemotherapy, radiotherapy and biophosphonates which may be considered for the management of metastatic disease.

Metastatic prostate cancer is an intensively pursued area in both clinical and scientific research. One of the most interesting features of prostate cancer metastasis is its predilection to metastasise to bone. Bone metastasis is the most common metastatic site of prostate cancer; approximately 90% of patients with advanced prostate cancer have skeletal metastases (Bubendorf *et al.*, 2000). Morbidity from bone metastasis is the most common complication in patients with advanced prostate cancer, which includes bone pain, hypercalcemia, pathologic fractures, and spinal cord compression. There are few effective treatments available for treating skeletal metastases, and none are curative. Molecular and cellular mechanisms leading to bone metastasis of prostate cancer are unclear but have been under intensive investigation in recent years. Despite some progress in this area, most key issues remain unanswered. For example, A) is there any specific genetic predisposition that enables the prostate cancer cells more prone to spreading to bone, B) what factors are involved in the development of bone metastasis in the local microenvironment, C) what are the interactions between metastatic prostate cancer cells and bone marrow endothelial cells, osteoblasts, and osteoclasts that assist

prostate cancer cells to develop into fully metastatic tumours? Answers to these important questions may reveal why prostate cancer so readily metastasises to bone.**1.2 Fundamental biology of bone**

The bone is a highly specialized form of connective tissue which comprises of metabolically active cells and mineralized matrix. There are two types of bone tissues: the compact bone which is dense and solid in appearance, while the cancellous bone is characterized by open space partially filled with an assemblage of needle-like structures. Bones constitute the skeleton, which differ in size and shape including long bone, short bone, flat bone and irregular bone. The skeleton consists of approximately 80% compact bone, largely in peripheral bones, and 20% cancellous bone, mainly in the axial skeleton. The amount of compact bone varies in different site according to the need for mechanical support. While cancellous bone accounts for the minority of total skeletal tissue, it is the site of greater bone turnover because its total surface area is much greater than that of compact bone. The principal functions of the skeleton are support, protection, movement, a source of inorganic ions, maintenance of calcium homeostasis and haematopoiesis in the bone marrow.

1.2.1 Bone cells

Bone is composed of four different cell types: osteoblasts, osteoclasts and bone lining cells that are present on bone surfaces, and osteocytes that are embedded in the mineralized bone matrix.

1.2.1.1 Osteoblasts

Osteoblasts originate from mesenchymal stem cells which are also the progenitors of chondrocytes, myocytes and adipocytes. Osteoblasts are aligned on the bone surface, and secret non-mineralized bone matrix called osteoid, which is primarily comprised of type I collagen and mineralises to become bone. Osteoblasts also regulate the mineralisation during the bone formation by secreting alkaline phosphatase (ALP). Another important function of osteoblast is the regulation of osteoclast differentiation through various factors including the receptor activator of nuclear factor-κB ligand (RANKL), macrophage colony-stimulating factor (M-CSF), interleukin-1 (IL-1), IL-6, and IL-11 (Ishimi *et al.*, 1990; Girasole *et al.*, 1994; Quinn *et al.*, 1998; Yao *et al.*, 1998; Jimi *et al.*, 1999; Lum *et al.*, 1999). After bone formation, osteoblasts may have one of these four different fates: 1. to become embedded in the bone matrix as osteocytes; 2. to be transformed into inactive osteoblasts and become bone-lining cells; 3. to undergo apoptosis; or 4. to transdifferentiate into cells that deposit chondroid or chondroid bone (Franz-Odendaal *et al.*, 2006).

1.2.1.2 Bone lining cells

Bone lining cells are essentially inactive osteoblasts. They cover all of the available bone surface and function as a barrier for certain ions.

1.2.1.3 Osteocytes

Osteocytes originate from osteoblasts which have migrated into and become trapped and surrounded by bone matrix which they themselves have produced. The spaces which they occupy are known as lacunae. An osteocyte has numerous cellular protrudes in

order to reach out and meet other osteocytes, or other cells on the bone surface probably, for the purpose of communication (Palumbo *et al.*, 1990). The exact role of osteocytes has yet to be fully determined, but it is believed that osteocytes are involved in sensing mechanical stresses in the bone matrix. On the other hand, the mechanical stress is also crucial for maintaining the viability of osteocytes (Takai *et al.*, 2004). It has also recently been reported that osteocytes are constitutive negative regulators of osteoclastic activity and may also play an important role in regulating osteoblasts' function (Takai *et al.*, 2004; Gu *et al.*, 2005).

1.2.1.4 Osteoclasts

Osteoclasts are large multinucleated cells that originate from the monocyte lineage/macrophage and are responsible for bone resorption. They secrete bone-reabsorbing enzymes, such as tartrate resistant acid phosphatase from their characteristic ruffled border, and these enzymes digest bone matrix. Osteoclasts are located on bone surfaces in what are called Howship's lacunae. These lacunae, or resorption pits, are left behind after the breakdown of bone and often present as scalloped surfaces. Because the osteoclasts are derived from a monocyte stem-cell lineage, they are equipped with engulfment strategies similar to circulating macrophages. Osteoclasts mature and/or migrate to discrete bone surfaces. Upon arrival they secrete active enzymes against the mineral substrate. Once the bone matrix is degraded, some factors released as the result of degradation can promote the differentiation and activity of osteoblasts.

1.2.2 Bone matrix

The bone matrix comprises of inorganic and organic parts. The inorganic fraction is mainly crystalline mineral salts and calcium, which is present in the form of

hydroxyapatite. The matrix is initially laid down by osteoblasts as unmineralised osteoid. After the subsequent mineralization, osteoblasts secret vesicles containing alkaline phosphatase to cleave the phosphate groups which later act as the foci for calcium and phosphate deposition.

The organic part of matrix is mainly Type I collagen. This is synthesised intracellularly as tropocollagen and then exported. Fibres of this collagen comprise 90% of the organic material in the mineralized bone matrix. Bone matrix is enriched with various growth factors and cytokines, such as TGF-β1 and bone morphogenetic proteins (BMP). The functions of these factors are not fully known. Bone matrix also contains a number of non-collagenous proteins (NCPs), including fibronectin, osteonectin, thrombospondin-2, βig-h3, bone gla protein (BGP, or osteocalcin), matrix gla protein (MGP), Small Integrin-Binding Ligand N-linked Glycoproteins (SIBLINGS) and Small Leucine-Rich Proteoglyans (SLRPs).

One of the most abundant NCPs in bone matrix is fibronectin, which is accumulated extracellularly at sites of osteogenesis and plays a profound role in the differentiation, proliferation and survival of osteoblasts (Moursi *et al.*, 1996; Moursi *et al.*, 1997; Globus *et al.*, 1998). Osteonectin ('bone connector') was initially called 'bone-specific nucleator' of mineralization as it has high affinity for both collagen and mineral (Termine *et al.*, 1981). It has been subsequently found to be present throughout the body, particularly at sites of tissue remodelling and matrix assembly. Evidence suggests that it is crucial in maintaining bone turnover (Delany *et al.*, 2000). Thrombospondin-2 is also abundant in bone, and may promote bone resorption and inhibit the bone formation through negatively controlling the differentiation of bone cell precursors (Bornstein *et*

al., 2000; Hankenson and Bornstein, 2002; Hankenson *et al.*, 2005). Another abundant NCP βig-h3, which is induced by TGF-β, inhibits the differentiation of osteoblasts through interacting with the integrins $\alpha_V\beta_3$ and $\alpha_V\beta_5$ (Skonier *et al.*, 1994; Thapa *et al.*, 2005). Osteocalcin may inhibit bone formation (Ducy *et al.*, 1996), while MGP is a powerful inhibitor of mineralisation in arteries and cartilage (Luo *et al.*, 1997). Members of the SIBLINGS family include: bone sialoprotein (BSP), osteopontin (OPN), dentin matrix protein (DMP), dentin sialophosphoprotein (DSPP) and matrix extracellular protein (MEPE). BSP has been suggested to be involved in hydroxyapatite nucleation (Hunter and Goldberg, 1993), and to promote adhesion, differentiation and some other biological functions in osteoclasts (Ganss *et al.*, 1999). Osteopontin is crucially involved in anchoring osteoclasts to the mineral matrix of bone surface via the integrin $\alpha_V\beta_3$ (Reinholt *et al.*, 1990; Hultenby *et al.*, 1993). Osteopontin is required, and probably indispensable, during the process of bone resorption (Ihara *et al.*, 2001; Ishijima *et al.*, 2002). Nine of 12 known SLRPs have been found in skeletal tissue (Young, 2003). The best characterized SLRP in bone is biglycan, which plays an important role in the differentiation of osteoblast precursors (Wadhwa *et al.*, 2004). It is also involved in osteoblast differentiation induced by BMP2/4 (Chen *et al.*, 2004d; Mochida *et al.*, 2006).

1.2.3 Bone marrow

Bone marrow is a specialised type of soft, diffuse connective tissue that is also called myeloid tissue. It produces blood cells and is found in the medullar cavities of certain long bones and in the spaces of spongy bones. There are two types of bone marrow: red marrow and yellow marrow. In an infant or child's body, all of the bones contain red

bone marrow which produces red blood cells. As an individual grows, the red marrow is gradually replaced by yellow marrow. In yellow marrow, the marrow cells have become saturated with fat, and are inactive in the production of blood cells.

Bone marrow contains two types of stem cells: haematopoietic stem cells and mesenchymal stem cells. Haematopoietic stem cells give rise to the three classes of blood cell that are found in the circulation: white blood cells (leukocytes), red blood cells (erythrocytes), and platelets (thrombocytes). Mesenchymal stem cells are found arrayed around the central sinus in the bone marrow. They have the capability to differentiate into osteoblasts, chondrocytes, myocytes, and many other types of cell.

1.2.4 Bone formation and resorption

Bone formation and resorption are crucial processes during skeletal development, skeletal homeostasis, bone turnover, healing fracture and some other diseases, particularly in bone metastasis. The process of bone formation (osteogenesis) involves three main steps: production of the extracellular organic matrix (osteoid); mineralization of the matrix to form bone; and bone remodelling by resorption and reformation. There are two categories of factors that are involved in the formation and resorption of bones:

1. Systemic hormones/factors: parathyroid hormone, 1,25-dihydroxyvitamin D_3, thyroxine (T4), and prostaglandins.
2. Local factors: bone morphogenetic proteins (BMPs), TGF-β, insulin-like growth factor (IGF), interleukin-1 (IL-1) and IL-6.

The cellular activities of osteoblasts, osteocytes, and osteoclasts are essential to the process of bone formation and resorption. Osteoblasts synthesize the collagenous precursors of bone matrix and also regulate its mineralisation. As the process of bone formation progresses, the osteoblasts come to reside in the tiny spaces (lacunae) within the surrounding mineralised matrix and are then called osteocytes. The cellular protrudes of osteocytes occupying the minute canals (canaliculi) permit the circulation of tissue fluids. To meet the requirements of skeletal growth and mechanical function, bone undergoes dynamic remodelling by a coupled process of bone resorption by osteoclasts and reformation by osteoblasts. Bone lesions are formed when the regulation of bone mass, which is maintained by a balance between bone-forming osteoblasts and bone-reabsorbing osteoclasts, is disturbed. Several reviews summarise the understanding of molecular interactions between osteoblasts and osteoclasts during the process of bone formation and resorption have recently been published (Sommerfeldt and Rubin, 2001; Roodman, 2004; Raubenheimer and Noffke, 2006). Probably, the best understood molecular crosstalk between osteoblasts and osteoclasts is RANK and RANKL (Figure 1.3). RANK is a transmembrane receptor expressed on osteoclast precursor cells, while RANKL is expressed by osteoblast which, upon binding to RANK, leads to osteoclast formation. This process can be interrupted by osteoprotegerin (OPG), a soluble competitive decoy receptor for RANKL, which can be secreted by stromal cells, B lymphocytes, dendritic cells and osteoblasts (Simonet *et al.*, 1997; Hofbauer *et al.*, 2000). This crosstalk also appears to be the mechanism underlying the response of bone to some hormones or local factors, including parathyroid hormone, 1,25-dihydroxyvitamin

D_3, oestrogen, IL-11 and prostaglandin E_2 (Sommerfeldt and Rubin, 2001; Roodman, 2004; Guise *et al.*, 2006; Lee and Lorenzo, 2006).

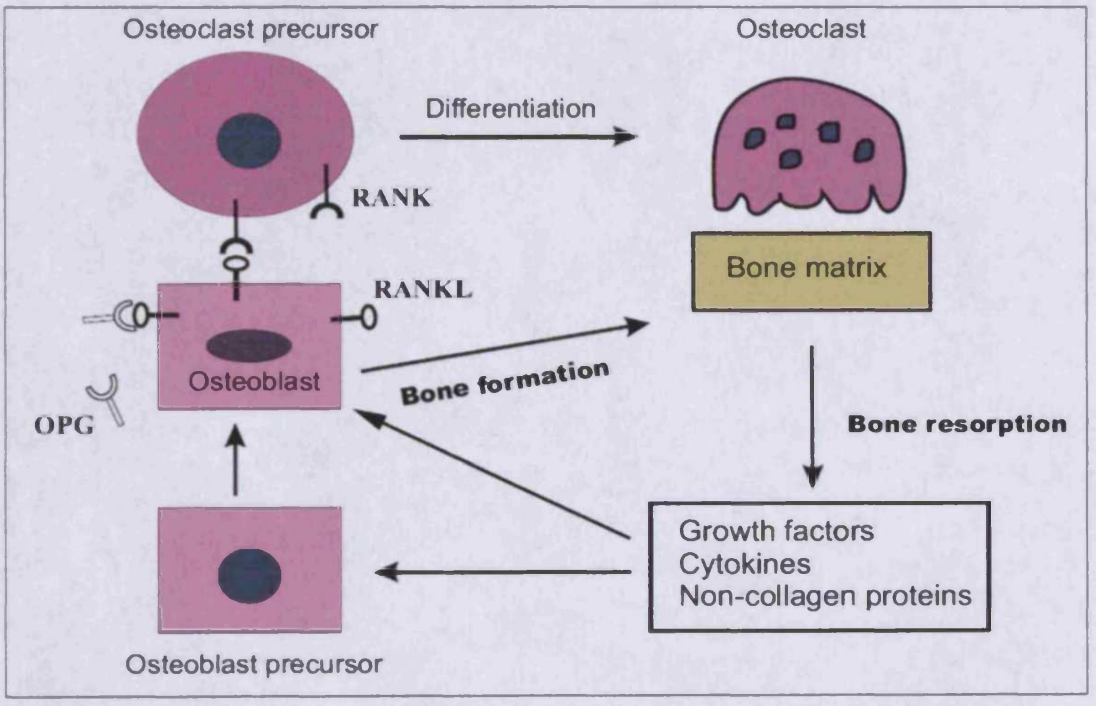

Figure 1.3 Interactions amongst the osteoblasts, osteoclasts and bone matrix during the bone formation and bone resorption.

1.3 Mechanisms of bone metastasis in prostate cancer

Bone metastasis is a frequent complication of certain solid tumours. For example, breast cancer and prostate cancer have the highest frequency in developing bone metastasis, whereas lung and kidney tumours are less frequently involved in bone metastasis (Mundy, 2002). Bone is the most common metastatic site of prostate cancer. Approximately 90% of patients with advanced prostate cancer (haematogenous metastasis) have skeletal metastasis(Bubendorf *et al.*, 2000). Importantly, once tumours metastasise to bone, they are incurable and can result in significant morbidity prior to a patient's death (Clark and Torti, 2003; Roodman, 2004). Bone metastasis can lead to pain, pathological fractures, nerve compression syndromes, and hypercalcemia. Current treatments for metastatic bone tumours are palliative.

A little more than a century ago, Peget proposed the "seed and soil" theory to describe the mechanisms by which tumour cells disseminate (Paget, 1989). Ever since, the knowledge in this area has expanded significantly. Key developments include the role of certain signal pathways, such as epithelial-mesenchymal transition (EMT) and the interaction between tumour cells and bone tissues, during the development of metastatic bone lesions. However, the mechanisms underlying are still unclear and current therapies are mainly palliative. A greater understanding of the complex multistep process of bone metastasis will undoubtedly shed light to the development of novel therapies or prevention.

1.3.1 Modes of disseminating prostate cancer

At an early stage, prostate cancer cells are confined to the prostate gland within a thin surrounding capsule. As disease progresses, some cancer cells, as the result of genetic predisposition or environmental interaction/stimulation or indeed the combination of both elements, become more aggressive and begin to breach the surrounding structure. These cells would either directly invade the surrounding tissue, or disseminate via lymphatic and haematogenous routes. Direct invasion may result in direct spreading of cancer cells to the erectile nerves, seminal vesicles, bladder and rectum nearby the prostate. The lymphatic and vascular routes, however, frequently result in the systemic spread of cancer cells to distant organs, including bones, lung, and liver, for example (Walsh *et al.*, 2002b).

The primary lymphatic drainage of the prostate is via the internal iliac, perivesical, external iliac, obturator, and presacral nodes. The secondary lymphatic drainage includes the inguinal, common iliac and para-aortic nodes (Naitoh *et al.*, 2000). These nodes are therefore prime locations when one searches for involved positive lymph nodes. Both lymphatic and haematogenous dissemination frequently occur, even at an early stage of the disease, and are very common in patients who have advanced prostate cancer (Walsh *et al.*, 2002b).

1.3.2 Process of bone metastasis from prostate cancer

The process of bone metastasis is complex, and incorporates multiple cells, factors and stages (Figure 1.4). A few reviews summarising this process have been recently published (Cooper *et al.*, 2003; Roodman, 2004; Raubenheimer and Noffke, 2006).

During the development and progression of primary tumour, certain clones of tumour cells which have acquired genotypic and phenotypic characteristics would enable themselves to interact with local microenvironment. For example, tumour cells release VEGF to initiate the angiogenesis, thus enhance the blood supply to the tumour. The stroma cells are rich sources of protein factors that directly act on cancer cells thus drive the growth of tumours and dissemination of cancer cells. On the other hand, some of the stromal cell derived factors will directly induce angiogenesis, thus support tumour growth and spread. A good example of these stromal derived protein factors is hepatocyte growth factor (HGF), a cytokine secreted by the stroma cells, which has been implicated in the angiogenesis and the dissemination of tumour cells (Jiang *et al.*, 2005c). The disruption of the intercellular adhesion in the tumour causes some tumour cells to detach from the tumour mass (**detachment**), and invade through the extracellular matrix (**invasion).** This invasion incorporates motility of tumour cells and breakdown of extracellular matrix. Some tumour cells will penetrate the blood vessel, thus enter the circulation (**intravasation**). From this point, tumour cells move away from the primary site, circulate in the blood circulation, and become viable to the host immune defences and subject to the mechanical stresses of blood flow. Some tumour cells may survive and exit the blood circulation (**extravasation**), in which cells adhere and penetrate the blood vessel. Once the tumour cells have escaped from the circulation, they may survive and finally develop a secondary tumour at another site, in this case in bone. This complex process requires the integration of multiple factors and events, such as tumour cells' invasion, angiogenesis, and the interaction of tumour cells with the local

microenvironment of bone (Parr and Jiang, 2001; Chambers *et al.*, 2002; Cooper *et al.*, 2003).

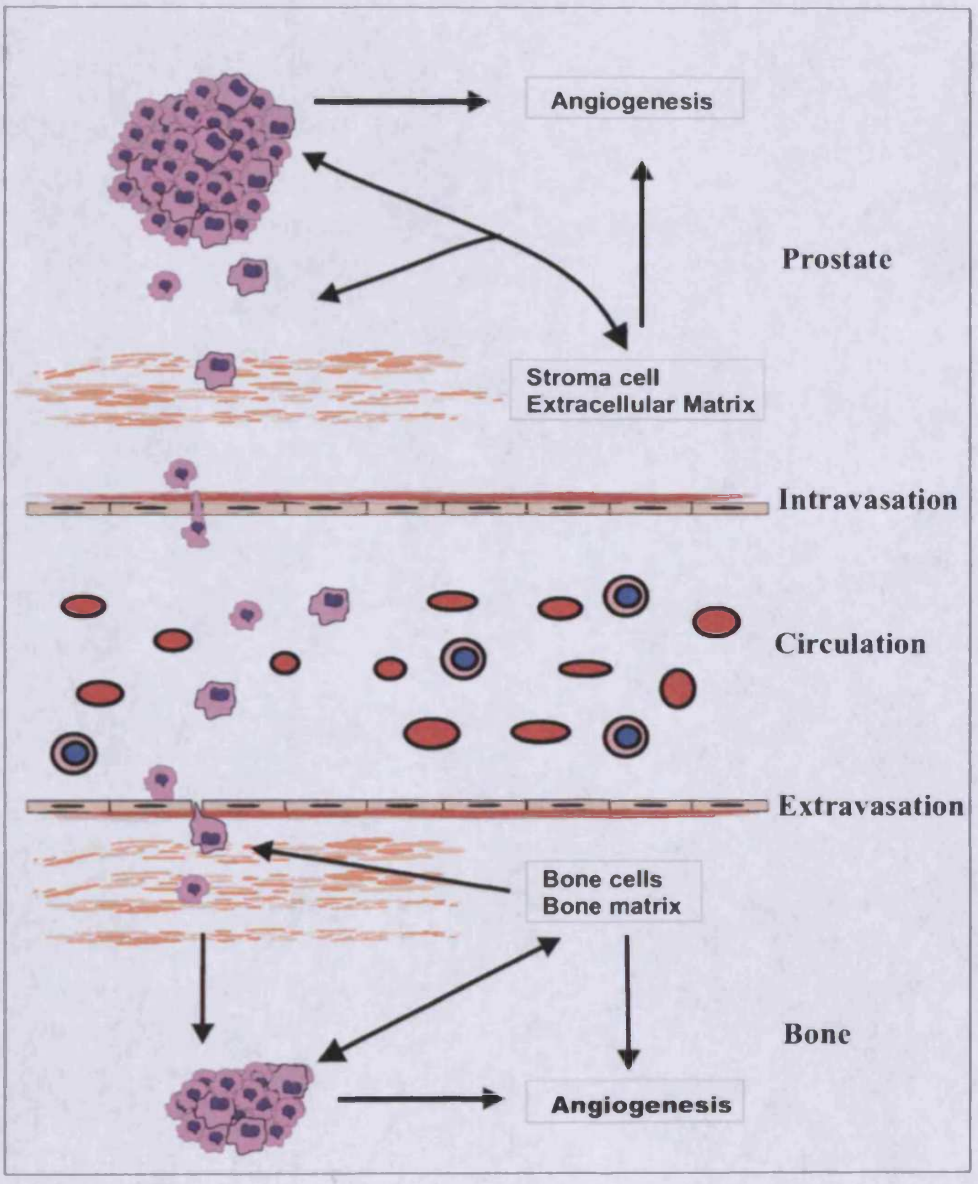

Figure 1.4 Schematic illustration of the bone metastatic process from prostate cancer.

1.3.3 The orientation metastases to bone in prostate cancer

The question of why the bone is the most preferred metastatic site of prostate cancer has aroused intense interest for investigation. One would first contemplate the anatomical characteristics of the prostate gland. The venous drainage of prostate may provide a shortcut for the haematogenous dissemination of tumour cells from prostate to certain bone. A rich venous plexus surrounds the prostate and connects to the venous drainage of the spine: this collection of veins (Batson's plexus) is potentially one of the reasons why the lumbosacral spinal metastases are common in advanced prostate cancer (Batson, 1995). However, the anatomical explanation is not able to explain why the other axial skeleton, skull and ribs may also be so commonly involved in bone metastasis from prostate cancer.

The 'seed and soil' theory proposed by Paget may provide some clue from a different standpoint (Paget, 1989). Osteotropic 'seeds' (tumour cells) may be developed during the progression of prostate cancer. These tumour cells may have acquired specific genetic phenotypes, or activated a specific set of cytokines and proteases. The elevated expression of BMPs and TGF-β in prostate cancer cells has been implicated in the development of bone metastasis (Autzen *et al.*, 1998; De Pinieux *et al.*, 2001; Shariat *et al.*, 2001; Masuda *et al.*, 2003). The "seeds" may also attach to the bone endothelium more effectively than to the endothelia of other organs (Lehr and Pienta, 1998). It has been suggested that the protease-activated receptor PAR1 and integrin $\alpha_v\beta_3$ which are highly expressed in primary prostate cancer cell lines and metastatic prostate cancer cells derived from bone metastasis, may contribute to the bony metastases through facilitating the attachment of tumour cells to blood vessel walls and the process of

extravasation (Chay *et al.*, 2002; Cooper *et al.*, 2002; Cooper *et al.*, 2003; Kumar, 2003). The vascular endothelial growth factor (VEGF) secreted by the tumour cells may also contribute to bone metastasis due to both the promotion of angiogenesis and the activation of osteoblasts (Krupski *et al.*, 2001; Chen *et al.*, 2004c; Dai *et al.*, 2004).

On the other hand, bone also provides a fertile "soil" for the "seeds". The bone matrix synthesised by osteoblasts has a particular abundance of cytokines and non-collagen proteins, which may "attract" prostate cancer cells and allow them to survive and proliferate in the bone matrix. For example, BMPs and TGF-β enriched in bone matrix can facilitate the development of the bone metatstasis. Osteonectin, osteopontin, osteocalcin, and bone sialoprotein can also modulate the properties of prostate cancer cells that facilitate spread and growth (Jacob *et al.*, 1999; Rosol, 2000; Denhardt *et al.*, 2001; Fizazi *et al.*, 2003; Zhang *et al.*, 2003; Khodavirdi *et al.*, 2006). Bone turnover, as a characteristic of adult bone, occurs most often in bone rich in trabecular bone, such as the vertebrae, proximal femur, calcaneous, and distal radius. During bone turnover, cytokines and NCPs released or synthesized through bone resorption and bone formation generate a fertile 'soil'. This may supplement the explanation of the favourite locations in bone metastases.

1.3.4 Tumour-derived osteotropic factors contribute to the predominantly osteoblastic metastases in prostate cancer

Bone metastases have been characterised as either osteolytic or osteoblastic. This classification actually represents two extremes of a continuum in which dysregulation of the normal bone remodeling process occurs. Patients can have both osteolytic and osteoblastic metastasis or mixed lesions containing both elements. Most patients with

breast cancer bone metastases have predominantly osteolytic lesions. In contrast, the metastatic lesions from prostate cancer are predominantly osteoblastic. During osteoblastic bone metastases, the balance between bone resorption and bone formation is tipped in favour of the latter. Patients may suffer bone pain and the poor quality of bone produced in osteoblastic bone metastases may lead to pathological fractures. Models to investigate osteoblastic metastases are rather rare, compared with models of osteolytic metastasis. Mechanisms which result in whether a metastatic lesion becomes osteoblastic or osteolytic, remain unclear. However, a number of factors produced by cancer cells, such as platelet-derived growth factor (PDGF), insulin-like growth factors (IGFs), fibroblast growth factors (FGFs), VEGF, Wingless and /NT-1 (WNT1), parathyroid hormone related protein (PTHrP), urokinase-type plasminogen activator (uPA), prostate specific antigen (PSA), endothelin-1 (ET-1) and BMPs, have been implicated in osteoblastic lesions.

PDGF is a dimeric polypeptide growth factor. Its subunit A and subunit B, form AA, BB and AB isoforms. The BB isoform is a potent osteotropic factor, which contributes to the osteoblastic lesions through promoting the migration and proliferation of osteoblasts (Yi *et al.*, 2002; Mehrotra *et al.*, 2004).

IGF system consists of two ligands, IGF-I and IGF-II, two receptors and seven binding proteins (IGFBPs). IGFs can elicit mitogenic stimulation of osteoblasts, increase bone matrix apposition and decrease the degradation of collagen. Evidence exists to implicate the osteoblast-stimulating factor IGF-I in the formation of metastasis from prostate cancer: first, serum IGF-I levels have been found to correlate with the risk of developing prostate cancer (Chan *et al.*, 1998), second, plasma IGFBP-3 levels were

lowest in patients with bone metastases, while IGFBP-2 levels were elevated in prostate cancer patients (Chan *et al.*, 2002; Shariat *et al.*, 2002). Although high IGF-I levels and low IGFBP-3 levels may predict the risk of developing advanced-stage prostate cancer (Chan *et al.*, 2002), a more recent study showed that IGF-I is neither necessary nor sufficient for the osteoblastic response to the metastases of prostate cancer (Rubin *et al.*, 2006). The role of the IGF system in bone metastasis of prostate cancer still requires further investigation.

FGFs, both acidic (FGF-1) and basic (FGF-2) are expressed in prostate cancer cells (Mansson *et al.*, 1989). Both FGFs can promote the proliferation of osteoblasts, while FGF-2 is able to suppress the formation of osteoclasts (Dunstan *et al.*, 1999). The implication of the interplay between these FGFs in the bone metastasis remains unclear.

VEGF has been shown to promote bone formation through directly activating the osteoblasts, and facilitating angiogenesis, thus making a contribution indirectly (Midy and Plouet, 1994; Gerber *et al.*, 1999; Street *et al.*, 2002). Elevated levels of VEGF have been implicated in the development of bone metastases in prostate cancer (Krupski *et al.*, 2001; Chen *et al.*, 2004c; Dai *et al.*, 2004).

WNT1 was elevated in the prostate cancer cells of advanced metastatic prostate carcinoma (Chen *et al.*, 2004a). Wnts produced by prostate cancer cells act in a paracrine fashion to induce osteoblastic activity in the bone metastases (Hall *et al.*, 2006). WNT signalling can be inhibited by its WNT antagonist DKK1 (Tian *et al.*, 2003). Inhibition of WNT signalling in osteoblasts can suppress osteoblast function and result in the osteolytic phenotype. DKK-1 production occurs early in the development of skeletal metastases, which results in the masking of osteogenic Wnts, thus favoring

osteolysis at the metastatic site. As metastases progress, DKK-1 expression is decreased, thus allowing the unmasking of Wnt's osteoblastic activity and ultimately resulting in osteosclerosis at the metastatic site (Hall *et al.*, 2006).

PTHrP is an osteolytic factor, which has been found in bone metastases of prostate cancer. However, even in a metastatic tumour in which PTHrP is highly expressed, the osteoblastic lesions remain predominant. The explanation for this paradox is that NH2-terminal fragments of PTHrP share strong sequence homology with ET-1, and thus stimulate new bone formation by activating the endothelin receptor type A (ET_AR) (Schluter *et al.*, 2001). The osteoblastic fragments of PTHrPs are the products of the cleavage of PTHrPs by prostate-specific antigen (PSA). This provides a partial molecular explanation for the osteoblastic phenotype of PTHrP-positive prostate cancer bone metastases (Cramer *et al.*, 1996).

uPA is also implicated in osteoblastic bone metastasis. uPA produced by prostate cancer cells has been shown to increase osteoblastic bone metastases (Rabbani *et al.*, 1990; Achbarou *et al.*, 1994). uPA can cleave and activate TGF-β which is produced in a latent form by osteoblasts. TGF-β regulates osteoblast and osteoclast differentiation but also regulates the growth of tumour cells themselves. uPA stimulated osteoblast proliferation may also be due to hydrolysing IGF-binding proteins and a resultant increasing level of free IGF (Koutsilieris, 1993).

PSA is a kallikrein serine protease, which is secreted by prostate cancer cells and used routinely as a marker of prostate cancer progression. PSA can not only cleave PTHrP to release osteoblastic PTHrP fragments, it may also activate osteoblast growth factors such as TGF-β (Killian *et al.*, 1993). PSA can also cleave IGF binding protein IGFBP3,

thereby IGF1 is capable of binding to its receptor and stimulating osteoblast proliferation (Cohen *et al.*, 1992; Cohen *et al.*, 1994).

MDA-BF-1 is a 45-kDa secreted form of the ErbB3 growth factor receptor (Vakar-Lopez *et al.*, 2004). Immunohistochemical analyses show that MDA-BF-1 is expressed in prostate cancer cells that have metastasised to bone, but not in cancer cells from primary tumours of patients with localised disease. Moreover, MDA-BF-1 has not been found in prostate cancer cells that have metastasised to the liver, adrenal glands, or lungs. Its function is mediated through a receptor expressed by osteoblasts (Liang *et al.*, 2005). Further functional studies show that MDA-BF-1 mediate specific interactions between prostate cancer cells and bone and assist in the osteoblast-mediated progression of prostate cancer in bone (Choueiri *et al.*, 2006).

ET-1 is a well known vasoconstrictor and is also a mitogenic factor for osteoblasts (Takuwa *et al.*, 1990). Serum level of ET-1 has been found to be increased in patients with bone osteoblastic lesions (Nelson *et al.*, 1995). ET-1 tends to be elevated in androgen-independent advanced prostate cancers (Granchi *et al.*, 2001), and its expression can also be enhanced by bone contact (Chiao *et al.*, 2000). ET-1 has been suggested to be a central mediator of osteoblastic metastasis (Mohammad and Guise, 2003). ET-1 mediates its effects on bone formation through the Endothelin A receptor, ET_AR. An ET_AR antagonist (atrasentan) has been shown to prevent osteoblastic bone metastases in mouse model and reduced skeletal morbidity in men with advanced prostate cancer (Carducci *et al.*, 2003; Yin *et al.*, 2003). ET-1 can increase prostate cancer cell proliferation and enhance the mitogenic effect of other growth factors, including IGF-1, PDGF and EGF (Nelson *et al.*, 1996). More recent evidence suggests

that ET-1 increases osteoblast proliferation, and new bone formation, by activating the Wnt signalling pathway through suppression of the Wnt pathway inhibitor DKK1(Clines *et al.*, 2006).

BMP belong to the TGF-β superfamily and stimulate osteoblast differentiation through the activation of transcription factors, in particular Runx-2 (McCarthy *et al.*, 2000). Some BMPs are highly expressed in bone metastases from prostate cancer, such as BMP-6, BMP-7 and GDF-15 (Thomas *et al.*, 2001; Masuda *et al.*, 2003; Masuda *et al.*, 2004; Dai *et al.*, 2005). Noggin, a BMP antagonist can prevent the development of both osteoblastic and osteoclastic prostate cancer metastases (Haudenschild *et al.*, 2004; Feeley *et al.*, 2006).

1.3.5 Cycle of osteoblastic metastases in prostate cancer

During the development of osteoblastic metastases from prostate cancer, the interactions among tumour cells, bone cells and bone matrix constitute a "vicious cycle" of osteoblast-mediated bone metastasis (Reddi *et al.*, 2003; Choueiri *et al.*, 2006). In the early stage of bone metastasis, prostate cancer cells produce osteogenic factors such as ET-1, BMPs and PDGF, which activate osteoblasts. The osteoblasts differentiate from their progenitor cells, proliferate and deposit new matrix for bone formation. However this unmineralised new matrix provides a more fertile 'soil' to tumour cells, which is enriched with growth factors and noncollagenous proteins (NCPs). These factors help prostate cancer cells survive and proliferate in the bone microenvironment. The prostate cancer cells then further activate osteoblasts. In addition to this cycle, both tumour-derived factors and osteoblasts expressing RANKL can activate osteoclasts, leading to a

degree of bone resorption, and subsequently generates a bigger space for dominant osteoblastic lesion. The cytokines and NCPs released from bone matrix during bone resorption can also enhance this cycle through facilitating proliferation of both prostate cancer cells and osteoblast (Figure 1.5).

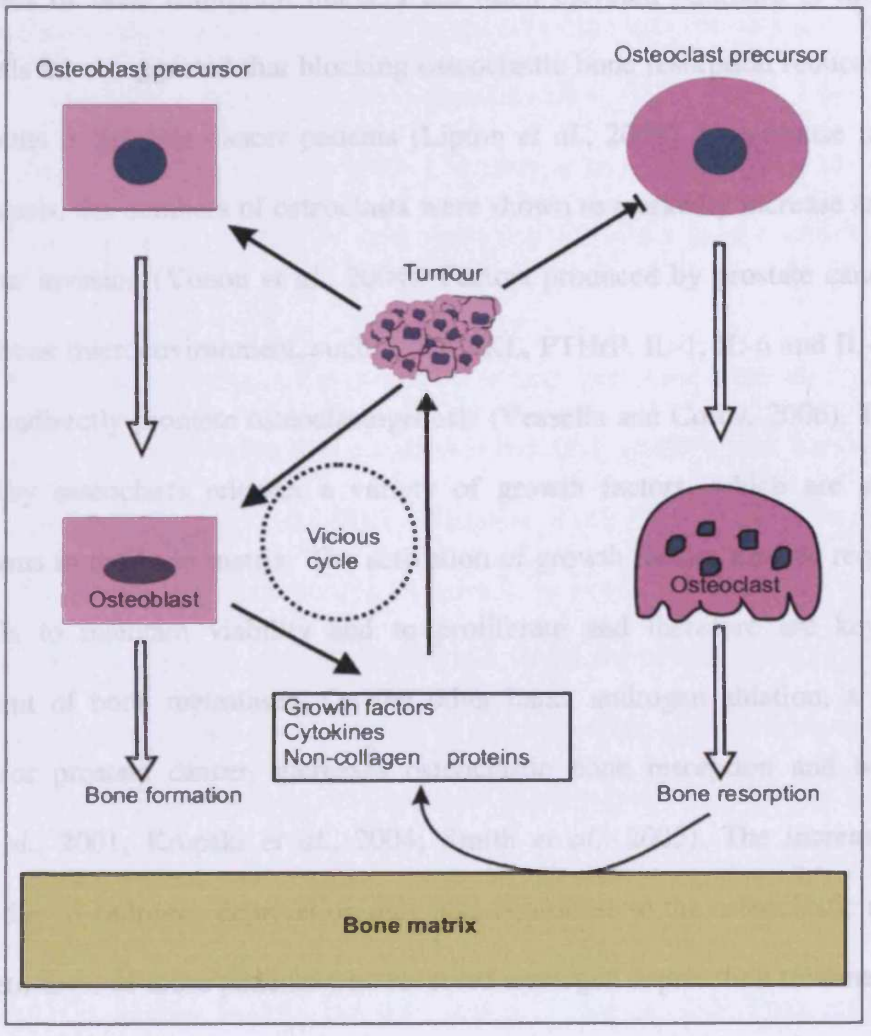

Figure 1.5 Vicious cycle of the osteoblastic metastasis in prostate cancer. Interactions between tumour and bone microenvironment which includes osteoblasts, osteoclasts and bone matrix, contribute to the predominant osteoblastic lesions in bone metastases from prostate cancer.

1.3.6 The role of osteolytic activity in bone metastases of prostate cancer

It has been demonstrated that osteoblastic metastases also involve considerable osteolysis (Oades *et al.*, 2002; Yonou *et al.*, 2004). Both osteolysis itself and the factors released from bone matrix during bone resorption contribute to the cycle of osteoblastic lesion formation. In prostate cancer patients with clinical osteoblastic lesions, blood and urinary levels of bone resorption markers are often elevated (Garnero *et al.*, 2000). Clinical trials have suggested that blocking osteoclastic bone resorption reduces related skeletal events in prostate cancer patients (Lipton *et al.*, 2002). In a mouse model of bone metastasis, the numbers of osteoclasts were shown to markedly increase at sites of early tumour invasion (Yonou *et al.*, 2004). Factors produced by prostate cancer cells within the bone microenvironment, such as RANKL, PTHrP, IL-1, IL-6 and IL-11, may directly or indirectly promote osteoclastogenesis (Vessella and Corey, 2006). The bone resorption by osteoclasts releases a variety of growth factors, which are stored as inactive forms in the bone matrix. The activation of growth factors may be required by cancer cells to maintain viability and to proliferate and therefore are key to the establishment of bone metastases. On the other hand, androgen ablation, a standard treatment for prostate cancer, increases osteoclastic bone resorption and bone loss (Smith *et al.*, 2001; Krupski *et al.*, 2004; Smith *et al.*, 2005). The increased bone resorption due to androgen deprivation may also contribute to the osteoclastic activities in bone metastases of those patients who received androgen deprivation treatment. Bone resorption inhibitors, such as biphosphonates which can prevent bone loss, may also decrease skeletal metastases (Paule and Cicco, 2001; Conti, 2005). Taken together, both

osteoblasts and osteoclasts "cooperate" to drive the settlement and growth of prostate cancer in bone.

1.4 Bone morphogenetic proteins and their signalling pathway

1.4.1 Bone morphogenetic proteins

Bone morphogenetic proteins (BMPs) are members of the transforming growth factor-beta (TGF-β) superfamily, which was first named by Urist (Urist, 1965). BMP proteins were first purified and cloned in late 1980s (Wozney *et al.*, 1988; Celeste *et al.*, 1990; Lee, 1990; Ozkaynak *et al.*, 1990). To date, more than 20 BMPs have been identified in humans (Table 1.3).

Bone morphogenetic proteins are synthesized as large precursor molecules, consisting of an amino-terminal pro-region and a carboxyl-terminal ligand which contains seven conserved cysteines (Wozney *et al.*, 1988; Ozkaynak *et al.*, 1990; Wozney *et al.*, 1990). Each BMP ligand has seven conserved cysteines, in which six cysteines construct a cysteine knot, and the seventh cysteine contributes to the dimerisation (Butler and Dodd, 2003). Presently, little is known with regard to the processing of the precursor molecule or secretion of BMPs. However, it has been shown that some of the proprotein convertases (PCs), such as furin, proprotein convertase subtilisin/kexin type 6 (PCSK6) and proprotein convertase subtilisin/kexin type 5 (PCSK5), which belong to a subtilisin-like proprotein convertase family, can proteolytically activate BMP precursors at the sequence of R-X-K/R-R or R-X-X-R (Cui *et al.*, 1998; Constam and Robertson, 1999; Tsuji *et al.*, 1999; Hashimoto *et al.*, 2005). The pro-region of the precursor BMP protein controls the stability of the processed mature protein, and the amino acid motif adjacent

to the cleavage site determines the efficiency of cleavage(Constam and Robertson, 1999). Amongst the BMPs, growth differentiation factor-9 (GDF9A) and BMP15 (GDF9B) may be an exception, and have only six cysteines in the mature form without the seventh cysteine. This characteristic of BMP15 and GDF9 may help to define its ligand-receptor binding properties (Mazerbourg and Hsueh, 2006). The pro-region of some BMPs, for example GDF-8 and GDF-9, remains non-covalently associated with the mature ligand even after secretion from the cell (Lee and McPherron, 2001; Brown *et al.*, 2005).

Once processed and activated, BMP proteins are biologically active both as homodimer, and as heterodimer molecules, in which two chains are connected by disulfide bonds. Interestingly, the heterodimers of BMP4/7, BMP2/6, BMP2/7 and BMP7/GDF7 are more effective than when they form homodimers (Aono *et al.*, 1995; Israel *et al.*, 1996; Suzuki *et al.*, 1997; Butler and Dodd, 2003).

Table 1.3 Members of Bone Morphogenetic Protein and Growth Differentiation Factors (Identified in Humans).

Official Symbol	Alternative Name	Gene Location in homo sapiens	Year of identification
BMP2	BMP2A	20p12	1988
BMP3		4p14-q21	1988
BMP4	ZYME; BMP2B; BMP2B1	14q22-q23	1988
BMP5	MGC34244	6p	1990
BMP6	VGR; VGR1	6p24-p23	1990
BMP7	OP-1	20	1990
BMP8A		1p35-p32	2002
BMP8B	BMP8; OP2	1p35-p32	1992
BMP10		2p13.3	1999
BMP15	GDF9B, ODG2	Xp11.2	1998
GDF1		19p12	1991
GDF2	BMP-9; BMP9	10q11.22	1994
GDF3		12p13.1	2000
GDF4		?(Reserved)	?
GDF5	CDMP1	20q11.2	1994
GDF6		8q22.1	1999
GDF7	BMP12	2p24-2p23	1998
GDF8	MSTN, myostatin	2q32.1	1997
GDF9		5q23-5q33.1	1993
GDF10	BMP-3b	10q11.22	1995
GDF11	BMP-11	12q13.13	1998
GDF15	PLAB, MIC-1, PDF, MIC1, NAG-1, PTGFB	19p13.1-13.2	1997

Data collected from HGNC and Entrez Gene. Based on literature published BMP2(Wozney *et al.*, 1988); BMP3(Wozney *et al.*, 1988); BMP4(Wozney *et al.*, 1988); BMP5(Celeste *et al.*, 1990); BMP6(Celeste *et al.*, 1990); BMP7(Ozkaynak *et al.*, 1990); BMP8A(Strausberg *et al.*, 2002); BMP8B(Ozkaynak *et al.*, 1992); BMP10(Neuhaus *et al.*, 1999); BMP15(Dube *et al.*, 1998); GDF1(Lee, 1990); GDF2(Celeste *et al.*, 1994a); GDF3(McPherron and Lee, 1993); GDF5(Hotten *et al.*, 1994); GDF6(Davidson *et al.*, 1999); GDF7(Lee *et al.*, 1998); GDF8(McPherron *et al.*, 1997); GDF9(McPherron and Lee, 1993);GDF10(Cunningham *et al.*, 1995); GDF11(Gamer *et al.*, 1999); GDF15(Yokoyama-Kobayashi *et al.*, 1997).

1.4.2 BMP receptors

BMP signals are mediated by receptors which are dedicated to TGF-β signalling, and include Type I and Type II serine/threonine kinase receptors, seven Type I receptors and five Type II receptors in humans (Table 1.4). Six of the 7 Type I receptors and three of the 5 Type II receptors are responsible for BMP signalling. BMPR1A, BMPR1B and BMPR2 are specific for the BMPs; whilst ACVRL1, ACVR1, ACVR1B, ACVR2B, and ACVR2A are also the receptors for activin; TGFBR1(ALK5) is known as the type I receptor for TGF-β1, 2 and 3 (Figure 1.6).

Both types of the BMP serine/threonine kinase receptors consist of an N-terminal extracellular ligand binding domain, a transmembrane region and a C-terminal serine/threonine kinase domain. The structure of the extracellular ligand binding domain of both receptors is similar. It has a three-finger toxin fold, with each finger formed by a pair of anti-parallel β strands(Greenwald *et al.*, 1999; Kirsch *et al.*, 2000). The intracellular region of the type I receptors, but not type II receptors, contains a highly reserved GS domain enriched in glycines and serines. The region is located in the intracellular juxtamembrane region of the receptor (Attisano *et al.*, 1994; Wrana *et al.*, 1994). Type II receptors recruit type I receptors by phosphorylating the GS domain of type I receptor during signal transduction.

Table 1.4 Transmembrane serine/threonine kinase receptors.

Type I receptor	Type II receptor
ACVRL1 (ALK-1, ACVRLK1, ALK1, SKR3)	TGFBR2 (TGFR-2, TGFbeta-RII)
ACVR1 (ALK2, ACTRI, ACVRLK2, FOP, SKR1)	TGFBR3
BMPR1A (ALK3, ACVRLK3, CD292)	***BMPR2*** (BMPR-II, BMPR3, BMR2, BRK-3, T-ALK)
ACVR1B (ALK4, ACTRIB, ACVRLK4, SKR2)	***ACVR2B*** (ActR-IIB)
TGFBR1 (ALK-5, ACVRLK4, SKR4, TGFR-1)	***ACVR2A*** (ACTRII, ACVR2)
BMPR1B (ALK-6, ALK6, CDw293)	
ACVR1C (ALK7, ACVRLK7)	

There are seven Type I and five Type II transmembrane serine/threonine kinase receptors identified in humans. Six Type I receptors and three Type II receptors that have been found involved in the signal transduction of BMPs, which are ***bold italic*** in the table. ACVRL1, activin A receptor type II-like 1; ACVR1, activin A receptor, type I; BMPR1A, bone morphogenetic protein receptor, type IA; ACVR1B, activin A receptor, type IB; TGFBR1, transforming growth factor, beta receptor I; BMPR1B, bone morphogenetic protein receptor, type IB; ACVR1C, activin A receptor, type IC; TGFBR2, transforming growth factor, beta receptor II; TGFBR3, transforming growth factor, beta receptor III; BMPR2, bone morphogenetic protein receptor, type II; ACVR2B, activin A receptor, type IIB; ACVR2A, activin A receptor, type IIA.

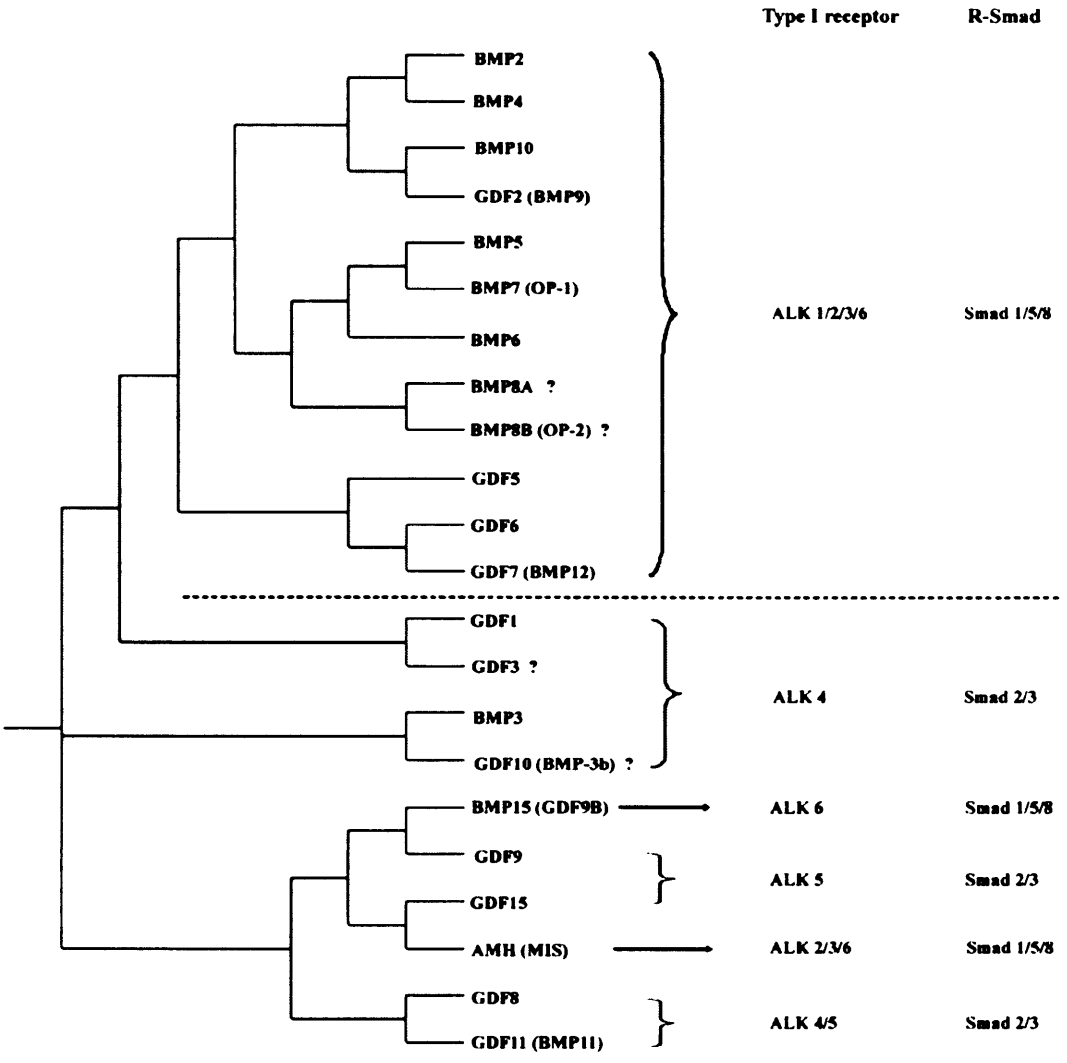

Figure 1.6 Dendrogram tree and key downstream signaling molecules of BMP/GDF. Phylogenetic analyses was performed using the ClustalW (http://www.ebi.ac.uk/clustalw/), and the dendrogram tree was drawn by using the Treeview (Version 1.6.6, http://taxonomy.zoology.gla.ac.uk/rod/treeview.html). ? is unknown.

1.4.3 BMP signal transduction

Smad proteins are important signaling molecules downstream of the BMP receptors. Smad is a nomination from both Sma (small family member, identified in *Caenorhabditis elegans*) and MAD (mothers against decapentaplegic homolog, MAD) (Derynck *et al.*, 1996). Eight Smads have been identified in humans, and comprise three subgroups: pathway restricted Smads (receptor regulated Smads) (referred to as R-Smads which include Smad 1, 2, 3, 5 and 8) (Table 1.5), common mediator Smad (Co-Smad, Smad4), and inhibitory Smads (I-Smads, Smad 6 and 7) (Shi and Massague, 2003; Nohe *et al.*, 2004). R-Smads 1, 5 and 8 are substrates of the type I receptors (ALKs 1, 2, 3 and 6), whereas R-Smads 2 and 3 are substrates of the type I receptors (ALKs 4, 5 and 7) (Kretzschmar and Massague, 1998; Chen and Massague, 1999; Jornvall *et al.*, 2001; Shi and Massague, 2003). All Smad proteins share considerable homology in their primary sequences. R-Smads and Co-Smad contain two highly conserved Mad homology domains: the Mad homology 1 (MH1) domain in the amino-terminal part and the Mad homology MH2 domain in the carboxy-terminal part. The MH1 domain can bind to specific DNA sequences, and the MH2 domains are responsible for homo- and heteromeric complex formation. R-Smads contain the carboxyl-terminal SSXS motif which is phosphorylated by the Type I receptor during signal transduction of BMP's (Nohe *et al.*, 2004).

There are two categories of signaling pathway for BMPs and BMP receptors: the Smad dependent pathway and the Smad independent pathway (Figure 1.7). Type I and type II BMP receptors are required for both pathways. When a dimeric ligand of BMPs binds to two different types of serine-threonine kinase transmembrane receptors, the Type-II receptors then transphosphorylate the GS domain of the Type-I

receptors(Moustakas and Heldin, 2002). This forms a ligand-receptor complex consisting of a dimer of each ligand, Type-I and Type-II receptors. If the BMP ligand binds simultaneously to the preformed hetero-oligomeric complexes (PFC), this leads to activation of the Smad dependent pathway(Nohe *et al.*, 2002; Nohe *et al.*, 2004). It includes recruitment of the pathway-restricted Smads (R-Smads, Smads1, 2, 3, 5 or 8), and regulates the transcription of target genes; this is known as the Smad dependent pathway.

Unlike other members of TGF-β superfamily, BMPs have a higher affinity for the Type-I receptors, rather than the Type II receptors. Thus, BMP ligand can also bind to ALK3 or ALK6, and then recruits BMPRII into a hetero-oligomeric complex (BMP-induced signalling complexes, BISC) which leads to the activation of the Smad independent pathway (Nohe *et al.*, 2002; Nohe *et al.*, 2004). During intracellular signal transduction, the X-linked inhibitor of apoptosis protein (XIAP) functions as an adaptor protein bridging between the Type I receptor and TGF-ß activated binding protein (TAB1/2/3), which is an activator of the MAPKKK TGF-ß activated tyrosine kinase 1 (TAK1) (Yamaguchi *et al.*, 1995; Shibuya *et al.*, 1996; Yamaguchi *et al.*, 1999). The activation of TAK1 can lead to activation of p38, a mitogen-activated protein kinase (MAPK) (Moriguchi *et al.*, 1996; Kimura *et al.*, 2000; Nohe *et al.*, 2002). TAK1 can also activate Jun N-terminal kinases (JNKs), NF-kappaB (NF-kB) and Nemo-like kinase (NLK) (Shirakabe *et al.*, 1997; Ishitani *et al.*, 1999; Lee *et al.*, 2002).

Table 1.5 Receptors and R-Smads involved in BMP signalling.

Official Symbol	Type II receptor	Type I receptor	R-Smad
BMP2	BMPRII ActRIIA	ALK 3/6	Smad 1/5/8
BMP3	ActRIIA	ALK 4	Smad 2/3
BMP4	BMPRII ActRIIA	ALK 3/6	Smad 1/5/8
BMP5		ALK 3	Smad 1/8
BMP6	ActRIIA ActRIIB BMPRII	ALK 1/2/3/6	Smad 1/5
BMP7	BMPRII ActRIIA	ALK 2/3/6	Smad 1/5/8
BMP8A			
BMP8B			
BMP10	BMPRII ActRIIA	ALK 3/6	Smad 1/5/8
BMP15	BMPRII	ALK 6	Smad 1/5/8
GDF1	ActRIIB	ALK 4	Smad 2/3
GDF2	ActRIIA ActRIIB BMPRII	ALK 1	Smad 1/5
GDF3			
GDF5	BMPRII ActRIIA	ALK 3/6	Smad 1/5/8
GDF6	BMPRII ActRIIA	ALK 3/6	
GDF7	BMPRII ActRIIA	ALK 3/6	
GDF8	ActRIIB	ALK4/5	Smad 2/3
GDF9	BMPRII	ALK5	Smad 2/3
GDF10			
GDF11	ActRIIA ActRIIB	ALK4	Smad 2/3
GDF15			Smad 2/3

BMP2 (Koenig *et al.*, 1994; Yamaji *et al.*, 1994; Liu *et al.*, 1995; Namiki *et al.*, 1997); BMP3 (Daluiski *et al.*, 2001); BMP4 (Koenig *et al.*, 1994; ten Dijke *et al.*, 1994; Yamaji *et al.*, 1994; Nohno *et al.*, 1995; Rosenzweig *et al.*, 1995; Aoki *et al.*, 2001); BMP5 (Beck *et al.*, 2001; Zuzarte-Luis *et al.*, 2004); BMP6 (Ebisawa *et al.*, 1999; Ahmed *et al.*, 2001; Aoki *et al.*, 2001); BMP7 (ten Dijke *et al.*, 1994; Liu *et al.*, 1995; Rosenzweig *et al.*, 1995; Aoki *et al.*, 2001); BMP10 (Mazerbourg *et al.*, 2005); BMP15 (Moore *et al.*, 2003); GDF1 (Cheng *et al.*, 2003); GDF2 (Brown *et al.*, 2005; Lopez-Coviella *et al.*, 2006); GDF5 (Nishitoh *et al.*, 1996; Aoki *et al.*, 2001; Nakahara *et al.*, 2003; Sammar *et al.*, 2004; Chen *et al.*, 2006); GDF6 (Mazerbourg *et al.*, 2005); GDF7 (Mazerbourg *et al.*, 2005); GDF8 (Rebbapragada *et al.*, 2003); GDF9 (Mazerbourg and Hsueh, 2006); GDF11 (McPherron *et al.*, 1999; Oh *et al.*, 2002; Andersson *et al.*, 2006); GDF15 (Xu *et al.*, 2006).

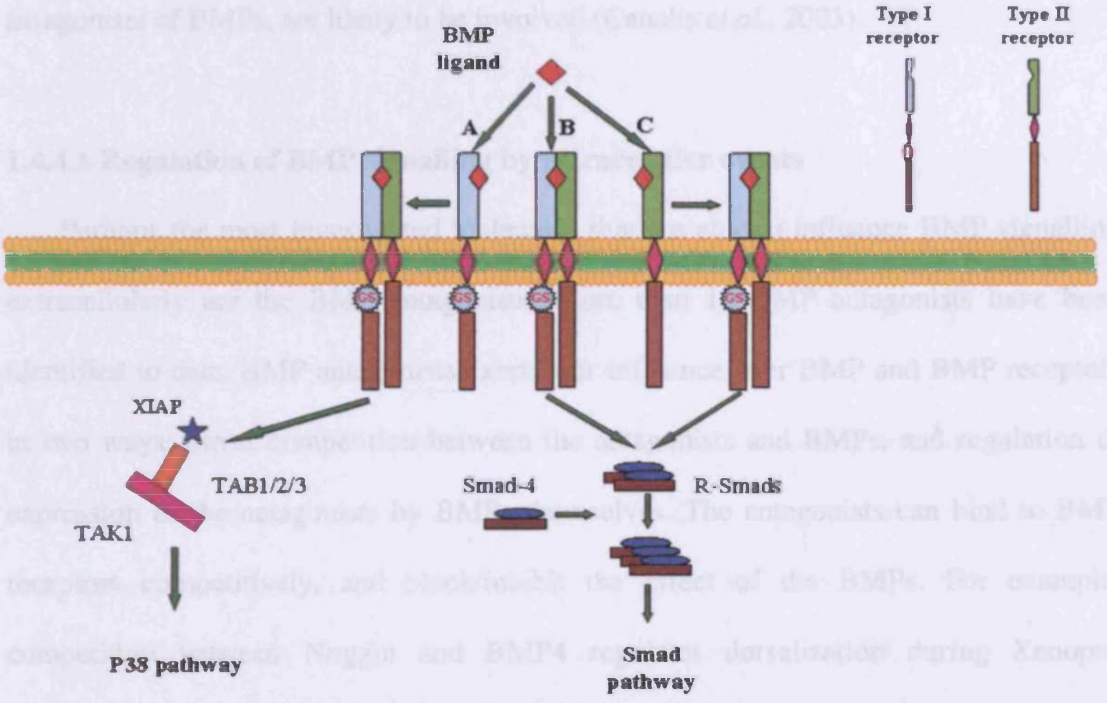

Figure 1.7 Signalling pathway of BMPs. (A) BMP ligand binds to the type I receptors with higher affinity and then recruit the type II receptors. After the phosphorylation by type II receptors, the type I receptors activate TAB1/2/3 through XIAP, leading to the activation of p38 pathway; (B) BMPs ligand binds to type I and type II simultaneously. After the phosphorylation, type I receptors recruit R-Smads, and then leads to activation of the Smad-dependent pathway; (C) The members of TGF-β superfamily, typically bind to the type II receptors firstly, then recruit and phsophorylate the type I receptors, thus leading to the activation of Smad-dependent pathway.

1.4.4 Regulation of BMPs' signalling

The regulation of BMP signalling may occur extracellularly during the process of ligand binding to the receptors, or intracellularly during signal transduction (Table 1.6). Recent evidence suggests that BMPs can also regulate their function through a negative feedback loop, in which the pseudoreceptor, Inhibitory Smads (Smad 6 and 7) antagonists of BMPs, are likely to be involved (Canalis *et al.*, 2003).

1.4.4.1 Regulation of BMP signalling by extracellular events

Perhaps the most investigated molecules that are able to influence BMP signalling extracellularly are the BMP antagonists. More than 10 BMP antagonists have been identified to date. BMP antagonists exert their influence over BMP and BMP receptors in two ways: direct competition between the antagonists and BMPs, and regulation of expression of the antagonists by BMPs themselves. The antagonists can bind to BMP receptors competitively, and block/inhibit the effect of the BMPs. For example, competition between Noggin and BMP4 regulates dorsalization during Xenopus development (Re'em-Kalma *et al.*, 1995). On the other hand, noggin expression in osteoblasts can be induced by BMP2, 4 and 6. Therefore, the BMPs are able to modulate their effect via a negative feed back loop by upregulation of the expression of their antagonist(Gazzerro *et al.*, 1998).

Besides the BMP antagonists, there are other possible mechanisms by which BMP signalling is regulated extracellularly. One of these extracellular mechanisms is the expression of co-receptors or dominant negative non-signalling pseudoreceptors in a cell. The pseudoreceptor, BMP and activin membrane bound inhibitor (BAMBI), is a

transmembrane protein which has an extracellular domain similar to that of the Type I BMP receptor. However, the pseudoreceptor lacks the intracellular serine/threonine kinase domain. BAMBI binds to ligand competitively, and then interferes with the signalling of BMPs and other TGF-β molecules (Onichtchouk *et al.*, 1999). BMP4 can also induce the expression of BAMBI in mouse embryonic fibroblasts(Grotewold *et al.*, 2001), and in doing so, BMP4 creates a negative feedback loop to regulate BMP function.

Recent evidence suggests that, like other members of the TGF-β family, there are co-receptors for the BMP ligand, which enhance the signaling of BMPs. DRAGON is the first co-receptor reported for BMP, and is a glycosylphosphatidylinositol-anchored member of the repulsive guidance molecule family. DRAGON binds directly to BMP2 and BMP4, but not BMP7 or other TGF-β ligands. The interaction between DRAGON and BMPs enhances the signaling and ultimately leads to a stronger biological response from the cell. Interestingly, this enhanced effect due to the DRAGON/BMP interaction can be reduced by the BMP2/4 antagonist, Noggin (Samad *et al.*, 2005). A homologue of the Dragon, repulsive guidance molecule (RGMa), has been identified as another co-receptor for BMPs (Babitt *et al.*, 2005).

1.4.4.2 Regulation of intracellular signalling by BMP/BMP receptors

Inhibitory Smads

Once the BMP ligand binds to the BMP receptors, inhibitory Smad (Smad 6 and 7), Smad binding protein (Ski and Tob) and Smad ubiquitin regulatory factor (Smurf 1 and 2) can also regulate the intracellular signal transduction of BMPs.

Smad 6 and 7 inhibit signal transduction of BMPs, by interference with the activation of Smad 1 and 5, which are phosphorylated by the BMP Type I receptor. Smad 6 and 7 also inhibit the heterodimerization between Smad1/5 and Smad 4 (Hayashi *et al.*, 1997; Imamura *et al.*, 1997). There is also evidence suggesting that BMPs can adjust their signalling by up-regulating the expression of Smad 6 and 7 (Takase *et al.*, 1998; Ishisaki *et al.*, 1999).

Smad binding proteins

Smad binding proteins suppress BMP signalling by associating with the MH2 binding domain of Smads. Sloan-Kettering retrovirus (Ski) binds Smad 1, 2, 3, 5 and 4 and inhibits BMP signalling (Luo *et al.*, 1999; Wang *et al.*, 2000; Xu *et al.*, 2000). The transducer of ErbB-2 (Tob) is probably associated with the MH2 domain of Smad 1, 5, 6, 7 and 8(Yoshida *et al.*, 2000; Yoshida *et al.*, 2003).

Molecules that facilitate degradation of the Smads

Smurf 1 and 2 modulate TGF-β signaling by selectively targeting the receptors and Smad proteins for degradation and ubiquitination (Arora and Warrior, 2001). Smurf 1 can directly interact with Smad 1/5, and facilitate their degradation (Zhu *et al.*, 1999). It can also indirectly interact with the BMP Type I receptor through I-Smad 6 and 7, and induce ubiquitination and degradation of the receptors(Murakami *et al.*, 2003). TNFα has been shown to inhibit osteoblastic bone formation through upregulation of Smurf 1 and 2 (Kaneki *et al.*, 2006).

NEDD4-2 (neural precursor cell expressed, developmentally down-regulated 4-2) has recently been found to be a direct binding partner of Smad7(Kuratomi *et al.*, 2005). NEDD4-2 is structurally similar to Smurfs 1 and 2 (Smad ubiquitin regulatory factors). It can interact with Type I receptor via Smad 7, and induce its degradation. It can also bind to Smad 2 and 3 in the ligand-dependent manner, and degrade Smad 2, but not Smad 3. Over-expression of NEDD4-2 inhibits the transcriptional activity induced by TGF-β and BMPs. Wicks and Haros *et al.* recently reported a novel ubiquitin: C-terminal hydrolase (UCH37). UCH37 is a deubiquitinating enzyme that can potentially reverse Smurf-mediated ubiquitination. It forms a stable complex with Smad 7, which deubiquitinates and stabilizes the type I TGF-beta receptor (Wicks *et al.*, 2005). However, its role in BMP signaling remains unclear.

The associated molecule with the SH3 domain of STAM (AMSH) is a direct binding partner for Smad6 and has been found to inhibit the interaction between Smad6 and the activated BMP type I receptor, thereby allowing more efficient BMP receptor-induced phosphorylation of R-Smads. In addition, AMSH was found to interfere with the interaction between Smad6 and the activated R-Smad. Thus, AMSH promotes BMP signaling by negatively regulating the function of I-Smads (Itoh *et al.*, 2001).

Table 1.6 Regulatory factors on BMP signalling.

Location	Category	Official Symbol	Target
Extracellular	*Antagonist*	Noggin	BMP2, 4, 6 and 7; GDF5 and GDF6
		Chordin	BMP4, 7
		Chordin like 2(CHL2)	BMP2, 4, 5, 6, 7 and GDF5
		Follistatin	BMP6, 7, 11 and 15, GDF8 and 9
		Ventroptin	BMP4
		FLRG	BMP2
		Twisted gastrulation (Tsg)	BMP2, 4
		Gremlin(DRM)	BMP2, 4 and 7
		Dan	BMP2, 4 and GDF5
		Cerberus	BMP2, 4
		(PRDC)	BMP2, 4
		Sclerostin (SOST)	BMP6 and 7
		Caronate	BMP2, 4 and 7
		(DAND5)	BMP4
	Enhancer	Kielin/Chordin like	BMP7
Membrane	*Pseudoreceptor*	BAMBI	BMP4
	Co-receptor	*Dragon*	BMP2, 4
		RGMa	BMP2, 4
Intracellular	*Inhibitory Smads*	Smad6 and 7	R-Smad, Co-Smad
	Smad binding protein	Ski	Smad 2, 3 and 4
		SKIL/SnoN	Smad 2, 4
		Tob	Smad 1, 5 and 8
		AMSH	Smad6
	Ubiquitination and degradation of Smad	Smurf1 and 2	Smad 1, 5, 6 and 7
		NEDD4-2	Smad 2
	Deubiquitination of Smad	UCH37	Smad7

The regulation of BMP signalling can happen during the process of ligand binds to receptor, and the intracellular signal transduction. Dan, Cerberus, Gremlin, PRDC, Sclerostin, Caronate and DAND5 belong to DAN/Cerberus family. Based on literatures published: ***Noggin*** (Re'em-Kalma *et al.*, 1995; Chang and Hemmati-Brivanlou, 1999; Haudenschild *et al.*, 2004; Pera *et al.*, 2004; Zhu *et al.*, 2006); ***Chordin*** (Sasal *et al.*, 1995; Piccolo *et al.*, 1996; Dale *et al.*, 1999); Kielin/Chordin like(Lin *et al.*, 2005); ***Chordin like 2, CHL2*** (Nakayama *et al.*, 2004); ***Follistatin*** (Fainsod *et al.*, 1997; Iemura *et al.*, 1998; Otsuka *et al.*, 2001; Balemans and Van Hul, 2002; Pierre *et al.*, 2005); Sclerostin(Kusu *et al.*, 2003); ***Ventroptin*** (Sakuta *et al.*, 2001); ***FLRG***(Tsuchida *et al.*, 2000); ***Gremlin*** (Hsu *et al.*, 1998; Merino *et al.*, 1999); ***Twisted gastrulation*** (Chang *et al.*, 2001; Ross *et al.*, 2001); ***Dan*** (Hsu *et al.*, 1998; Dionne *et al.*, 2001; Gerlach-Bank *et al.*, 2004); ***Cerberus*** (Piccolo *et al.*, 1999); Protein related to DAN and Cerberus, ***PRDC*** (Sudo *et al.*, 2004); Dan domain family member 5, ***DAND5*** (Marques *et al.*, 2004); ***Caronate*** (Yokouchi *et al.*, 1999); ***BAMBI***(Onichtchouk *et al.*, 1999; Grotewold *et al.*, 2001); ***Dragon*** (Samad *et al.*, 2005); RGMa (Babitt *et al.*, 2005); ***Ski***(Luo *et al.*, 1999); Ski like, ***SKIL/SnoN*** (Stroschein *et al.*, 1999; Vignais, 2000);***Tob*** (Yoshida *et al.*, 2000); SH3 domain of STAM, ***AMSH*** (Itoh *et al.*, 2001); Smad ubiquitination regulatory factor, ***Smurf*** (Arora and Warrior, 2001; Murakami *et al.*, 2003); Neural precursor cell expressed, developmentally down-regulated 4-2, ***NEDD4-2*** (Kuratomi *et al.*, 2005); ubiquitin C-terminal hydrolase, ***UCH37***(Wicks *et al.*, 2005).

1.5 BMP and receptor signalling in prostate cancer

1.5.1 The Expression of BMPs in Prostate Cancer

Bone is the most common metastatic site for prostate cancer. The interaction between prostatic tumour cells and bone contributes significantly to this organ tropism and the predominant osteoblastic characteristics of prostate metastases. As a group of the most powerful bone inductive factors, the expression of the BMPs in prostate cancer has stimulated much interest since the early 1990s (Table 1.7).

1.5.1.1 Expression of BMPs in prostate cancer

The mRNA level of BMP 1-6 has been examined in prostatic tissue with benign hyperplasia, localised prostatic carcinoma and metastatic prostatic carcinoma. BMP-6 expression was detected in the prostate tissues of over 50% of patients with clinically defined metastatic prostate adenocarcinoma, but was not detected in localised adenocarcinoma or benign prostate samples (Bentley *et al.*, 1992). The initial finding suggests BMP-6 may have an important role to play in progression and the development of bone metastasis in prostate cancer. Therefore, both mRNA and the protein level of BMP-6 were assessed in subsequent studies. An elevated level of BMP-6 is associated with higher grades of primary tumour and with advanced prostate cancer which developed metastasis. It also may contribute to the progression of prostate cancer in the absence of androgens (Barnes *et al.*, 1995; Hamdy *et al.*, 1997; Tamada *et al.*, 2001).

Table 1.7 Level of expression of BMP signalling in prostate cancer.

	Features	BMP-2	BMP-3	BMP-4	BMP-5	BMP-6	BMP-7	PLAB (GDF15, MIC)	BMPRIA	BMPRIB	BMPRII	Smad4	Smad8
Normal		+	+	++		±	++	++	++	++	++	++	++
Malignant		±	+	+	+	+	+	±	±	+	-	±	-
	Lower grade	±				+	+	±	+	+	+	+	+
	Higher grade	-				++	±	-	±	±	±	±	±
Malignant	Primary tumour (localized)					+							
	Primary tumour (metastatic)					++							
	Primary tumour					+	+	±					
	Bone metastasis					++	++	++					

Based on the literature published: BMP2(Harris *et al.*, 1994; Kim *et al.*, 2000; Horvath *et al.*, 2004); BMP4(Harris *et al.*, 1994); BMP5; BMP6(Bentley *et al.*, 1992; Harris *et al.*, 1994; Barnes *et al.*, 1995; Hamdy *et al.*, 1997; Tamada *et al.*, 2001); BMP7(Masuda *et al.*, 2004); PLAB(Thomas *et al.*, 2001; Kakehi *et al.*, 2004); BMPR1A(Kim *et al.*, 2000); BMPR1B(Kim *et al.*, 2000); BMPR2(Kim *et al.*, 2000; Kim *et al.*, 2004); Smad4(Horvath *et al.*, 2004); Smad8(Horvath *et al.*, 2004).

In contrast to BMP6 which has an elevated level in more aggressive prostate cancers, BMP2/4, BMP7 and GDF15 are expressed predominantly in normal prostate tissue, and their expression tends to be lower or absent during progression of prostate cancer (Harris *et al.*, 1994; Thomas *et al.*, 2001; Horvath *et al.*, 2004; Masuda *et al.*, 2004). Expression of GDF15 is higher in the androgen–sensitive LNCaP cells than in androgen-insensitive PC-3 and DU-145 cells. The level of GDF15 in prostate cancer cells was seen to rise after cells were exposed to androgens (Kakehi *et al.*, 2004). And similarly, androgen-dependent expression of BMP-7 has been demonstrated in a mouse model (Thomas *et al.*, 1998). This latter feature was subsequently identified in humans: the expression of BMP-7 in prostate epithelial cells increases in response to dihydrotestosterone (DHT) (Masuda *et al.*, 2004). Taken together, the loss or reduction in expression of BMP7 and GDF15 may be due to a shift in the tumour cell phenotype from androgen dependent to androgen independent in prostate cancer cells.

More interestingly, GDF15 and BMP-7 (expression of which has been reduced or lost in primary tumours), can be re-expressed in metastatic bone lesions (Thomas *et al.*, 2001; Masuda *et al.*, 2003). This suggests that selected BMPs may play differential roles in primary tumours and secondary tumours.

1.5.1.2 BMPs signaling molecules in prostate cancer

The expression of BMPRIA, BMPRIB, and BMPRII in human prostate cancer tissues has also been investigated and found to correlate with tumour grade. Using immunohistochemistry and Western blot analyses, it has been shown that there is frequent loss of expression of these three receptors in high-grade prostate cancer. But it appears that only the loss of expression of BMPRII correlates with poor prognosis in prostate cancer patients (Kim *et al.*, 2000; Kim *et al.*, 2004).

Intracellular signaling molecules downstream of BMP receptors have also been shown to alter in prostate cancer. The level of Smad 4 and Smad 8 in the nuclei is thought to be associated with the development of prostate cancer, and loss of Smad 4 is related to progression to a more aggressive phenotype (Horvath *et al.*, 2004).

Taken together, these findings support the hypothesis that the BMPs and their signalling pathways play a significant role in the osteoinductive activity of prostate cancer during metastases. The pattern of expression of BMPs may be important in the pathogenesis of osteoblastic-type metastases in prostate cancer.

1.5.2 The biological function of BMPs in prostate cancer

The notion that the BMPs may play a profound role in the progression of primary prostate tumours and the development of secondary tumours, especially bone metastasis, has been supported by lines of biologically based investigations. However, the precise mechanism underlying this remains unclear. The application of recombinant human BMPs (rh-BMPs) and artificial manipulation of the expression of BMPs or the signaling molecules makes it possible to investigate the biological functions of BMPs in prostate cancer *in vitro*.

1.5.2.1 Effects of BMPs on growth and proliferation of prostate cancer cells

As shown in Figure 1.8, BMPs can be classified into sub-groups according to the homology of their protein sequence. An anti-proliferation function has been found in two of these BMP subgroups.

BMP-2 and 4 inhibit the growth of the androgen-sensitive prostate cancer cell line LNCaP, but not the androgen-insensitive PC-3. The inhibitory effect of BMP-2/4 on cell proliferation is related to the activation of Smad 1, up-regulation of the

cyclin-dependent kinase inhibitor (CDKI) p21 (CIP1/WAF1), and phosphorylation of the retinoblastoma (Rb) (Brubaker *et al.*, 2004). Further investigation shows that BMP-2 decreases the phosphorylation of retinoblastoma (Rb) protein induced by treatment with DHT. DHT promotes proliferation of LNCaP cells through induction of cyclin A and cyclin-dependent kinase 2 (CDK2) and the transcription factor E2F-1, which can be inhibited by co-treatment with BMP-2. This suggests that BMP-2 inhibits DHT-induced growth of LNCaP cells through a decrease in E2F protein expression and suppression of E2F activity by hypophosphorylation of Rb (Tomari *et al.*, 2005).

On the other hand, another subgroup of BMPs, BMP-6 and 7, are more likely to inhibit the proliferation of both androgen-sensitive and androgen-insensitive prostate cancer cells. BMP-6 inhibits the proliferation of both LNCaP and DU-145 cells, by up-regulation of several cyclin-dependent kinase inhibitors such as p21/CIP, p18 and p19. The inhibitory effect on cell growth by this subgroup can be either prevented by the application of the recombinant Noggin(Haudenschild *et al.*, 2004), or by up-regulation of Noggin by BMP-6 itself, as discussed earlier. Under certain culture conditions (1% Foetal bovine serum in culture medium), BMP-7 inhibits the proliferation of the LNCaP, PC-3 and DU-145 cells in a concentration-dependent manner (5-500ng/ml), possibly through the up-regulation of the cyclin-dependent kinase inhibitor (CDKI) $p21^{CIP1/WAF1}$. Interestingly, BMP7 can also induce a concentration-dependent biphasic effect on the proliferation of LNCaP in the absence of exogenous androgen. It promotes proliferation at lower concentrations (20ng/ml), but inhibits proliferation at higher concentrations (80ng/ml). Exogenous androgen can prevent this biphasic effect (Miyazaki *et al.*, 2004). If the FBS concentration in the culture medium is reduced to 0.5%, the anti-proliferative effect of rh-BMP7 at a

concentration of 50ng/ml was only seen in the cell line representing benign prostatic epithelial hyperplasia (BPH-1), but not in the invasive PC-3 and DU-145 cells (Yang *et al.*, 2005). Under *in vitro* conditions in which 10% FBS was supplied in the culture medium, BMP 6 did not alter the rate of cell growth of C4-2B or LuCaP 23.1 (Dai *et al.*, 2005). C4-2B is a variant of LNCaP with a propensity for bone metastasis(Hsieh *et al.*, 1993; Wu *et al.*, 1994; Chen *et al.*, 1998).

The nature of the diverse, sometimes contrasting effects of different BMPs is interesting, but the underlying mechanism(s) remain unclear. While BMPs themselves may hold some of the answers, BMP receptors are probably also determining factors in distinguishing between the pro- or anti-proliferation effects seen in prostate cancer cells. Further understanding of the expression pattern of BMPRIA, BMPRIB, and BMPRII and their relationship to the development and progression of prostate cancer may provide more information on this phenomenon. For example, Kim *et al* demonstrated that transfection of a domain negative BMP-RII (BMP-RIIDN) into PC-3 cells (PC3M), resulted in a growth rate 10 times higher than that of the control cells in a murine tumour model (Kim *et al.*, 2004). But once the PC-3 cells express a constitutively active BMPRIB (c.a.-BMPRIB) in a tetracycline (Tet)-regulated manner, the Tet/doxycycline-regulated expression of the c.a.-BMPRIB results in the inhibition of both *in vitro* cell proliferation and the tumour growth *in vivo* (Miyazaki *et al.*, 2004).

A biphasic effect on the proliferation of LNCaP can be induced by rh-BMP2 under appropriate hormonal conditions. A decrease in cell proliferation in response to rhBMP2 was elicited in the presence of an androgen, which was thought to be the result of up-regulation of BMPR-IB expression. Conversely, an increase in cell growth was seen in the absence of androgen (Ide *et al.*, 1997b). Similar biphasic

effects were also revealed in LNCaP on exposure to rh-BMP7 (Miyazaki *et al.*, 2004). This may partially help to explain some other results whereby identical inhibition by BMP-2 and -4 on cell growth was not seen on another androgen-sensitive prostate cancer cell line: LuCaP 23.1, because of the absence of exogenous androgen (Dai *et al.*, 2005).

1.5.2.2 BMPs and Apoptosis

Apoptosis or programmed cell death is the key event for physiological growth control and regulation of tissue homeostasis. Aberration in the rate of apoptosis plays a crucial role during oncogenesis and subsequent tumour development. BMPs have been shown to regulate the apoptosis of malignant cells. The apoptotic response to BMPs is dependent upon cell type and, within the same cell type, is dependent on phenotype, hormone and growth factors status, and *in vitro* culture condition. For example, BMP2 induces apoptosis in medulloblastoma cells and colonic epithelial cells (Hallahan *et al.*, 2003; Hardwick *et al.*, 2004), but prevents apoptosis in breast cancer cells (MCF-7) (Clement *et al.*, 2000). On the other hand, in the myeloma cell lines, BMP4 can inhibit DNA synthesis and induce apoptosis in two IL-6 dependent myeloma cells (OH-2 and IH-1), but not the IL-6 independent ANBL-6 cells (Hjertner *et al.*, 2001).

BMPs regulate the expression of the molecules involved in the procedure of apoptosis, forming a basis for the previous observations. BMPs can directly affect apoptosis by regulating the transcription of the caspases. For example, BMP2 partially prevents an increase in caspase-3 mRNA level in MCF-7 cells as the result of withdrawal of serum in cell culture (serum free culture condition) (Clement *et al.*, 2000). Expression of the apoptosis mediators DRP-1 death kinase and ZIP kinase

may be regulated by BMPs through the Type I receptor, as demonstrated by expressing constitutively active (ca)BMP type I receptors in the cells (Korchynskyi *et al.*, 2003). Also, senescent cells as the result of BMP4 treatment had lower ERK activation, VEGF expression, and Bcl2 expression than wild-type cells. This is consistent with a less proliferative, less angiogenic phenotype that has an increased susceptibility to death by apoptosis(Buckley *et al.*, 2004).

BMPs alter apoptosis through several signalling pathways. BMP2 activates p38 mitogen-activated protein kinase (MAPK) pathway in medulloblastoma cells leading to apoptosis, which can be prevented by Noggin (Hallahan *et al.*, 2003). BMP2 can also rescue MCF-7 cells from hypoxic cell death via activation of the MAPK ERK1/2 and the basic helix-loop-helix transcription factors Id-1 pathways (Raida *et al.*, 2005). Anti-Mullerian hormone (AMH) is a member of the TGF-β family, which can trigger different pathways leading to inhibition of cell growth and apoptosis in various cell lines: it activates the NFκB pathway in both breast and prostate cancer cell lines(Segev *et al.*, 2002; Hoshiya *et al.*, 2003), but enhances p16 and modulates the E2Fs in ovarian cancer cell lines (Ha *et al.*, 2000). GDF-15 is indispensable for the pro-apoptotic activity of several apoptosis-inducing agents including the retinoid-related molecules (CD437 and ST1926) (Xu *et al.*, 2006).

Signaling mediated by BMPR-IB is believed to contribute to apoptosis during the development of the embryonic limb(Zou and Niswander, 1996). BMP4 induces apoptosis of myeloma cells through ALK3 and ALK6; BMP5 acts partially by ALK3, whereas BMP6 and 7 rely on ALK2(Ro *et al.*, 2004).

Recent studies have begun to uncover the role of BMPs in apoptosis in prostate cancer cells. BMP7 can stabilise the level of survivin in prostate cancer cells (LNCaP and C4-2B), and restore the activity of c-jun NH2-terminal kinase (JNK), both of

which contribute to the anti-apoptotic activity of BMP7 (Yang *et al.*, 2005; Yang *et al.*, 2006).

1.5.2.3 Influence of BMPs on cellular Motility and Invasion

Invasion and metastasis are the major causes of cancer related mortality. The motility and invasiveness of cancer cells are some of the important determining factors regarding the metastatic spread of a tumour. Recent evidence demonstrates that BMPs also regulate cellular motility and the invasiveness of some malignant cells, including lung cancer cells (A549 and H7249), malignant melanoma cells, and breast cancer cells (MCF-7) (Langenfeld *et al.*, 2003; Clement *et al.*, 2005; Rothhammer *et al.*, 2005). Similar to the diverse effects on cell growth, the effect on cell motility also appears to be dependent on the particular BMP and the type of tumour cell. For example, recombinant human BMP-2 can inhibit the invasion and metastasis of rat brain glioma cells under certain conditions (Zhang *et al.*, 2002).

In the case of prostate cancer cells, studies have revealed that the motility and invasiveness of prostate cancer cells can be increased by BMPs. BMP-2 and BMP-7 promote the migration and invasion of osteoblastic prostate cancer cells (LAPC-4 and LAPC-9) in a dose-dependent manner, but BMP-4 does not have this effect (Feeley *et al.*, 2005). BMP-2 and BMP-6 can increase the in vitro invasive ability of the prostate cancer cell lines C4-2B and LuCaP (Dai *et al.*, 2005). BMP-2 and, to a lesser extent, BMP-4 will stimulate PC-3 cell migration and invasion in a dose-dependent fashion, an effect which Noggin can subsequently inhibit (Feeley *et al.*, 2006).

Further details of the underlying pathways and precise mechanisms of BMP induced cell migration and invasion are sparse. However, in addition to the receptors

implicated in the previous discussion, BMP2 has been shown to activate the P38 MAPK and JNK signaling pathway to induce the expression of tenascin-W in tumour stroma, an effect that was thought to contribute to the stimulation of migration of tumour cells. Tenascin-W belongs to a family of extracellular matrix glycoproteins with distinctive expression patterns. Higher expression in the stroma around tumours is associated with a high potential for development of metastases (Scherberich *et al.*, 2005).

1.5.2.4 Epithelial homeostasis and epithelial-mesenchymal transdifferentiation

The BMP pathway is important in epithelial homeostasis. Inactivating mutations of the *Smad4* and *BMPR-IA* genes account for up to 50% the junvenile polyposis syndrome (JPS). This is an autosomal hamartoma syndrome with high risk of developing gastrointestinal polyps and colorectal cancer(Radtke and Clevers, 2005). The concurrent inactivation of BMPs (BMP-3b and BMP-6) with activation of the Ras signalling pathway is important in lung carcinogenesis(Kraunz *et al.*, 2005). This suggests that an aberration of BMP signalling in the epithelia can result in a disturbance of epithelial homeostasis, which may lead to carcinogenesis.

Epithelial-mesenchymal transdifferentiation/transformation (EMT) is an important event during the development of certain pathological processes including cancer. In normal development, BMP-2 acts synergistically with TGF-β3 in the initiation of EMT during the generation of the endocardial cushion(Nakajima *et al.*, 2000). The application of the BMP antagonist, Noggin, disrupts the EMT induced by BMPs during the development of the chicken heart(Romano and Runyan, 2000). The EMT induced by BMP-7 contributes to the repair of tubular injury in a fibrotic kidney(Zeisberg *et al.*, 2003; Zeisberg *et al.*, 2005).

An aberration of BMP signalling will not only impair epithelial homeostasis which may lead to carcinogenesis, it may also induce EMT in prostate cancer cells leading to a more aggressive phenotype. In the bone metastasis-derived PC-3 prostate cancer cell line, BMP7 has been shown to induce epithelial-mesenchymal transdifferentiation with classical changes in morphology, and the promotion of both motility and invasiveness in prostate cancer cells (Yang *et al.*, 2005).

Our understanding of the mechanisms underlying BMP-induced EMT is poor. The induction of inhibitor of differentiation factors (ID-1, ID-2 and ID-3), and activation of the proto-oncogene phosphoinositide 3-kinase (PI3K)/mammalian target of rapamycin (mTOR) signaling pathway by some BMPs (BMP-2 and BMP-7) has been implicated in BMP-induced EMT, but further exploration is required (Ogata *et al.*, 1993; Kowanetz *et al.*, 2004; Langenfeld *et al.*, 2005).

Taken together, these findings suggest that BMPs are able to modulate the biological behaviour of prostate tumour cells in diverse ways and in a cell specific manner, and point to certain mechanisms by which these secreted signalling molecules may contribute to prostate cancer growth and metastasis.

1.5.3 Regulation of the expression of BMPs

1.5.3.1 BMP and Androgen

In prostate cancer, androgens play an important part in the carcinogenesis, progression and metastasis of the disease, and controlling the level of circulating androgens constitutes the only effective therapy in advanced disease. Androgen-deprivation therapy (ADT) by orchidectomy or an leutenising hormone releasing hormone (LHRH) agonist is the mainstay of treatment for metastatic and locally advanced prostate cancer (Labrie, 2004). Prostate cells are highly hormone-sensitive

until late in the disease. Depriving androgen-sensitive cells of testosterone results in tumour cell undergoing apoptosis, a consequent reduction in tumour size and a delay in symptomatic progression. In most patients, the development of androgen resistance to hormonal therapy is the harbinger of disease specific mortality (Klotz, 2000).

Androgens can induce the expression of some BMPs, BMP receptors and intracellular signaling molecules. With regard to the receptors, androgens induce the expression of BMPR-IB mRNA, but not the expression of BMPR-IA and BMPR-II mRNAs in the androgen-sensitive human prostate cancer cell line LNCaP. As discussed above, rh-BMP-2 induces a biphasic effect on the proliferation of LNCaP. In the presence of an androgen, there is a decrease in cell proliferation in response to rhBMP2. This is thought to be the result of up-regulation of BMPR-IB expression. Conversely, an increase in cell growth is seen in the absence of androgen. Thus, the induction of BMPR-IB expression by an androgen appears to result in a signal which inhibits cell proliferation in response to stimulation by BMPs (Ide *et al.*, 1997b).

Turning to the BMPs themselves, the level of BMP-7 mRNA can be affected by manipulating the level of androgens in a murine model; orchidectomy results in a decrease in the expression of BMP-7 and administration of testosterone or dihydrotestosterone caused an increase in the expression level (Thomas *et al.*, 1998). However, androgen deprivation appears to have no effect on BMP-6 production in the normal rat prostate, suggesting an alternative and androgen-independent gene regulation for this particular protein (Barnes *et al.*, 1995).

1.5.3.2 BMP and DNA methylation

During cancer progression, besides the known inactivation of tumor suppressor genes by hypermethylation, activation of BMP-6 by selective demethylation occurs

and may also contribute to the shift to a more aggressive phenotype in prostate cancer (Tamada *et al.*, 2001). Aberrant methylation of BMP-2 has also been recorded, and the resultant loss of BMP-2 expression has been implicated in the carcinogenesis of gastric tumours (Wen *et al.*, 2006).

Kitazawa *et al* also noted abnormal methylation in an unusual case of desmoid-type fibromatosis which had features of metaplastic bone development. They observed that hypermethylation of the BMP and activin membrane-bound inhibitor (BAMBI) promoter caused a decreased expression of the BAMBI gene, which resulted in an enhanced responsiveness to BMP signaling and thus the abnormal bone formation (Kitazawa *et al.*, 2005).

1.5.3.3 Other regulatory factors

There are several other growth factors involved in the regulation of the BMPs. Nacamuli *et al* demonstrated that BMP3 expression can be controlled by recombinant human fibroblast growth factor in calvarial osteoblasts (Nacamuli *et al.*, 2005). EGF can also influence BMP expression. The expression of BMP6 has been shown to be reduced in breast cancer tissues, a reduction accompanied by a concurrent reduction in EGF receptor expression. The relation between BMP6 expression and EGF was further confirmed by the inductive expression of BMP6 in breast cancer cells (MCF-7) in vitro by EGF through EGF receptor activation (Clement *et al.*, 1999). Retinoid induces expression of BMP2 in retinoid-sensitive cell lines (Hallahan *et al.*, 2003), Rapamycin induced BMP4 expression but reduced follistatin expression in PC3 cells (van der Poel *et al.*, 2003).

1.5.4 BMP and Bone Metastasis

Bone is the most common site of metastasis for certain tumour types. Prostate cancer, breast cancer and lung cancer all preferentially spread to bone (Mundy, 2002). Bone metastases can generally be categorised as osteoclastic (osteolytic) leading to bone destruction, or osteoblastic (osteosclerotic) leading to bone formation. The osteoblastic lesion is the predominant form of bone metastasis formed by prostate cancer, and is always associated with a significant increase in tumour-induced osteolysis (Demers *et al.*, 1995; Garnero *et al.*, 2000; Demers *et al.*, 2003). There are a number of factors in the bone microenvironment known to contribute to the development of bone metastasis (Figure 1.8). Well documented factors include ET-1, BMPs, prostaglandins, tumor necrosis factor alpha (TNFα), IL-1, IL-6, PTHrP, PDGF and RANKL (Yin *et al.*, 2005; Yoneda and Hiraga, 2005). Some interesting patterns have been reported recently, by comparing the expression profile of certain genes in two prostate cancer cell lines that develop different bone metastasis: PC-3 which induces osteoclastic lesions in vivo, and LAPC-9 which produces osteoblastic lesions. PC-3 cells expressed RANKL, IL-1, and TNF-alpha, which are associated with osteoclastogenesis. In contrast, LAPC-9 cells showed expression of osteoprotegrin, which blocks osteoclast production, results in minimal amounts of TNF-alpha and undetectable levels of RANKL or IL-1. Both these cells also secreted BMP-2, -4, -6, and IL-6, which are associated with bone formation (Lee *et al.*, 2003).

The role of BMPs in bone malignancies has been investigated in several primary and secondary malignant deposits in bone. BMP-2 is expressed in more than half of osteosarcomas, but not in chondrosarcomas or Ewing's sarcomas (Yoshikawa *et al.*, 1994). The expression of the BMP type II receptor was found to correlate with the presence of metastases in osteosarcomas, which implicates the BMP pathway in

tumor progression. BMP-2, -4, and -6 also are expressed in osteosarcoma and other sarcoma tissues, indicating a potential for autocrine or paracrine growth stimulation in these tumors (Guo *et al.*, 1999).

1.5.4.1 Adaptable Expression of BMPs in bone metastases from prostate cancer

As discussed earlier, a specific expression pattern of BMPs (BMP-2, 4, 7 and GDF15) is associated with disease progression in primary prostate cancer. The role of BMP-2, 4, 6 and 7 in bone metastases from clinical prostate cancer has also been investigated. It was found that BMP-7 and GDF15 are re-expressed in bone metastasis (Masuda *et al.*, 2003), suggesting that these molecules contribute to the development of metastatic bone lesions (Figure 1.8). This extends their pivotal roles in primary tumor development to include secondary tumour formation in bone.

On the other hand, the expression of BMP-6 is consistently elevated in both primary and secondary tumours of prostate cancer (Autzen *et al.*, 1998; De Pinieux *et al.*, 2001). The elevated expression of BMP-6 within the primary tumor may be due to selective demethylation of its gene promoter during disease progression, which results in tumour cells with a more aggressive phenotype (Tamada *et al.*, 2001).

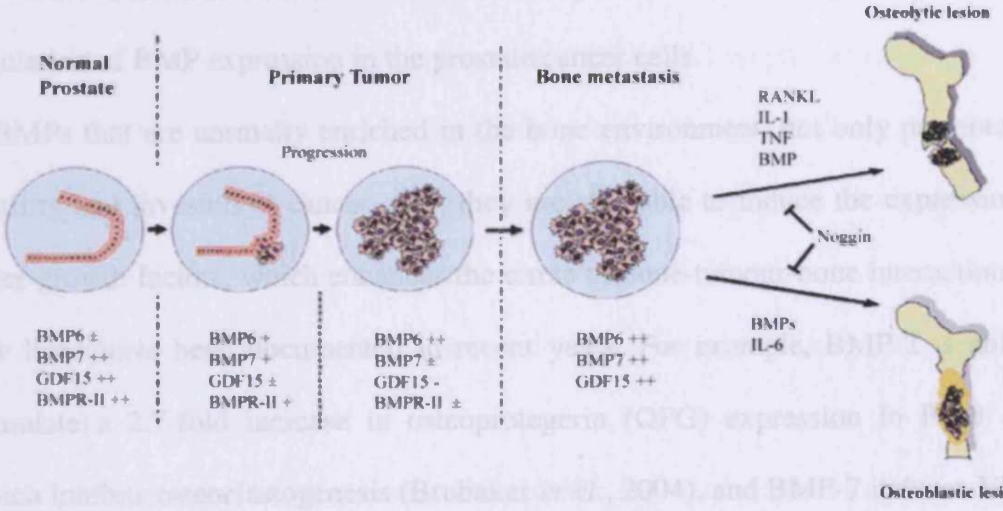

Figure 1.8 BMPs in the bone metastasis of prostate cancer.

1.5.4.2 Role of BMPs in the crosstalk between cancer cells and the bone micro-environment

From the moment a metastatic cell settles in bone, there is constant interaction between the tumour cell and its residing microenvironment. Host factors from the bone environment and factors generated by the cancer cell exhibit a reciprocal influence over each other, the BMPs secreted by the cancer cells would certainly influence remodeling of the bone, including osteoblastic and osteoclastic activity. However, it remains unclear as to how exactly the local factors participate in the regulation of BMP expression in the prostate cancer cells.

BMPs that are normally enriched in the bone environment, not only promote the motility and invasion of cancer cells, they are also able to induce the expression of other growth factors, which enhances the circle of bone-tumour-bone interactions. A few links have been documented in recent years. For example, BMP-2 is able to stimulate a 2.7-fold increase in osteoprotegerin (OPG) expression in PC-3 cells which inhibits osteoclastogenesis (Brubaker *et al.*, 2004), and BMP-7 induces VEGF protein and mRNA expression in C4-2B cells, which contributes to the pro-osteoblastic activity of C4-2B cells.

1.5.4.3 BMPs and Angiogenesis

Angiogenesis is an important event during the development and progression of both primary and secondary tumours. It has been demonstrated that BMPs, including BMP-2, 4, 6, 7 and GDF5, are capable of inducing angiogenesis. This may be one of the ways in which they contribute to the process of bone formation (Yamashita *et al.*, 1997; Mori *et al.*, 1998; Yeh and Lee, 1999; Glienke *et al.*, 2000). The experimental evidence suggests that BMPs promote angiogenesis indirectly through up-regulation

of the expression of VEGF in both cancer cells and osteoblasts: since Noggin, the BMP antagonist, produces the same effect as anti-VEGF antibody: it diminishes the pro-osteoblastic activity of osteoblast cells which is induced by conditioned medium from C4-2B cells (Yeh and Lee, 1999; Deckers *et al.*, 2002; Dai *et al.*, 2004). Also, the early stage of bone induction by rhBMP-2 can be blocked by the anti-angiogenic agent (TNP-470) (Mori *et al.*, 1998). This evidence indicates that the control of angiogenesis is, to some extent, integrated with the influence which BMPs have over osteoblastic activity.

Dai *et al* have demonstrated that it is possible for BMP-7 to promote osteosclerosis through VEGF in the skeletal metastases from prostate cancer (Dai *et al.*, 2004). This angiogenesis induced by BMPs can also be synergized by basic fibroblast growth factor (bFGF) and TGF-β1 (Ramoshebi and Ripamonti, 2000), which suggests that the angiogenesis induced by BMPs is a vital event during the initial stage of bone metastasis development.

In summary, the phenotypic pattern of BMPs and their signalling pathways in prostate cancer are different in the primary tumor compared to that in secondary deposits in bone. Most BMPs and receptors are detectable at a relatively higher level in normal prostate tissue. Their expression decreases in a manner which correlates with progression of the primary tumor, except BMP6, which shows an increase. The expression of BMP7, GDF15 and BMPR-IB can be induced by exposure to androgens in the androgen-sensitive prostate cancer cell lines and the prostate epithelial cell lines (Ide *et al.*, 1997b; Thomas *et al.*, 1998; Tamada *et al.*, 2001; Kakehi *et al.*, 2004). Aberrant expression of BMP and BMP associated molecules have also been shown to have prognostic value (Kim *et al.*, 2004). The modification of the BMP phenotype has a clear and close involvement in the development and

progression of primary prostate tumors, and it also contributes to the onset and development of bone metastases. For example, BMP6 remains highly expressed in both primary and metastatic bone lesions, whereas BMP7 and GDF15, which are expressed at low levels in normal prostate and in primary prostate tumours, are re-expressed at a higher level in skeletal metastatic lesions (Thomas *et al.*, 2001; Masuda *et al.*, 2003). BMPs not only contribute to the development of an osteoblastic-type lesion in bone metastases from prostate cancer, they are also partially responsible for the osteolytic appearance of occasional lesions. In an *in vivo* bone tumor model, exposure to Noggin, an antagonist of BMPs, can reduce the size of bone lesions by decreasing both osteoblastic and osteolytic processes. These findings collectively indicate a promising therapeutic value for BMPs and their antagonists in the management of bone metastases.

1.6 Aims of this study

BMPs clearly play a profound role in the development, progression, and metastasis of prostate cancer. If the mechanisms underlying the adaptation of the BMP phenotype in both primary tumor and bone metastasis can be elucidated, it will provide a greater understanding of the pathogenesis of prostate cancer and may provide clues for novel therapies for managing advanced disease.

The aims of this study are:

1. To determine the expression of the most recently identified BMPs and molecules involved in their signalling in prostate cancer cell lines and tissues. Some BMPs have been implicated in the bone metastasis of prostate cancer; however, the roles of the most recently discovered BMPs in cancer, particularly in prostate cancer are still unknown. The present study will investigate the role of two such BMPs, BMP-9 and BMP-10 in prostate cancer.

2. Among the seven Type 1 and three Type 2 receptors, BMPR-IB and BMPR-II have been implicated in the development and progression of prostate cancer. Therefore, further investigation of signalling involved in prostate cancer was developed using ribozyme transgenes to knockdown the expression of these two specific receptors. Knockdown of these two receptors will enable us to investigate whether they are involved in the function of BMP-9 and BMP-10 in prostate cancer.

3. Most studies to date have exposed the cancer cells to exogenous BMPs (BMP-2, 4, 6 and 7). However little is known about the role of endogenous BMPs which are produced by cancer cells themselves. To investigate the impact of BMPs (BMP-7, BMP-9 and BMP-10) on biological behavior of prostate cancer cells, their expression was manipulated within the cells. Knockdown of BMP-7 will elucidate the funciton of endogenous BMP-7 in prostate cancer. On the other hand, over-expression of

BMP-9 and BMP-10 respectively, and subsequently examination of their influences on cellular biology in prostate cancer will be studied. There is no commercial source of recombinant human BMP-9 and BMP-10, and generation of recombinant human BMPs (rh-BMP-9 and rh-BMP-10) will be required. Therefore, the signal transduction of these BMPs will be elucidated through utilisation of the cells in which the receptors have been knocked down.

Chapter 2

Materials and Methods

2.1 General Materials

2.1.1 Cell lines

Seven prostate cancer or prostatic epithelial cell lines were used in the study. PC-3 cells were acquired from the ECACC (European Collection of Animal Cell Culture, Salisbury, UK). DU-145, LNCaP-FGC, CA-HPV10 and PZ-HPV-7 were supplied by the ATCC (American Type Culture Collection). PNT-1A and PNT-2C2 were generous gifts provided by Professor Norman Maitland (University of York, England, UK). The cells were routinely maintained in DMEM-F12 medium supplemented with 10% foetal calf serum and antibiotics. Full details of these seven cell lines are provided in Table 2.1.

2.1.2 Primers

Three different categories of primers were designed using Beacon Designer (PREMIER Biosoft International, Palo Alto, CA, USA) for this study. The software incorporates features including automated search for reaction conditions, and possible homology of the amplicon with other genes etc. The first set were able to detect mRNA level of a particular gene through conventional RT-PCR or Real-time Quantitative PCR (Table 2.1); the paired forward and reverse primers for each gene reside in one of the two adjacent exons and the amplified sequence includes at least one intron boundaries of its genomic sequence (Table 2.2); cDNA of human normal prostate tissue was used as template; the third category of primers were designed according to the secondary structure of a gene transcript, and were used to synthesise a hammerhead ribozyme for the gene silence study (Table 2.3).

2.1.3 Antibodies

2.1.3.1 Primary antibodies

Full details about the primary antibodies used in this study are in Table 2.5.

Table 2.1 Seven prostatic cell lines used in current studies.

Cell Line	Organism	Morphology	Ethnicity	Gender	Age	Source and Feature
PC-3	*Homo sapiens* (human)	epithelial	Caucasian	Male	62	**Disease:** adenocarcinoma **Tumor stage:** grade IV **Derived from metastatic site:** bone **Isolation date:** 1979 **Antigen Expression:** HLA A1, A9
DU-145	*Homo sapiens* (human)	epithelial	Caucasian	Male	69	**Disease:** carcinoma **Derived from metastatic site:** brain **Isolation date:** 1978 **Antigen Expression:** Blood Type O; Rh+
LNCaP	*Homo sapiens* (human)	epithelial	Caucasian	Male	50	**Disease:** carcinoma **Derived from metastatic site:** left supraclavicular lymph node **Isolation date:** 1977 **Androgen receptor:** positive; **Estrogen receptor:** positive; **Cellular Products:** human prostatic acid phosphatase; prostate specific antigen
CA-HPV-10	*Homo sapiens* (human)	epithelial	Caucasian	Male	63	**Cell type:** human papillomavirus 18 (HPV-18) transfected **Disease:** adenocarcinoma **Isolation date:**1994 **Antigen Expression:** kallikrein **3,** KLK3 (prostate specific antigen, PSA); Homo sapiens, not expressed
PZ-HPV-7	*Homo sapiens* (human)	epithelial	Caucasian	Male	70	**Tissue:** epithelium **Cell type:** human papillomavirus 18 (HPV-18) transformed
PNT1A	*Homo sapiens* (human)	epithelial		Male	35	**Tissue:** epithelium **Cell type:** Established by immortalisation of normal adult prostatic epithelial cells by transfection with a plasmid containing SV40 genome with a defective replication origin.
PNT2-C2 (PNT2)	*Homo sapiens* (human)	epithelial		Male	33	**Tissue:** epithelium **Cell type:** Human prostate normal, immortalized with SV40 **Applications:** Biology of prostate cells, model of differentiated prostate epithelial cells.

Table 2.2A Primers for conventional RT-PCR and real time quantitative PCR

Gene	Name of Primer	Sequence of Primers	Optimal Annealing Temperature	Size of Products (bps)
BMP-2	BMP2F1	5'-AGACCACCGGTTGGAGAG	55°C	120 (NM_001200, 1070-1171)
	BMP2ZR	5'-ACTGAACCTGACCGTACAGTTGTTTTCCCACTCGTTT		
BMP-3	BMP3F1	5'-GATGCCTATTATTGCTCTGG	55°C	117 (NM_001201, 1503-1601)
	BMP3ZR	5'-ACTGAACCTGACCGTACACCCCACAGCTCTCACTATAC		
BMP-4	BMP4F1	5'-CAACACCGTGAGGAGCTT	55°C	111 (NM_001202, 818-910)
	BMP4ZR	5'-ACTGAACCTGACCGTACATGAGGTTAAAGAGGAAACGA		
BMP-5	BMP5F1	5'-CACTTAACGCCCATATGAAT	55°C	134 (NM_021073, 1878-1993)
	BMP5ZR	5'-ACTGAACCTGACCGTACAGATGGCATTTAATTTGGTTG		
BMP-6	BMP6F1	5'-AGTCTTACAGGAGCATCAGC	55°C	141 (NM_001718, 1013-1135)
	BMP6ZR	5'-ACTGAACCTGACCGTACAACAACCCACAGATTGCTAGT		
BMP-7	BMP7F1	5'-AGAAGCACGAGCTCTATGTC	55°C	100(NM_001719)
	BMP7ZR	5'-ACTGAACCTGACCGTACACTTCACAGTAATACGCAGCA		
BMP-8A	BMP8AF8	5'-GCCTCTATGTGGAGACTGAG	56°C	352
	BMP8AR8	5'-CACTCCCCCTCACAGTAATA		
BMP-8B	BMP8BF8	5'-CAACAGGGAGTCTGACTTGT	56°C	483
	BMP8BR8	5'-CACTCCCCCTCACAGTAATA		
BMP-9	BMP9ZF	5'-ACTGAACCTGACCGTACACAGTCACGAGGAGGACAC	55°C	142 (NM_016204, 1057-1180)
	BMP9R1	5'-GATGTCCTCGAAGTTTACCC		
BMP-10	BMP10F1	5'-CTGCCAACATCATTAGGAGT	55°C	108 (NM_014482, 461-550)
	BMP10ZR	5'-ACTGAACCTGACCGTACAATGGACACATTGAAGAGGAG		
BMP-11	BMP11F1	5'-CACAGACCTGGCTGTCAC	55°C	98 (NM_005811, 836-915)
	BMP11ZR	5'-ACTGAACCTGACCGTACATGTTCTCTAGGACTCGAAGC		
BMP-12	BMP12F1	5'-GATCACCGGCTTCACAGA	55°C	109 (NM_182828, 936-1026)
	BMP12ZR	5'-ACTGAACCTGACCGTACAGTCGTTAAGGCTGGACAC		
Noggin	NOGGINF1	5'-cagcgcctaagcaagaag	55°C	100
	NOGGINZR1	5'-actgaacctgaccgtacagtcgttccacgcgtacag		
Follistatin	FOLLISTF1	5'-acctgagaaaggctacctg	55°C	100
	FOLLISTZR1	5'-actgaacctgaccgtacacaaccttgaaatcccataaa		

Table 2.2B Primers for conventional RT-PCR and real time quantitative PCR

Gene	Name of Primer	Sequence of Primers	Optimal Annealing Temperature	Size of Products (bps)
Smad1	SMAD1F1	5'-tcactgatccttccaacaat	55°C	86(HSU59423)
	SMAD1ZR1	5'-actgaacctgaccgtacacctggtgttttcaatagtgg		
Smad2	SMAD2F1	5'- gaagccgtctatcagctaac	55°C	102 (AF027964)
	SMAD2ZR1	5'- actgaacctgaccgtacagcaaggagtacttgttaccg		
Smad3	SMAD3F1	5'-AGTCTCCCAACTGTAACCAG	55°C	98 (HSU68019)
	SMAD3ZR1	5'-ACTGAACCTGACCGTACAGAACTCCTGGTTGTTGAAGA		
Smad4	SMAD4F1	5'- TTTTGTTTGGGTCAACTCTC	55°C	110 (BC002379)
	SMAD4ZR1	5'-5'-ACTGAACCTGACCGTACACAAACATCACCTTCACCTTT		
Smad5	SMAD5F1	5'-AGCTCACCAAAATGTGTACC	55°C	109 (AF009678)
	SMAD5ZR1	5'-ACTGAACCTGACCGTACATGAAGATGAATCTCAATCCA		
Smad6	SMAD6F1	5'-AACCCCTACCACTTCAGC	55°C	96(AF035528)
	SMAD6ZR1	5'-ACTGAACCTGACCGTACACAGATCCAGTGGCTTGTACT		
Smad7	SMAD7F1	5'-AACAGGGGGAACGAATTAT	55°C	119 (AF015261)
	SMAD7ZR1	5'-ACTGAACCTGACCGTACACCACTCTCGTCTTCTCCTC		
Smad8	SMAD8F1	5'-CGTGTATGAACTGACCAAGA	55°C	113 (NM_005905)
	SMAD8ZR1	5'-ACTGAACCTGACCGTACAGATGAATCTCAATCCAGCAG		
BMPR-IB	BMPR1BF1	5'-ATGGAACTTGCTGTATTGCT	55°C	107 (NM_001203, 1301-1389)
	BMPR1BZR	5'-ACTGAACCTGACCGTACACAACTCGAGTGTTAGGTGGT		
BMPR-II	BMPR2F1	5'-TTTGGGAAAGAAACAAATCT	55°C	130 (NM_001204, 2047-2158)
	BMPR2ZR	5'-ACTGAACCTGACCGTACATGGATAAGGACCAATTTTTG		
β-actin	BACTF	5'-ATGATATCGCCGCGCTCG	55°C	580 (NM_001101, 81-660)
	BACTR	5'-CGCTCGGTGAGGATCTTCA		
	BACTINZF	5'-GGACCTGACTGACTACCTCA	55°C	117 (NM_001101, 622-720)
	BACTINZR	5'-ACTGAACCTGACCGTACAAGCTTCTCCTTAATGTCACG		

Table 2.3 Primers designed for amplifying coding sequence of BMPs

Gene	Name of Primer	Sequence of Primers	Optimum Annealing Temperature	Size of Products (bps)
	T7F	5′-TAATACGACTCACTATAGGG		
	BGHR	5′-TAGAAGGCACAGTCGAGG		
BMP-9	BMP9EXF1	5′-ATGTGTCCTGGGGCACTGT	64-66	1290
	BMP9EXR1	5′-CTACCTGCACCCACACTCTG
	rhBMP9EXR1	***5′-CCTGCACCCACACTCTG***
	Bmp9exf2	5′-ATGTGTCCTGGGGCACTGT
	Bmp9exf3	5′-ATGTGTCCTGGGGCACTGT
BMP-10	BMP10EXF1	5′-ATGGGCTCTCTGGTCCTG	58	1275
	BMP10EXR1	5′-CTATCTACAGCCACATTCGGAGA
	rhBMP10EXR1	***5′-TCTACAGCCACATTCGGAGA***
	Bmp10exr2	5′-CTATCTACAGCCACATTCGGA
	Bmp10exr3	5′-CTATCTACAGCCACATTCGG
	Bmp10exr4	5′-CTATCTACAGCCACATT

Table 2.4 Primers for synthesis of ribozymes

Ribozyme	Name of Primer	Sequence of Primers
	T7F	5′-TAATACGACTCACTATAGGG
	RBBMR	5′-TTCGTCCTCACGGACTCATCAG
	RBTPF	5′-CTGATGAGTCCGTGAGGACGAA
BMPR-IB ribozyme-1	BMPR1BRIB1F	5′-CTGCAGTCTGTGCAGCATTCAATTCTGATGAGTCCGTGAGGA
	BMPR1BRIB1R	5′-ACTAGTCCCATTCCTCATCAAAGAAGATTTCGTCCTCACGGACT
BMPR-IB ribozyme-2	BMPR1BRIB2F	5′-CTGCAGCTTCCTCTGTGGTGACTGATGAGTCCGTGAGGA
	BMPR1BRIB2R	5′-ACTAGTAGCTGTGAAAGTGTTTTCGTCCTCACGGACT
BMPR-IB ribozyme-3	BMPR1BRIB3F	5′-CTGCAGATATCTGCAGCAATCTGATGAGTCCGTGAGGA
	BMPR1BRIB3R	5′-ACTAGTGAAAACATTTTGGGTTTTCGTCCTCACGGACT
BMPR-II ribozyme-1	BMPR2RIB1F	5′-CTGCAGTATGTTCCATTCTCTGATGAGTCCGTGAGGA
	BMPR2RIB1R	5′-ACTAGTACCACTCCTCCCTCAATTTTCGTCCTCACGGACT
BMPR-II ribozyme-2	BMPR2RIB2F	5′-CTGCAGAAATCTGTGCTACAACAGCACTGATGAGTCCGTGAGGA
	BMPR2RIB2R	5′-ACTAGTCAGAATGGAACATACCGTTTTTCGTCCTCACGGACT
BMPR-II ribozyme-3	BMPR2RIB3F	5′-CTGCAGTAAATATCTCCCAATACTGATGAGTCCGTGAGGA
	BMPR2RIB3R	5′-ACTAGTAGACATGTGTGCTCTTGGACTAATTTCGTCCTCACGGACT
BMP-7 ribozyme-1	BMP7RIB1F	5′-CTGCAGTGTTGCTGGTGGCTGTCTGATGAGTCCGTGAGGA
	BMP7RIB1R	5′-ACTAGTGGCTGGTGTTTGACATTTCGTCCTCACGGACT
BMP-7 ribozyme-2	BMP7RIB2F	5′-TGGACCTCCGTGGCCTTCTGATGAGTCCGTGAGGACTGCAG
	BMP7RIB2R	5′-ACTAGTCCTTCATGGTGGCTTTCTTTTCGTCCTCACGGACT

Table 2.5 Primary antibodies utilised in current studies.

Name	Source	Molecular Weight (kDa)	Commercial Origin	Product Code
Anti-BMP7	Goat polyclonal antibody	55	SANTA CRUZ BIOTECHNOLOGY, INC.	Sc-9305
Anti-BMP9	Goat polyclonal antibody	**13kDa(monomeric)**	SANTA CRUZ BIOTECHNOLOGY, INC.	SC-27820
Anti-BMP10	Rabbit polyclonal antibody	12, **48**, 60 and 120	Orbigen	PAB-10450
Anti-BMPR-IB	Goat polyclonal antibody	45	SANTA CRUZ BIOTECHNOLOGY, INC.	SC-5679
Anti-BMPR-II	Goat polyclonal antibody	70-80	SANTA CRUZ BIOTECHNOLOGY, INC.	SC-5683
Anti-Actin	Mouse monoclonal antibody	42	SANTA CRUZ BIOTECHNOLOGY, INC.	SC-8432
Anti-Noggin	Goat polyclonal antibody		SANTA CRUZ BIOTECHNOLOGY, INC.	SC-16627
Anti-Follistatin	Goat polyclonal antibody		SANTA CRUZ BIOTECHNOLOGY, INC.	SC-23553
Anti-Smad-1	Mouse monoclonal antibody	52/56	SANTA CRUZ BIOTECHNOLOGY, INC.	SC-7965
Anti-Smad-5	Goat polyclonal antibody	43	SANTA CRUZ BIOTECHNOLOGY, INC.	SC-26418
Anti-Smad-8	Rabbit polyclonal antibody	52	SANTA CRUZ BIOTECHNOLOGY, INC.	SC-11393
Anti-p-Smad-1	Goat polyclonal antibody	52/56	SANTA CRUZ BIOTECHNOLOGY, INC.	SC-12353
Anti-Phosphoserine /threonine	Rabbit polyclonal antibody		Abcam plc	ab17464
Anti-His-probe	Mouse monoclonal antibody		SANTA CRUZ BIOTECHNOLOGY, INC.	SC-8036
Anti-PAR-4	Mouse monoclonal antibody	47	SANTA CRUZ BIOTECHNOLOGY, INC.	SC-1666
Anti-Paxillin	Mouse monoclonal antibody	68	BD Transduction Laboratories	610051
Anti-FAK	Mouse monoclonal antibody	125	BD Transduction Laboratories	610088

2.1.3.2 Secondary antibodies

Peroxidase (horseradish peroxidase, HRP) conjugated rabbit anti-goat IgG, goat anti-rabbit IgG and rabbit anti-mouse IgG antibodies were obtained from Sigma (Poole, Dorset, UK). TRITC conjugated secondary antibody to rabbit IgG (produced in goat) was obtained from Sigma (Poole, Dorset, UK). FITC conjugated secondary antibodies to mouse (produced in sheep) and goat (produced in rabbit) IgG were obtained from Santa-Cruz Biotechnology (Santa-Cruz, California, USA).

2.1.4 General reagents and solutions

2.1.4.1 Reagents and chemicals

Protein-A/G agarose beads used during immunoprecipitation were obtained from Santa-Cruz Biotechnology (Santa-Cruz, California, USA). The OptiMax Wash Buffer (BioGenex, San Ramon, USA) was used in the immunochemical staining and immunofluorescent staining (IF). The VECTASTAIN® ABC system (Vector Laboratories, Inc., Nottingham, England, UK) was used for the immunochemical staining. SDS-6H (Sigma-Aldrich, Inc., Poole, Dorset, England, UK), a protein molecular weight marker mixture was used to determine the protein size. The Supersignal™ West Dura system (Pierce Biotechnology, Inc., Rockford, IL, USA), a highly sensitive chemiluminescence substrate was used to detect the horseradish peroxidase (HRP) in western blot. The suppliers of the general reagents used in current study are listed in Table 2.6. All other chemicals or reagents were purchased from Sigma, unless otherwise stated.

Table 2.6 Reagents and suppliers

Reagent	Supplier
acetic acid	Fisher Scientific, Leicestershire, UK
agarose	Melford Laboratories Ltd., Suffolk, UK
amino black	EDWARD GURR Ltd., London, UK
Boric acid	Duchefa Biochemie, Haarlem, Netherlands
bromophenol blue	Sigma-Aldrich, Inc., Poole, Dorset, England, UK
chloroform	Sigma-Aldrich, Inc., Poole, Dorset, England, UK
Coomassie Brilliant Blue	Sigma-Aldrich, Inc., Poole, Dorset, England, UK
DEPC	Sigma-Aldrich, Inc., Poole, Dorset, England, UK
dimethylsulphoxide (DMSO)	Sigma-Aldrich, Inc., Poole, Dorset, England, UK
EDTA	Duchefa Biochemie, Haarlem, Netherlands
ethanol	Fisher Scientific, Leicestershire, UK
ethidium bromide	Sigma-Aldrich, Inc., Poole, Dorset, England, UK
glycine	Melford Laboratories Ltd., Suffolk, UK
isopropanol	Sigma-Aldrich, Inc., Poole, Dorset, England, UK
KCl	Fisons Scientific Equipment, Loughborough, UK
KH2PO4	BDH Chemicals Ltd., Poole, England, UK
methanol	Fisher Scientific, Leicestershire, UK
Na2HPO4	BDH Chemicals Ltd., Poole, England, UK
NaCl	Sigma-Aldrich, Inc., Poole, Dorset, England, UK
NaOH	Sigma-Aldrich, Inc., Poole, Dorset, England, UK
SDS	Melford Laboratories Ltd., Suffolk, UK
sucrose	Fisons Scientific Equipment, Loughborough, UK
Tris-Cl	Melford Laboratories Ltd., Suffolk, UK
Tween 20	Melford Laboratories Ltd., Suffolk, UK

2.1.4.2 General solutions

The following solutions are generally used throughout the study.

Tris-Boric acid-EDTA (TBE)

For a 5×TBE buffer (1.1M Tris; 900mM Borate; 25mM EDTA; pH 8.3), dissolve 540g Tris-Cl (Melford Laboratories Ltd., Suffolk, UK), 275g Boric acid (Duchefa Biochemie, Haarlem, Netherlands) and 46.5g EDTA (Duchefa Biochemie, Haarlem, Netherlands) in 9.5 litres of distilled water. Adjust pH to about 8.3 using NaOH, and then make up to a final volume of 10 litres with distilled water.

Tris Buffered Saline (TBS)

A 10× TBS stock (0.5M Tris, 1.38 M NaCl, pH 7.4) solution was made up by dissolving 24.228 Tris and 80.06g NaCl in 1 litre distilled H_2O and adjusting the pH to 7.4 with concentrated HC1. This solution contained 200mM Tris and 1.37M NaC1.

Balanced Salt Solution (BSS)

A 5 litre stock solution of lx BSS consists of 137mM NaCl, 2.6mM KCl (Fisons Scientific Equipment, Loughborough, UK), 1.7mM Na_2HPO_4 and 8.0mM KH_2PO_4 and was made by dissolving 40g NaCl, lg KCl, 5.72g Na_2HPO_4 and 1 g KH_2PO_4 in dH_2O and adjusting the pH to 7.4 with 1M NaOH.

0.05M EDTA in BSS

A 5 litre stock solution at lxBSS contained 137mM NaCl, 2.6mM KCl, 1.7mM Na_2HPO_4 and 8.0mM KH_2PO_4 and 0.05M EDTA, which were dissolved in 5 litres distilled H_2O and adjusted the pH to 7.4 before autoclaving.

Loading buffer (for DNA electrophoresis)

A stock solution was made by dissolving 25mg bromophenol blue and 4g sucrose in distilled water to a final volume of 10ml. Store at 4°C to avoid mould growing in the sucrose until use.

Ethidium bromide solution

A stock solution of ethidium bromide (10mg/ml) was made by dissolving 200mg ethidium bromide in 20ml distilled water, and protected from light by covering the tube in aluminium foil.

Transfer buffer (for Western blot)

Dissolve 15.15g Tris, 72g glycine in distilled water, add 1 litre methanol (Fisher Scientific, Leicestershire, UK), and make to final volume of 5 litres with distilled water.

0.5% amino black staining solution

2.5g amino black (Edward Gurr Ltd., London, UK), 50ml acetic acid (Fisher Scientific, Leicestershire, UK), 125ml ethanol (Fisher Scientific, Leicestershire, UK) were added into 325ml distilled water to make a final volume of 500ml.

Amino black distaining solution

100ml acetic acid and 250ml ethanol were added into 650ml of distilled water for a 1 litre amino black destaining solution.

Running buffer (for SDS-PAGE)10×

A 10× stock solution (0.25M Tris, 1.92M glycine, 1% SDS, pH8.3) was made by dissolving 303g Tris, 1.44kg glycine and 100g SDS in 10 litres distilled water.

2.2 Cell culture and storage

2.2.1 Preparation of growth medium and maintenance of Cells

- The culture medium used in the study was Dulbecco's Modified Eagle's Medium (DMEM / Ham's F-12 with L-Glutamine; E15-813, PAA Laboratories, Austria) (pH 7.3) containing; 2mM L-glutamine, and 4.5mM $NaHCO_3$;
- DMEM was then supplemented with 10% heat inactivated foetal calf serum (PAA Laboratories, Austria); 50 ml FCS in 500 ml DMEM/HAM F12.

- Antibiotics were added to the medium at a final concentration of 100 units/ml (=60μg/ml) for benzylpenicillin (Britannia, Pharmaceuticals, Ltd) and 100 μg/ml for streptomycin (Streptomycin Sulfate salt, Sigma-Aldrich Co.). Benzylpenicillin (Britannia, Pharmaceutical, Ltd.) powder 600mg (=$1x10^6$units) in each bottle was dissolved in 5ml sterilized water, and kept at 4 °C in a fridge until ready for use. The concentration of streptomycin stock solution was 250mg/ml. 200μl of streptomycin was dispensed into each 500 ml of culture medium, to give a final concentration of 100μg/ml.

- The cell lines were cultured in either $25cm^2$ or $80cm^2$ culture flasks (Cell Star, Germany).

- Culture flasks were loosely capped and placed in an incubator at 37 °C with a 98% humidification (water tray in the incubator) and 5% CO_2.

- The flasks were then left until sub-confluent (2-3 days) for experimental work or fully confluent (7 days) for subculture.

2.2.2 Trypsinisation and counting of cells

- All handling of cells performed under sterile conditions using class II hoods and autoclaved instruments to keep conditions.

- Following removal of culture medium, the flasks were rinsed once with 5ml of sterile BSS buffer to remove all possible traces of serum, which would inhibit the enzymatic action of trypsin.

- 1-2ml of trypsin EDTA, which has trypsin 0.01% (w/v) and EDTA 0.05% (w/v) in BSS buffer, was added to the flasks, which were incubated for 5 minutes at 37°C to allow cell detachment.

- Once the cells had detached from the surface of the flask, 5ml of DMEM was added and the cells were then placed in a universal container.
- The cells were centrifuged at 1,500 rpm for 5 minutes.
- The excess medium was aspirated and the pellet re-suspended in 5ml of DMEM.
- The cells were then re-cultured in flasks, counted for immediate experimental work or stored by freezing in liquid nitrogen (see below).
- Cell counts were performed using an improved Neubauer haemocytometer counting chamber with an inverted microscope (Reichert, Austria) at 10×10 magnification.

2.2.3 Storage of cell lines in liquid nitrogen

- The cell lines were stored in liquid nitrogen by resuspending at a cell density of $1x10^6$ cells/ml in DMEM containing 10% (v/v) dimethylsulphoxide (DMSO; Fisons, UK).
- 1 ml aliquots of cell suspension were transferred into cryopreserve tubes;
- Transferred to -80 ^{o}C for 24 hours before storage in liquid nitrogen (- 196 ^{o}C) until required.

2.2.4 Resuscitation of cells

- After removal from liquid nitrogen, the cells were allowed to thaw rapidly to 37 ^{o}C in 1-2 minutes;
- The cell suspension was transferred to a universal container, with 2ml of pre-warmed DMEM. The cells were then incubated at 37 ^{o}C for 10 minutes.

- The cells were then centrifuged at 1500 rpm for 5 minutes and the excess medium removed.
- The cell pellet was re-suspended in DMEM and washed twice to remove any possible trace of DMSO.
- After the final wash, the cell pellet was re-suspended in 5ml of DMEM and the cell suspension transferred to a $25cm^2$ tissue culture flask. The cells were incubated at 37°C, 98% humidification and 5% CO_2 in air.

2.3 Methods for Detecting mRNA

2.3.1 Total RNA isolation

Ribonucleic acid (RNA) is present within the nucleus, cytoplasm and mitochondria of all living eukaryotic cells. The total cytoplasmic RNA is composed of three main sub types which are classified as; ribosomal (rRNA), transfer (tRNA) and messenger (mRNA) RNA. Although mRNA accounts for only 1-2% of total cellular RNA, it is of particular importance as it carries the genetic information for protein formation. The presence of specific mRNA sequences indicates which protein is being produced by a cell at any given time.

RNA is susceptible to the degradation by RNases and therefore, special care must be taken to minimise this during its isolation. All methods involving RNA isolation rely on the use of strong denaturants to inhibit the action of endogenous RNases for preserving intact RNA during the isolation. Guanidine, thiocyanate and chloride used for the RNA isolation are amongst the most effective protein denaturants and inhibitors of ribonucleases. The guanidine thiocyanate method described by Chomczynski and Sacchi in 1987 (Chomczynski and Sacchi, 1987), has evolved as a

rapid procedure which combines acid guanidium thiocyanate, phenol and chloroform in a single step RNA extraction. Using this method, the extraction of RNA is set under acidic conditions, so that the DNA is selectively partitioned into the organic phase whilst the RNA remains in the aqueous phase. The quality and concentration of the RNA isolated can then be detected using a spectrophotometer at a wavelength of A_{260nm}/A_{280nm}.

2.3.1.1 Homogenisation

After the aspiration of culture medium, cells in mono-layer were lysed directly in the culture flask by adding the RNA reagent (1ml / 3.5cm petri dish, or 1ml/ 5-10 x 10^6 cells). The resultant cell lysate should be transferred immediately to eppendorf or polypropylene tubes. Washing the cells before addition of the RNA reagent was avoided as this might increase the possibility of mRNA degradation.

2.3.1.2 RNA extraction

Following homogenisation,

- Store the homogenate for 5 minutes at 4°C to permit the complete dissociation of nucleoprotein complexes.
- Add 0.2ml of chloroform per 1ml of RNA reagent, cover the samples tightly, shake vigorously for 15 seconds and place on ice at 4°C for 5 minutes.
- Centrifuge the homogenate at 12,000g (4°C) for 15 minutes.

The homogenate will form two phases: the lower phase is the organic phase and the upper phase is the aqueous phase. DNA and protein are in the organic phase and in

the interface while RNA is in the aqueous phase. The volume of the aqueous phase should be about 40–50% of the total volume of the homogenate plus chloroform.

2.3.1.3 RNA precipitation

- Carefully transfer the aqueous phase to a fresh tube while taking care not to disturb the interface.
- Add an equal volume of isopropanol and store samples for 10 minutes at 4°C.
- Centrifuge at 12,000g (4°C) for 10 minutes.
- RNA precipitation forms a white pellet at the bottom of the tube after the centrifugation.
- In some cases RNA might precipitate along the sides of the tube. Care should be taken not to contaminate the side while washing the precipitate.

2.3.1.4 RNA wash

- Remove the supernatant and wash RNA pellet twice with 75% ethanol (prepared using DEPC treated distilled water) by vortexing and subsequent centrifugation for 5 minutes at 7,500g (4°C).
- At the end of the procedure, briefly dry the pellet at 50°C for 5–10 minutes in a hybridiser drying oven..
- It is important not to let the RNA pellet dry completely, as it will greatly decrease its solubility. However, as much ethanol as possible should be removed, without completely drying the pellet.

- Dissolve the RNA pellet in 50–100µl of DEPC treated water by vortexing for 1 minute.

2.3.1.5 Qualification and quantification of RNA

The concentration and purity of RNA was determined by measuring its absorbance at wavelength A260nm/A280nm (WPA UV 1101, Biotech Photometer). The ratio of A260nm/A280nm can give an estimate of the purity of the RNA. Pure RNA solutions have an optical density ratio of 2.0. Optical density values less than 1.5 indicates ethanol or protein contamination. The RNA samples were either stored at -80°C until used later or ready for reverse transcription (RT).

2.3.2 Reverse transcription (RT)

RT-PCR is a simple, versatile and sensitive technique, which has greatly enhanced the study of genes and how they are controlled. It provides an alternative and more sensitive approach for the analysis of mRNA, compared with other procedures such as; Southern blots for DNA analysis and Northern blots for RNA analysis. This technique has the advantage over more traditional methods in that it requires a smaller amount of RNA, and is yet more sensitive and rapid. In this study, cDNA was synthesized by using the DuraScript™ RT-PCR KIT (Sigma-Aldrich, Inc.). According to the manufacturer's instructions, a 20-µl-reaction mixture was added in a polypropylene tube (Eppendorf):

0.25µg of total RNA template (volume depends on concentration)

PCR H_2O (volume=8µl – volume of the RNA template)

1µl of deoxynucleotide mix (500 µM of each dNTP)

1µl of anchored oligo $(dT)_{23}$

The samples were heated at 70°C for 10 minutes to denature RNA secondary structure which allowed for more efficient reverse transcription, and were then placed on ice. The following components were added to the samples:

6 µl PCR H_2O

2µl 10×buffer for DuraScript RT

1µl RNase inhibitor

1 µl DuraScript reverse transcriptase

The resultant total volume in each eppendorf tube is 20 µl. The samples were incubated at 50°C for 50 minutes. A negative control which using PCR H_2O instead of RNA tamplet was set up for each individual experiment. The cDNA samples were then diluted to 1:4 by adding 60 µl of PCR H_2O. The samples are ready for amplification using PCR or they were stored at -20°C until required.

2.3.3 Polymerase chain reaction (PCR)

The polymerase chain reaction is a very powerful technique for enzymatically amplifying a nucleic acid target sequence. It is devised by Karey Mullis in 1983, for which he was awarded the Nobel prize in 1994. A particular gene was amplified by using a REDTaq™ ReadyMix PCR reaction mix (Sigma-Aldrich, Inc.). A 12-µl-reaction mixture was prepared in a thin wall PCR tube:

1µl of cDNA template

1µl of forward primer (at a working concentration of 1 µM)

1µl of reverse primer (at a working concentration of 1 µM)

6µl of 2×REDTaq™ ReadyMix

3µl of PCR H_2O

Cycling conditions for the 12-µl-reaction mixture were 94 °C for 5min, followed by 30-36cycles of 94°C for 30s, 55 °C for 30s, and 72 °C for 40s. This was followed by a final extension of 10 min at 72 °C. Cycling conditions might be different according to differences of primers and size of PCR products. PCR products were visualized on a 0.8% or 2% agarose gel through staining with ethidium bromide after electrophoresis. A negative control, which had all the components except template, ie. cDNA, was always run alongside the test samples.

2.3.4 Agarose gel DNA electrophoresis

Agarose gel electrophoresis is the easiest and commonest way of separating and analyzing DNA. The purpose of the gel might be to look at the DNA, to quantify it or to isolate a particular band. The DNA is visualised in the gel by addition of ethidium bromide. This binds strongly to DNA by intercalating between the bases and is fluorescent meaning that it absorbs invisible UV light and transmits the energy as visible orange light.

A 0.8% gel will show good separation (resolution) of large DNA fragments (1–10kb), while a 2% gel will show good resolution for small fragments (<1kb). In the present study, 20mls of agarose gel solution at the appropriate concentration was poured into an universal container (Sterilin, UK) and cooled to about 55°C before casting the gel in the mould. A well forming comb was then inserted into the gel mould and the gel was allowed to set at room temperature for about 30-40 minutes.

Once the gel had set, TBE buffer was carefully poured into the electrophoresis tank until it reached a level of about 5mm from the surface of the gel. The PCR products were loaded into the wells (6µl per well) by placing the gel loading tip through the buffer and locating it just above the bottom of the well. The sample was slowly and delicately delivered into the well. This procedure was continued until all the samples had been loaded into the gel. A 1Kb DNA ladder (Cat No. 15615-016, Invitrogen Inc., USA) was prepared according to the manufacturer's instructions, and delivered into the well (5µl per well) in the same manner as for the PCR products.

A power pack (Gibco BRL, Life Technologies Inc.), was connected to the electrophoresis apparatus and the gel was run at a constant voltage of 100 Volts. Electrophoresis was continued for 30-50 minutes or until the samples had migrated about two-thirds of the way down the agarose gel (depending on the size of the PCR products). The PCR products were stained using ethidium bromide (10mg/ml) for 5 minutes with continuous agitation to ensure even staining of the agarose gel. This was followed by destaining in distilled water for about 1 hour, to reduce the background staining on the agarose gel from the fluorescent dye. PCR products were then visualised on the agarose gel using an UV Transilluminator (UVP, Inc, Cambridge, England, UK). Gel images were printed using a Mitsubishi thermoprinter (Mitsubishi UK, London) and saved as a TIFF image file using a default image saving facility. Typically, a band is easily visible if it contains about 20ng of DNA.

2.3.5 Extraction of PCR products from agarose gel

PCR products of interest were extracted using GelEluteTM Gel Extraction Kit (Sigma-Aldrich, Inc., Poole, Dorset, England, UK). Following the DNA

electrophoresis, the PCR products of interest were excised from the agarose gel with a clean and sharp scalpel. The excess gel was trimed away to minimise the amount of agarose. After weighing the gel slice in an eppendorf, 300µl of the Gel Solubilisation was added to each 100mg of the gel slice. The gel mixture was incubated at 55°C for 10 minutes, or until the gel slice was completely dissolved. The gel mixture was vortexed briefly every 2-3 minutes during the incubation to help dissolving the gel. Meanwhile, the binding column can be prepared. For which, the GenElute Binding Column G was placed into a provided 2ml collection tube, and 500µl of the Column Preparation Solution was added to each binding column. The flow-through liquid was discarded following a 1-minute centrifugation. Once the gel slice was completely dissolved, the colour of the mixture should be yellow, otherwise added 3 M sodium acetate buffer (pH 5.2) until the mixture was yellow. 100µl of isopropanol to each 100mg of the original gel slice was added into the mixture, and the gel solution was then loaded in the prepared binding column. Following a brief centrifugation of 1 minute, the binding column was washed with 700µl Wash Solution, and the PCR products were finally eluted using 50 µl of Elution Solution. The purified PCR products were were store at -80°C, unless were used immediately.

2.4 Methods for Detecting Protein

Three different methods were employed in present study to assess the expression of a certain gene at protein level. Three methods were western blot, immunochemical staining and immunofluorescent staining.

2.4.1 SDS-polyacrylamide gel electrophoresis (SDS-PAGE) and western blot

2.4.1.1 Preparation of cell lysates

- Remove cells from the base of the culture flask using a disposable cell scraper or alternatively decant the medium and trypsinise the cells. Transfer cells, using a pastette, to a clean universal.
- Centrifuge at 2,000 rpm for 5 minutes.
- Decant supernatant and resuspend the cell pellets in 200-300 µl of lysis buffer (20 µl per 500,000 cells) and transfer the resultant lysates into 1.5ml eppendorf tubes.
- Incubate samples at 4°C for 40 minutes with continuous rotation in order to extract protein from the cell lysate.
- Centrifuge at 13,000 rpm for 15 minutes in order to remove cellular debris and collect the protein. Transfer the supernatant to a new tube and discard the pellet. The protein samples were quantified and utilised for SDS-PAGE, or were stored at -20°C until used.

2.4.1.2 Determination of protein concentration of cell lysates

This is based on a protocol supplied by BIO-RAD, from whom the protein assay kit was purchased.

- Preparation of working reagent. Add 20 µl of reagent S to each ml of reagent A that will be needed for the run. (This working reagent A' is stable for 1 week even though a precipitate will form after 1 day. If precipitate forms, warm the solution and vortex. Do not pipette the undissolved precipitate, as this will likely plug the tip of the pipette, thereby altering the volume of reagent that is added to the sample.) If samples do not contain detergent, step #1 can be skipped and simply use reagent A as supplied.
- Serial dilute bovine serum albumin stock with known concentration (Sigma; 100mg/ml) prepared in the same cell lysis buffer to give a working concentration range between 50-0.79mg/ml. A standard curve should be prepared each time the assay is performed. For best results, the standard was always prepared in the same buffer as the sample.
- Pipet 5 µl of standards and samples into a 96-well plate.
- Add 25 µl of reagent A' or reagent A (see note from step 1) into each well.
- Add 200 µl of reagent B into each well. The microplate reader has a mixing function available and has been programmed to shake the plate for 5 seconds.
- After 15 minutes, absorbance can be read at 590 nm. The absorbance will be stable for about 1 hour.
- Construct a standard protein curve for the bovine serum albumin and determine the unknown protein concentrations of the cell lysate samples.

- Adjust protein concentrations to a working range of 1-2mg/ml by diluting in cell lysis buffer.
- For immunoprecipitation experiments see below, otherwise prepare crude cell lysates for SDS-PAGE by diluting a portion of the protein sample to be analysed 1:1 (v/v) with a 2x sample buffer (containing 2x mercaptoethanol).
- Denature crude cell lysate samples by boiling at 100°C for 5 minutes, remembering to pierce the top of the tube with a needle. Cool at room temperature for 5 minutes. (If cooled on ice – the SDS will precipitate) and centrifuge to collect droplets.
- Flash spin to bring down condensation.
- The samples may be subsequently loaded on a gel, or stored at -20°C until required.

2.4.1.3 Preparation of immunoprecipitates

Immunoprecipitation is an invaluable technique used to analyse intracellular phosphorylation events occurring following extracellular stimulation. The process of immunoprecipitation involves cell lysis, followed by the addition of a specific antibody directed against the target protein present within the cell lysate sample. The resultant antigen-antibody complexes are then collected by the addition of staphylococcal protein A, protein G or their mixture, which is covalently attached to sepharose or agarose. These immune complexes are precipitated by centrifugation, separated by SDS-PAGE and analysed by immunoprobing. A brief description of the immunoprecipitation method used in this study is outlined in the following paragraph.

- Add antibody for the protein of interest to the cell lysate, the concentration or dilution of the antibody followed the corresponding instruction of the antibody used.
- Incubate samples at 4°C for 1 hour with constant agitation on a rotating wheel.
- 50ul of conjugated A/G protein agarose beads (Santa Cruz Biotechnology, supplied by Insight Biotechnologies Inc, Surrey, England, UK) are added into each sample, and then the samples are rotated on the rotating wheel for 1 hour to allow to the antibody-antigen complex to get attached to the beads.
- Centrifugation at 7000 - 8000 rpm for 5 minutes, to remove unbound protein or access antibodies from the supernatant fraction.
- Wash the protein pellets twice using 200-300µl of lysis buffer.
- Resuspend in 40-60µl of 2x sample buffer, and denatured by boiling at 100°C for 5 minutes.
- Store samples at -20°C until required for use.

2.4.1.4 Gel Preparation

- Clean and dry four glass plates (2 large rectangular and 2 small rectangular plates) and assemble two gel cassettes on a casting stand. Insert alignment card to verify glass plates and spacers are aligned properly. Tighten thumb screws to hold glass (and spacers) in place – Do not over tighten- the alignment card should drop out when the cassette is lifted from gel casting assembly.

- Tighten screws further if necessary. Fit the gel cassette tightly in the gel casting assembly.
- Fill the space between the glass plates with some alcohol to test seal for leaks. Remove cassette and wipe away alcohol.
- Prepare the polyacrylamide resolving gel. After adding the specified amount of TEMED and 10% APS, stir gently to mix.
- Using another plastic pipette, immediately apply the resolving gel by carefully running the solution down one side between the glass plates until it reaches a level about 1 cm below the top of the smaller plate.
- Using a new pipette, slowly cover the top of the resolving gel with 0.1% solution of SDS until a layer of about 2mm formed on top of the gel solution. This ensures the gel will set with a smooth surface.
- Allow the gels to polymerize at room temperature for about 30 minutes. When the gel has set a sharp refractive change at the overlay/gel interface will be visible on polymerization. Furthermore, the unused resolving gel in the universal will have set.
- Pour off the SDS solution and rinse with deionized or distilled water. Remove excess water with some tissue paper.
- Prepare the stacking gel remembering not to add the TEMED and APS until ready to use.
- Add stacking gel solution immediately to the gel cassette (on top of the resolving gel) in the same manner as the resolving gel, until its upper surface is flush with the smaller glass plate).

- Gently insert a well forming Teflon comb immediately (taking care not to trap bubbles between the glass plates) into the layer of stacking gel, until it reached within 1mm from the top of the spacers.
- Allow stacking gel to polymerize for 30minutes at room temperature. Refractive changes around the comb will indicated when the gel has set, and the unused portion of stacking gel will have set.
- Once the stacking gel has set, carefully remove the Teflon comb without tearing the edges of the polyacrylamide wells. Rinse wells with distilled water and clamp the gel cassettes in a gel electrophoresis rig with the small glass plate facing the silicone gasket.
- Insert the gel rig into the electrophoresis chamber and fill the central reservoir formed by the gel plates with running buffer so that the top of the wells is completely covered.
- Now fill the chamber with sufficient 1x running buffer to immerse the thumb screws.

2.4.1.5 Loading the samples

- Load equal volumes, approximately 10-15µl, (1-10µg total protein) of crude cell lysates or precipitated proteins (containing sample buffer) into the wells. This is accomplished using a 50µl syringe (Hamilton) with a flat-tipped needle, and carefully locating the tip of the needle just above the bottom of the wells and then slowly delivering the protein into the well.

- Load control wells with 10µl of pre-stained molecular weight standard. Document the sequence the protein samples were added. Attach the lid of the tank over the apparatus and connected the leads.

2.4.1.6 Running the gel

- Connect the red high voltage lead to the red outlet and the black high voltage lead to the black outlet. Switch on the power supply and run the gel at a constant current of 40mA at 125V (20mA per gel.). Stop electrophoresis when the dye front is about 1cm from the bottom of the gel. Usual running time is about 40-60 minutes.

2.4.1.7 Preparation of membrane

- While the gel is running, cut a piece of nitrocellulose membrane (Hybond C, Ammersham, Cardiff) to the dimensions of the gel (7.5×7.5cm) and immerse in 1× transfer buffer for about 10-20 minutes to ensure proper binding of the protein to the membrane. Similarly, cut four sheets of filter paper to the same dimensions (7.5×7.5cm) and soak in 1× transfer buffer for 10-20 minutes or until ready to use. Always wear gloves and use blunt forceps as the membrane can be easily contaminated and damaged during the handling.

- Upon completion of the electrophoresis, turn off the power supply and disconnect the leads. Remove the lid and discard the running buffer. Disassemble the apparatus. To separate the glass plate from the gel, use one of the spacer between the plates as a lever to pry open the glass plate, exposing the gel. Then carefully remove most of the stacking with the edge of

a spacer and cut a small triangle off one corner of the gel so that after transfer, the lanes will appear on the membrane in the desired order. This will ensure that the gel is oriented correctly in the transfer apparatus. Soak the gel still attached to the back plate in transfer buffer for about 5 mins.

2.4.1.8 Electroblotting: Transfer proteins from gel to membrane

- Place two pieces of pre-soaked filter paper bottom electrode graphite base (Anode +). Avoid trapping air bubbles by laying gels, membranes and filter paper on electroblot at an angle.
- Place the pre-soaked nitrocellulose membrane on top of filter papers previously placed on electrode. Note: The membrane is on the same side as the red, positive electrode.
- Holding the gel and the filter paper together, carefully remove them from the tray of blot buffer and transfer the paper and gel to a pad of the blot cell with the gel facing up. Carefully remove the gel from the glass plate by inverting onto 3MM paper, then pull the paper and the gel away from glass plate.
- Carefully transfer the gel on top of the nitrocellulose membrane taking care not to trap air bubbles between gel and membrane. Keep the stacking gel off of the paper until the last moment, since it tends to stick and make repositioning difficult.
- To complete the sandwich, lay two more sheets of wet filter paper on top of gel creating a sandwich of paper-nitrocellulose-gel-paper (Figure 2.1).

- Use a clean plastic test tube to roll out air bubbles. Roll a glass rod across the surface to remove any air bubbles and ensure good contact between the gel and nitrocellulose.
- The surface of this sandwich was carefully smoothed out, using a transfer pipette as a rolling pin to remove the formation of air bubbles which may interfere with protein transfer.
- Firmly position the cover, containing cathode plate of blotter, on top of transfer "sandwich" and connect the high voltage leads to the power supply. Apply a constant current of at 5 Volts, 500 mA and 8 Watts for 30-40 minutes.
- Note: Transfer time depends upon the molecular weight of proteins, with high molecular weight proteins requiring more time to transfer. Failure to closely monitor the electrophoresis buffer or temperature can result in a fire.
- After transfer is complete, turn off power supply and remove cathode plate of blotter. Remove transfer membrane and label the lower right corner of membrane to mark orientation of gel.
- Place the sandwich, nitrocellulose side down, onto a glass plate and remove the other filter paper.

To check if the proteins are all transferred to the nitrocellulose, lift one corner of the gel to see if any blue is left in the gel. In other words, the gel should be clear when the transfer is complete.

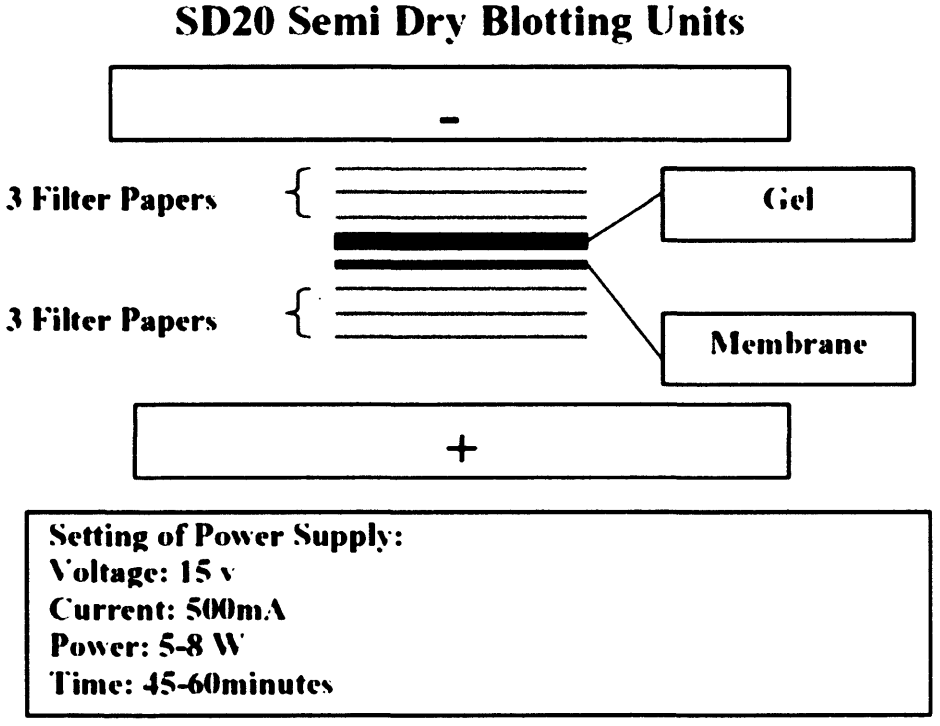

Figure 2.1 Diagram of assembling the semi dry blotting unit.

2.4.1.9 Ponceau S Staining Protocol:

- After transfer, immerse the membrane in Ponceau S Stain (Sigma-Aldrich, Poole, Dorset) for approximately 1 minute at room temperature. Rinse the membrane with distilled water until bands are visible.
- Use a pencil to mark the position of molecular weight markers. Cut the top left (or top right) corner of the membrane to enable orientation during detection. Retain Ponceau stain for re-use. Cut the blot into strips if required.
- Proceed to the immunostaining protocol.

Note: The staining of proteins on nitrocellulose membranes using Ponceau S has two functions: firstly, it verifies if proteins have been transferred to the membranes and secondly, it aids in the visualization of the molecular weight markers. In addition, the Ponceau S stain is a reversible protein stain and does not interfere with subsequent immunoprobing steps.

2.4.1.10 Coomassie blue used for staining the gel after electroblotting

- Place the electroblotted gel in a plastic tray and Coomassie blue stain in Coomassie blue solution for 1 hr to overnight.
- Pour off the used stain and destain the background staining by multiple washes in destain solution. The gel may be left for days in the destaining solution. Protein bands stain dark blue.

2.4.1.11 Specific Protein Detection – Immunoprobing Procedure

- After Ponceau S staining, transfer the membrane from the staining tray into a clean 50ml polypropylene tubes (Falcon) ensuring that the membrane surface which was in contact with the gel is facing upward.
- Incubate the blotted membrane in this blocking solution (solution A) with agitation for 40-60 minutes at room temperature or overnight at 4°C, in order to block non-specific protein binding of the antibody on membrane.
- Pour off solution A, and incubate membrane with 10ml of solution B for 15 mins.
- Incubate the membrane with 5ml of diluted primary antibody (1:200 diluted in the solution B) for one hour at room temperature.
- Pour off the diluted primary antibody solution and wash membranes for 30 minutes with agitation, changing the wash buffer every 10 minutes in 10ml of solution B.
- Pour off the solution B, and incubate the membranes with 5 ml of diluted HRP conjugated secondary antibody (typically 1:1,000 in solution B) with agitation for one hour at room temperature.
- Wash the membranes in 10ml of solution B twice, each for 15 mins.
- Wash the membranes twice using 10ml per wash of the solution C, and finally wash twice for 15 minutes each in TBS to remove residual detergent and transferred to weighing boats containing TBS solution using forceps until ready for chemiluminescent detection.

Solution A

10% milk powder (5g)

0.1% Tween 20 (50ul)

Dissolve above in 50ml TBS

Solution B

3% milk powder (3g)

0.1% Tween 20 (100ul)

Dissolve above in 100ml TBS

Solution C

0.2% Tween 20 (60ul) in 30ml TBS

2.4.1.12 Chemiluminescent detection of protein

- The Supersignal™ West Dura system (Pierce Biotechnology, Inc., Rockford, IL, USA), which has a highly sensitive chemiluminescence substrate, was used to detect the horseradish peroxidase (HRP) in western blot. Mix the two substrate components at a 1:1 ratio with final volume regarding of 0.125ml/cm^2 (for a mini gel – 4ml of each reagent – be sure to change pipettes in between reagents.)
- Decant wash buffer and remove excess TBS buffer from the membrane by draining the membrane over a piece of folded tissue paper and briefly touching the edge of the membrane.

- Immerse the membrane with protein side down in a clean tray containing the chemiluminescence working solution. Agitate the tray to allow the solution to cover the surface of the membrane for 5 mins.
- Use a pair of tweezers to move membrane from the tray (drain excess reagent mix along the edge of the tray and onto some tissue paper) and transfer the membrane to a clean piece of saran wrap face down in the prepared autoradiography film cassette (large enough to cover a open film cassette)
- Wrap the membrane up in the saran wrap and place it in a plastic tray with the right-side facing up. Smooth over the covered blot to remove air bubbles and excess substrate. Place membrane down on saran wrap, remove bubbles and wrap membrane completely. The chemiluminescence signal was captured and visualised by using a UVITech imager (UVITech, Inc., Cambridge, England, UK). The protein bands were then quantified by using UVIband software (UVITEC, Cambridge, UK).

2.4.1.13 Amido Black Staining Protocol

- After all the film has been developed, remove the membranes from the cassette and immerse in Amido Black stain for approximately 15-30 seconds.
- Destain the membrane in a solution containing 10% acetic acid /10% isopropanol until bands are clearly observed.
- Rinse thoroughly with water.

- The Amido black stain provided a permanent record of the membrane which can then be compared to corresponding images from the chemiluminescence assay, to aid in the orientation of the membrane.

2.4.2 Immunohistochemical staining

A routine method was modified and reported previously (Davies *et al.*, 1999; Martin *et al.*, 2003; Jiang *et al.*, 2005b). Prostate tissue samples were available following collection from the patients at the Department of Urology, University Hospital of Wales. All research samples were snap-frozen in liquid nitrogen immediately after radcial prostatectomy, transurethral prostatectomy or prostate biopsy. All protocols were reviewed and approved by the local ethical committee (03/5048, Cardiff and Vale Local Ethics Committee) and all patients gave written informed consent. Similarly, paraffin embedded samples from the same patient were also available.

2.4.2.1 Immnunohistochemical staining procedures for frozen sections

- Frozen specimens were sectioned at 5 microns (μm), and allowed to dry for 20-30 minutes at room temperature.
- Fix in acetone or 50/50 acetone-methanol mix for 15-20 minutes.
- The sections were then air dried for 10-20 minutes.
- Stain immediately or stored at -20 ^{o}C in foil wrapped slide trays.
- Place sections in PBS for 5 minutes. If the sections have been stored at -20 ^{o}C, allow them to reach room temperature first.

- Draw around sections with Dako pen (water proof marker) to form a reservoir for the staining solutions to be confined in.
- Block with diluted serum for 20 minutes, i.e. the same serum that the secondary antibody is made up in (in our case horse serum). 1 drop to 5 ml washing buffer.
- Wash in washing buffer 4 times.
- Incubate with optimally diluted primary antibody at optimal temp for optimum time, [usually carry out a study on times and temps to discover this factor before.], 1:100~150 primary antibody to blocking solution, for 1 hour at room temperature. Primary antibodies were stored at 1:5 dilutions (in 100µl in eppendorf vials).
- Wash in washing buffer 4 times.
- Incubate with secondary antibody for 30 minutes at room temperature.
- Wash in washing buffer 4 times.
- Incubate in ABC complex for 30 minutes at room temperature
- Wash in washing buffer 4 times.
- DAB chromogen for 5 minutes in dark (covered by a tray).
- Wash in water for 2 minutes.
- Counterstain with Mayer's Htx for 1 minute.
- Wash in water for 5 minutes.

ABC Complex (Vector Laboratories Inc., Burlingame, USA)

4 drops Reagent A to 20 ml of wash buffer;

Then add 4 drops Reagent B to the same mixing bottle, mix immediately;

Allow the VECTASTAIN ABC reagent to stand for about 30 minutes before use.

DAB Chromogen

Add the following reagents in order and shake each time, 2 drops buffer, 4 drops DAB and 2 drops hydrogen peroxide in 5 ml distilled water:

2.4.2.2 Immunohistochemical staining procedure for paraffin sections

- Fixation and Section. Human prostate tissue samples were processed on a Reichert-Jung automatic tissue processor, fixed for 48 hours using neutral buffered formalin, and embedded in pastillated paraffin wax. 7μm sections were placed on slides and incubated overnight at 60°C.
- To remove the wax of sections, treating of pure xylene (2 times) and pure methanol (3 times), several minutes for each, followed by treating with the hydrogen peroxide in pure methanol (5 ml hydrogen peroxide in 300 ml pure methanol) for 15 minutes to block the endogenous peroxidase activity.
- Antigen retrieval was carried out by placing slides on a plastic rack in 1 litre of EDTA solution (pH adjusted to 8.0) for 25minutes in a microwave, after which open door of microwave and leave for 5 minutes, slides were then washed in running water for 5 minutes. Slides were placed in Optimax working buffer solution for 2 minutes.
- Primary antibody was added (in a pre-determined dilution) and incubated at room temperature for 45 minutes. Slides were then washed in Optimax working buffer before and followed by the addition of secondary antibody (in horse serum/buffer solution). Avidin/Biotin complex was added for 30

minutes followed by washes in Optimax, Diaminobenzadine (DAB) was applied for 5 minutes, in a darkened box, to visualise the antibody/antigen complex before being counterstained in Mayer's Haemotoxylin and placed in running tap water. Finally slides were dehydrated in alcohol, cleared in xylene and mounted. A negative control was also included in which primary antibody was not applied during the immunochemical staining procedure.

Blocking Solution for endogenous peroxidase:

283.2ml methanol

4.8ml H_2O_2(30%v/w)

EDTA solution for antigen retrieval:

Mix 4ml EDTA with 1996ml double distilled water adjusting pH to 8 using 1N NaOH solution or 0.1N HCl. Allow this mixture to equilibrate for 30 minutes then check pH again before use.

2.4.3 Immunocytochemical staining

Cells were fixed with 4% neutralised formalin after the treatment, and then permeabilized with 0.1% Triton in TBS. Following a blocking with horse serum in OptiMax Wash Buffer (BioGenex, San Ramon, USA), probed a particular protein with its specific primary antibody, and then stained by using a VECTASTA I N® ABC system (Vector Laboratories, Inc.). The procedure was otherwise similar to that given in the immunohistochemical staining protocol. The staining was quantified by using Optimas 6.0. The procedure was performed as following:

- Gently remove cell culture medium by aspiration and wash cells twice with TBS buffer to remove culture medium proteins.
- Add 4% buffered formalin and incubate at room temperature for 10 minutes. The fixation time can be from 5 -15 minutes to optimize label signal.
- Aspirate fixative and wash cells twice with TBS buffer.
- Add Permeabilisation buffer mixture (0.1% Triton in TBS buffer). Incubate for 10 min.
- Descant permeabilisation buffer and wash cells twice with washing buffer.
- Block with diluted serum for 20 minutes, i.e. the same serum that the secondary antibody is made up in (in our case horse serum). 1 drop to 5 ml washing buffer.
- Wash in washing buffer for 4 times.
- Incubate with optimally diluted primary antibody at optimal temp for optimum time, for 1 hour at room temperature.
- Wash in washing buffer for 4 times.
- Incubate with secondary antibody for 30 minutes at room temperature.
- Wash in washing buffer for 4 times.
- Incubate in ABC complex for 30 minutes at room temperature.
- Wash in washing buffer for 4 times.
- DAB chromogen for 5 minutes in dark area (covered by a tray).
- Wash in water for 2 minutes.
- Counterstain with Mayer's Htx for 1 minutes.
- Wash in water for 5 minutes.

2.4.4 Immunofluorescent Staining

This fluorescent staining method was previously reported (Jiang *et al.*, 1999b; Parr *et al.*, 2001; Ye *et al.*, 2003).

- 20,000 cells in 200µl aliquots per well were seeded into a 16-well chamber slide (Nalge NUNC International, LAB-TEK®), which had been pre-coated with or without Matrigel (5µg/well), and then incubated at 37 oC with 5%CO2 overnight.
- After incubation or treatment, aspirated medium and fixed cells with ice-cold ethanol at -20 oC for 20 minutes.
- Rehydrated in BSS buffer for 20 minutes at RT.
- Permeabilised cells with 0.1% Triton×100 for 5 minutes.
- Blocking was performed for 20 minutes using blocking buffer (2 drops of horse serum in 5ml wash buffer).
- Washed twice with wash buffer after blocking.
- Probed with primary antibody for 1 hour (1:100 made up in wash buffer with horse serum for blocking).
- Washed twice with wash buffer.
- Incubated with specific secondary antibody for 1 hour in the dark according to the primary antibody used which labelled with FITC or TRITC (1:100 made up in wash buffer with horse serum for blocking).
- Wash twice with wash buffer.

- Mount slides with a fluorescence mounting medium, Flour-Save, CalBiochem, Nottingham, England) .
- View cells under fluorescent microscope (Olympus), take photos. Analysis was carried out using Cell Analyser software (Olympus).

2.5 Topo TA Cloning

TOPO TA Expression system provides a highly efficient, 5 minute, one step cloning strategy ("TOPO Cloning") for the direct insertion of *Taq* polymerase amplified PCR products into a plasmid vector for high-level expression in mammalian cells. No ligase, post-PCR procedure, or PCR primers containing specific sequences are required. Once cloned, analysed, and transfected into a mammalian host cell line, the PCR product can be constitutively expressed (Figure 2.2).

The plasmid vectors pEF6/V5-His-TOPO and pcDNA3.1/NT-GFP-TOPO (Invitrogen, Inc., Paisley, UK) are used in current study. These plasmid vectors were supplied linearised with:

- Single 3´ thymidine (T) overhangs for TA Cloning
- Topoisomerase covalently bound to the vector (this is referred to as "activated" vector)

Taq polymerase has a nontemplate-dependent terminal transferase activity that adds a single deoxyadenosine (A) to the 3´ ends of PCR products. The linearised vector supplied in this kit has single, overhanging 3´ deoxythymidine (T) residues. This allows PCR products to ligate efficiently with the vector.

2.5.1 TOPO TA cloning reaction

Spontaneous ligation between vector and appropriate insert occurs when approximately 10 ng of insert (0.5-0.2 µl of a typical PCR sample) is mixed gently with the vector at correct ratio (dependant upon vector), and the reaction is made up to 5 µl with sterile water, then left for five minutes at room temperature.

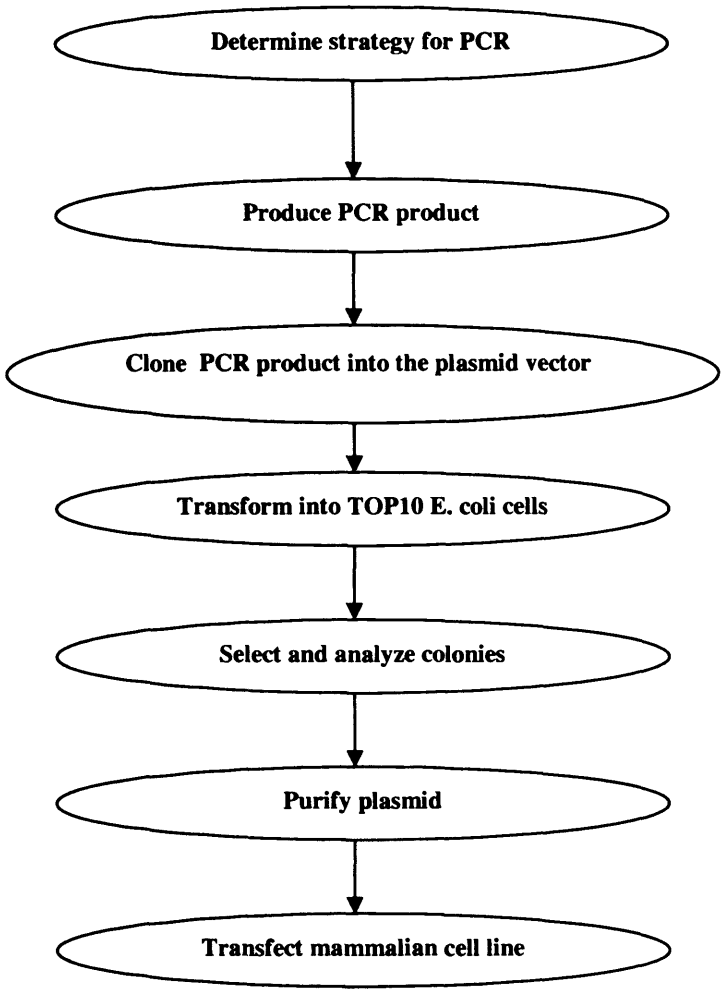

Figure 2.2 Flow chart of TOPO TA cloning procedure.

Following ligation, the cloning reaction should be transformed immediately into *E. coli*, otherwise the transformation efficiency may decrease.

2.5.2 Transform plasmid into E.coli

The cloning reaction was transformed into the chemically competent *E. Coli* cells (OneShot^{tm} TOP10 E.Coli, Invitrogen Inc.) as follows: a 100 µl aliquot of the chemically competent bacteria (stored at -70°C) was thawed by immersion in an ice-bath for 5 minutes. Following this, the cloning reaction was added and gently mixed using a pipette; this suspension was then placed on ice for 30 minutes. Cells were then heat-shocked, in a water bath, at exactly 42°C for 30 seconds, then immediately placed back on ice for 2 minutes. Following which, 250µl of SOC medium was added. These cells were then incubated for 60 minutes at 37°C with continuous shaking at approximately 225 rpm. The resultant transformation mix was then plated out (at two different volumes) onto pre-warmed selective LB-agar plates containing ampicillin (50 µg/ml) to the plasmid vector resistance and incubated at 37°C overnight.

LB (Luria-Bertani) medium and agar plates (1 liter)

Dissolve l0 g tryptone (Duchefa Biochemie, Haarlem, The Netherlands), 5 g yeast extract (Duchefa Biochemie, Haarlem, The Netherlands), and l0 g NaCl in 950 ml deionised water. Then adjust the pH to 7.0 with NaOH, and made up to 1 liter. Autoclave the solution, allow cooling, and adding the appropriate antibiotic (Ampicillin was used in the current study), this can then be stored at room temperature. To create LB plates, add 15g of agar to the one liter of LB medium before autoclaving. Autoclave, then when cooling add the desired antibiotic and pour

into petri dish plates (Bibby Sterilin Ltd., Staffs, UK). Allow to set, then store inverted at 4°C.

2.5.3 Selection and analysis of colonies

Following overnight incubation, the plates should reveal a large number of bacterial colonies containing the plasmid vector. The plasmid vector encodes a gene to enable resistance to specific antibiotics and when transformed into the *E. coli*, confers this resistance to these cells. Ampicillin resistance gene was present in both vectors used in the present study. Thus, selection occurs in the presence of the antibiotic, as cells without the plasmid vector will not survive. The next step is to establish which of these surviving cells containing the plasmid vector also has the insert ligated into the vector with right orientation. Analysis of the colonies is required to determine which of the colonies grown on the plate, contains the vector plus insert in the correct arrangement, prior to amplification.

Screening involves PCR, of approximately 10 colonies or as appropriate, to amplify the target sequence of insert DNA at the correct position within the plasmid vector. Individual colonies are examined by using a pipette tip touched against a labeled colony then placed into the PCR reaction cocktail ready for specific amplification of the desired sequence. This is achieved through the use of the forward primer for the plasmid and the reverse primer specific for the inserted PCR products. This ensures that amplified products, at the expected size, are that of the plasmid and insert in the correct orientation. These colonies are then ready for amplification.

2.5.4 Amplification and purification of plasmid DNA

Following identification of positive colonies with the appropriate vector and insert positioning, a single positive colony is transferred, aseptically, to inoculate 2ml of LB medium, containing Ampicillin at a final concentration of 100 μg/ml, and incubated until culture grows to mid-log phase at 37°C in a rotary shaker. At which stage, the resultant culture was then added into 100 ml LB medium (plus ampicillin), and incubated overnight at 37°C under rotation. The resulting amplification of recombinant plasmids within *E.coli,* then requires plasmid DNA extraction via a plasmid DNA purification kit (Filter Maxi System, QIAGEN, West Sussex, UK), as described below.

This method uses QIAGEN Maxi filter cartridges to recover plasmid DNA from the 100 ml of bacterial cells. To harvest the culture, centrifuge the cells in a refrigerated centrifuge (at 4 °C) at 6000g for 15 minutes, then remove the medium so that only the cell pellet remains. This pellet is then resuspended in 10 ml of resuspension buffer, which contains RNase inhibitors (available in the pack). To lyse the cells, 10 ml of cell lysis buffer is added and the solution is mixed gently to avoid shearing of genomic DNA. Following a 5-minute incubation at room temperature, 10 ml of neutralization buffer is added and mixed, and then transferred to the QIAGEN filter cartridge. After 10 minutes at room temperature, the cell lysate is filtered into the barrel of the QIAGEN tip, which is then allowed to enter the resin by gravity flow. The plasmid DNA binds to the anion-exchange resin.

To remove all contaminants from the plasmid preparation, the resin is washed through with wash buffer. RNA, proteins, dyes, and low molecular weight impurities are removed by this medium-salt wash. The DNA was eluted from the

resin through the addition of a high salt elution buffer, and was collected in a 50 ml universal tube. Plasmid DNA was then concentrated and desalted by isopropanol (10.5ml) precipitation, followed by a series of centrifugation and washing steps. The pellet was then dried and resuspended in a suitable volume of water. The yield of DNA was determined through quantification, following which, small amount of plasmid DNA was run on agarose gel (0.8%) to check both plasmid purity and size. After that, the DNA inserts were isolated by restriction digestion, if required.

Mini-preparation was also used when to verified the cloning efficiency, for which a Qiagen mini kit was used. The procedure was similar to Maxi, except that all were in a smaller scale.

2.5.5 Transfection via electroporation of mammalian cells

Once the plasmid DNA has been isolated, purified and quantified, it is ready to be introduced into cultured mammalian cells. The method employed during this study, utilized electroporation of cultured cells to allow plasmid DNA to be incorporated into the cells.

The electroporation technique used the Easy Jet Plus system (Flowgen, Staffordshire, UK), which passed a voltage of upto 310 volts across the cells to produce small perforations in the cell wall integrity, thus allowing passage of plasmid DNA across cell membranes to be integrated into the cells.

For a transfection, 3 pg of plasmid DNA was added to resuspended (- 1x10~) cells and mixed. The mixture was left to stand at room temperature for 2-5 minutes. The mixture was then transferred into an electroporation cuvette (Euro Gentech, Southampton, UK) ready for electroporation. The cuvette was loaded into the

electroporator and a pulse of electricity (250-310 volts, depending on cell types) was passed through the cuvette. The mixture was then immediately (within 10 seconds) transferred into 10 ml of pre- warmed culture medium (must be within 30 seconds). This reaction was then cultured under the usual incubation conditions.

2.5.6 Establishing a stable expression mammalian cell line

To create a stable cell line that expresses the gene of interest, the culture must first be selected to yield only a population of cells expressing the plasmid-insert construct, which either constitutively induce or express the molecule of interest.

The above electroporated cells were allowed to growing to semi-confluence. Selection of plasmid positive cells relies on the presence of an additional drug (antibiotic) resistance gene in the plasmid. Plasmids used in this study have dual resistance genes, i.e. one for prokaryotic selection (as already mentioned earlier) and one for mammalian selection. For the latter, modified antibiotics that are capable of entering mammalian cells are used, such as G418 (for pCDN4/GFP-TOPO) or blasticidin (for pEF6/V5-His-TOPO). Thus the respective antibiotics are added to cultured cells at an appropriate concentration (100 pg/ml for G418 and 5 pg/ml for blasticidin) to kill plasmid absent cells. This antibiotic selection period may continue for a number of weeks (two weeks for G418 and 1 week for blasticidin), at which point the cells remaining should all contain the plasmid and the inserted DNA fragment. Cells are routinely tested for the presence of the plasmid and insert, using RT-PCR. Once the plasmid has been incorporated into the mammalian cells, and the inserted DNA fragment were expressed. The transfectants may then be employed in a

series of *in vitro* studies, to examine for the presence and influence of the expressed gene.

2.6 Knockdown of gene transcripts Using Ribozyme Transgenes

The hammerhead ribozyme was first discovered as a self-cleaving domain in the RNA genome of different plant viroids and virusoids (Forster and Symons, 1987). Soon thereafter, it was demonstrated that the hammerhead motif could be incorporated into short synthetic oligonucleotides and transformed into a true, multiple turnover catalyst, suitable for cleaving in trans a variety of RNA targets (Uhlenbeck, 1987; Haseloff and Gerlach, 1988). All hammerhead motifs share a typical secondary structure consisting of three helical stems (I, II and III) that enclose a junction characterized by several invariant nucleotides (i.e., the 'catalytic core'). In most trans-acting hammerhead ribozymes, helix II is formed intramolecularly by the catalyst, whereas helices I and III are formed by hybridization of the ribozyme with complementary sequences on the substrate. The best triplets in terms of cleavage rates were found to be AUC, GUC and UUC (Figure 2.3).

To knockout or knockdown a specific gene by using a hammerhead ribozyme transgene, we designed primers according to secondary structure of the gene generated by using Zuker's RNA mFold programme (Zuker, 2003), targeting at a specific GUC or AUC site. We synthesised ribozymes with a Touchdown PCR procedure, and cloned ribozymes in a suitable vector which followed by transformation and transfection using an electroporator. After 3-4 weeks selection with a specific antibiotic, a stable cell line with a transgene was verified by using RT-PCR and/or Western-blot. This method has been extensively used and reported previously in our laboratory (Jiang *et al.*, 2001; Jiang *et al.*, 2003; Jiang *et al.*, 2005a;

Jiang *et al.*, 2005b). According to the similar procedure, a hammerhead ribozyme transgene was designed and constructed for BMPR-IB, BMPR-II and BMP-7, respectively.

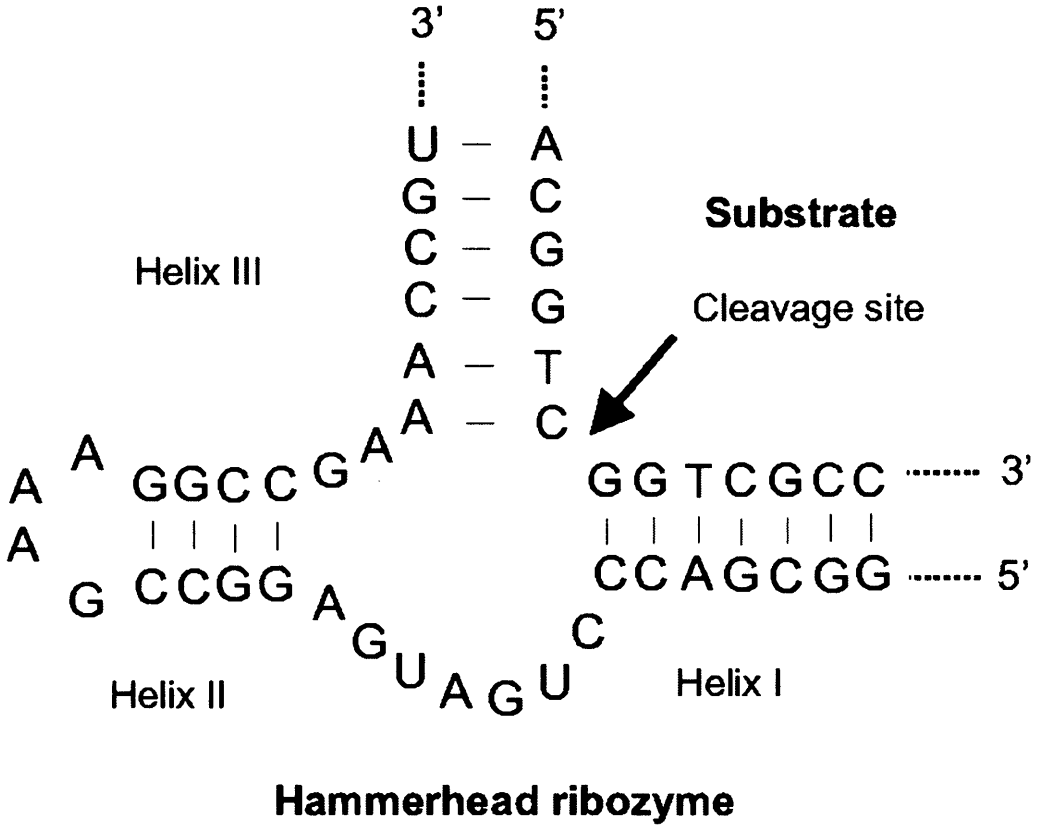

Figure 2.3 Secondary structure of the hammerhead ribozyme with bound substrate.

2.7 Gene Over-expression

We designed the primers according to the mRNA sequence of a particular gene, which are capable to amplify the whole coding sequence with or without a stop codon. The primers were designed to amplify the coding sequence of BMP-9 and BMP-10 (Table 2.3). The PCR parameters were optimised, and the high fidelity long and accurate PCR (LA-PCR) was performed using DuraScript™ RT-PCR kit (Sigma-Aldrich, Inc., Poole, Dorset, England, UK). The resultant of PCR products were subsequently cloned into to the plasmid vector a pEF6/V5-His-TOPO vector according to the TOPO TA cloning procedure as introduced in 2.5. Briefly, following by transformation of plamids into One-Shot *E. coli* (Invitrogen Ltd.), the analysis and amplification were performed. Plasmid was then purified with GenElute™ Plasmid Miniprep Kit (Sigma-Aldrich, Inc.). The transgene or an empty plasmid (for control) was subsequently transfected into cells respectively, followed by selection with blasticidin. Stable BMP-9 transfectants, BMP-10 transfectants and empty plasmid transfectants were established, and were utilized in this study. Therefore, the transgene obtained will generate native copies of the complete coding sequence.

2.8 *In vitro* Functional Assays

2.8.1 In vitro cell growth assay.

We used the method previously reported by Jiang *et al* (Jiang *et al.*, 2005b). Briefly, the respective cells were plated into a 96-well plate equally (2,500cells/well). Cells were fixed in 10% formaldehyde at the day of plating; days 1, 3, and 5 after plating; and then stained with 0.5% (w/v) crystal violet. Following washing, stained crystal was extracted with 10% (v/v) acetic acid and absorbance determined at a wavelength

of 540nm by using a spectrophotometer (BIO-TEK, ELx800, Wolf Laboratories, York, England).

2.8.2 In vitro migration assay (wounding assay)

The migration of cells across a wounded surface of a near-confluent cell monolayer was examined, which has been described in a previous study (Jiang *et al.*, 1999a). Cells at a density of 50,000/well were seeded into a chamber slide and allowed to reach near confluence. The layer of cells was then scraped with a fine gauge needle to create a wound of approximately 200 mm. A treatment was then added with appropriate control. The movement of cells to close the wound was recorded using a time lapse video recorder and analysed using the motion analysis feature in a software package Optimas 6.0.

2.8.3 In vitro motility assay using Cytodex-2 beads

We followed the protocol described by Rosen and Jiang (Rosen *et al.*, 1990; Jiang *et al.*, 1995b). In this *in vitro* motility assay, the cells will adher the surface of beads after a period of incubation, the beads which carry the cells will be transfered into a culture plate. Cells will move from beads onto the surface of culture plate and was stained and counted which indicate the cellular motility. 1×10^6 cells were incubated with 100µl of beads in 10 ml DMEM overnight. The beads were washed to remove dead cells in 5ml DMEM twice, and then resuspended in 800µl DMEM. 100µl of beads/cells were transferred into each well of a 24-well plate, and repeated in triplicate. After incubation for 4 hours, the medium was aspirated and cells were fixed with 4% formalin for 5 minutes. They were then stained with 0.5% crystal

violet for 5 minutes. The cells were washed and allowed to dry before counting. Counting minimum 3 random fields per well, i.e. should have more than 9 counts if samples are set up in triplicate for statistical analysis.

2.8.4 In vitro invasion assay

This technique was previously reported and modified in our laboratory (Jiang *et al.*, 1995a). The technique works upon the principle that a culture plate is equipped with an insert which has one end sealed with a polycarbonate membrane. The polycarbonate membrane has a pore size of 8μm in diameter, which is sufficiently large enough to allow cells to migrate through it. The surface of this membrane is then coated with an extracellular matrix protein solution, Matrigel (rich in basement membrane), to form a thin layer of gel matrix. Since this technique determines the capacity of tumour cells to penetrate through the gel matrix and porous membrane, it presents an indication of invasive capacity. The following method briefly outlines the procedure used during this study.

Cell culture inserts (Becton-Dickinson) for *in vitro* invasion, were placed into a 24 well plate (Nunclon) using forceps. To prevent irreversible gelling of Matrigel the following procedure was carried out at 4°C. A stock solution of Matrigel was prepared at a concentration of 0.5mg/ml in pre-cooled sterile water and 100μl aliquots of Matrigel (50μg per insert) were added to these pre-chilled cell culture inserts. Once the inserts had a thin even coating of Matrigel, they were incubated at 45°C in a drying owen, to dry out the Matrigel. Prior to use, the Matrigel layers were rehydrated by incubating at room temperature for 1 hour using 300μl of sterile water, and then aspirating the water from each insert.

Cell suspensions were added to each insert and treated. After a culture time of upto 72 hours at 37°C, the Matrigel layer together with the non-invasive cells were removed from the inside of the insert using a cotton swab. This step was performed as Matrigel is stained in addition to the cells, thus making it difficult to resolve between invading cells and background. The cells which had invaded into the Matrigel and migrated through the porous membrane, were fixed in 4% formaldehyde, for 10 minutes at room temperature. The cells were washed twice using distilled water and stained with 0.5 % crystal violet for 10 minutes at room temperature. Excess stain was removed by washing the cells twice in distilled water. The cells were allowed to air dry and the numbers of invading cells were counted using a light microscope, prior to being photographed.

2.8.5 *In vitro* cell-matrix adhesion assay

100µl serum free medium that contained 5µg Matrigel (BD Matrigel™ Matrix, Matrigel™ Basement Membrane Matrix, Cat No. 354234) was added in each well of 96-well plate (NUNC™, TC Microwell 96F, Cat No. 167008), and then the Matrigel was dried at 55°C for about one hour in oven. Rehydrated the Matrigel in 100µl sterile water per well at room temperature for 40 minutes, and then aspirated the medium. 40,000-50,000 cells per well were seeded since the plate with Matrigel were ready. Incubated the cells with or without treatment of some factor at 37 °C with 5%CO_2 for 40 minutes. After the incubation or treatment with some specific factors, the medium was discarded. The non adherent cells were washed off 3-4 times using BSS buffer. The cells were then fixed with 100µl per well of 4% formaldehyde for a minimum of 5 minutes. The formaldehyde was discarded and the cells washed with BSS buffer. 100µl of crystal violet solution (0.5% crystal violet in distilled water)

was added into each well for up to 5 minutes, washed with BSS buffer, and then left to dry at RT. The number of adherent cells were counted under a microscope from random fields from triplicate samples and compared to the number of adherent cells that remained on the Matrigel after HGF/SF treatment.

2.8.6 Flow cytometric analysis of apoptosis

In normal live cells, phosphatidylserine (PS) is located on the cytoplasmic surface of the cell membrane. However, in apoptotic cells, PS is translocated from the inner to the outer leaflet of the plasma membrane, thus exposing PS to the external cellular environment. In leukocyte apoptosis, PS on the outer surface of the cell marks the cell for recognition and phagocytosis by macrophages. The human anticoagulant, annexin V, is a 35–36 kD Ca^{2+}-dependent phospholipid-binding protein that has a high affinity for PS. Annexin V labeled with a fluorophore or biotin can identify apoptotic cells by binding to PS exposed on the outer leaflet. Propidium iodide (PI) is a red-fluorescent nucleic acid binding dye. PI is able to permeate through integral cell membrane, thus it stains dead cells with red fluorescence by binding tightly to the nucleic acids, but not the live cells and the apoptotic cells. In this study, we utilised the Vybrant® Apoptosis Assay Kit (Invitrogen, Inc., Paisley, UK) to perform the apoptosis assay, which contains the recombinant annexin V conjugated to fluorescein (FITC annexin V) and PI solution. After staining, the apoptotic cells show green fluorescence, the dead cells show red and green fluorescence, and the live cells show little or no fluorescence. These populations can easily be distinguished using the Partec CyFlow® SL flow cytometer and the accompanied FloMax software package (Partec GmbH, Munster, Germany).

Cells were harvested the cells including the cells floating in the culture medium after a period of incubation, and washed in cold phosphate-buffered saline (PBS). The washed cells were Re-centrifuged, the supernatants were discarded and the cells were then resuspended in 1X annexin-binding buffer. Determine the cell density and dilute in 1X annexin-binding buffer to ~1 × 10^6 cells/ml, preparing a sufficient volume to have 100 µl per assay. Add 5 µl of FITC annexin V and 1 µl of the PI working solution (100 µg/ml) to each 100 µl of cell suspension. Incubate the cells at room temperature for 15 minutes. After the incubation, add 400 µl of 1X annexin-binding buffer, mix gently and keep the samples on ice. As soon as possible, analyze the stained cells by using the flow cytometer and FlowMax software package, measuring the fluorescence emission at 530 nm (e.g. FL1) and >575 nm (e.g. FL3).

2.8.7 Cell cycle analysis of fixed cells stained with PI

In this study, ethanol was used to fix and permeabilized cells to make them accessible to propidium iodide (PI). After fixation, the cells were rinsed with PBS and stained with PI in a solution containing Triton ×100 and RNase A. Triton ×100 additionally permeabilized the cells. Because double-standed sections of RNA are also stainable with PI, RNase A is used to digest these sections and thereby to increase the specificity of DNA staining.

Cells from the culture flasks were collected by trypsinisation, and pooled with the cells floating in the medium which contained detached mitotic, apoptotic and dead cells. The cells were centrifuged and washed twice with cold PBS, and then counted. 1×10^6 to 1×10^7 cells were resuspended in 0.5ml of PBS, and fixed at 4°C for at lest 2 hours by adding 4.5ml of 70% ethanol. The fixed cells were washed with PBS, and resuspended in 1ml of PI staining solution. After a 30 minutes incubation at room

temperature (in dark area), the fluorescence of PI was detected using the flow cytometer, and the cell cycle analysis was performed using the FlowMax software package.

2.9 Generation of recombinant human BMPs (rh-BMPs)

2.9.1 TOPO TA cloning

We designed the primers according to the complete mRNA sequence of a particular gene, which were almost same as primers designed for gene over-expression except a deletion of the stop codon (ATC) (Table 2.3). The PCR parameters were optimized and performed. The resultant of PCR products were subsequently cloned into to the plasmid vector a pEF6/V5-His-TOPO vector according to the TOPO TA cloning procedure as introduced in 2.5. Briefly, following by transformation of plamids into One-Shot *E. Coli* (Invitrogen Ltd.), the analysis and amplification were performed. Plasmid was then purified with GenElute™ Plasmid Miniprep Kit (Sigma-Aldrich, Inc.). The transgene or an empty plasmid (for control) was subsequently transfected into 3T3 cells (a murine fibroblast cell line obtained from ATCC) respectively, followed by selection with blasticidin. Stable BMP-9 or BMP-10 transfectants, or empty plasmid transfectants were established, and were utilized in this study. Therefore, the transgenes obtained will generate copies of the complete coding sequence with an additional Histidine-tag which transcribed from the downstream sequence in the pEF6/V5-His-TOPO plasmid vector.

2.9.2 Extraction and purification of rh-BMPs

rh-BMP-9 and rh-BMP-10 generated from the above carries a 6-histidine-tag at one end of the protein. The multi-histidine taq had high affinity to heavy metals (nickel in the present study). These proteins were extracted and purified using a HisTrap kit (Amersham Bioscience UK Ltd., Buckinhamshire, UK).

2.9.2.1 Preparation of protein for extraction

The 3T3 transfectants which were verified for the expression of BMPs, were grown to a large population. The cells were then lysed in a lysis buffer which is same as the lysis buffer (mentioned in 2.4), but without SDS.

2.9.2.2 Preparation of HiTrap chelating HP columms

- Fill the syringe with distilled water. Remove the stopper and connect the column to the syringe with the provided adaptor. "Drop to drop" to avoid introducing air into the column.
- Remove the twist-off end. Wash the column with 5 ml distilled water. Do not use buffer to wash away the 20% ethanol solution as nickel salt precipitation can occur in the next step. If air is trapped in the column, wash the column with distilled water until the air disappears.
- Disconnect the syringe from the column, fill the syringe with 0.5 ml of the 0.1 M nickel salt solution ($NiSO_4$) which and load it on the column.
- Wash the column with 5 ml distilled water, using the syringe.

2.9.2.3 Purification of histidine-tagged rh-BMPs

- Prepare 24 ml binding buffer. Mix 3 ml Phosphate buffer 8x stock solution with 0.12 ml 2 M Imidazole and add water up to 24 ml. Check pH and adjust to pH 7.4-7.6 if necessary. This buffer will contain 20 mM phosphate, 0.5 M NaCl and 10 mM Imidazole.
- Prepare 8 ml elution buffer. Mix 1 ml Phosphate buffer 8x stock solution with 2 ml 2 M imidazole and add distilled water up to 8 ml. Check pH and adjust to pH 7.4-7.6 if necessary. This buffer will contain 20 mM phosphate (1x), 0.5 M NaCl and 500 mM imidazole.
- Using the syringe, equilibrate the column with 10 ml binding buffer.
- Apply the sample (from step 2.9.2.1) with the syringe. Collect the flow through fraction. Keep the flow rate at 1-3 ml/min.
- Wash with 10 ml binding buffer. Collect the wash fraction.
- Elute with 5 ml elution buffer. Avoid dilution of the eluate by collecting the eluate in 1 ml fractions. Fractions with colour (light green) were particularly collected as they are the franctions with the recombinant proteins.
- Check the purification by running an aliquot of the collected samples on SDS-PAGE. The purified protein is most likely to be found in the 2nd + 3rd ml of the elution step.
- After the protein has eluted, regenerate the column by washing it with Start buffer. The column is now ready for a new purification and there is no need to reload with metal. The reuse of HiTrap Chelating HP depends on the nature of the sample and should only be performed with identical recombinant proteins, to prevent cross-contamination.

8x Phosphate buffer, pH 7.4

To 1.42 g Na_2HPO_4 . $2H_2O$ (177.99 g/mol), 1.11 g NaH_2PO_4 . H_2O (137.99 g/mol) and 23.38 g NaCl (58.44 g/mol), add distilled water to 90 ml and dissolve completely. Adjust pH, to 7.4. Add distilled water to 100 ml and filterthrough a 0.45 μm filter.

2 M Imidazole, pH 7.4

To 13.62 g imidazole (68.08 g/mol) add distilled water to 90 ml and dissolve completely. Adjust pH to 7.4. Add distilled water to 100 ml and filter through a 0.45 μm filter.

0.1 M $NiSO_4$

To 2.63 g $NiSO_4$. $6H_2O$ (262.86 g/mol) add distilled water to 100 ml and dissolve completely. Filter through a 0.45 μm filter.

2.9.3 Desalting and buffer exchange using dialysis

A tubing (7000/1, Medical International Ltd., London, UK) of which the cut-off size is 7kD, was used for the dialysis.

- Cut the dry tubing to the proper length, allowing an additional 10 cm for closing off the ends. Handle tubing only with powder-free gloves to avoid getting skin oils on membrane.
- Immerse the sections of tubing in distilled water and rub each between two fingers until the layers separate. Using a large wash bottle containing 50% ethanol, rinse the inside and outside of each section thoroughly. The ethanol rinse serves to remove glycerol (used as a humectant) and residual sulfides (from the manufacturing process).

- Mix 400 ml of 10 mM EDTA (pH 8.0) and 400 ml of 0.05 $NaHCO_3$ in a 1-liter beaker. Transfer the wetted and washed tubing to this beaker and stir for 30 min using a magnetic stirrer.
- Decant the EDTA/$NaHCO_3$ solution and replace with 800 ml distilled water. Stir 10 min on the magnetic stirrer, decant the water, and repeat the water wash. Transfer the tubing to fresh distilled water.
- Close one end of a washed section of tubing firmly with two simple overhand knots. Squeeze the tubing between two fingers to remove excess water from inside.
- Transfer the resultant protein sample into the tubing. When sample loading is complete, squeeze the tubing with the fingers to eliminate air space. Close the end shut with a knot the tubing carefully twice, and trim off excess tubing. Check for leakage at both ends by applying moderate pressure to the sample area.
- Place the filled dialysis bag in a beaker containing a volume at least ten times the sample volume of dialysis buffer at the desired temperature, making sure that the bag is completely immersed. Stir the dialysis buffer continuously with a magnetic stirrer.
- Follow the progress of the dialysis by measuring the conductivity of the dialysis buffer (if this is practical). Replace the used dialysis buffer with an equal volume of fresh buffer when the increase in conductivity slows down (indicating approach to equilibrium and a drop in the efficiency of the dialysis). Continue replacing the dialysis buffer in this way until the

conductivity of the buffer remains essentially unchanged after stirring for 1 to 2 hr.

- Remove the dialysis bag from the buffer and rinse the exterior with distilled water. While holding the bag just below the knot, or cut off the knot. Carefully tip the bag and pour the dialyzed sample into an appropriate container. Confirm that the desired salt concentration was achieved by comparing conductivity measurements of the dialyzed sample and unused dialysis buffer.

2.10 Statistical analysis

Statistical analysis was performed using Minitab statistical software (version 10). For non-normally distributed data we used the Mann-Whitney test, while the two samples t-test was used for normally distributed data. Graphs were constructed using Microsoft Excel software.

Chapter 3

Expression of BMPs and BMP Receptor Signalling Intermediate Molecules in Prostate Cancer

3.1 Introduction

As addressed in chapter one, BMPs which belong to the TGF-β superfamily may play a pivotal role in the bone metastasis from prostate cancer. As a group of the most powerful osteotropic factors, BMPs are enriched in bone matrix, which can be produced by both bone cells and prostate cancer cells. During the development of bone metastasis, these factors play profound roles in the local microenvironment of the bones. Via both paracrine and autocrine loops, BMPs are intensively involved in the interaction between the tumour cells and bone microenvironment.

BMPs exert their effects through a heteromeric receptor complex, which consists of two types of serine-threonine kinase transmembrane receptors, Type-I and Type-II (refer to Table 1.4 and Table 1.5). After binding of BMPs to at least one homodimer of each type receptor, the Type-II receptor kinase phosphorylates a regulatory region within the Type-I receptor known as the GS domain, resulting in kinase activation. The activated Type-I receptor then recognises and phosphorylates the carboxy-teminal SXS motif of receptor-regulated Smad proteins (R-Smad). After forming a heterodimer or heterotrimer with Smad-4, the Smad signal complex is translocated into the nucleus, where the complex either induces or represses the transcription of target genes. This pathway is known as the Smad dependent pathway. Smad 6 and 7 can inhibit this process. The other pathway downstream of the BMP receptors is known as the Smad independent pathway, in which extracellular-signal-regulated kinases (ErK, ErK-1 and ErK-2), mitogen-activated protein kinases (MAPKs, p38 or c-Jun amino-terminal kinase (JNK)), and RAS pathway may be involved (Nohe *et al.*, 2004).

BMPs have recently been implicated in prostate cancer. An elevated level of BMP-6 is associated with the high grade of primary tumour and with advanced prostate

cancer which developed metastases. It also may contribute to the progression of prostate cancer in the absence of androgens (Bentley *et al.*, 1992; Barnes *et al.*, 1995; Hamdy *et al.*, 1997; Tamada *et al.*, 2001). In contrast, BMP2/4, BMP7 and GDF15 are expressed predominantly in normal prostate tissue, and their expression tends to be lower or absent during development of the primary tumour. Some of these 'suppressed' BMPs may be re-expressed in the metastatic tumours of the prostate in the bone (Harris *et al.*, 1994; Thomas *et al.*, 2001; Masuda *et al.*, 2003; Horvath *et al.*, 2004; Masuda *et al.*, 2004).

Among Type-I and Type-II receptors, the expression of BMPRIA, BMPRIB, and BMPRII in human prostate cancer tissue has been found to correlate with tumour grade, although only the loss of expression of BMPRII has been shown to correlate with poor prognosis in prostate cancer patients (Kim *et al.*, 2000; Kim *et al.*, 2004). Intracellular signalling molecules of BMP receptors have also been implicated in the development and progression of prostate cancer. The levels of Smad 4 and Smad 8 in the nuclei are also thought to be associated with the development of prostate cancer, and in particular loss of Smad 4 may be related to a more aggressive phenotype (Horvath *et al.*, 2004).

The role of most recently discovered members of the BMP family in prostate cancer remains unclear. The studies presented in this chapter, were aimed to evaluate the expression profile of some key BMPs, their receptors, receptor antagonists, and some of the signalling intermediate molecules. The following were assessed: BMP-2, 4, 6, 7, 8A, 8B, 9, 10, 11 and 12), BMP antagonists (Noggin and follistatin), BMP receptors and intracellular signalling molecules, in seven prostate cell lines. We also examined the expression of BMP receptors (BMPR-IB and BMPR-II), BMP-9 and BMP-10 in human prostate specimens.

3.2 Materials and Methods

3.2.1 Reagents and Antibodies.

Polyclonal goat anti-BMPR-IB IgG (SC-5679), polyclonal goat anti-BMPR-II IgG (SC-5683), polyclonal goat anti-BMP-9 (SC-27820) and were obtained from Santa Cruz Biotechnology (California, USA). Polyclonal rabbit anti-BMP-10 was purchased from Orbigen Inc. (San Diego, USA). Other reagents or materials if not mentioned were purchased from Sigma-Aldrich Ltd (Poole, UK).

3.2.2 Cell lines.

Seven prostate cell lines were employed for this study as outlined in section 2.1 and Table 2.1. The cells were routinely maintained in DMEM-F12 medium supplemented with 10% foetal calf serum and antibiotics.

3.2.3 Prostate tissue samples.

Prostate tissue samples were available following collection from the patients at the Department of Urology, University Hospital of Wales. All research samples were snap-frozen in liquid nitrogen immediately after radcial prostatectomy, transurethral prostatectomy or prostate biopsy. All protocols were reviewed and approved by the local ethical committee and all patients gave written informed consent. Similarly, paraffin embedded samples from the same patient were also available.

3.2.4 RNA Isolation and RT-PCR.

RT-PCR was performed in the same procedure described in section 2.3. The details of primers have also been given in Table 2.1. The PCR products were then visualized on a 2% agarose gel which was stained with ethidium bromide after electrophoresis, and photographed.

3.2.5 Immunohistochemical staining procedures for frozen prostate tissue

Frozen specimens of prostate cancer tissue (n =8) and normal prostate (n = 18) were cut at a thickness of 6 μm using a Leica CM 1900 cryostat (Leica, Wetzlar, Germany). The immunohistochemical staining of BMPR-IB, BMPR-II, BMP-9 and BMP-10, was performed by using the specific primary anti-body for each protein (details in Table 2.5). Positive controls were no particularly examined in current study, as there is no tissue avaliabe which has been reported expressing either BMP-9 or BMP-10, and also for both BMP receptors as they have been shown expressed in normal prostate tissue. Negative controls were performed in which only the secondary antibody was applied.

3.2.5 Immunohistochemical staining procedures for paraffin embedded specimens

Human prostate specimens that were embedded in paraffin wax were cut into 7μm sections. The same primary antibodies were used as for the frozen specimens. The IHC staining was carried out according to the method (described in section 2.4.2.2).

3.3 Results

3.3.1 The expression of BMPs and BMP antagonists in prostate cell lines

Seven prostate cell lines were employed in this study: PC-3, DU-145, LNCaP and CA-HPV-10 are cancer cell lines, whereas PZHPV-7, PNT-1A and PNT2-C2 are immortalised prostatic epithelial cell lines. We screened these cell lines to assess the expression of BMPs and BMP antagonists, Noggin and Follistatin, using RT-PCR. The mRNA level of BMP-2, 4, 6, 7, 8A, 8B, 9, 10, 11 and 12 in seven different prostate cell lines together with Noggin and Follistatin are illustrated in Figure 3.1. BMP-2 was expressed at a relatively higher level in CA-HPV-10 cells, and was also detectable in LNCaP and PNT2-C2 cells. BMP-4 was expressed at a higher level or detectable in most of these cell lines except DU-145. BMP-6 was expressed highly in PNT2-C2, and detectable in PC-3 and DU-145 cells. In contrast, BMP-8A and BMP-9 are expressed at a relatively higher level. BMP-9 expression is higher in two prostate cancer cell lines DU-145 and CAHPV-10, but not in PC-3. BMP-10 was only detectable in DU-145. The expression of BMP-7 was relatively higher in CA-HPV-10 and PNT-1A cells, at an intermediate level in DU-145 cells, and was also detectable in PC-3 and PZHPV-7 cells. Both antagonists, Noggin and Follistatin, were expressed at relatively high level in all these seven prostate cell lines in comparison with the expression of the BMPs.

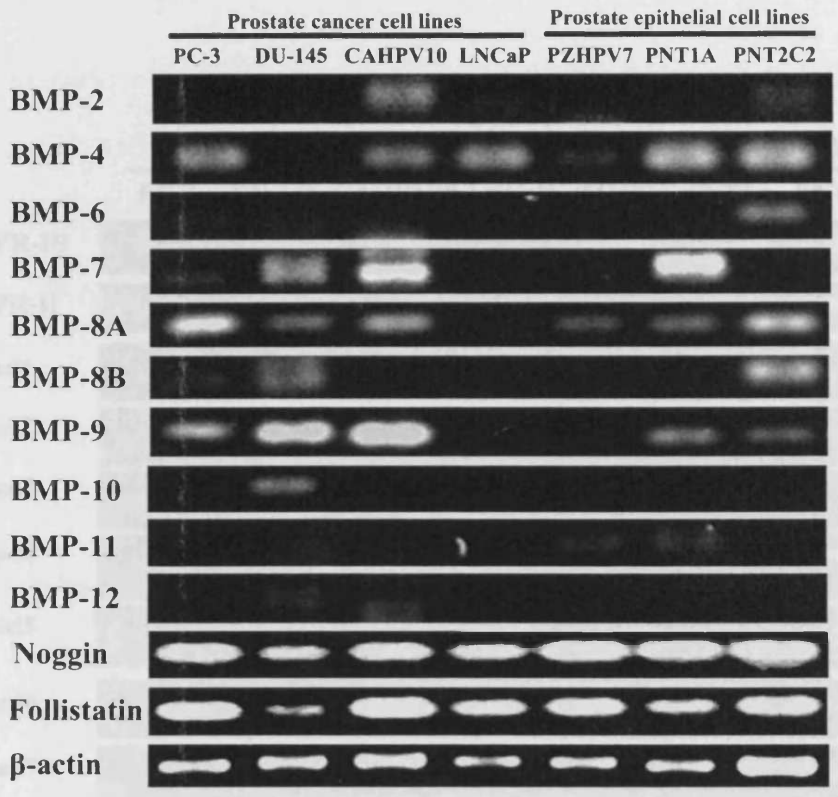

Figure 3.1 The expression of BMPs and BMP antagonists in prostate cell lines was assessed using RT-PCR. 38 cycles were performed for these PCR reactions.

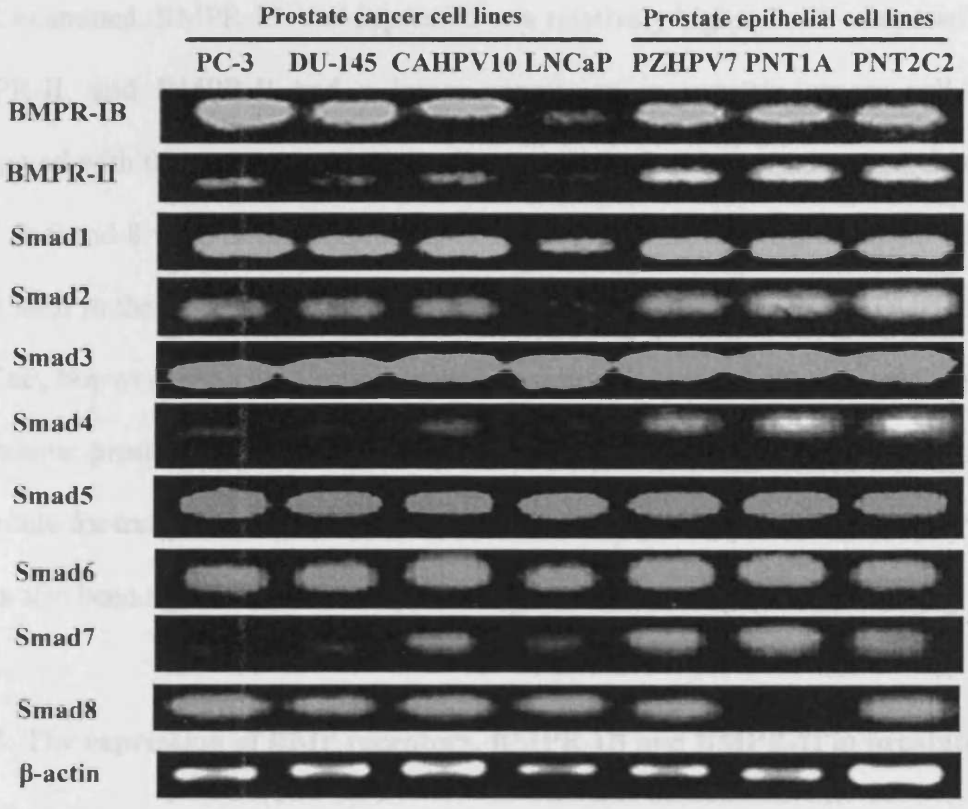

Figure 3.2 mRNA levels of BMPR-IB, BMPR-II and Smad family in seven prostatic cell lines were revealed by conventional RT-PCR. High levels of expression were revealed in BMPR-IB, Smad 1, 2, 3, 5, 6 and 8. 38cycles were performed for these PCR reactions.

3.3.2 The expression of BMP receptors and intracellular signaling molecules in prostate cell lines

We also utilised these seven prostate cell lines for assessing the expression of the two BMP receptors and the intracellular signal molecules using conventional RT-PCR. Figure 3.2 illustrates the subtle variations in the level of the gene transcripts of the two receptors. Both receptors were detectable in all seven prostate epithelial cell lines examined. BMPR-IB was expressed at a relatively higher level compared with BMPR-II, and BMPR-II had a lower expression in prostate cancer cell lines compared with the prostate epithelial cell lines. Eight Smads were detected, Smad-1, 2, 3, 5, 6 and 8 were clearly expressed in all cell lines. Low levels of Smad-4 and 7 were seen in the three more aggressive prostate cancer cell lines, PC-3, DU-145 and LNCaP, but were more easily seen in the prostatic epithelial cell lines and the less aggressive prostate cancer cell line CA-HPV-10. Smad-4 is not only an important molecule for translocation of Smad complex during signal transduction of BMP, and it has also been reported as onco-suppressor gene.

3.3.3. The expression of BMP receptors, BMPR-IB and BMPR-II in prostate tissue

We examined the expression of the BMP receptors, BMPR-IB and BMPR-II in prostate tissues (frozen specimens), using immunohistochemistry. BMPR-IB staining (Figure 3.3) was stronger in the plasma of normal prostate epithelia, but weak or absent in tumour cells. Weak staining was also demonstrated in heterogeneous cells, such as in the stromal cells. A similar pattern of BMPR-II staining was revealed in prostate tissue (frozen specimens) using immunohistochemical staining (Figure 3.4). IHC staining of BMPR-II was stronger in the normal prostate epithelia compared

with the cancer cells. Both receptors showed a weak staining in cancer cells where no prostate gland structure exists.

3.3.4 The expression of BMP-9 and BMP-10 in prostate tissue

The IHC staining of BMP-9 and BMP-10 were performed using both human frozen specimens and paraffin specimens. The staining of BMP-9 exhibits a similar pattern in both frozen and paraffin specimens, which revealed a stronger staining in normal epithelial plasma compared to cancer cells. The staining of BMP-9 disappeared in high grade tumour particularly where the structure of gland was totally disturbed (Figure 3.5 and Figure 3.6). Some degree of the staining was also revealed in the stroma in both frozen and paraffin specimens.

The staining of BMP-10 was stronger in normal prostatic epithelia, and there was also some degree of staining in the stromal tissue. Prostate cancer cells in the frozen specimens showed virtually no staining for BMP-10. There was no staining revealed in paraffin specimens of both normal prostate tissue and prostate cancer specimens (Figure 3.7 and Figure 3.8).

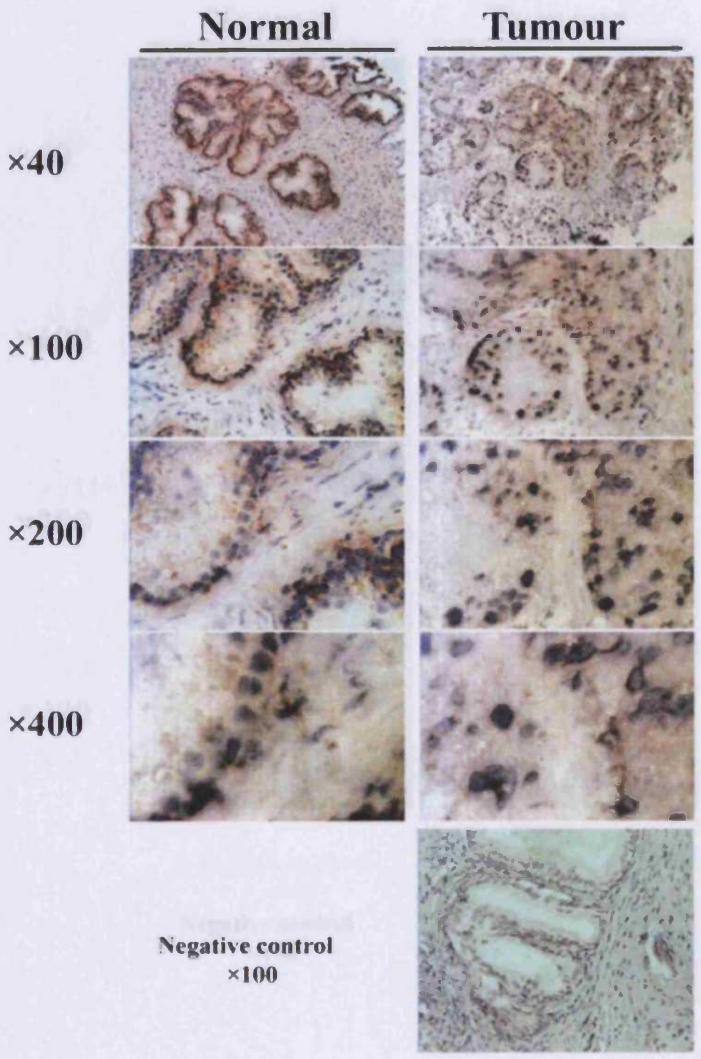

Figure 3.3 Immunohistochemical staining of BMPR-IB in human prostate frozen specimens.

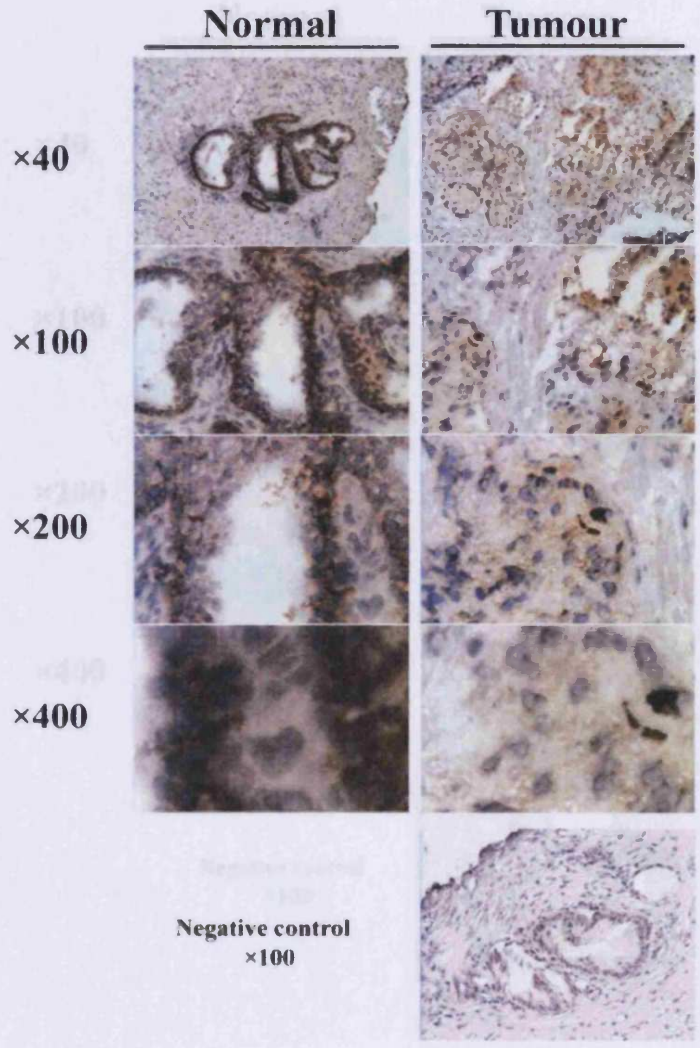

Figure 3.4 Immunohistochemical staining of BMPR-II in human prostate frozen specimens.

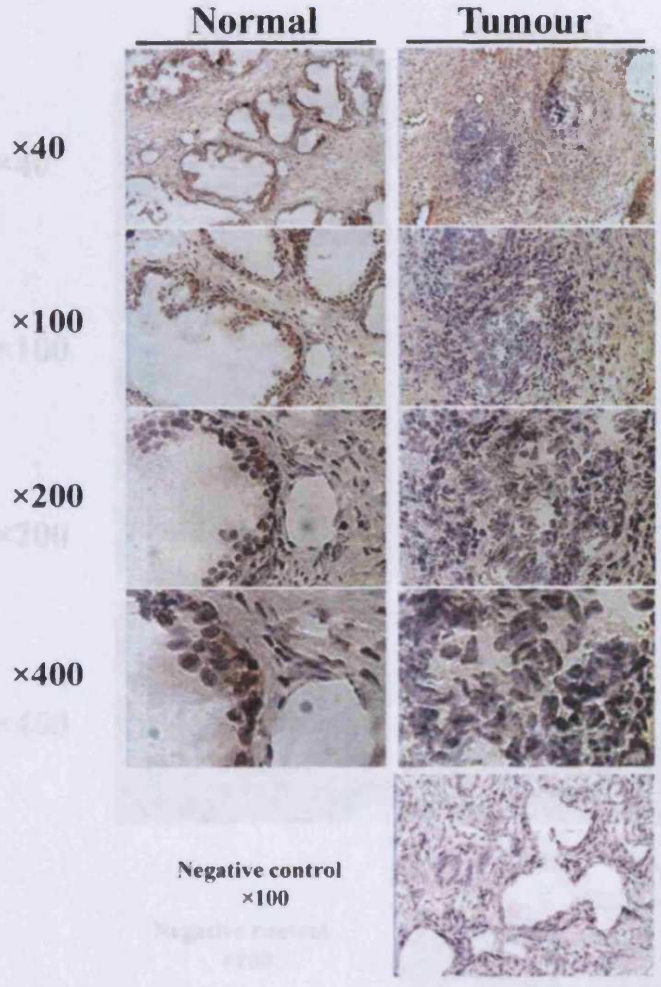

Figure 3.5 Immunohistochemical staining of BMP-9 in human prostate specimens (frozen sections).

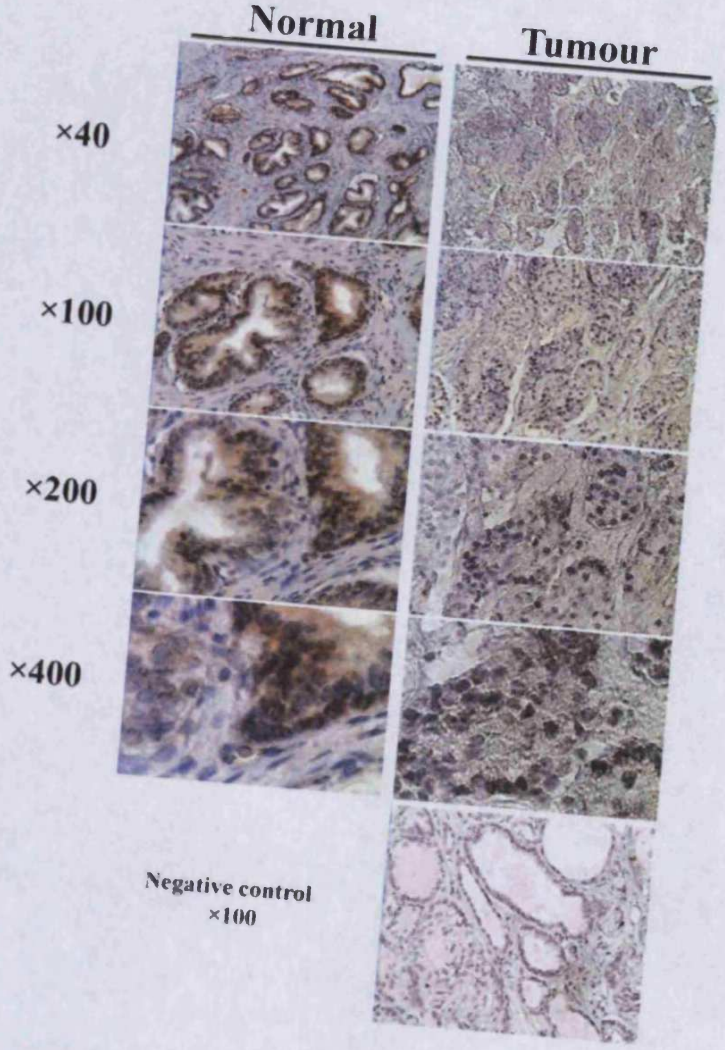

Figure 3.6 Immunohistochemical staining of BMP-9 in the prostate specimens (paraffin sections)

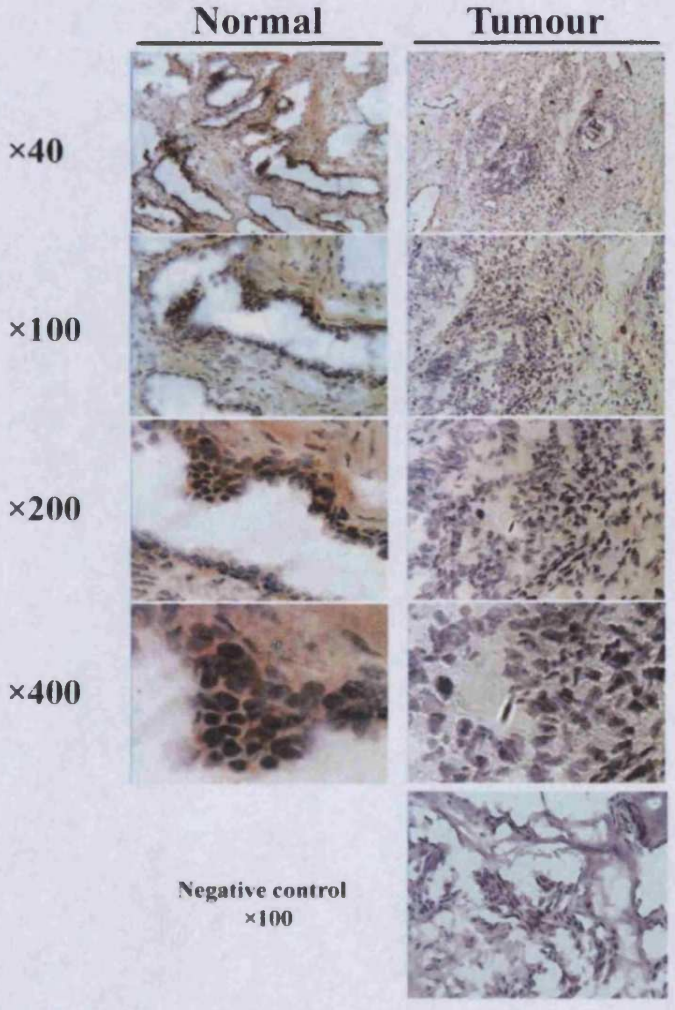

Figure 3.7 Immunohistochemical staining of BMP-10 in human prostate specimens (frozen sections)

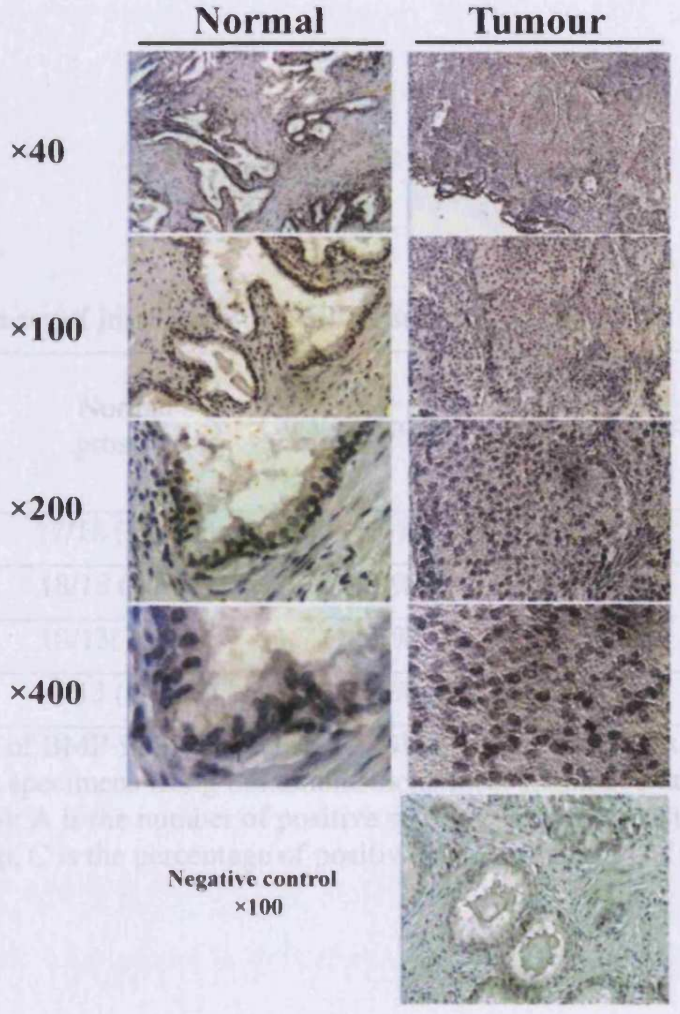

Figure 3.8 Immunohistochemical staining of BMP-10 in human prostate specimens (paraffin sections).

Table 3.1 Summary of immunohistochemical staining results

Molecule	Normal prostate	Prostate cancer		
		Gleason score ≤7	Gleason score >7	Total
BMPR-IB	17/18 (94.4%)	0/7 (0%)	0/1 (0%)	0/8 (0%)
BMPR-II	18/18 (100%)	1/7 (14.3%)	0/1 (0%)	1/8 (12.5%)
BMP-9	10/13(76.9%)	1/7 (14.3%)	0/1 (0%)	1/8 (12.5%)
BMP-10	11/13 (84.6%)	1/7 (14.3%)	0/1 (0%)	1/8 (12.5%)

The expression of BMP-9, BMP-10, and two BMP receptors were examined in human prostate specimens using immunohistochemical staining. Data shown in the table A/B (C %): A is the number of positive staining samples, B is the total number of this subgroup, C is the percentage of positive staining samples of this subgroup.

3.4 Discussion

The seven prostate cell lines used in this study may represent different clinical characteristics of prostate cancer according to their origin. PC-3, DU-145, LNCaP and CA-HPV-10 represent prostate carcinomas which were derived from either primary tumour or secondary tumour, whereas PZ-HPV-7, PNT-1A and PNT2-C2 are immortalised prostate epithelial cell lines. Among the four prostate cancer cell lines, PC-3, DU-145 and LNCaP were derived from various metastatic sites and are more aggressive than CA-HPV-10, which was isolated from a primary tumour. LNCaP is an androgen sensitive cell line, whereas PC-3 and DU-145 are androgen insensitive. These cell lines have been in the past provided different models for the *in vitro* investigation of prostate cancer. We initially examined the mRNA level of BMPs, BMP receptors and intracellular signalling molecules in these seven prostate cell lines using RT-PCR. The subtle variations of BMPs expression have been demonstrated in these cell lines. Although the variation is insufficient in providing a clear distinction for BMPs expression between prostate cancer cells from normal prostate epithelial cells, the results however provided some key and original information for profiling these genes in the prostate cell lines. Furthermore, the results have been instrumental in the subsequent selection of a suitable cell line (or cell lines) to manipulate the expression of BMPs and their receptors. For example, PC-3 was chosen for BMP-9 and BMP-10 over expression as it has a relatively low expression for both BMPs.

The mRNA level of Smad4 and Smad7 were relatively lower in the three more aggressive prostate cancer cell lines compared with the other four cell lines, while Smad1, 2, 3, 5, 6, 8 were expressed at relatively higher and consistent level in these seven cell lines. The loss or reduction of Smad4 has been implicated in the development of prostate cancer (Horvath *et al.*, 2004; Perttu *et al.*, 2006). Our results

are consent with these earlier findings. In addition, the reduction of Smad7 has been observed in most of the prostate cancer cell lines used in the study. Further to the observations reported in the literatures, it is possible that Smad7 may act as an inhibitory factor for BMP signal transduction and may have profound implications in the development and progression of prostate cancer.

We further examined the expression of BMPR-IB and BMPR-II at protein level in human prostate specimens. There was a markedly decreased expression of both receptors in prostate cancer compared with the normal prostate tissues, an observation consistent with the other recent reports (Ide *et al.*, 1997a; Kim *et al.*, 2000; Kim *et al.*, 2004). These two receptors are amongst the most important BMP receptor types in the development and progression of prostate cancer. In the studies represented in the following chapters, we have focused on the role of these two receptors in prostate cancer, particularly their involvement in BMP-9 and BMP-10 signal transduction.

The protein levels of BMP-9 and BMP-10 as visualised by IHC were reduced in prostate cancer tissue compared with normal prostate tissue. This suggests that both BMP-9 and BMP-10 may play important roles in the development and progression of prostate cancer. BMPs, like other members of TGF-β are inhibitory factors of epithelial proliferation (Siegel and Massague, 2003). However, their inhibitory effect on proliferation may be dependent on the expressing pattern of BMP receptors. For example, BMPR-IB and BMPR-II are receptors that mediate the inhibitory effect on cellular proliferation and are decreased in prostate cancer (Kim *et al.*, 2004; Miyazaki *et al.*, 2004). On the other hand, certain BMPs may contribute to the more aggressive features of prostate cancer cells during the progression of disease. For example, BMP-6 stimulates the invasiveness and motility of prostate cancer cells and

may contribute to the bone metastasis of prostate cancer (Haudenschild *et al.*, 2004; Dai *et al.*, 2005). The roles of BMP-9 and BMP-10 in prostate cancer are still unknown.

In addition, the immunohistochemical staining of both receptors and BMP-9 were performed successfully using both frozen specimens and paraffin specimens. BMP-10 staining was not seen in the paraffin specimens, while shown in the frozen specimens. This may due to the degradation of the antigen or the nature of the antibody itself which may not work well in paraffin processed tissues. Improved staining may be achieved through the improvement of retrieving and staining procedures and using an alternative antibody.

In summary, we have assessed the expression of these two receptors, BMP-9 and BMP-10 in human prostate specimens. A large scale retrospective or prospective study, particularly for BMP-9 and BMP-10 may further highlight their clinical value in prostate cancer. The following chapters present further investigation into the molecular and cellular impact of manipulating their expression on prostate cancer cells.

Chapter 4

Knockdown of BMPR-IB and BMPR-II by Hammerhead Ribozyme Transgenes Promotes Cell Growth in Prostate Cancer Cells

4.1 Introduction

Bone morphogenetic proteins (BMPs) are members of the TGF-β superfamily and have been shown to be involved in the development of bone metastasis in prostate cancer. Loss of expression of BMP receptors, type I (BMPR-IA, BMPR-IB), and type II (BMPR-II) , especially BMPR-II in both prostate cancer tissue and cell lines, has been implicated in the progression of prostate cancer (Ide *et al.*, 1997a; Kim *et al.*, 2000; Kim *et al.*, 2004). This inhibitory effect on tumour growth, mediated through BMPR-II, had been demonstrated in an *in vivo* study, by using a nude mice model which were inoculated subcutaneous with a BMPR-II knock-out prostate cancer cell line (PC3M) (Kim *et al.*, 2004). While the PC-3 cells constitutively express an active BMPR-IB (c.a.-BMPR-IB) in a tetracycline (Tet)-regulated manner, the Tet/doxycycline-regulated expression of the c.a.-BMPRIB results in the inhibition of both the *in vitro* cell proliferation and tumour growth *in vivo* (Miyazaki *et al.*, 2004). These studies suggest that both BMPR-IB and BMPR-II play crucial roles in the control of the cellular behaviour of prostate cancer cells. However, the role played by these two receptors in the cells and the molecular signalling pathways elicited by BMP-9 and BMP-10 in prostate cancer cells are still unclear, and formed the main aim of our following studies. Therefore, we constructed a ribozyme transgene targeting each receptor.

4.2 Materials and Methods

4.2.1 Materials.

Polyclonal goat anti-BMPR-IB IgG (SC-5679), polyclonal goat anti-BMPR-II IgG (SC-5683), and monoclonal mouse anti-Actin (SC-8432) were obtained from Santa

Cruz Biotechnology (Santa Cruz, California, USA). Western blotting luminol reagent Peroxidase-conjugated anti-goat and anti-mouse IgG for western blotting were purchased from Sigma-Aldrich Ltd (Poole, Dorset, England, UK). PC-3 cells were routinely maintained in DMEM-F12 medium supplemented with 10% foetal calf serum and antibiotics.

4.2.2 Construction of ribozyme transgenes targeting at BMPR-IB and BMPR-II.

A hammerhead ribozyme was designed based on the secondary structure of the BMPR-1B or BMPR-2 mRNA. Figure 4.1A shows the secondary structure of BMPR-1B, which was generated using Zuker's RNA mFold programme (Zuker, 2003). The sequence in the mFold programme was the entire coding region of human BMP-R1B. According to both the cleavage site of target gene and the sequence of hammerhead ribozyme, the primers were designed (refer to Table 2.4). These oligo primers had the following characteristics: restriction sites (Spe1 (TGATCA) on the 5' end of the reverse primer and Pst1 (CTGCAG) on the 5' end of the forward primer) were included for cloning purpose; the primers permit template free amplification during PCR; Hammerhead ribozyme and antisense were pre-arranged in order that correctly oriented ribozymes were amplified.

The ribozymes were synthesized by using touchdown PCR (Figure 4.1B). The ribozymes thus generated carried an A- overhang at the 3' end of the product. The ribozyme was subsequently TA cloned into a mammalian expression pEF6/V5-His-TOPO plasmid vector (Invitrogen Ltd., Paisley, UK) (Figure 4.1C), using a protocol as already described in chapter-2. Following ligation, the vector was then transformed into *E. Coli*, using the heat shock method. After one-hour incubation in

SOC medium which allows the bacteria with transgenes to generate resistance to the antibiotic, the bacteria were plated and incubated overnight at 37°C. The clones were then analysed using direction specific PCR, which verified both presence and direction of the ribozymes in the clone (Figure 4.1D). Each colony was tested used two separated PCR reactions: one using T7F primer coupled with RBBMR primer and the other using T7F with RBTPF primer (sequences of primers in Table 2.4). Colonies with T7F/RBBMR reaction positive (and with the correct /sided product) and T7F/RBTPF negative were regarded as the colonies with correctly oriented ribozyme insert were grown (i.e. colonies C1-C4 in figure 4.1D). These colonies were then carefully picked and grown up in large volume of LB medium (with ampicillin). The respective plasmid was finally extracted, and verified using DNA electrophoresis (Figure 2.1E).

4.2.3 Transfection of PC-3 cells and establishment of the stable transfectants.

Ribozyme transgenes and empty plasmid vectors were then transfected into separate groups of PC-3 cells using an electroporator (Easjet Plus, EquiBio Ltd, Kent, UK), with a voltage at 270v. The cells were immediately transferred to 25 cm^3 tissue culture flasks containing 5ml of pre-warmed culture medium. Selection of transfectants began when the cells reached 50%-70% confluence. The selection of positive cells was with a medium that contained the antibiotic blasticidin (Sigma-Aldrich, Inc., Poole, Dorset, England, UK) at 5μg/ml. After selection, the surviving cells were then expanded into a larger population, and used for verification for the presence of the ribozyme and effects of the ribozymes on the expression of the respective target gene transcript using RT-PCR. Verified transfectant were cultured

in maintenance medium (blasticidin 0.5μg/ml) and grown to sufficient numbers for experimental studies. The selection took upto to 2 weeks.

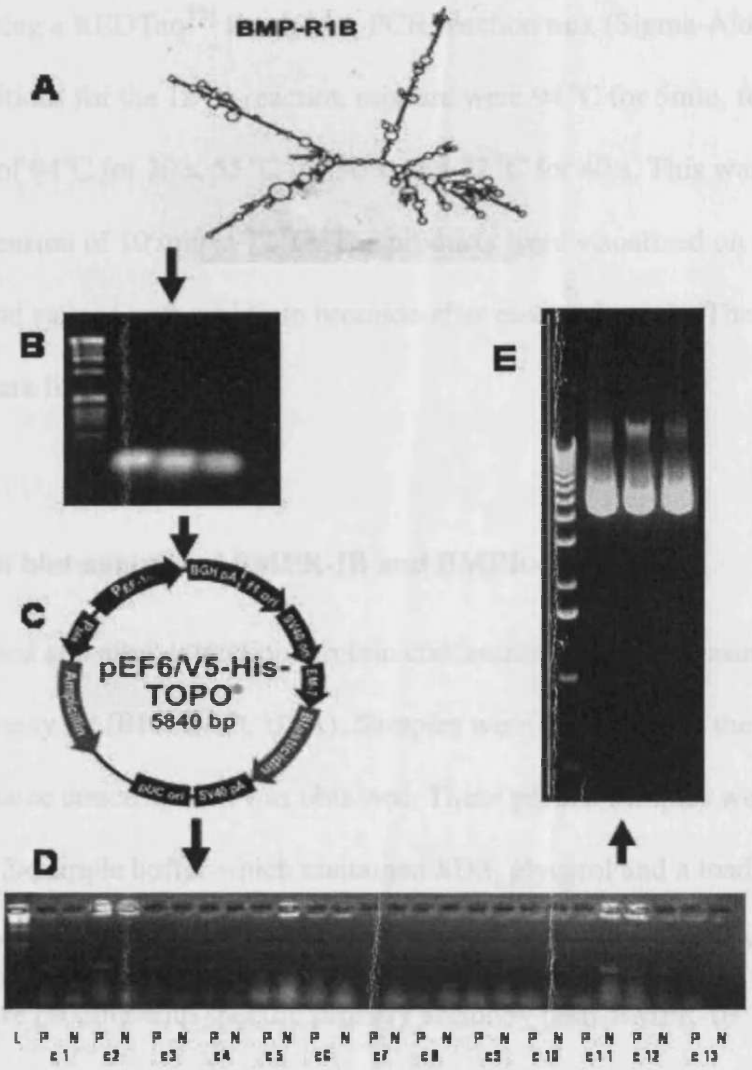

Figure 4.1 Construction of ribozyme transgenes.
(A) is the secondary structure of BMPR-IB mRNA. The ribozymes were synthesised using touchdown PCR procedure (B), and then were cloned into the pEF6/V5-His-TOPO plasmid vector (C). (D) The clones were analysed using PCR after transformation. L is the DNA ladder, P is the right orientation, N is the wrong orientation. The clones (c1-4) are the clones which the ribozymes were inserted in the right orientation. The clones (c5-8) are empty plasmid vector only. The clones (c9-13) have the ribozymes inserted in the reverse (wrong) orientation. The ribozyme transgenes were finally extracted, and verified using DNA electrophoresis (E).

4.2.4 RT-PCR for BMPR-IB, BMPR-II and β-actin.

RNA was isolated from the cells, and cDNA was synthesised by reverse transcription using 0.25μg RNA in a 20-μl-reaction mixture as described in section 2.3. PCR was undertaken using a REDTaq™ ReadyMix PCR reaction mix (Sigma-Aldrich, Inc.). Cycling conditions for the 12-μl-reaction mixture were 94 °C for 5min, followed by 30-40 cycles of 94°C for 30 s, 55 °C for 30 s, and 72 °C for 40 s. This was followed by a final extension of 10 min at 72 °C. The products were visualized on a 2% agarose gel and stained with ethidium bromide after electrophoresis. The PCR primers used are listed in Table 2.1.

4.2.5 Western blot analysis of BMPR-IB and BMPR-II.

Cells were lysed and after extraction, protein concentrations were measured using the DC Protein Assay kit (BIO-RAD, USA). Samples were diluted using the lysis buffer in order that same concentration was obtained. These protein samples were then mixed with a 2×sample buffer which contained SDS, glycerol and a loading dye. After electrophoresis, proteins were blotted onto nitrocellulose sheets, followed by blocking before probing with specific primary antibody (anti-BMPR-IB 1:250 or anti-BMPR-II 1:200), and corresponding peroxidase-conjugated secondary antibodies (1:1000). Protein bands were visualized with a SupersignalTM West Dura system (Pierce Biotechnology, USA).

4.2.6 *In vitro* cell growth assay

We used the method previously reported by Jiang *et al* (Jiang *et al.*, 2005b). Cell growth was assessed after a period of incubation (up to 5 days). Crystal violet was

used to stain cells, and absorbance which represents cells number was determined at a wavelength of 540nm using a spectrophotometer (BIO-TEK, Elx800, UK). The growth rate was calculated as a percentage using the absorbance of day 1 as a baseline.

4.2.7 *In vitro* invasion assay

This technique was previously reported (Jiang *et al.*, 1995a). Transwell inserts with 8 μm pore size were coated with 50 μg Matrigel and dried. The Matrigel was rehydrated before use. 20,000 cells were added to each well. After 96 hours cells that had migrated through the matrix to the other side of the insert were fixed (4% formalin), stained with 0.5% (weight/volume) crystal violet and counted under a microscope.

4.3 Results

4.3.1 The effect of ribozyme transgenes on mRNA level of BMPR-IB and BMPR-II in PC-3 cells

BMPR-IB and BMPR-II are both detectable in PC-3 cells. In addition, it is also the cell line we use for forced expression experiments BMP-9 and BMP-10, as the levels of both BMPs are low or absent. Therefore, we transfected PC-3 cells with empty plasmids and the ribozyme transgenes which target BMPR-IB or BMPR-II, respectively. The expression of BMPR-IB mRNA was completely eliminated from PC-3 cells by the ribozyme transgene ($PC\text{-}3^{\Delta BMPR\text{-}IB}$) in comparison to the level of expression seen in wild type ($PC\text{-}3^{WT}$) cells and PC-3 empty plasmid ($PC\text{-}3^{pEF/His}$) cells (Figure 4.2A). After optimisation of the PCR parameters by running more

cycles for the PCR reactions, we were able to identify a decrease of BMPR-II transcripts in PC-3$^{\Delta BMPR\text{-}II}$ cells, compared to both PC-3^{WT} and PC-3$^{pEF/His}$ cells (Figure 4.2B).

4.3.2 Knockdown of BMPR-IB and BMPR-II transcripts in PC-3 cells by ribozyme transgenes results in loss of the respective BMP receptor protein

We also examined if there was a resultant reduction of protein levels following the knockdown of both receptors' mRNA in the PC-3 cells. Western blot analysis was employed here. As shown in figure 4.3A, there was a significant reduction of BMPR-IB protein (45kDa) in PC-3$^{\Delta BMPR\text{-}IB}$ cells, in comparison to the PC-3^{WT} and PC-3$^{pEF/His}$ cells (Figure 4.3A top panel). In fact, the BMP- R1B protein was not detectable in PC-3$^{\Delta BMPR\text{-}IB}$ cells. The protein yield of BMPR-II (70-80kDa) was also decreased after the knockdown of BMPR-II transcripts in PC-3$^{\Delta BMPR\text{-}II}$ cells, which is shown in Figure 4.3B.

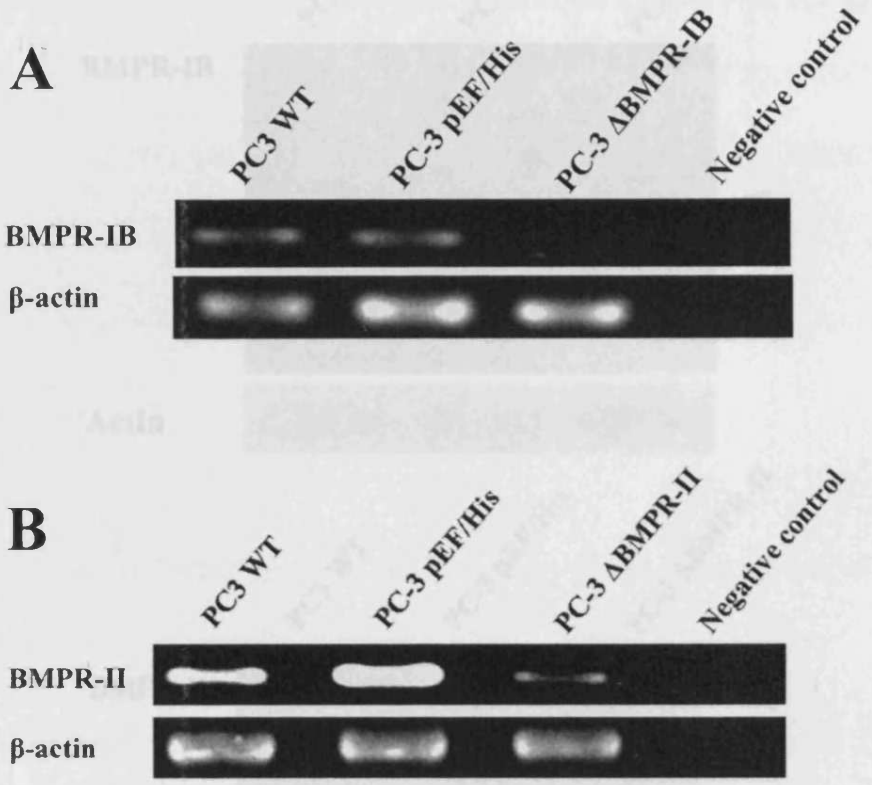

Figure 4.2 RT-PCR for mRNA level of BMPR-IB and BMPR-II in PC-3 cells following knockdown by ribozyme transgenes.
(A) The gene transcripts of BMPR-IB were diminished in the PC-$3^{\Delta BMPR\text{-}IB}$ cells by ribozyme transgenes. The PCR reactions were performed 30 cycles.
(B) The mRNA level of BMPR-II was also markedly reduced in the PC-$3^{\Delta BMPR\text{-}II}$, compared with the PC-$3^{WT}$ and PC-$3^{pEF/His}$. The PCR reactions were run 40 cycles. Shown are representative results of three replicate PCR reactions..

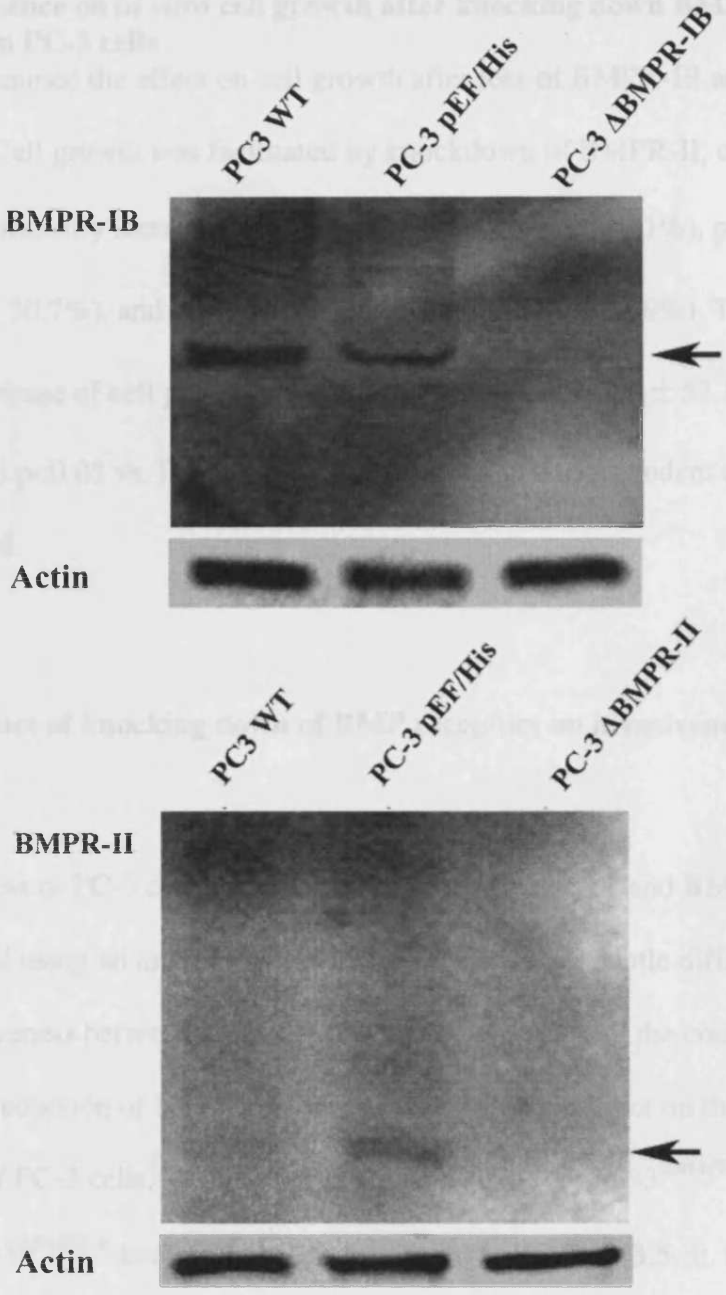

Figure 4.3 Western blot analysis for protein production of BMPR-IB and BMPR-II in PC-3 cells following knockdown using ribozyme transgenes.
(A) The protein production of BMPR-IB was eliminated in the PC-$3^{\Delta BMPR\text{-}IB}$ cells, compared with the PC-3^{WT} and PC-$3^{pEF/His}$. 15ug total protein of each sample was loaded for the SDS-PAGE.
(B) A similar reduction of BMPR-II protein was also revealed in PC-$3^{\Delta BMPR\text{-}II}$, compared with both PC-$3^{WT}$ and PC-$3^{pEF/His}$ cells. Approximate 25ug total protein of each sample was used for the western blot analysis of BMPR-II.
Shown are representative experiments of three experiments for each receptor.

4.3.4 The influence on *in vitro* cell growth after knocking down BMPR-IB and BMPR-II from PC-3 cells

We further examined the effect on cell growth after loss of BMPR-IB and BMPR-II in PC-3 cells. Cell growth was facilitated by knockdown of BMPR-II, cell growth at day 4 was significantly increased in PC-$3^{\Delta BMPR\text{-}II}$ (543.8%$\pm$119.1%), $p<0.01$ vs. PC-3^{WT} (239.3%$\pm$30.7%), and $p<0.05$ vs. PC-$3^{pEF/His}$ (209.9%$\pm$26.9%). There was also a markedly increase of cell growth in PC-$3^{\Delta BMPR\text{-}IB}$ cells (423.4%$\pm$57.1%), $p<0.01$ vs. PC-3^{WT} and $p<0.05$ vs. PC-$3^{pEF/His}$ (Figure 4.4). Three independent experiments were performed.

4.3.5 The impact of knocking down of BMP receptors on invasiveness of PC-3 cells

The invasiveness of PC-3 cells after knocking down BMPR-IB and BMPR-II from was determined using an *in vitro* invasion assay. There were subtle differences of cellular invasiveness between the BMPRs knockdown cells and the control cells. However, the reduction of both receptors has no significant effect on the invasiveness of PC-3 cells, the number of invading cells for PC-$3^{\Delta BMPR\text{-}IB}$ being 5.0 $\pm$ 2.0 and PC-$3^{\Delta BMPR\text{-}II}$ being 5.2 $\pm$ 2.9, compared to PC-3^{WT} (3.5 $\pm$ 1.2) and PC-$3^{pEF/His}$ (4.3 $\pm$ 2.3) (Figure 4.5).

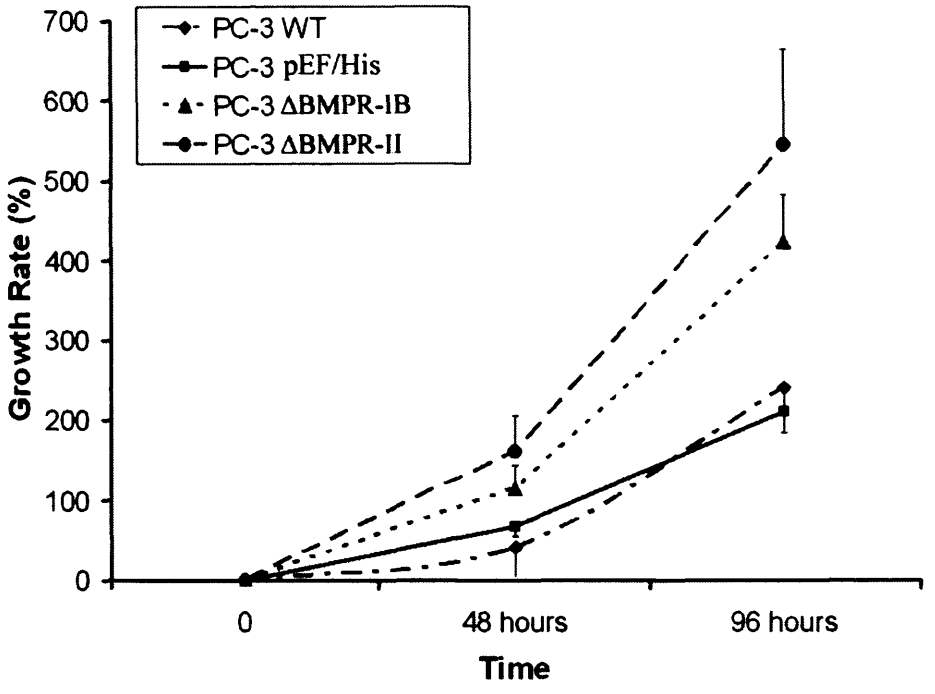

	PC-3 WT (mean±SD, n=6)	PC-3 pEF/His (mean±SD, n=6)	PC-3$^{\Delta BMPR-IB}$ (mean±SD, n=6)	PC-3$^{\Delta BMPR-II}$ (mean±SD, n=6)
48 hrs	**41.0±37.2%**	**66.1±12.1%**	**114.0±28.6%**	**159.8±46.0%**
96 hrs	**239.3±30.7%**	**210.0±23.9%**	**423.4±57.1%**	**543.8±119.1%**

Figure 4.4 Effect on cell growth of PC-3 cells by knockdown of BMPR-IB and BMPR-II using *in vitro* cell growth assay. The error bars represents standard deviation.

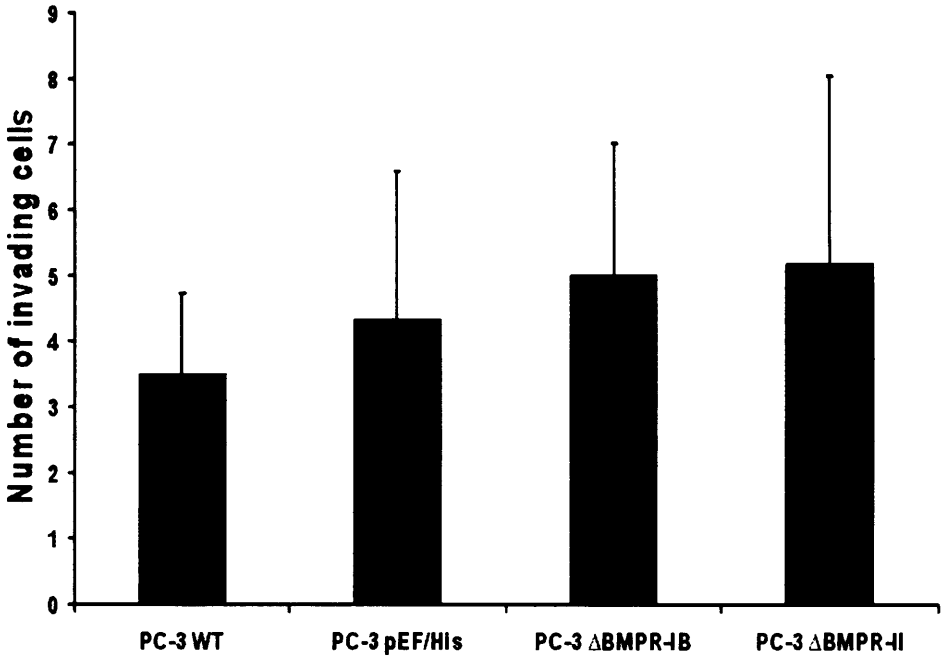

Figure 4.5 Influence on the invasiveness of PC-3 cells by knockdown of BMPR-IB and BMPR-II using *in vitro* invasion assay. Error bars represent standard deviations, n=9 and the experiment were repeated three times.

4.4 Discussion

BMPR-IB and BMPR-II have been demonstrated that express at lower level in prostate cancer, which is consistent with our observations in prostate specimens using immunohistochemical staining (Chapter 3). It has also been demonstrated that both receptors are involved in the inhibitory effects of BMPs on *in vitro* cell proliferation and *in vivo* tumour growth (Ide *et al.*, 1997a; Kim *et al.*, 2004). The reduced expression of both receptors is partially responsible for the uncontrolled growth of tumour, particularly in prostate cancer. The studies collectively indicate possible implications of both BMPR-IB and BMPR-II.

In current studies, we utilised the hammerhead ribozymes to interfere the expression of BMPR-IB and BMPR-II after transcription. BMPR-IB and BMPR-II expression can be successfully down-regulated by the application of ribozyme transgenes *in vitro*. The ribozymes described here are highly effective and have dramatically reduced the levels of the respective receptor at both mRNA and most importantly protein levels. These tools not only allow generation of successful cell models in dissecting the impact of the individual receptor in the mediation of a given BMP, but may also have an important therapeutic role.

Loss of BMPR-IB and BMPR-II from prostate cancer cells is associated with increased growth. These demonstrated that both BMPR-IB and BMPR-II are receptors mediating inhibitory effects of BMPs on cellular growth in prostate cancer. The current study is unable to answer which specific BMP may contribute to this receptor-controlled cell growth. However, it is anticipated that one or more of the endogenous BMPs that are expressed in the cells may be responsible. For example, BMP-2, 4, 6 and 7, which are expressed in prostate cancer cells (Chapter 3, Figure 3.1). These endogenous BMPs and BMP antagonists, Noggin and Follistatin, are

secreted by tumour cells and may contribute to cell growth restriction. The effects on cell growth of these BMPs have been discussed in Chapter 1.

We also investigated the effects on the invasiveness of prostate cancer cells by knocking down BMPR-IB and BMPR-II. There is no significant alteration of invasiveness after loss of either receptor. This suggests these two receptors may not be responsible for the promotion of invasiveness and motilities of tumour cells by BMPs.

Taken together, we have developed a hammer head ribozyme transgene targeting each receptor, BMPR-IB and BMPR-II. These cells in which the receptors have been knocked down will be utilised for further investigation of signal transduction of BMP, and the mediated effects on the biological behaviours of prostate cancer cells.

CHAPTER 5

Endogenous BMP-7 Controls the Motility of Prostate Cancer Cells through Regulation of BMP Antagonists

5.1 Introduction

The interaction between prostatic tumour cells and factors in the bone microenvironment appear to contribute to their predilection for boney sites in metastatic prostate cancer, and also the predominantly osteoblastic character of metastases from prostate tumours. BMPs are some of the most powerful bone inductive factors isolated from bone matrix, and have been implicated in the development of boney metastases from prostate cancer. Bentley *et al* detected BMP-6 expression in the prostate tissue of over 50% of patients with metastatic prostate adenocarcinoma, but it was not detected in non-metastatic or benign prostate samples. They concluded that BMPs play a role in the osteoinductive activity of prostate metastases and that the pattern of expression of individual BMPs may be important in the pathogenesis of osteoblastic type metastases associated with prostate adenocarcinoma (Bentley *et al.*, 1992). An elevated level of BMP-6 is associated with higher grade primary tumours and advanced prostate cancer with metastasis. It may also contribute to the progression of prostate cancer independently from androgen stimulation (Barnes *et al.*, 1995; Hamdy *et al.*, 1997; Tamada *et al.*, 2001). BMP-6 can promote the metastasis of prostate cancer to bone through a dual mechanism, in which BMP-6 not only facilitates the invasion of prostate cancer cells, it can also induce osteoblastic activity once they arrive in the bone microenvironment (Dai *et al.*, 2005).

In contrast to this seeming close relationship between BMP-6 and bone metastasis, the relationship has not been consistently demonstrated with other BMPs. For example, BMP-2, -4 and BMP-7 are expressed predominantly in normal prostate tissues. They tend to exhibit lower levels or loss of expression during the

development and the progression of prostate cancer (Harris *et al.*, 1994; Thomas *et al.*, 2001; Horvath *et al.*, 2004; Masuda *et al.*, 2004).

The expression of BMP-7 transcripts is decreased in local recurrent prostate cancer tissues after hormonal therapy and is increased by di-hydrotestosterone, suggesting that its expression is androgen-dependent in the human prostate (Masuda *et al.*, 2004). Thus, the loss of BMP7 expression in prostate tumours may be related to the shift in phenotype from androgen-dependent to androgen-independent activity within the cancer cells. However, it is interesting to note that BMP-7 is re-expressed in metastatic bone lesions at a much higher level than that found in the normal bone tissue surrounding the lesion, implicating it in the development of osteoblastic metastases (Masuda *et al.*, 2003). Furthermore, evidence from Yang *et al* demonstrates that the expression of BMP-7 is increased with the growth of prostatic adenocarcinoma in the *Pten* conditional deletion mouse model of prostate cancer (Yang *et al.*, 2005). These studies collectively suggest that BMP-7 plays an important role in the development and progression of bony metastases from prostate cancer.

Despite these observations, the biological function of BMP-7 on prostate cells remains highly controversial. For example, it has been shown in a recent study that BMP-7 inhibits the proliferation of both androgen-sensitive and androgen-insensitive prostate cancer cells (Miyazaki *et al.*, 2004). It can also induce an epithelial-mesenchymal transdifferentiation in PC-3 cells which promotes their invasive potential (Yang *et al.*, 2005). However, in other studies using the same cell lines, BMP-7 was found to have no effect on proliferation, migration or invasion (Feeley and Lieberman, 2006). Although the use of different models, different cell lines, different experimental settings such as different concentrations of the BMPs and

different source of BMPs employed may have contributed to the obvious discrepancies, the possibility also exists that the source of the BMP (i.e. exogenous vs endogenous), the involvement of BMP antagonists (both exogenous and endogenous), and difference in the receptor status (thus intracellular signalling pathways) may also have a role to play. For example, Noggin is an antagonist to BMP-7 and other BMPs (Re'em-Kalma *et al.*, 1995; Chang and Hemmati-Brivanlou, 1999; Haudenschild *et al.*, 2004; Pera *et al.*, 2004; Zhu *et al.*, 2006), and Noggin expression can be induced in osteoblasts by exposure to exogenous recombinant human BMP2, BMP4 and BMP6 (Gazzerro *et al.*, 1998). Furthermore, as shown in earlier chapters, different cell lines have different expression pattern of endogenous BMPs and have different patterns of BMP receptors in these cells.

In order to investigate what role endogenous BMP-7 plays in the control of growth and migration of prostate cancer cells, we created BMP-7 knockdown cell line using hammerhead ribozymes, specific to human BMP-7. We also evaluated the role of endogenous BMP-7 in regulation of BMP antagonists, Noggin and Follistatin.

5.2 Materials and Methods

5.2.1 Materials.

The following human prostate cancer cell lines were used: PC-3, DU-145, LNCaPFGC, CA-HPV-10, PZ-HPV-7, PNT-1A and PNT-2C2. The cells were routinely maintained in Dulbecco's Modified Eagle Medium (DMEM) -F12 medium supplemented with 10% foetal calf serum and antibiotics. Anti-BMP7, anti-Noggin and anti-Follistatin antibodies were obtained from Santa Cruz Biotechnology (Santa Cruz, California, USA). Both mouse anti-paxillin IgG and mouse anti-FAK IgG were

purchased from BD Transduction Laboratories (Lexington, KY, USA). The recombinant human BMP-7 (rh-BMP-7) was obtained from R&D System, Inc. (R&D System, Ltd. Abingdon, UK).

5.2.2 Construction of Ribozyme Transgene Targeting Human BMP-7

Anti-human BMP-7 hammerhead ribozymes were designed based on the secondary structure of the gene which was generated using Zuker's RNA mFold programme (Zuker, 2003). The ribozymes were synthesized by touchdown PCR, followed by ligation into the pcDNA3.1/NT-GFP-TOPO vector using the GFP Fusion TOPO TA Expression Kit (Invitrogen Ltd., Paisley, UK) (table-1) (Jiang *et al.*, 2005b). The vector was then transformed into *E. Coli* and amplified. Following verification of the presence and direction of the ribozymes (same as the procedure introduced in Chapter 4, section 4.2.2), *E. coli* colonies with correctly oriented ribozyme insert were grown and the plasmid extracted using an extraction kit (Genelute Plasmid Mini-prep Kit, Sigma-Aldrich, Inc., Poole, Dorset, England, UK).

5.2.3 Electroporation and Establishment of Stable Transfectants

Ribozyme transgenes and control empty plasmids were transfected into PC-3 cells individually through an electroporation. After up to 3 weeks selection with G418 at 100μg, the transfectants were verified. The stable transfectants were then cultured in maintenance medium (G418 concentration = 25μg/ml), and were used in the following studies.

5.2.4 RNA Isolation and Reverse Transcription PCR

RNA was isolated from the cells using Total RNA Isolation Reagent (ABgene, Epsom, England, UK). cDNA was synthesized by using 0.25μg RNA in a 20-μl-reaction mixture as per the protocol contained in the DuraScript™ RT-PCR kit (Sigma-Aldrich, Inc., Poole, Dorset, England, UK). PCR was undertaken using a REDTaq™ ReadyMix PCR reaction mix (Sigma-Aldrich, Inc., Poole, Dorset, England, UK) (primer sequences in Table-1). Cycling conditions were 94 °C for 5min, followed by 36 cycles of 94°C for 30 s, 55 °C for 30 s, and 72 °C for 40 s. This was followed by a final extension of 10 min at 72 °C. The products were visualized on a 2% agarose gel and stained with ethidium bromide after electrophoresis.

5.2.5 SDS-PAGE and Western Blot Procedure

Cells were lysed in HCMF buffer with addition of 1% Triton, 0.1% SDS, 2 mM $CaCl_2$, 100 μg/ml phenylmethylsulfonyl fluoride, 1 μg/ml leupeptin, and 1 μg/ml aprotinin for 30 min before clarification in a centrifuge at 13,000 × g for 10 min. Protein concentrations were measured using the DC Protein Assay kit (BIO-RAD), and were quantified using a spectrophotometer (BIO-TEK, ELx800). Equal amounts of protein from each cell sample were loaded onto a 10% polyacrylamide gel. After electrophoresis, proteins were blotted onto nitrocellulose sheets and blocked in 10% skimmed milk for 60 min before probing with the appropriate primary antibody and peroxidase-conjugated secondary antibodies. A molecular weight marker mixture (SDS-6H, Sigma-Aldrich, Inc., Poole, Dorset, England, UK) was used to determine the protein size. Protein band signal was visualized with the Supersignal™ West Dura system (Pierce Biotechnology, Inc., Rockford, IL, USA), and images obtained using an UVITech imager (UVITech, Inc., Cambridge, England, UK).

5.2.6 Immunocytochemical Staining for BMP-7

We used a standard procedure described in section 2.4.3. Cells in glass chamber slides were fixed after each experiment, and then permeabilized with 0.1% Triton for 5 minutes in TBS. Following blocking with horse serum in the OptiMax Wash Buffer (BioGenex, San Ramon, USA), anti-BMP-7 antibody (used at dilution 1:200 from the original) was added to the cells for 60 minutes. After extensive washing, a biotinylated secondary antibody (used at 1:1000) and ABC solution was added, separated by extensive washings. The staining was visualised using the DAB kit (VECTASTA I N® ABC system, Vector Laboratories, Inc., Nottingham, England, UK).

5.2.7 *In vitro* cell growth assay

This was based on previously described method (section 2.8.1). Cell growth was assessed after a period of incubation (upto 3 days). Crystal violet was used to stain cells, and the absorbance was determined at a wavelength of 540nm using a spectrophotometer (BIO-TEK, Elx800, UK). The absorbance represents the cell number.

5.2.8 *In vitro* invasion assay

We used a standard procedure as previously described in section 2.8.4. Transwell inserts with 8 μm pore size were coated with 50 μg Matrigel and air-dried. The Matrigel was rehydrated before use. 20,000 cells were added to each well. After 96

hours, cells that had migrated through the matrix and pores were fixed with 4% formalin, stained with 0.5% crystal violet and counted.

5.2.9 *In vitro* motility assay using Cytodex-2 beads

We followed a protocol previously described in section 2.8.3.

5.2.10 *In vitro* Cell-matrix adhesion assay

The cell-Matrix adhesion was analysed according to the method introduced in Chapter 2, section 2.8.5. 8 wells were set for each cell lines, and the experiment was performed three times.

5.2. 11 Immunofluorescent Staining of Paxillin and FAK

We used a standard procedure as previously described (Jiang *et al.*, 1999b; Parr *et al.*, 2001; Ye *et al.*, 2003). Wild type PC-3 cells ($PC\text{-}3^{WT}$), plasmid control cells ($PC\text{-}3^{pcDNA/GFP}$) and ribozyme transgene cells ($PC\text{-}3^{\Delta BMP7}$), were seeded in Matrigel-coated chamber slides (Nunc, Denmark), at a density of 20,000 cells/well. After 60 minutes incubation, the cells were fixed in ice cold ethanol, and were then rehydrated and permeabilized (0.1% Triton-X100) before staining. Anti-paxillin or anti-FAK antibody was added (used at 1:1500 dilution from the original) and then, following extensive washing, labelled with anti-mouse IgG TRITC conjugate (Sigma-Aldrich, Inc., Poole, Dorset, England, UK). The staining was visualized by fluorescent microscopy (Olympus, BX51, Olympus UK Ltd., London, UK) using a cooled digital camera (Hamamatsu, C4742-80, Hamamatsu Photonics (UK) Ltd.,

Hertfordshire, UK). Imaging process and analysis was conducted using analySIS imaging analysis package (verision 5.0, Olympus Soft Imaging System GmbH, Helperby, North Yorkshire, UK).

5.2.12 Data Analysis

The Minitab statistical software package (version 14) was used for analysis. Non-normally distributed data was assessed using the Mann-Whitney test, and the two sample t-test was used for normally distributed data. Differences were considered to be statistically significant at $p<0.05$.

5.3 Results

5.3.1 Expression of BMP-2, 4, 6 and 7, Noggin, Follistatin and BMP receptors in prostate cancer cell lines

PC-3, DU-145, LNCaP and CA-HPV-10 are cancer cell lines, whereas PZHPV-7, PNT-1A and PNT2-C2 are immortalised prostatic epithelial cell lines. We screened these cell lines for the expression of BMP-2, 4, 6 and 7, two BMP receptors, Noggin and Follistatin, using conventional reverse transcription PCR (RT-PCR), which were described previously in Chapter 3, section 3.3.1 (Figure 3.1) and section 3.3.2 (Figure 3.2).

5.3.2 Manipulation of BMP-7 expression by ribozyme transgene

To investigate the role of endogenous BMP-7 in prostate cancer, we used PC-3 cells, a cell line originally derived from a bony metastasis. It expresses a low but

detectable level of BMP-7, which may closely reflect the clinical situation in advanced prostate cancer.

The expression of BMP-7 mRNA was completely eliminated from PC-3 cells by the ribozyme transgene in comparison to the level of expression seen in wild type ($PC\text{-}3^{WT}$) cells and PC-3 empty plasmid ($PC\text{-}3^{pcDNA/GFP}$) cells (Figure 5.1A). It was accompanied with an obvious reduction in the BMP-7 protein level in PC-3 ribozyme transgene ($PC\text{-}3^{\Delta BMP7}$) cells (Figure 5.1B and 5.1C).

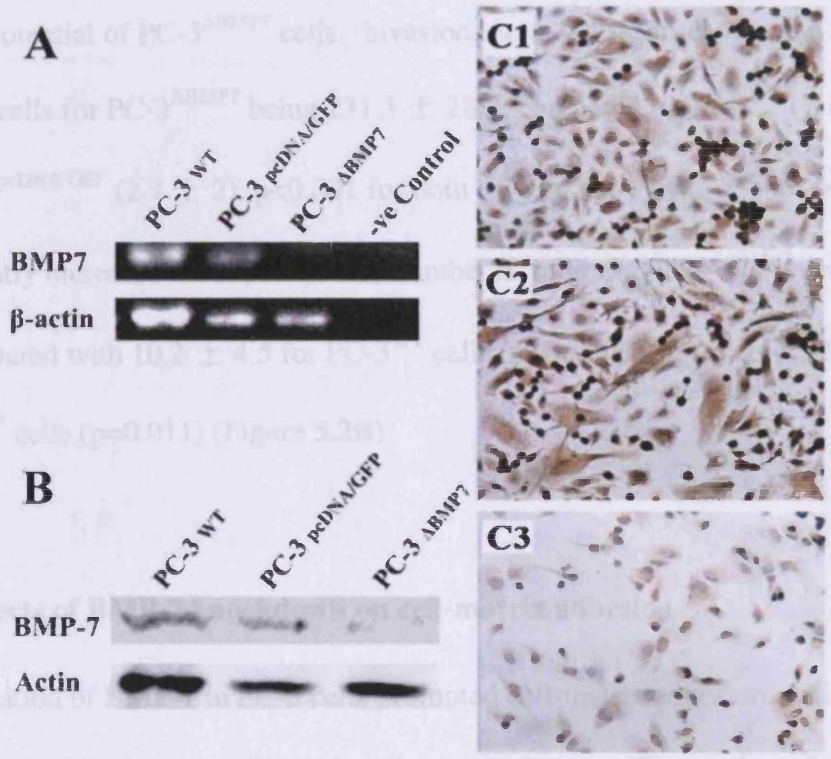

Figure 5.1 The expression of BMP-7 in PC-3 cells after transfection with the ribozyme transgene.

(A) The level of BMP-7 mRNA was qualitatively detected using RT-PCR. BMP-7 transcripts were detectable in the PC-3 wild type cells ($PC\text{-}3^{WT}$) and PC-3 empty plasmid cells ($PC\text{-}3^{pcDNA/GFP}$), but not in PC-3 ribozyme transgene cells ($PC\text{-}3^{\Delta BMP7}$).

(B) The protein level of BMP-7 was also reduced by the ribozyme transgene, as revealed by western blot and,

(C) immunocytochemical staining($\times 100$). C1: immunostaining of BMP-7 in $PC\text{-}3^{WT}$ cells; C2: BMP7 staining in PC-3 $^{pcDNA/GFP}$ cells; C3: BMP-7 staining in $PC\text{-}3^{\Delta BMP7}$ cells.

5.3.3 Loss of endogenous BMP-7 resulted in an increase in both invasion and motility in PC-3 cells

Loss of BMP-7 (PC-$3^{\Delta BMP7}$) had no significant effects on the rate of cell growth (Figure 5.2D). However, there were significant changes in both the invasion and motility potential of PC-$3^{\Delta BMP7}$ cells. Invasion increased significantly, the number of invading cells for PC-$3^{\Delta BMP7}$ being 231.3 $\pm$ 28.6, compared to PC-3^{WT} (7.1 $\pm$ 4.4) and PC-$3^{pcDNA/GFP}$ (2.7 $\pm$ 2), $p<0.001$ for both (Figure 5.2A). PC-$3^{\Delta BMP7}$ cells also significantly increased the motility. The number of migrating PC-$^{3\Delta BMP7}$ cells 24 $\pm$ 7.5, compared with 10.2 $\pm$ 4.5 for PC-3^{WT} cells ($p<0.01$) and 11.3 $\pm$ 7.5 for the PC-$3^{pcDNA/GFP}$ cells ($p=0.011$) (Figure 5.2B).

5.3.4 Effects of BMP-7 knockdown on cell-matrix adhesion

Elimination of BMP-7 in PC-3 cells promoted cell-matrix adhesion, which assessed using the *in vitro* cell-matrix adhesion technique. The number of adherent cells for the PC-$3^{\Delta BMP7}$ line being 38.2$\pm$15.2, vs 8.42$\pm$ 4.01 for PC-3^{WT} ($p<0.001$), and 6.83$\pm$2.89 for PC-$3^{pcDNA/GFP}$ ($p<0.001$) (Figure 5.2C). We further assessed the downstream events following cell adhesion to the matrix surface by staining for two of the matrix adhesion regulatory molecules, Paxillin and FAK ($p125^{FAK}$). The staining for both FAK and paxillin in the BMP-7 knockdown PC-3 cells (PC$3^{\Delta BMP7}$) was dramatically enhanced at the focal adhesion sites (Figure 5.3).

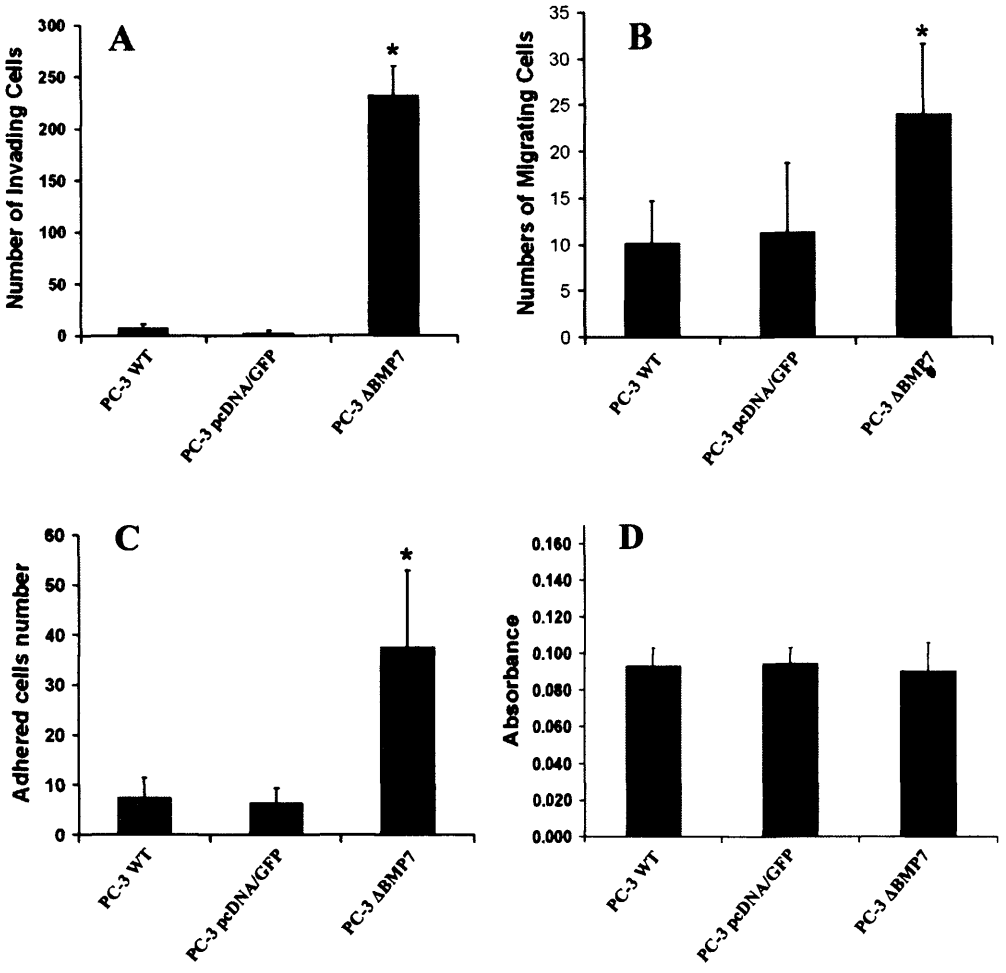

Figure 5.2 Loss of BMP-7 and its effect on invasion (A), motility (B), adhesion (C) and growth (D) in PC-3 cells.

(A) The invasiveness of PC-$3^{\Delta BMP7}$ cells (reduced BMP7 expression) was increased by approximately 30 times that of PC-3 wild type cells. * $p<0.01$, vs. PC-3^{WT} and PC-$3^{pcDNA/GFP}$ cells.

(B) The motility was also increased in PC-$3^{\Delta BMP7}$ cells. * $p<0.01$, vs. PC-3^{WT} and PC-$3^{pcDNA/GFP}$ cells.

(C) Matrix Adhesion in PC-$3^{\Delta BMP7}$ cells was increased, as demonstrated by the cell-matrix adhesion assay. * $p<0.01$ vs PC-3^{WT} and $p<0.05$ vs PC-$3^{pcDNA/GFP}$.

(D) Shown is the absorbance of day 3 which represent the cells number of each cell lines. The reduction of endogenous BMP-7 has no effect on the growth of PC-$3^{\Delta BMP7}$ cells.

Error bars represent the standard deviation. All experiments were repeated three times.

The original data was supplemented on the following page.

Supplementary data for Figure 5.2

(A) Invasion assay

	PC-3 WT (n=9)	PC-3 pEF/His (n=9)	PC-3 ΔBMP7 (n=9)
Mean	7.1	2.7	231.3
sd	4.4	2.0	28.6

(B) Motility assay

	PC-3 WT (n=6)	PC-3 pEF/His (n=6)	PC-3 ΔBMP7 (n=6)
Mean	10.2	11.3	24.0
sd	4.5	7.5	7.5

(C) Adhesion assay

	PC-3 WT (n=8)	PC-3 pEF/His (n=8)	PC-3 ΔBMP7 (n=8)
Mean	7.5	6.5	37.5
sd	4.0	2.9	15.2

(D) Growth assay

	PC-3 WT (n=6)	PC-3 pEF/His (n=6)	PC-3 ΔBMP7 (n=6)
Mean	0.093	0.095	0.091
sd	0.010	0.009	0.015

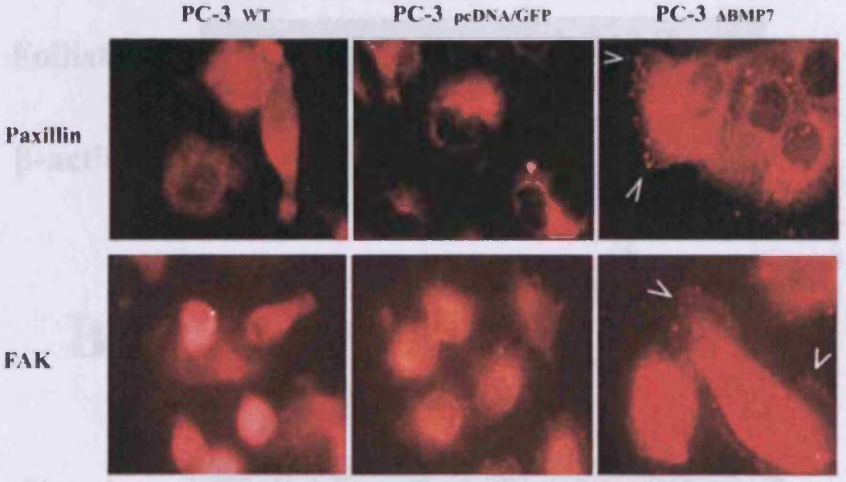

Figure 5.3 Immunofluorescent staining of Paxillin and FAK.
There was enhanced staining of Paxillin and FAK (indicated by the arrows) at the focal adhesion site in PC-$3^{\Delta BMP7}$ cells (right panels), compared with the staining in both PC-3^{WT} (left panels) and PC-$3^{pcDNA/GFP}$ cells (middle panels). Each cell line was duplicated in each experiment, and the experiments were repeated three times.

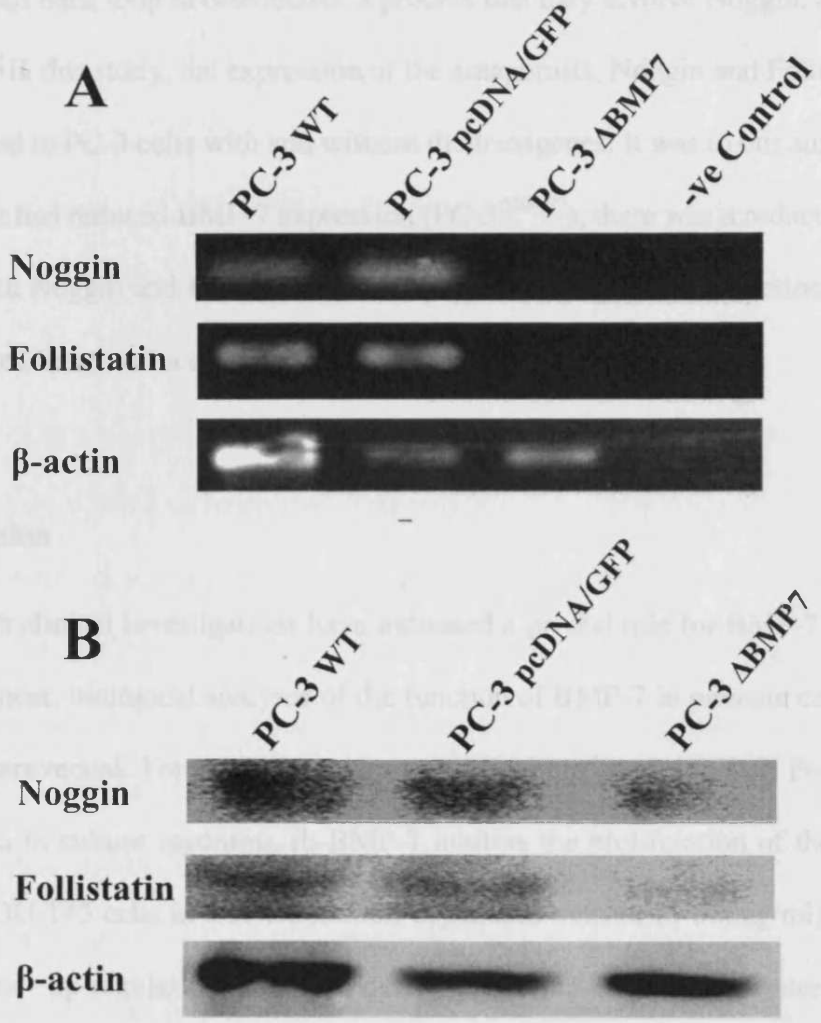

Figure 5.4 Impact of loss of endogenous BMP-7 on the expression of Noggin and Follistatin in PC-3 cells.
The transcription of Noggin and Follistatin was down-regulated with loss of the expression of BMP-7 in PC-3 cells,

(A) This was revealed using conventional RT-PCR (30 cycles).

(B) The protein level of these two antagonists was also lower in the PC-$3^{\Delta BMP7}$ cells, here demonstrated using western blot analysis.

5.3.5 Relationship between the BMP antagonists and BMP-7

It has been demonstrated that BMP-2, 4 and 6 regulate their functions through a negative feed back loop in osteoblasts, a process that may involve Noggin, a BMP antagonist. In this study, the expression of the antagonists, Noggin and Follistatin, was detected in PC-3 cells with and without the transgenes. It was to our surprise that in cells that had reduced BMP-7 expression (PC-$3^{\Delta BMP7}$), there was a reduction in the level of both Noggin and Follistatin mRNA. Concordant with this reduction in the mRNA level, there was a decrease in both proteins (Figure 5.4).

5.4 Discussion

Although clinical investigations have indicated a pivotal role for BMP-7 in human prostate cancer, biological analyses of the function of BMP-7 in prostate cancer cells remain controversial. For example, under certain culture condition (1% Fetal bovine serum, FBS in culture medium), rh-BMP-7 inhibits the proliferation of the LNCaP, PC-3 and DU-145 cells in a concentration-dependent manner (5-500ng/ml), possibly through the up-regulation of the cyclin-dependent kinase inhibitor (CDKI) $p21^{CIP1/WAF1}$ (Miyazaki *et al.*, 2004). Conversely, when the FBS concentration is reduced to 0.5%, an anti-proliferation effect by rh-BMP7 has been observed in the cell line representing benign prostatic epithelial hyperplasia (BPH-1), but not in PC-3 and DU-145 cell lines (Yang *et al.*, 2005). In serum free medium, rhBMP-7 has no effect on the proliferation, migration or invasion of PC-3 cells (Feeley and Lieberman, 2006).

Recent evidence has shown that BMP-7 can stabilise the level of survivin in prostate cancer cells (LNCaP and C4-2B), and restore the activity of c-jun NH2-

terminal kinase (JNK) (Yang *et al.*, 2005; Yang *et al.*, 2006). These both contribute to the anti-apoptotic activity of BMP7. These observations are in contrast to clinical evidence where a decrease in the expression of BMP-7 has been correlated with the progression of primary tumours (Masuda *et al.*, 2003; Masuda *et al.*, 2004).

Our first task was to assess if endogenous BMP-7 in prostate cancer cells has any influence on cellular behaviour. To accomplish this, we constructed cell lines with a greatly reduced level of endogenous BMP-7 by using a ribozyme transgene. We have shown that the reduction of endogenous BMP-7 in PC-3 cells promotes cellular invasion, motility and adhesion, but has no effect on cell proliferation, under the specific culture conditions employed. This indicates that endogenous BMP-7 plays an important role in inhibiting these functions in PC-3 cells. However, this observation itself is not sufficient to explain the discrepancies in the literature discussed previously. Yang *et al* demonstrated that in serum free conditions, PC-3 cells exposed to rh-BMP-7 at a high concentration (50ng/ml) for four days showed epithelial mesenchymal transformation (EMT), with classic changes in morphology, motility, invasiveness, and molecular markers (Yang *et al.*, 2005). Conversely, Feeley *et al* found that rh-BMP-7 has no effect on migration and invasion in PC-3 cells within a wide range of concentration from 1ng/ml to 500ng/ml(Feeley *et al.*, 2006). In the light of these findings, we would question whether the effects seen in PC-3 cells of reducing the level of endogenous BMP-7 may not be due solely to BMP-7 itself, but rather, the effects may be balanced by the involvement of the BMP antagonists, Follistatin and Noggin.

Noggin can inhibit cellular migration and invasion of BMP-2 and -4 stimulated PC-3 cells (Feeley *et al.*, 2006). On the other hand, noggin expression in osteoblasts can be induced by BMP2, 4 and 6. Thus, the effect of BMPs can be modulated

through a negative feed back loop with up-regulation of the expression of its antagonist(Gazzerro *et al.*, 1998).

Therefore, it is proposed that endogenous BMP-7 may control cellular motility through regulating Follistatin and Noggin expression. Noggin is the antagonist of BMP-2, 4, 6 and 7, GDF5 and GDF6(Re'em-Kalma *et al.*, 1995; Chang and Hemmati-Brivanlou, 1999; Haudenschild *et al.*, 2004; Pera *et al.*, 2004; Zhu *et al.*, 2006). Follistatin has been reported as an antagonist for BMP6, 7, 11 and 15, GDF8 and 9(Fainsod *et al.*, 1997; Iemura *et al.*, 1998; Otsuka *et al.*, 2001; Balemans and Van Hul, 2002; Pierre *et al.*, 2005). Most recent studies have confirmed that BMPs stimulate the motility and invasiveness of prostate cancer cells. Feeley *et al* established that BMP-2 and BMP-7 promote the migration and invasion of osteoblastic prostate cancer cells (LAPC-4 and LAPC-9) in a dose-dependent manner, but not BMP-4 (Feeley *et al.*, 2005). Dai *et al* confirmed that BMP-2 and BMP-6 increased the in-vitro invasive ability of the prostate cancer cell (C4-2B and LuCaP) (Dai *et al.*, 2005). Thus, BMP-2, and to a lesser extent, BMP-4, stimulate PC-3 cell migration and invasion in a dose-dependent fashion. This study corroborates previous studies that reveal a relationship between BMP-7 and cell migration and adhesion. The intracellular pathway for this connection is presently unknown. However, our study has provided evidence that this connection is synchronised, at least in part, by regulation of the assembly of focal adhesion complexes, and by regulation of the FAC regulators, FAK and paxillin. This interesting link requires additional investigation to further elucidate the pathways involved.

This study clearly demonstrates that there is a decreased level of both Noggin and Follistatin in PC-$3^{\Delta BMP7}$ cells where there is a loss of expression of BMP-7. This reduction was seen at both mRNA and protein levels. There appears to be an

association between the expression of endogenous BMP-7 and the antagonists, Noggin and Follistatin. In addition the effect on the motility of PC-3 cells when BMP-7 is reduced may be due to the enhanced influence of other BMPs, for example, BMP-4 which is expressed at a relatively higher level in PC-3 cells (Figure 3.1). The reduction in the level of Noggin and Follistatin occurring in response to the reduction of endogenous BMP-7 may contribute to this enhancing effect on the motility of PC-3 cells via the feed-back loop affecting other BMPs.

This study indicates that endogenous BMP-7 plays an important role in maintaining the dynamic balance between BMPs and their antagonists in prostate cancer cells. It is proposed that endogenous BMP-7 is an important regulator of the invasion, motility and adhesion of prostate cancer cells, by maintaining the expression of both Noggin and Follistatin. Further work is required to investigate the pathway(s) by which BMP-7 regulates Noggin and Follistatin expression in prostate cancer cells.

Chapter 6

Over-expression of BMP9 and BMP-10 in Prostate Cancer Cells, and the Influence on Cellular Growth, Motility and Cell-matrix Adhesion

6.1 Introduction

BMP-9, also known as growth differentiation factor 2 (GDF2), was originally cloned from a foetal mouse liver cDNA library (Celeste *et al.*, 1994a). BMP-9 gene is mapped to human chromosome 10 based on sequence similarity between the BMP-9 sequence and the chromosome 10 clone RP11-463P17. The immature and unprocessed human BMP-9 precursor protein has 429 amino acids (aa), whose molecular weight is predicted to be approximately 47kDa. As other BMPs, it is divided into a pro-region and a matured region (13kDa) after a post-translational cleavage. Once secreted, BMP-9 may exist as dimers of mature regions, or as BMP-9·pro-region complexes in which the pro-region of BMP-9 remains tightly associated with the mature ligand dimer after secretion. The BMP-9·pro-region complexes have equivalent biological activities as BMP-9 mature ligand dimers (Brown *et al.*, 2005).

The recombinant human BMP-9 (rh-BMP-9) binds with high affinity to two specific receptors that exist on HepG2 liver cancer cells and on rat hepatocytes, and stimulates the proliferation of these cells. The molecular weights of these two receptors were found to be approximately 54kDa and 80kDa, which were similar to the molecular weight of the Type I (50-55kDa) and Type II receptors (70-80kDa) of other BMPs (Song *et al.*, 1995). It has been demonstrated that Activin receptor-like kinase-1 (ALK-1), ALK-2 and BMPR-IB (ALK-6) are the putative Type-I receptors for BMP-9 signal transduction, while BMPR-II and ActR-IIA are the Type-II receptors with relatively higher affinity to BMP-9 (Brown *et al.*, 2005; David *et al.*, 2007; Scharpfenecker *et al.*, 2007).

BMP-9 has been demonstrated to be a pleiotropic cytokine, which is implicated in a number of physiological and developmental events, including bone

morphogenesis, hepatic reticulodendothelial system function, haematopoiesis, neuronal differentiation, glucose homeostasis, iron homeostasis and angiogenesis (Celeste *et al.*, 1994b; Ploemacher *et al.*, 1999; Helm *et al.*, 2000; Lopez-Coviella *et al.*, 2000; Chen *et al.*, 2003; Truksa *et al.*, 2006; David *et al.*, 2007). It is interesting to note that although the expression of BMP-9 was initially found to be restricted to the liver (Celeste *et al.*, 1994b; Song *et al.*, 1995), BMP-9 mRNA has been subsequently found to be present in a number of other cells and tissues including the central nerve system and bone (Lopez-Coviella *et al.*, 2000; Suttapreyasri *et al.*, 2006). The non-parenchymal cells of the liver (endothelial, Kupffer, and stellate cells), rather than hepatocytes, have been thought to be the major source of BMP9 in the body (Miller *et al.*, 2000).

From the point of view of sequence homology amongst BMPs, BMP-10 and BMP-9 share the highest homology and thus form a subgroup in the BMP family. The mouse BMP-10 gene was firstly cloned in 1999 (Neuhaus *et al.*, 1999). The BMP-10 amino acid sequence has a typical cleavage site (RRIR) which divides the 421 amino acid (aa) proprotein into a pro-region (309aa) and mature region (108aa). The mature domain contains the conserved seven cysteines. Unlike BMP-9, the expression of BMP-10 is most abundant in the trabeculae of the embryonic heart, whereas the expression is weaker in liver and lungs (Neuhaus *et al.*, 1999). BMP-10 deficient mice die in uterus between E9.5 and E10.5 due to a defect in cardiogenesis (Chen *et al.*, 2004b). These evidences suggest that BMP-10 plays an important role in the trabeculation of the embryonic heart. It has been demonstrated that the ALK1, BMPR-IA (ALK3) and BMPR-IB (ALK6) are candidate Type-I receptors for BMP-10, and BMPR-II and ActR-IIA are the candidate Type-II receptors for the protein (Mazerbourg *et al.*, 2005; David *et al.*, 2007).

Recent studies have shown that BMP-9 and BMP-10 play some crucial roles during the foetal or postnatal development, particularly during the morphogenesis of certain tissues. The roles played by these cytokines in cancer are largely unknown. As already shown in Chapter 3, expression of BMP-9 and BMP-10 is present in prostate cancer, cell lines and benign prostate tissues. The expression of both BMPs may be suppressed during the progression of prostate cancer. In the current study, both BMP-9 and BMP-10 were successfully cloned and over-expressed in human prostate cancer cells. Using the BMP9/10 modified cells, the cellular biological functions were investigated in order to establish the functional role of the BMPs in these cells.

6.2 Materials and Methods

6.2.1 Materials.

Polyclonal goat anti-BMP-9 (SC-27820) and monoclonal mouse anti-Actin (SC-8432) were obtained from Santa Cruz Biotechnology (Santa Cruz, California, USA). Polyclonal rabbit anti-BMP-10 was purchased from Obigen Inc. (San Diego, USA). PC-3 cells were routinely maintained in DMEM-F12 medium supplemented with 10% foetal calf serum and antibiotics.

6.2.2 Amplification of the coding sequences of BMP-9 and BMP-10 using LA-PCR.

According to the protocol of the DuraScript™ RT-PCR kit (Sigma-Aldrich, Inc., Poole, Dorset, England, UK), cDNA was first synthesised from normal human tissues. This was followed by a long range PCR, using the Extensor PCR master mix.

Briefly, 50μl LA-PCR reactions were prepared for BMP-9 and BMP-10 using cDNA of normal prostate tissue as template, respectively. The sequences of primers are in Table 2.3. Cycling conditions were 94 °C for 2min, followed by 40 cycles of 94°C for 20 s, 56 °C or 68 °C for 40 s, and 68 °C for 90 s. The optimal annealing temperature was 66 °C for BMP-9 and 56 °C for BMP-10, which were pre-determined using gradient PCR (Thermal Hybaid, Gradient block). This was followed by a final extension of 10 min at 68 °C. The products were visualized in 0.8% agarose gel stained with ethidium bromide. The discrete products of correct size were extracted for the agarose gel following the method in Chapter 2, section 2.3.5.

6.2.3 TOPO TA cloning of BMP-9 and BMP-10 into the pEF/His TOPO plasmid vector.

The correct LA-PCR products with the entire coding sequences of BMP-9 and BMP-10 were respectively cloned into the pEF/His TOPO plasmid vectors. Details of the methods are in Chapter 2, section 2.5. Primers used for analysis of transformed bacterial colonies (TOP10 *E. Coli)* are listed in Table 2.1 and Table 2.3. The strains that carried the correctly oriented inserts were then amplified. Plasmids were extracted following the methods described in Chapter 2, section 2.5.4. The constructed plasmids were verified using different pairs of primers designed for each respective BMP. The empty pEF/His TOPO plasmid vectors were used as a control.

6.2.4 Electroporation and selection.

Purified and verified BMP-9 plasmid, BMP-10 plasmid, or empty plasmid vector were then transfected into PC-3 cells using an electroporator (Easjet Plus, EquiBio Ltd, Kent, UK) at 270 volts. Following electroporation, the cells were

immediately transferred to 25 cm^3 tissue culture flasks containing 5ml of pre-warmed culture medium. Selection of transfectants began when the cells reached 50%-70% confluence. The selection of positive cells was with a medium that contained the antibiotic blasticidin (Sigma-Aldrich, Inc., Poole, Dorset, England, UK) at 5μg/ml. A stable transfectant with transgene was then cultured in maintenance medium (blasticidin 0.5μg/ml) and grown to sufficient numbers for storage and experimental studies. The selection and stocking took up to to 3 weeks.

6.2.5 RT-PCR for BMP-9, BMP-10 and β-actin.

This was carried out to verify the success of transfection. RNA was isolated from the aforementioned cells, and cDNA was synthesised by reverse transcription using 0.25μg RNA in a 20-μl-reaction mixture as described in the section 2.3 of Chapter 2. PCR was undertaken using a REDTaq™ ReadyMix PCR reaction mix (Sigma-Aldrich, Inc.). Cycling conditions for the 12-μl-reaction mixture were 94 °C for 5min, followed by 30-40 cycles of 94°C for 30 s, 55 °C for 30 s, and 72 °C for 40 s. This was followed by a final extension of 10 min at 72 °C. The products were visualized on a 0.8 or 2% agarose gel and stained with ethidium bromide after electrophoresis. Details of the primers used are provided in Table 2.1.

6.2.6 Verification of the presence of BMP-9 and BMP-10 proteins after over-expression in PC-3 cells using Western blot analysis.

Cells were first collected using a cell scraper and pelletted. The pellets were lysed using the HCMF lysis buffer as given in chapter-2. After extraction, protein concentrations were measured using the DC Protein Assay kit (BIO-RAD, USA),

and all protein samples were then adjusted to the same concentration (1-2mg/ml) using the lysis buffer. The protein samples were then added with sample buffer, boiled and loaded onto SDS gels. After electrophoresis, proteins were blotted onto nitrocellulose sheets, followed by blocking, before probing with anti-BMP-9 (1:250) and anti-BMP-10 (1:200), respectively. The blot was then probed with corresponding peroxidase-conjugated secondary antibodies. Protein bands were visualized with a SupersignalTM West Dura system (Pierce Biotechnology, USA), and images captured and documented by UVI-doc system (UVI, Cambridge, England, UK).

6.2.7 In vitro cell growth assay

This was based on previously described method (section 2.8.1). 6 wells were set for each cell line, and the experiment was performed three times.

6.2.8 In vitro invasion assay

We used a standard procedure as previously described in section 2.8.4. Each test was conducted in triplicate with 3 fields being counted for each sample, and the experiment was performed three times.

6.2.9 In vitro cell-Matrix adhesion assay

The cell-Matrix adhesion was analysed according to the method introduced in Chapter 2, section 2.8.5. 8 wells were set for each cell lines, and the experiment was performed three times.

6.2.10 Wounding assay

The influence on cellular migration was assessed using an established wounding assay, which has been introduced in Chapter 2, section 2.8.2. Three independent experiments were performed.

6.3 Results

6.3.1 Amplification of the entire coding region of human BMP-9 and BMP-10

The purpose of this part was for preparation of a mammalian expression construct for human BMP9 or BMP10. The primers were designed as such that, when successful, the PCR products would cover the entire the coding region of the respective BMPs. To ensure minimum the variation, a master mix with proof reading enzyme and allowing amplification of large products was used, namely, Extensor Long Range PCR master mix. The annealing temperature for each pair of primers was optimised using gradient PCR. The PCR products of right size were the coding sequences of BMP-9 (Figure 6.1) and BMP-10 (Figure 6.2). Both were amplified from cDNA of normal prostate tissue, and have a stop codon (ATC) at 3' end of the sequences in order to generate native proteins.

6.3.2 TOPO TA cloning of BMP-9 and BMP-10 DNA fragments into a mammalian expression plasmid vector.

Following the preparation of BMP-9 and BMP-10 genetic inserts, both were cloned into a mammalian expression plasmid vector (pEF/His TOPO TA plasmid vector). The recombinant plasmid vectors were transformed into the chemical competent TOP10 *E.Coli*, and the colonies were then analysed. The analysis of the colonies for BMP-9 cloning is demonstrated in Figure 6.3, and Figure 6.4A and 6.4B

show the analysis for BMP-10 cloning. Once the colonies carrying the recombinant plasmids with the respective BMP-9 and BMP-10 inserts at the correct orientation were amplified (marked with a * in figures 6.3, 6.4 and 6.5), the recombinant plasmid vectors were then extracted from a larger volume of the respective bacterial preparation (Figure 6.5) and utilised for the following experiments.

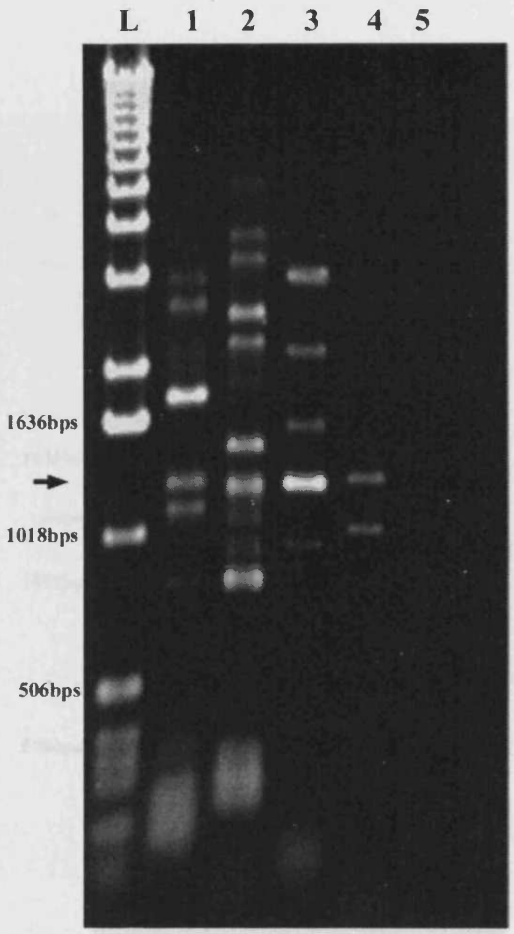

Figure 6.1 Amplification of the entire coding region of human BMP-9 using PCR. Annealing temperatures for the gradient PCR was 60°C (lane1), 62 °C (lane2), 64 °C (lane3), 66 °C (lane4), and 68 °C (lane5). Lane L is the 1kb DNA ladder. The optimal annealing temperature is 64-66 °C. Arrow indicates the correct products of BMP-9 (1290bps), which was subsequently extracted from the gel and used for cloning.

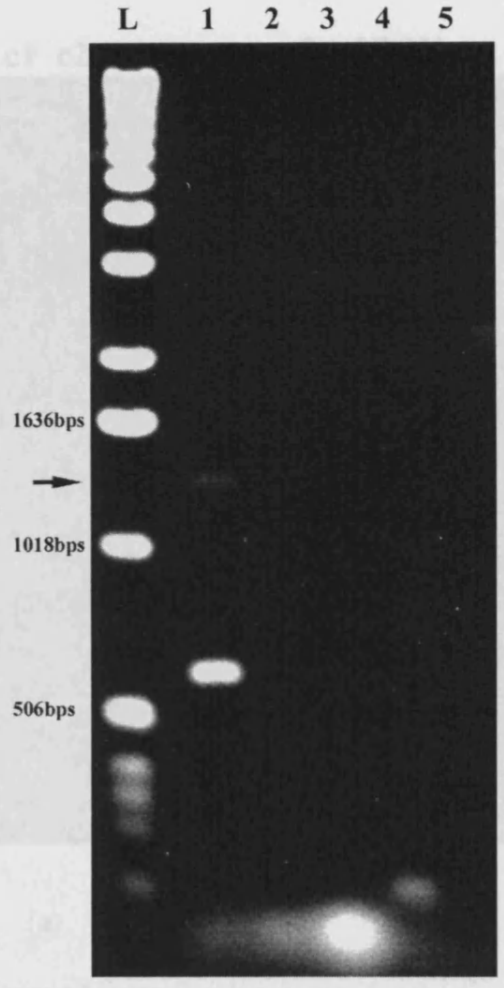

Figure 6.2 Amplification of the BMP-10 coding sequence using PCR. Annealing temperatures for the gradient PCR is 58°C (lane1), 60 °C (lane2), 62 °C (lane3), 64 °C (lane4), and 66 °C (lane5). Lane L is the 1kb DNA ladder. The optimal annealing temperature is approximate 58 °C. Arrow indicates the correct products of BMP-10 (1275bps), which was subsequently extracted from the gel and used for cloning.

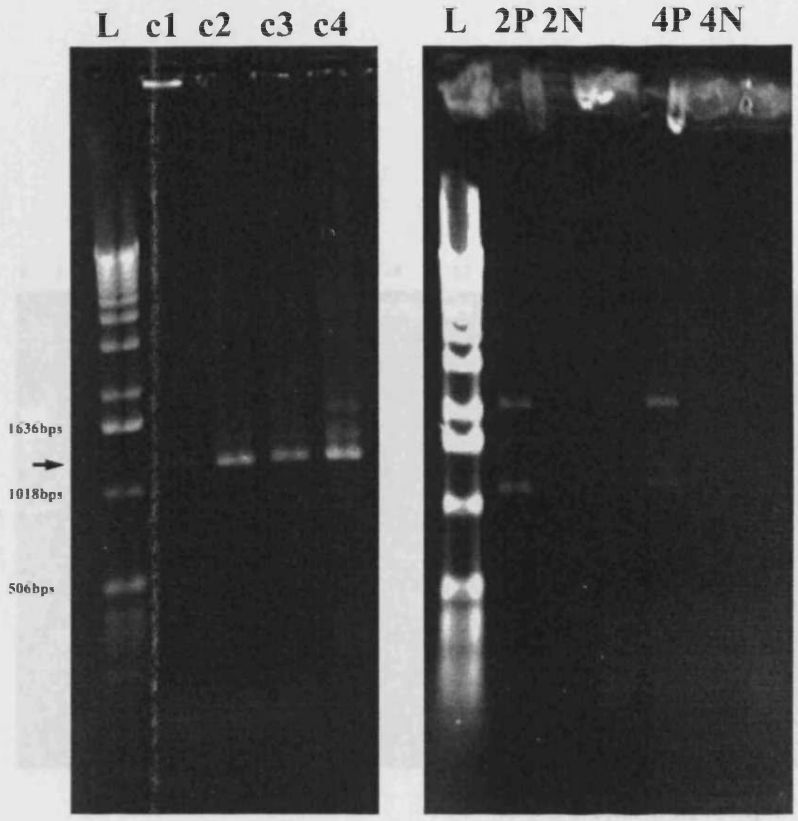

Figure 6.3 Analysis of recombinant *E.coli* colonies for the presence and orientation of the BMP-9 insert using orientation specific PCR.
In (a), colonies were analysed using T7F with BGHR for the PCR reactions, size of right products is approximate 1400bps (indicated by the arrow). Lane L is the 1kb DNA ladder. Four colonies were analysed (c1-4).
In (b), colony 2 and colony 4 were subsequently verified with PCR using different pairs of primers, i.e. to check the correct orientation using BMP9F8 coupled with BGHR. The size of product is approximate 1000bps (P, positive); to check wrong orientation using BMP9F8 coupled with T7F, size of product is approximate 1000bps (N, negative). Colony 2 was then used in the subsequent studies.

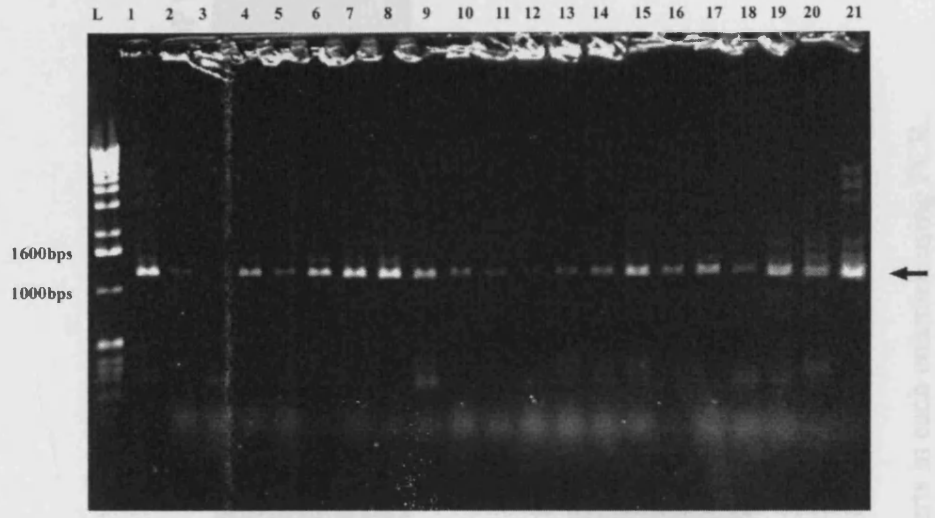

Figure 6.4A Analysis of individual colonies for presence of BMP-10 inserts using PCR.
To analyse the colonies, PCR reactions were run using TF7 and BGHR primers. The size of products was approximately 1400bps if the colony had the BMP-10 sequence inserted into the plasmid. In this case, most of the colonies that survived ampicillin selection have been transformed with the BMP10 plasmids.

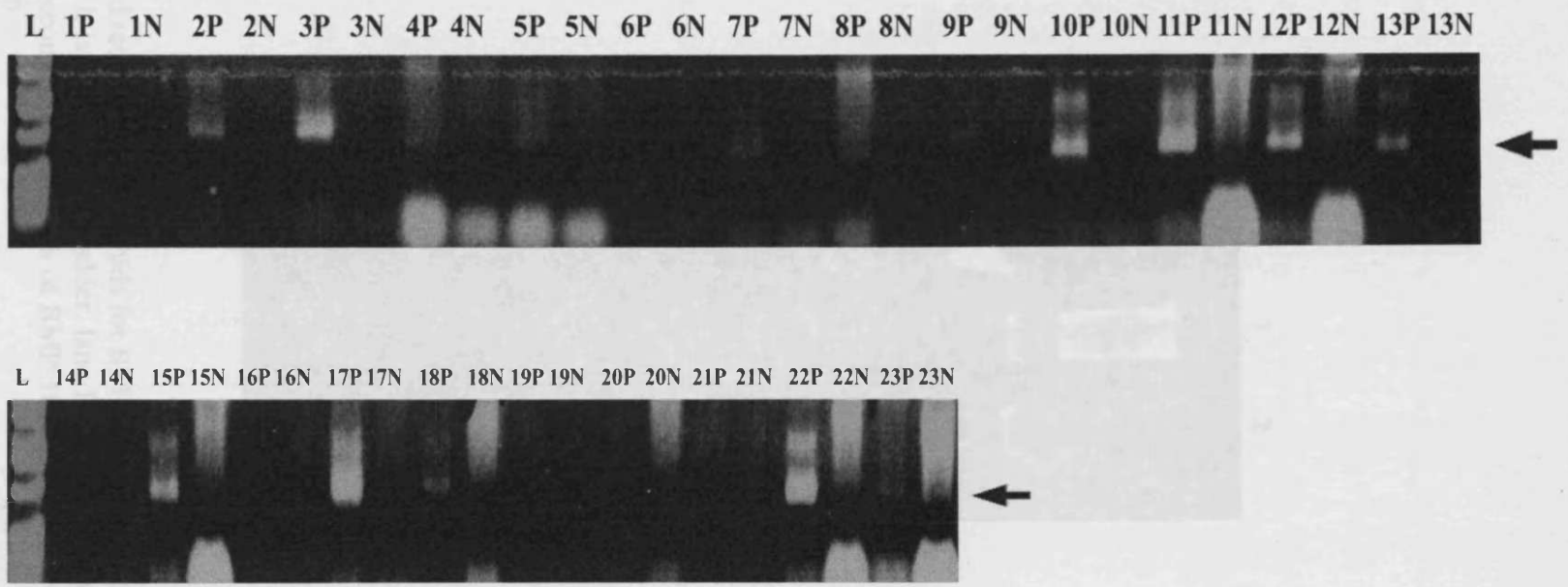

Figure 6.4B Analysis of the orientation of BMP-10 inserts in each colonies using PCR.
To verify the orientation of BMP-10 inserts, we performed PCR reactions using BMP10F1 primer coupled with T7F (N, in wrong orientation), or BGHR (P, in correct orientation). Colony 10 was then utilised for the subsequent experiments.

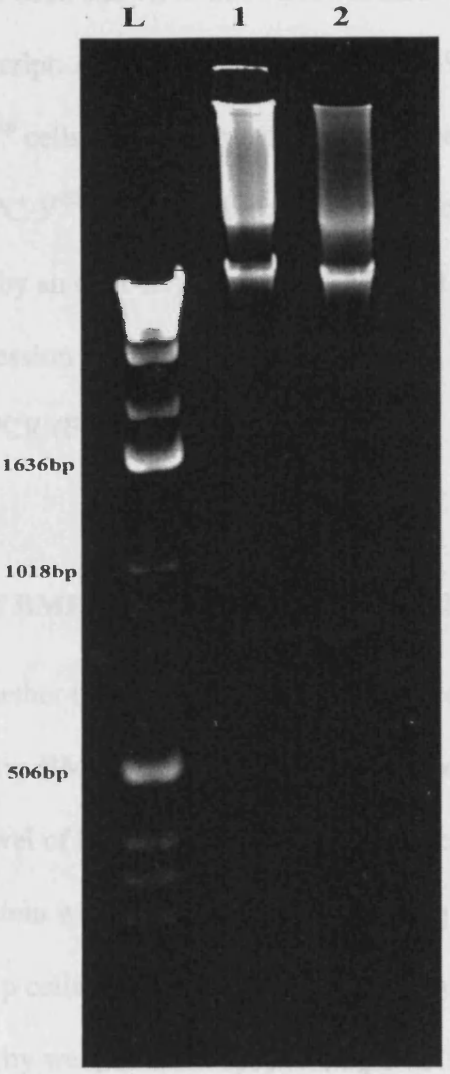

Figure 6.5 Purified recombinant plasmids for BMP-9 and BMP-10 visualised on the agarose gel. Lane L is the 1kb DNA ladder, lane 1 is BMP-9 recombinant plasmids and lane 2 is the recombinant plasmids of BMP-10, the sizes of both were approximately 7kb.

6.3.3 Over-expression of BMP-9 and BMP-10 in prostate cancer cell, at mRNA level

We transfected prostate cancer cells with the respective BMP-9 and BMP-10 recombinant construct, or empty control plasmids. In the current study, PC-3 cells were employed which has been shown to have a lower mRNA level of BMP-9 and absence of BMP-10 transcript. An over-expression of BMP-9 was successfully established in PC-$3^{BMP\text{-}9exp}$ cells after the transfection, compared with the PC-3 wild type cells (PC-3^{WT}) and PC-$3^{pEF/His}$ cells which were transfected with the empty vectors. This was shown by an over-expression of BMP-9 at mRNA level (Figure 6.6). A similar over-expression of BMP-10 was also seen in PC-$3^{BMP\text{-}10exp}$ cells, as demonstrated using RT-PCR (Figure 6.7).

6.3.4 Over-expression of BMP-9 and BMP-10 at protein level

To investigate whether the respectively transfected cells (which showed over-expression of the respective BMP transcript) would also produce BMP protein, we determined the protein level of BMP in the cells using western blot analysis. Over-expression of BMP-9 protein was confirmed with increasing protein production of BMP-9 in PC-3BMP-9exp cells (Figure 6.8). Over-expression of BMP-10 at protein level was also confirmed by western blot analysis (Figure 6.9).

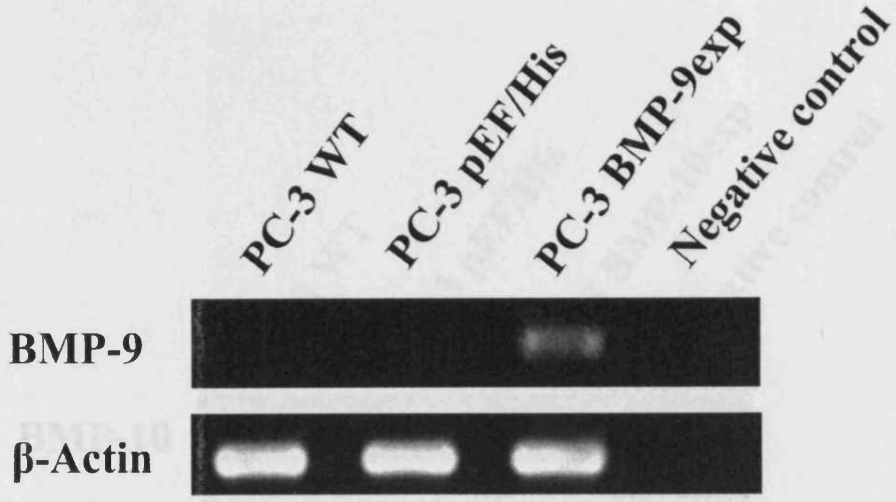

Figure 6.6 Verification of the over-expression of BMP-9 in PC-3 cells using RT-PCR. The expression of BMP-9 in PC-3 was significantly elevated after the transfection, and the BMP-9 transcripts were only detectable in PC-3$^{BMP\text{-}9exp}$ if the cycles' number of PCR reactions was reduced to 30.

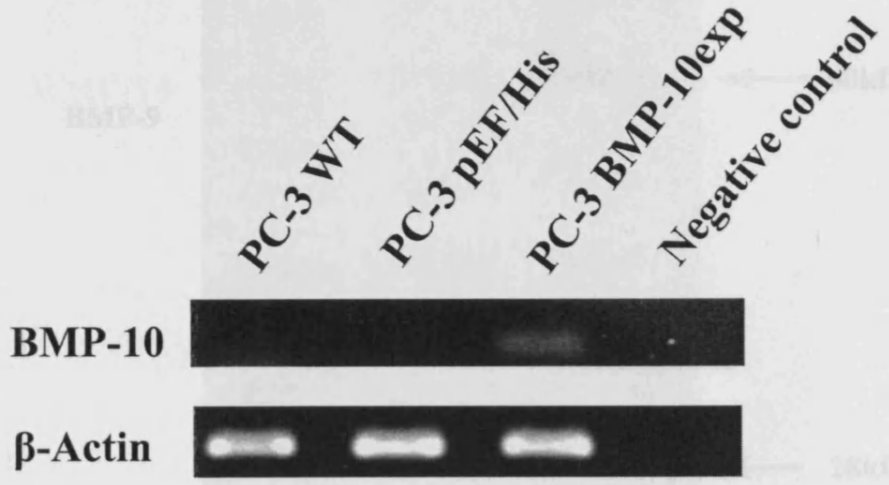

Figure 6.7 Verification of the over-expression of BMP-10 in PC-$3^{BMP\text{-}10exp}$ cells using RT-PCR. BMP-10 transcripts were only detectable in PC-$3^{BMP\text{-}10exp}$ cells using RT-PCR (40cycles).

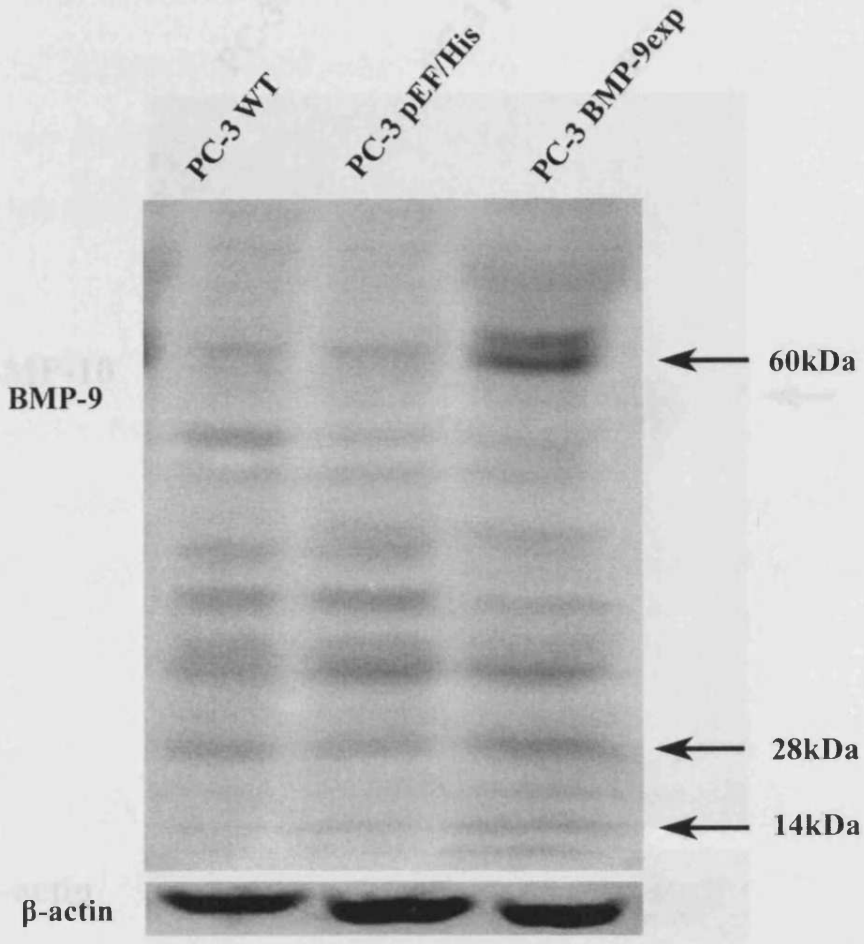

Figure 6.8 Over-expression of BMP-9 at protein level in PC-3$^{BMP\text{-}9exp}$ cells was verified using western blot analysis.

An increasing protein level was revealed in the PC-3$^{BMP\text{-}9exp}$ cells. Three bands shown on the western blot under reduced condition are BMP-9. The band of around 60kDa is the monomer of BMP-9 precursor protein, the bands of approximate 28 kDa and 14 kDa represent respective dimers and monomers of matured ligands.

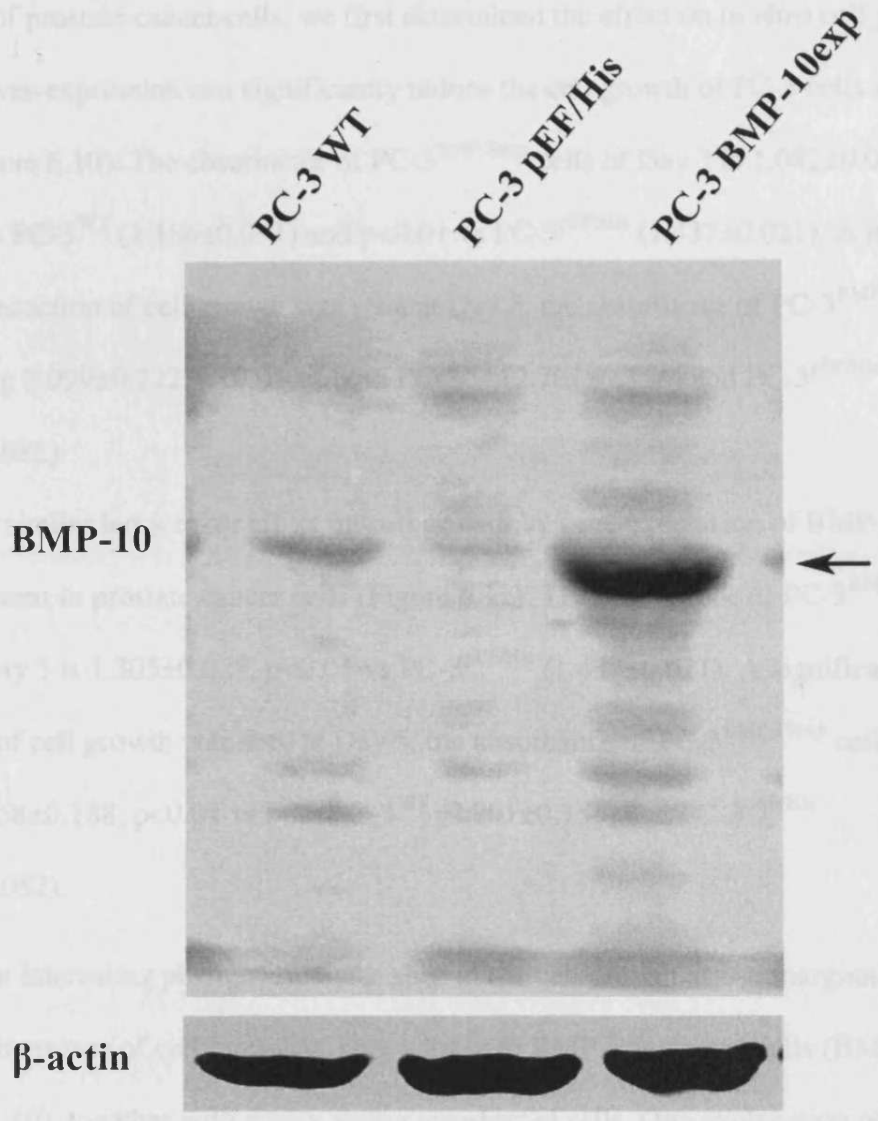

Figure 6.9 Over-expression of BMP-10 at protein level in PC-3$^{BMP\text{-}10exp}$ cells using western blot analysis.
An elevated expression of BMP-10 at protein level was seen in PC-3$^{BMP\text{-}10exp}$ cells. A 60kDa band was seen on western blot under reduced condition, which is the precursor protein of BMP-10.

6.3.5 Over-expression of BMP-9 and BMP-10 influences the cell growth of prostate cancer cells

To assess whether the over-expression of BMP-9 influences the biological function of prostate cancer cells, we first determined the effect on *in vitro* cell growth. BMP-9 over-expression can significantly reduce the cell growth of PC-3 cells *in vitro* (Figure 6.10). The absorbance of PC-$3^{BMP\text{-}9exp}$ cells of Day 3 is 1.082±0.052, $p<0.05$ vs PC-3^{WT} (1.186±0.091) and $p<0.01$ vs PC-$3^{pEF/His}$ (1.437±0.021). A more marked reduction of cell growth was seen at Day 5, the absorbance of PC-$3^{BMP\text{-}9exp}$ cells being 2.099±0.222, $p<0.01$ vs both PC-3^{WT} (2.701±0.156) and PC-$3^{pEF/His}$ (2.698±0.082).

A similar but weaker effect on cell growth by over-expression of BMP-10 was also seen in prostate cancer cells (Figure 6.11). The absorbance of PC-$3^{BMP\text{-}10exp}$ cells at Day 3 is 1.305±0.028, $p<0.01$ vs PC-$3^{pEF/His}$ (1.437±0.021). A significant decrease of cell growth was seen at Day 5, the absorbance of PC-$3^{BMP\text{-}10exp}$ cells being 2.258±0.188, $p<0.01$ vs both PC-3^{WT} (2.701±0.156) and PC-$3^{pEF/His}$ (2.698±0.082).

An interesting phenomenon was seen in the cell growth assay: marginal and transient increases of cell growth at Day 1 for both BMP-transfected cells (BMP-9 and BMP-10), together with empty vector transfected cells. One explanation of the transient change may be due to the change of the culture medium for the transfectants in the cell growth assay, in which there is absence of blasticidin.

6.3.6 Over-expression of BMP-9 and BMP-10 reduced the invasion of prostate cancer cells *in vitro*

BMP-9 over-expression markedly reduced the invasiveness of PC-3 cells; the number of invading cells for PC-$3^{BMP\text{-}9exp}$ being 3.7±2.1, $p<0.01$ vs both PC-3^{WT} cells (38.2±6.7) and PC-$3^{pEF/His}$ cells (34.1±5.4) (Figure 6.12).

Although the effect of BMP-10 over-expression on invasion was less powerful compared to that of BMP-9, the reduction of invasion in PC-$3^{BMP\text{-}10exp}$ cells was nonetheless significant. The number of the invading cells was 12.9±5.3 for PC-$3^{BMP\text{-}10exp}$ cells, $p<0.01$ vs both PC-3^{WT} cells (38.2±6.7) and PC-$3^{pEF/His}$ cells (34.1±5.4) (Figure 6.13).

6.3.7 Over-expression of both BMP-9 and BMP-10 'prevented' the cell-matrix adhesion of prostate cancer cells

Adhesion to extracellular matrix (ECM) is an important property and process of cancer cells during the metastasis. To investigate the impact of BMP-9 on ability of adhering to ECM in prostate cancer cells, we employed an established *in vitro* cell-matrix adhesion assay. Over-expression of BMP-9 markedly reduced the cell-matrix adhesion of PC-3 cells. The adhesion cells number of PC-$3^{BMP\text{-}9exp}$ is 7±2.4, $p<0.01$ vs both PC-3^{WT} (30±7.1) and PC-$3^{pEF/His}$ (37±10.3), as shown in Figure 6.14.

BMP-10 also reduces the cell-matrix adhesion of prostate cancer cells, but to a lesser degree than that of BMP-9 over-expression. The adhered cell number of PC-$3^{BMP10exp}$ was 24±12.3, $p<0.01$ vs that of both PC-3^{WT} and PC-$3^{pEF/His}$ cells (Figure 6.15).

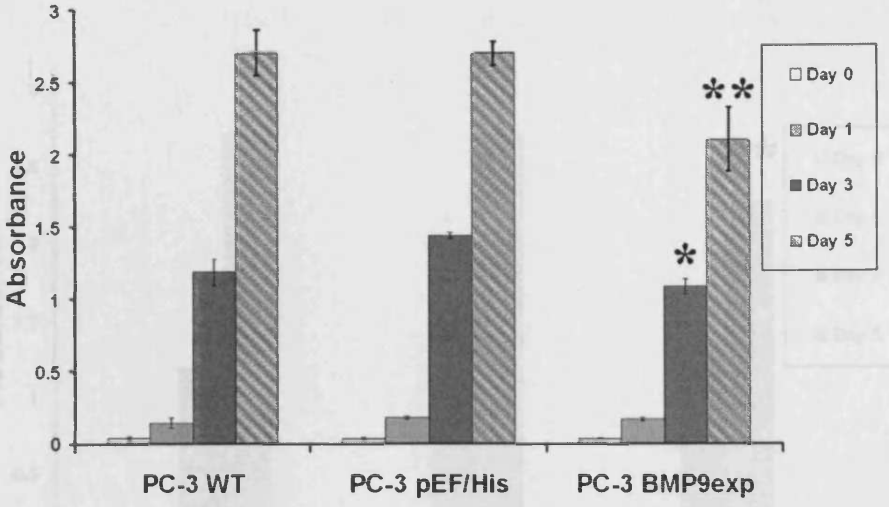

	PC-3 WT (mean±SD, n=6)	PC-3 pEF/His (mean±SD, n=6)	PC-3 BMP-9exp (mean±SD, n=6)
Day 0	**0.034±0.010**	**0.032±0.006**	**0.032±0.004**
Day 1	**0.143±0.032**	**0.177±0.009**	**0.167±0.011**
Day 3	**1.186±0.091**	**1.437±0.021**	**1.082±0.052**
Day 5	**2.701±0.156**	**2.698±0.082**	**2.099±0.222**

Figure 6.10 Over-expression of BMP-9 inhibits the growth of PC-3 cells using the *in vitro* cell growth assay.
Cell growth was slowed down by the over-expression of BMP-9 after 3 days of incubation. * $p<0.05$ and ** $p<0.01$, vs both $PC\text{-}3^{WT}$ and $PC\text{-}3^{pEF/His}$. Error bars are standard deviations.

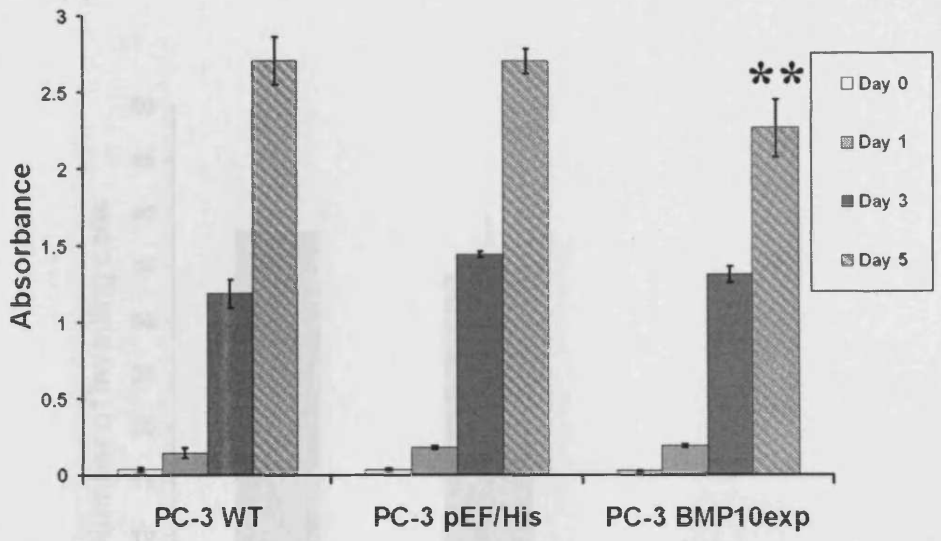

	PC-3 WT (mean±SD, n=6)	PC-3 pEF/His (mean±SD, n=6)	PC-3 BMP-10exp (mean±SD, n=6)
Day 0	**0.034±0.010**	**0.032±0.006**	**0.024±0.007**
Day 1	**0.143±0.032**	**0.177±0.009**	**0.187±0.020**
Day 3	**1.186±0.091**	**1.437±0.021**	**1.305±0.028**
Day 5	**2.701±0.156**	**2.698±0.082**	**2.258±0.188**

Figure 6.11 Over-expression of BMP-10 influences the *in vitro* growth of PC-3 cells as demonstrated in the *in vitro* growth assay.
Cell growth was prevented by the over-expression of BMP-10 in PC-3 cells. ** $p<0.01$ vs both $PC\text{-}3^{WT}$ and $PC\text{-}3^{pEF/His}$. Error bars are standard deviations.

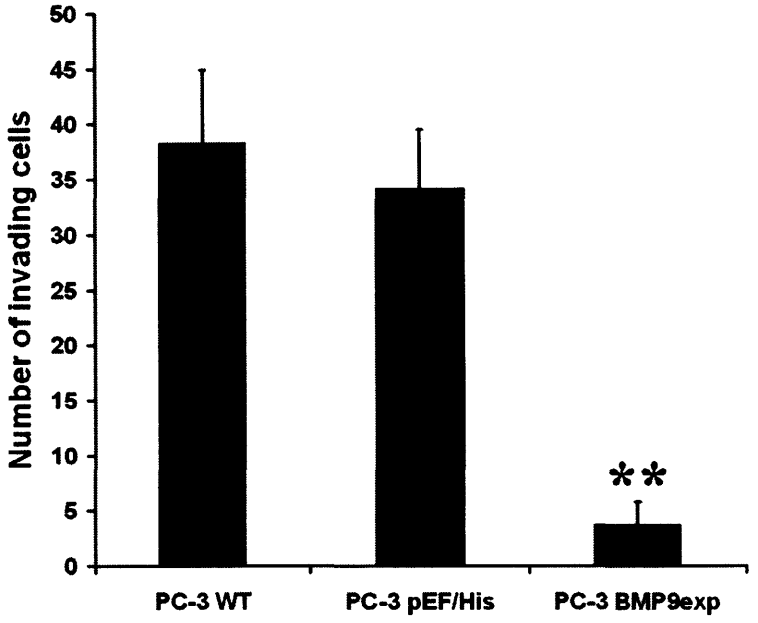

	PC-3 WT (n=9)	PC-3 pEF/His (n=9)	PC-3 BMP-9exp (n=9)
Mean	38.2	34.1	3.7
sd	6.7	5.4	2.1

Figure 6.12 The influence of BMP-9 over-expression on the invasiveness of prostate cancer cells using the *in vitro* invasion assay.
Over-expression of BMP-9 decreases the invasiveness of prostate cancer *in vitro*. ** $p<0.01$ vs $PC\text{-}3^{WT}$ and $PC\text{-}3^{pEF/His}$. Error bars are standard deviations.

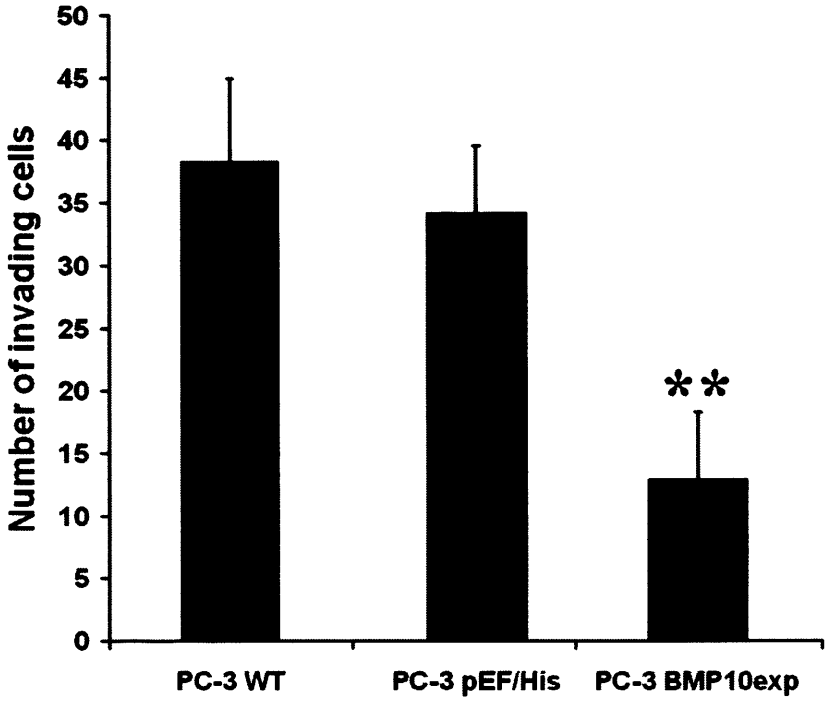

	PC-3 WT (n=9)	PC-3 pEF/His (n=9)	PC-3 BMP-10exp (n=9)
Mean	38.2	34.1	12.9
sd	6.7	5.4	5.3

Figure 6.13 The effect of BMP-10 over-expression on the invasiveness of prostate cancer cells using the *in vitro* invasion assay.
Over-expression of BMP-10 inhibits the invasiveness of prostate cancer *in vitro*. ** $p<0.01$ vs $PC\text{-}3^{WT}$ and $PC\text{-}3^{pEF/His}$. Error bars are standard deviations.

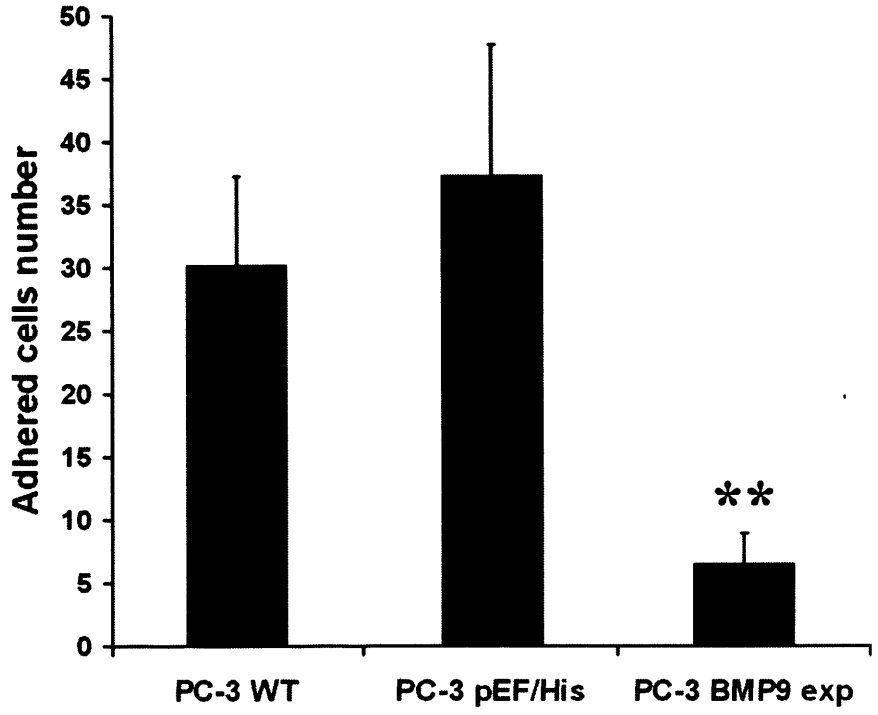

	PC-3 WT (n=8)	PC-3 pEF/His (n=8)	PC-3 BMP9exp (n=8)
Mean	30	37	7
Median	28.5	37	6.5
sd	7.1	10.3	2.4

Figure 14 Over-expression of BMP-9 influences the cell-matrix adhesion of PC-3 cells using the *in vitro* cell-matrix adhesion assay.
BMP-9 significantly reduces the adhesion of prostate cancer cells *in vitro*. Error bars are standard deviations.

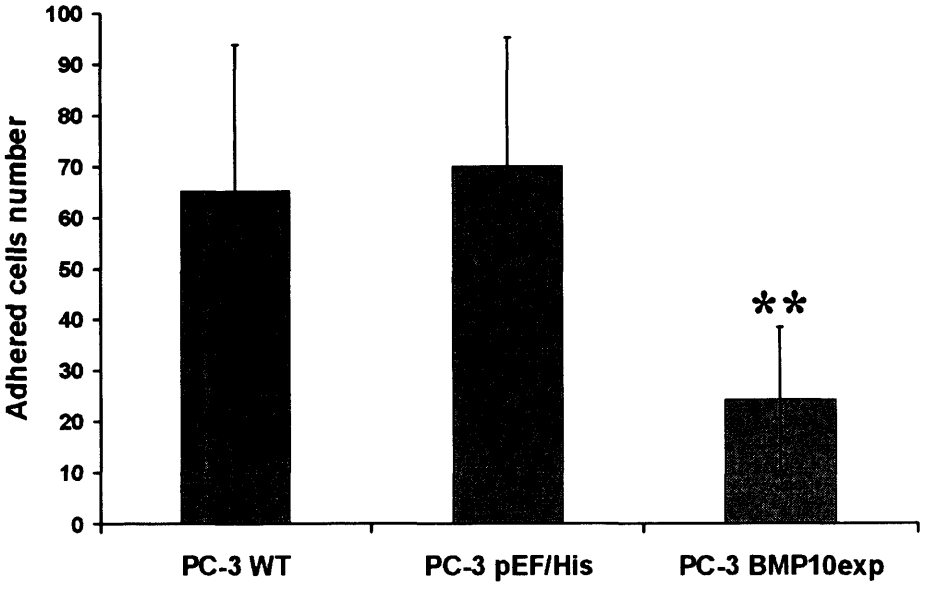

	PC-3 WT (n=8)	PC-3 pEF/His (n=8)	PC-3 BMP-10exp (n=8)
Mean	65	70	24
sd	28.6	25.1	12.3

Figure 6.15 Over-expression of BMP-10 inhibits the cell-matrix adhesion of PC-3 cells as demonstrated in the *in vitro* adhesion assay.
BMP-10 significantly prevented the adhesion of the prostate cancer cells *in vitro*. Error bars are standard deviations.

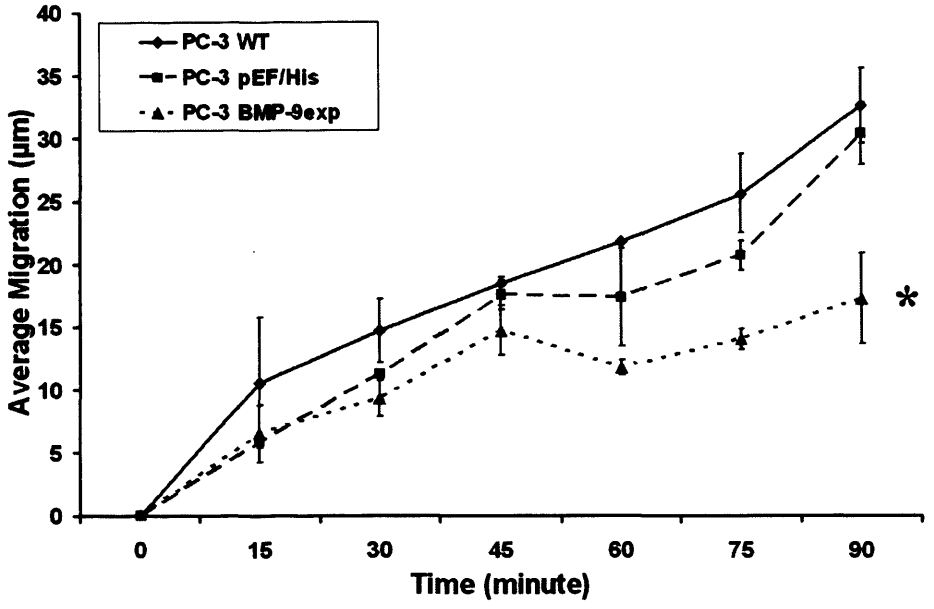

Migration at 90 mins (µm)

	PC-3 WT (n=3)	PC-3 pEF/His (n=3)	PC-3 BMP-9exp (n=3)
Mean (µm)	32.47	30.26	17.22
S.E.M	2.98	2.43	3.61

Figure 6.16 Over-expression of BMP-9 inhibits the migration of PC-3 cells using the *in vitro* wounding assay.
* $p<0.05$ vs both $PC\text{-}3^{WT}$ and $PC\text{-}3^{pEF/His}$. Error bars are standard error of means.

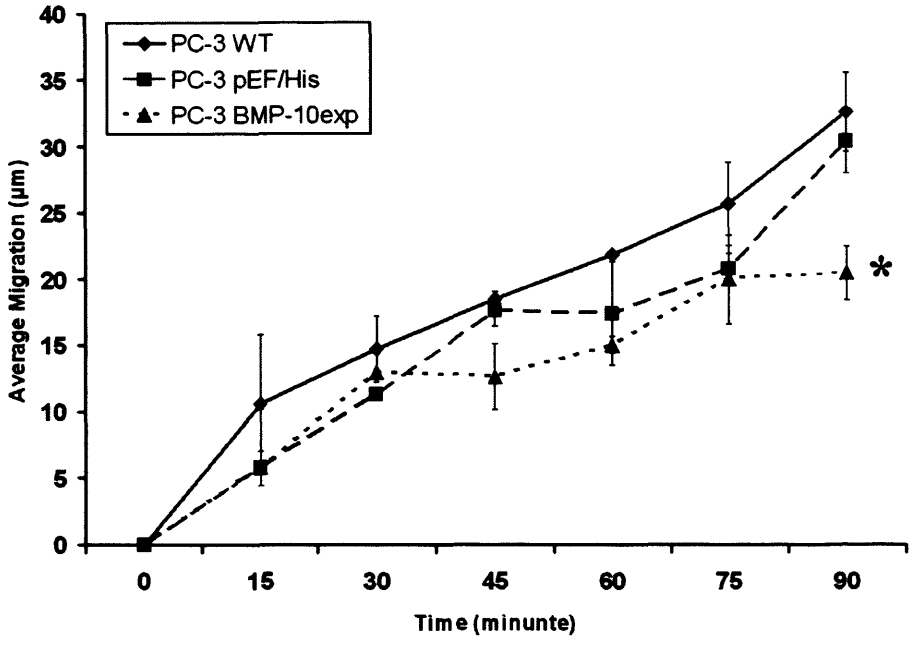

Migration at 90 mins (µm)

	PC-3 WT (n=3)	PC-3 pEF/His (n=3)	PC-3 BMP-10exp (n=3)
Mean (µm)	32.47	30.26	20.34
S.E.M	2.98	2.43	2.00

Figure 6.17 Over-expression of BMP-10 reduces the migration of PC-3 cells using the *in vitro* wounding assay.
* $p<0.05$ vs. PC-3 pEF/His, $p=0.057$ vs. PC-3 WT. Error bars are standard error of means.

6.3.8 Over-expression of BMP-9 and BMP-10 reduced the motility of prostate cancer

The effect of both BMPs on cellular motility was examined using an established *in vitro* cellular migration assay. $PC3^{BMP9exp}$ cells showed a significantly reduced cellular migration, compared with the controls. A reduction of migration distance was seen 60 minutes after wounding (figure 6.16). The average migration distance at 90 minutes for $PC\text{-}3^{BMP\text{-}9exp}$ cells was 17.22±3.61μm, $p<0.05$ vs both $PC\text{-}3^{WT}$ (32.47±2.98μm) and $PC\text{-}3^{pEF/His}$ (30.26±2.43μm) (Figure 6.16).

A decreased cell migration was also seen in $PC\text{-}3^{BMP\text{-}10exp}$ cells 90 minutes after wounding (20.34±2.00μm), $p<0.05$ vs $PC\text{-}3^{pEF/His}$ (30.26±2.43μm), $p=0.057$ vs $PC\text{-}3^{WT}$ (32.47±2.98μm) (Figure 6.17).

6.4 Discussion

Although the expression of BMP-9 was only demonstrated in the liver when it was firstly discovered in mouse (Celeste *et al.*, 1994a; Song *et al.*, 1995), subsequent studies have shown that the tissue distribution is much wider. As a pleiotropic factor, its expression has been revealed in a few other tissues, for example, bone (Suttapreyasri *et al.*, 2006) and central nerve system (Lopez-Coviella *et al.*, 2000). In the current study, we firstly demonstrated the presence of BMP-9 in human prostate at both mRNA level and protein level. BMP-9 mRNA was detectable in most of the currently available prostate cell lines in our laboratory (Figure 3.1). The immunochemical staining revealed an expression of BMP-9 protein in normal prostatic epithelia, which is decreased in prostate cancer cells as demonstrated in our pilot study using human prostate specimens (Figure 3.5 and Figure 3.6). This

suggests that BMP-9 is widely expressed in prostate tissues and may play an important role in the prostate cancer.

To investigate the biological functions of BMP-9 in prostate cancer cells, we over-expressed human BMP-9 in PC-3 cells which has a relatively lower level of expression. In the current study, we successfully constructed a mammalian expression system that contained the entire coding region of human BMP-9. One particular point was that the BMP9 insert carried a stop codon thus allowing production of native BMP-9 protein without any by-product from the downstream sequence of the plasmid vector. The over-expression of BMP-9 was verified at both mRNA level and protein level in PC-3 cells. Subsequent functional analyses were based on these successfully transfected cells.

Previously, it was shown that human recombinant BMP-9 (rh-BMP-9) would stimulate the proliferation of both human HepG2 liver tumor cells and rat hepatocytes (Song *et al.*, 1995). However most BMPs so far investigated inhibit the proliferation of prostate cancer cells, for example BMP-2 and 4 inhibit the growth of the androgen-sensitive prostate cancer cell line LNCaP (Brubaker *et al.*, 2004; Tomari *et al.*, 2005), while BMP-6 and BMP-7 are more likely to inhibit the proliferation of both androgen-sensitive and androgen-insensitive prostate cancer cells (Haudenschild *et al.*, 2004; Miyazaki *et al.*, 2004). The present study reveals an inhibitory effect of BMP-9 on cell growth of prostate cancer cells, which is in line with decreased expression of BMP-9 in prostate cancer and documented effects of other members of the BMP family in prostate cancer. It is noteworthy that there appears to be a different response to a given BMP by different cancer cell lines. Although a number of possibilities exist, later in this thesis, we have tangible

evidence to show that this may be due to the varied expressing pattern of the BMP receptors and intracellular signaling molecules.

The current study also reveals an inhibitory effect of BMP-9 on the motility of prostate cancers. Most interestingly, both migration and invasion of PC-3 cells were reduced after over-expression of BMP-9. These are somewhat very different from the effects on motility by other known BMPs, for example, BMP-2, 4, 6 and 7 can stimulate the migration and invasion of prostate cancer cells (Dai *et al.*, 2005; Feeley *et al.*, 2005; Feeley and Lieberman, 2006). The contrasting effect of BMP-9 on cellular motility of prostate cancer cells compared to other known BMPs points to a differential role of BMP-9 in prostate cancer.

Finally, the present study also shows that the adhesion to ECM was reduced by over-expressing BMP-9 in PC-3 cells. It suggests that BMP-9 may interfere with the aggressive growth of prostate tumour and the process of metastasis.

BMP-10, which is the closest member to BMP-9 in TGF-β superfamily plays a crucial role during the embryonic and postnatal development of heart. BMP10 has been found in heart, liver and lung. In current studies, we firstly demonstrated its expression in the prostate, and revealed a potential anticancer role of BMP10 in prostate cancer. BMP-10 mRNA was only detectable in DU-145 cells using conventional RT-PCR. Immunochemical staining revealed the presence of BMP-10 protein in normal prostate epithelia, and a decreased expression or absence in prostate cancer. Taken together, the present study demonstrates the presence of BMP-10 in prostate epithelia, and also suggests the potential implication of BMP-10 in prostate cancer.

In similar cellular models to that used in the BMP-9 study, we evaluated the impact of BMP-10 over-expression in the cellular function of PC-3 cells. BMP-10

displayed a similar impact on biological functions of PC-3 cells, although to a lesser extent compared with BMP-9. Over-expression of BMP10 inhibited the *in vitro* cell growth of PC-3 cells. BMP-10 also reduced the cell-matrix adhesion, migration and invasion of PC-3 cells *in vitro*.

Taken together, BMP-9 and BMP-10, which are the closest members in TGF-β and BMPs family, both inhibit *in vitro* cell growth, adhesion, invasion and migration of prostate cancer cells, the mechanisms of which are further reported in the following chapters.

Chapter 7

Generation of Recombinant Human BMP9 and BMP-10

7.1 Introduction

In Chapter 6, the inhibitory effects of both BMP-9 and BMP-10 on the some biological activities of prostate cancer cells, such as the cell growth, adhesion, migration and invasion, were demonstrated. These events are crucial for the metastasis of cancer cells. This was achieved way of transfection and forced expression. At the commencement of the current study, the corresponding signal pathways for both BMP-9 and BMP10 were not clear. There was no commercial recombinant protein available for either BMP, which may be one reason for the lack of major studies on the signalling pathways. To elucidate the signal transduction of these BMPs, and to further examine their implication in the development and metastasis of prostate cancer, a strategy to generate histidine-tagged recombinant human proteins of BMP-9 (rh-BMP-9) and BMP-10 (rh-BMP-10) was designed. Firstly, we utilised a mammalian expression plasmid vector, pEF/V5-His-TOPO plasmid vector, which has six histidine tag at downstream of the TOPO cloning site. Pairs of primers were designed for each BMP to amplify the complete coding region without a stop codon at the end of the region, thus enabling the recombinant plasmid vector to add the histidine tag at one end of the recombinant protein. Following the cloning, the recombinant plasmid vectors and empty plasmid were transfected into a murine fibroblast cell line, 3T3 cells which is one of the cell lines popularly used for producing recombinant proteins. As will be presented in the present chapter, the choice of 3T3 cells followed the initial failure to grow CHO cell, another cell line attempted to generate recombinant protein. The present chapter thus demonstrates the logic and procedure in producing recombinant BMP-9 and BMP-10 as well as ways to over-come the difficulties with the cells used for the study.

7.2 Materials and Methods

7.2.1 Materials.

The antibodies used in present study are same as those used for the studies in Chapter 6. 3T3 and CHO (Chinese hamster ovary) cells were routinely maintained in DMEM-F12 medium supplemented with 10% foetal calf serum and antibiotics.

7.2.2 Amplify complete coding sequence of respective BMP-9 and BMP-10 using PCR.

A pair of primer was used for each to amplify the coding sequence of full-length human BMP-9 and human BMP-10 (Table 2.3), minus a stop codon (compared with that presented in chapter-6). A high fidelity extensor PCR reaction was performed for each BMP following same procedure as described in Chapter 6, section 6.2.2 and section 6.2.3.

7.2.3 TOPO TA cloning of BMP-9 and BMP-10 into the pEF/His TOPO plasmid vector.

The coding sequences of full-length BMP-9 and BMP-10 were then cloned into the pEF/His TOPO plasmid vectors, respectively. Details of the methods are in Chapter 2, section 2.5. Primers used for analysis of transformed colonies are in Table 2.1 and Table 2.3.

7.2.4 Plasmids extraction

The resultant recombinant plasmids were then purified and utilised for the subsequent studies. Details of the methods are in Chapter 2, section 2.5.4.

7.2.5 Electroporation and selection.

BMP-9 and BMP-10 expression constructs (plasmids), and empty plasmids were then transfected into separate 3T3 and CHO cells using an electroporator (Easjet Plus, EquiBio Ltd, Kent, UK). The cells were immediately transferred to 25 cm^3 tissue culture flasks containing 5ml of pre-warmed culture medium. Selection of transfectants began when the cells reached 50%-70% confluence. The selection of positive cells was with a medium that contained the antibiotic blasticidin (Sigma-Aldrich, Inc., Poole, Dorset, England, UK) at 5μg/ml. A stable transfectant that carried the insert was then cultured in maintenance medium (blasticidin 0.5μg/ml) and grown to sufficient numbers for experimental studies. The selection took up to to 3 weeks. Different amount of plasmid DNA and different voltages were tested on both 3T3 and CHO cells in order to achieve the most effective transfection. However, despite repeated efforts trying to establish a CHO cell line, this proved unsuccessful, as all the cells subsequently died. Later evidence showed that this was likely to be the result of the dramatic growth inhibitory effect of both BMP9 and BMP10 in CHO cells. CHO cells were therefore dropped as the cell type to generate recombinant BMPs, and studies subsequently focused on using 3T3 cells.

In the case of BMP-9NSCD transfection, the cells were transfected with 2μl of the BMP-9NSCD (NSCD = no stop codon) recombinant plasmids which is nominated as $3T3^{BMP\text{-}9NSCD2}$, and $3T3^{BMP\text{-}9\ NSCD5}$ for the cells transfected with 5μl of the recombinant plasmids. The volume of the recombinant plasmids is 3μl for both

3T3 $^{BMP\text{-}9\ NSCDA}$ and 3T3$^{BMP\text{-}9\ NSCDB}$ cells. The voltage of electroporation for 3T3$^{BMP\text{-}9\ NSCD2}$, 3T3$^{BMP\text{-}9\ NSCD5}$ and 3T3 $^{BMP\text{-}9\ NSCDA}$ was found to be optimal at 190volts, and was 170volts for 3T3$^{BMP\text{-}9\ NSCDB}$. The transfection of BMP-10NSCD transgenes were performed in a same manner.

7.2.6 Verification of BMP-9 and BMP-10 over-expression in 3T3 cells using both immunocytochemical staining and Western blot analysis.

For immunocytochemical analysis, 3T3 cells stably transfected with BMP-9 or BMP-10 plasmid were seeded in the glass chamber slide in duplicate for each cell line. The cells were fixed with 4% formaldehyde (prepared in a neutralising buffer) after an overnight incubation. The immunochemical staining was performed using the method described in the section 2.4.3.

For WB analysis, cells were lysed from the tissue culture flasks, protein extracted and separated on SDS gels (10% SDS-PAGE gel). Proteins were blotted and probed with respective antibodies. Protein bands were visualized with a SupersignalTM West Dura system (Pierce Biotechnology, USA) and documented using the UVITech imager (UVITech, Inc., Cambridge, England, UK).

7.2.7 Purification of the histidine-tagged rh-BMP-9 and rh-BMP-10

Following verification, the transfectants for each BMP were grown to a sufficient amount. The cells were subsequently lysed using the lysis buffer in the absence of SDS. The recombinant proteins were then purified using affinity chromatography. The method has been described in detail in Chapter 2, section 2.9.2.

7.2.8 Desaltification of the purified rh-BMP-9 and rh-BMP-10

The imidazole in the purified recombinant proteins was removed using dialysis, as described in Chapter 2, section 2.9.3.

7.2.9 Quantification of the purified rh-BMP-9 and rh-BMP-10

The purified recombinant proteins and BSA standard (in a series of concentration) were run on a 10% SDS-PAGE gel, and stained with Coomassie blue, the bands were then photographed and quantified using UVIband software (UVITEC, Cambridge, UK). The concentration of rh-BMP-9 and rh-BMP-10 were subsequently calculated according to a standard curve generated from BSA.

7.2.10 *In vitro* cell growth assay

The biological activities of rh-BMP-9 and rh-BMP-10 were examined in PC-3 cells using the *in vitro* cell growth. The cells were incubated in DEME supplied with 10% FCS, and were exposed to different concentrations of rh-BMP-9 or rh-BMP-10 (0ng/ml, 1ng/ml, 10ng/ml and 50ng/ml). The cells were fixed after 3 days incubation, and stained with crystal violet (0.5% w/v). The absorbance which represents cell number was determined at a wavelength of 540nm using a spectrophotometer (BIO-TEK, Elx800, UK). 6 wells were set for the control, while 3 wells were set for each treated group. Two independent experiments were performed.

7.3 Results

7.3.1 Amplification of the full length coding region of human BMP-9 and BMP-10

In order to generate recombinant human BMP-9 and BMP-10, pairs of primers for each BMP with a deletion of the stop codon were designed. The coding sequence of full length human BMP-9 and BMP-10 was amplified and cloned into the pEF/V5-His TOPO TA plasmid vector (the same as use for the over-expression of BMPs in Chapter 6). The deletion of stop codon enables the recombinant plasmids adding a six-histidine tag to protein products of each BMPs. Therefore the recombinant proteins were able to be purified using the affinity chromatography.The coding sequences of full length human BMP-9 and BMP-10 were amplified, the PCR products of BMP-9 (Figure 7.1) and BMP-10 (Figure 7.2) were subsequently purified and utilised in the construction of the expression plasmid.

7.3.2 TOPO TA cloning of BMP-9 and BMP-10 using the pEF/V5-His-TOPO vector

The coding sequences of full-length human BMP-9 and BMP-10 were then cloned into the pEF/V5-His-TOPO plasmid vector, respectively. The colonies for BMP-9 cloning were analysed using PCR (Figure 7.3). Figure 7.4 shows the analysis of colonies for BMP-10 cloning. One colony was chosen for each cloning according to the analysis of the colonies. The recombinant plasmids were then extracted as shown in Figure 7.5.

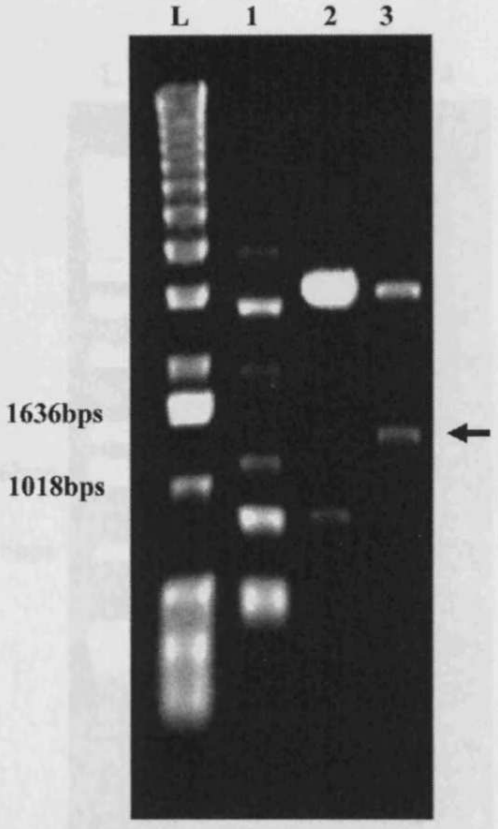

Figure 7.1 Amplification of the coding sequence for full-length human BMP-9 without stop codon (BMP-9NSCD) using LA-PCR. L is 1kb DNA marker, annealing temperature for LA-PCR in lane 1, lane 2 and lane 3 is 64°C, 66°C and 68°C, respectively. Right size of products is 1206 bps indicated by the arrow.

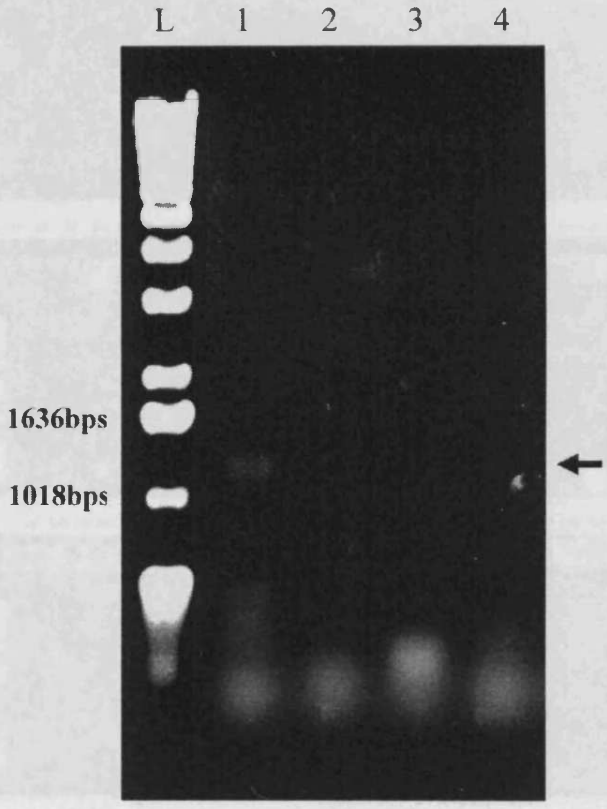

Figure 7.2 Amplification of the coding sequence for full-length human BMP-10 without stop codon (BMP-10NSCD) using LA-PCR. L is 1kb DNA marker, annealing temperature for LA-PCR in lane 1, lane 2, lane 3 and lane 4 is 60°C, 62°C, 64°C and 56°C, respectively. Right size of products is 1272 bps indicated by the arrow.

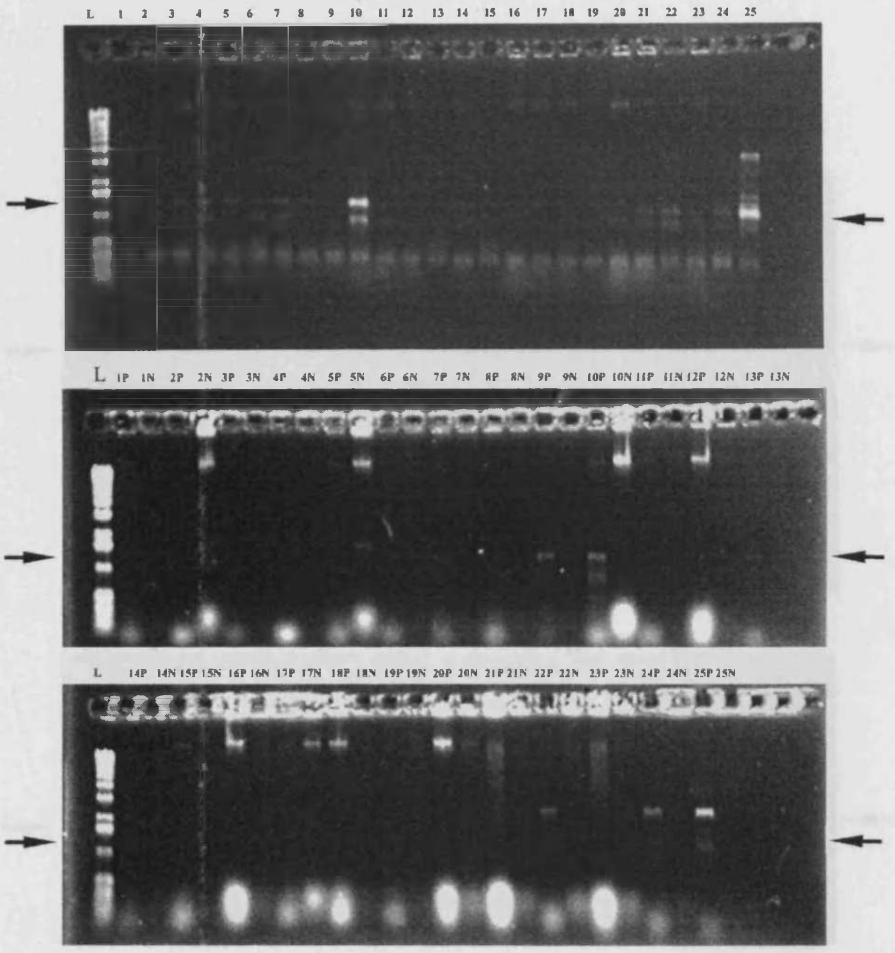

Figure 7.3 Analysis of the colonies *E. Coli* transformed with BMP-9 NSCD pEF/His TOPO plasmids vector using PCR. In the top panel, the presence of BMP-9NSCD inserts was analysed using T7F and BGHR primers, the right products are indicated by arrow (approximate 1400bps). In the middle and bottom panels, the presence and orientation of the BMP-9NSCD inserts were analysis using BMP9F8 coupled with either BGHR or T7F (wrong orientation). L is the 1kb DNA ladder. The products were marked with the number of the colony, P representing the BMP-9NSCD inserts in right orientation, and N indicating the BMP-9NSCD inserts in wrong orientation. The size of right products is approximate 1000bps. Colony 10 was utilised in the following experiments.

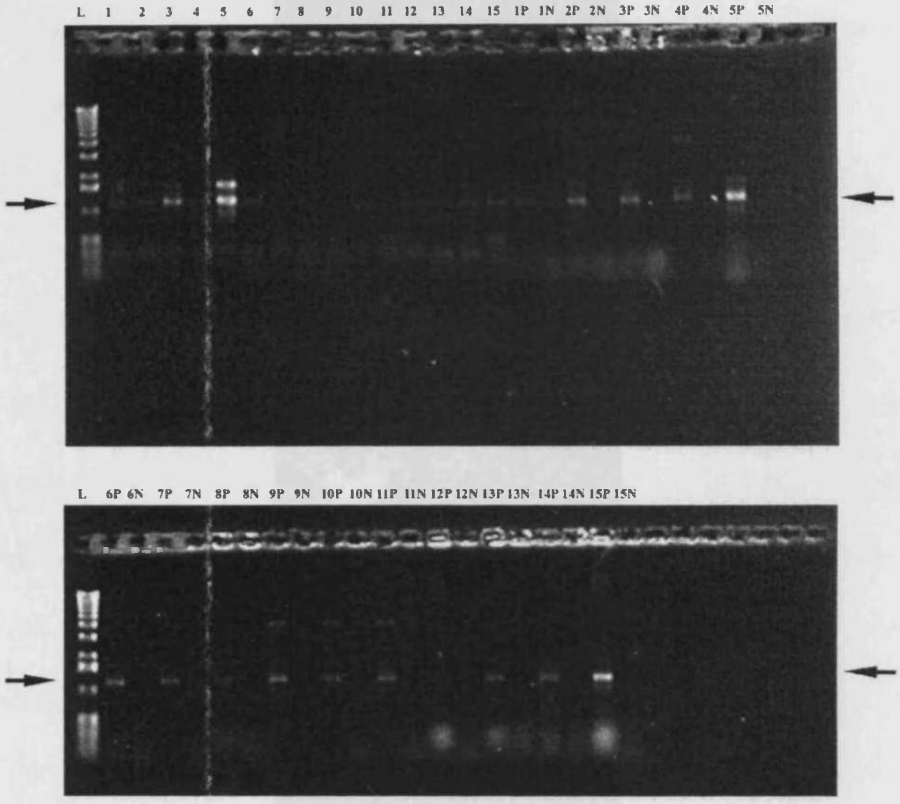

Figure 7.4 Analysis of the colonies *E. Coli* transformed with BMP-10 NSCD pEF/His TOPO plasmids vector using PCR. In the top panel (Lane 1-15), the presence of BMP-10NSCD inserts in 15 colonies was analysed using T7F and BGHR primers, the right products are indicated by arrow (approximate 1400bps). In the top and bottom panels, the presence and orientation of the BMP-10NSCD inserts were then analysis using BMP10F1 coupled either BGHR (right orientation), or T7F (wrong orientation). L is the 1kb DNA ladder. The products were marked with the number of the colony, P representing the BMP-10NSCD inserts in right orientation, and N indicating the BMP-10NSCD inserts in wrong orientation. The size of right products is approximate 1000bps. Colony 7 was utilised for the subsequent experiments.

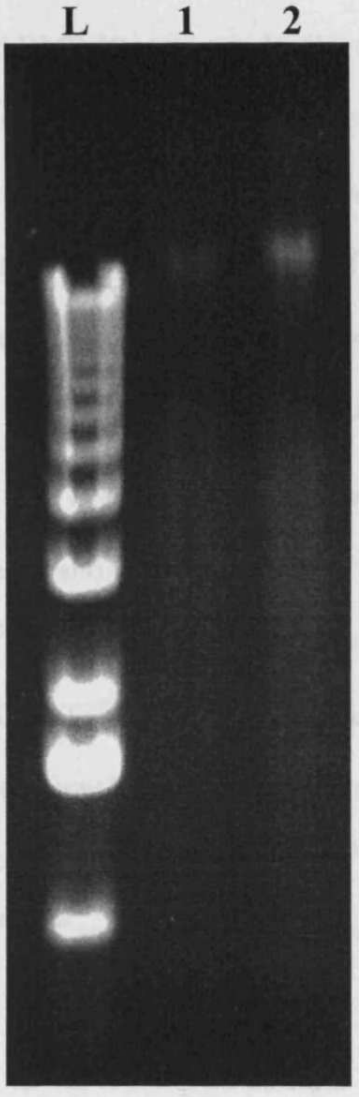

Figure 7.5 BMP-9 NSCD and BMP-10 NSCD transgenes were purified from the resultant transfectants, respectively. The purified plasmids were visualised on the agarose gel. Lane L is the 1kb DNA ladder, Lane 1 is BMP-9NSCD transgenes, and Lane 2 is the BMP-10NSCD transgenes.

7.3.3 Verification of the forced expression of human BMP-9 and BMP-10 in 3T3 cells

The BMP-9, BMP-10 expression constructs and empty vectors were transfected into the 3T3 cells, respectively. After 2 weeks' selection with blasticidin, the expression of BMP-9 and BMP-10 at protein level were found to be successful as shown by the immunochemical staining. Figure 7.6 shows the immunostaining of BMP-9, which is stronger in the four BMP-9NSCD transfectants compared to the wild type cells ($3T3^{WT}$) and the empty vector control ($3T3^{pEF/His}$). The staining is dense in the cytoplasm of the transfectants. The immunostaining of BMP-10 in the cytoplasm was also stronger in the four BMP-10NSCD transfectants (Figure 7.7).

The protein levels of both BMPs in 3T3 cells were further confirmed by western blot analysis. Figure 7.8 shows the protein level of BMP-9 was remarkably increased in both $3T3^{BMP\text{-}9NSCDA}$ and $3T3^{BMP\text{-}9NSCDB}$ cells, in comparison with the $3T3^{WT}$ and $3T3^{pEF/His}$ cells. The $3T3^{BMP\text{-}9NSCD2}$ was missing due to an accidental contamination. A higher protein level of BMP-10 was also revealed in the $3T3^{BMP\text{-}10NSCD2}$ and $3T3^{BMP\text{-}10NSCDB}$ cells, compared to the $3T3^{WT}$ and $3T3^{pEF/His}$ cells (Figure 7.9). Therefore the $3T3^{BMP\text{-}9NSCDB}$ and $3T3^{BMP\text{-}10NSCDB}$ were utilised for the subsequent experiments.

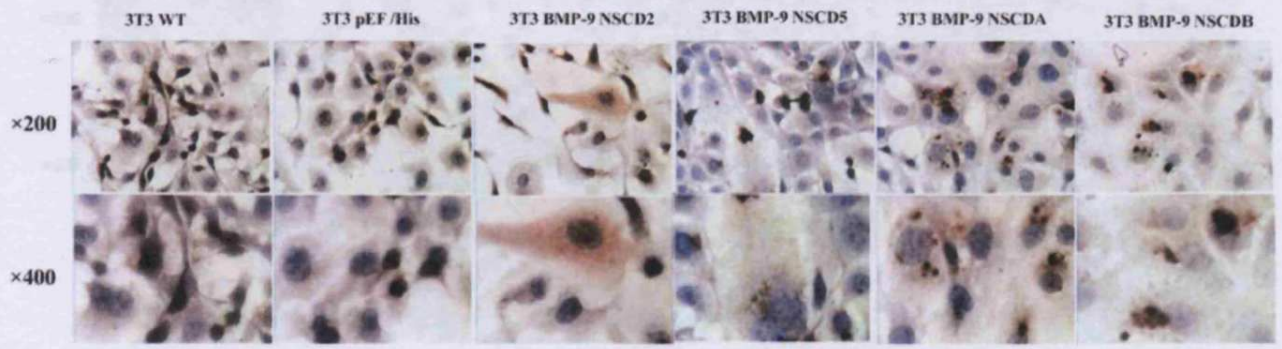

Figure 7.6 Verification of BMP-9 expression in 3T3 cells using immunochemical staining.
An intense immunostaining of BMP-9 was seen in the cytoplasm of a few cells in all the 3T3 BMP-9NSCD transfectants, in comparison with the wild type control (3T3 WT) and empty vector control (3T3 pEF/His).

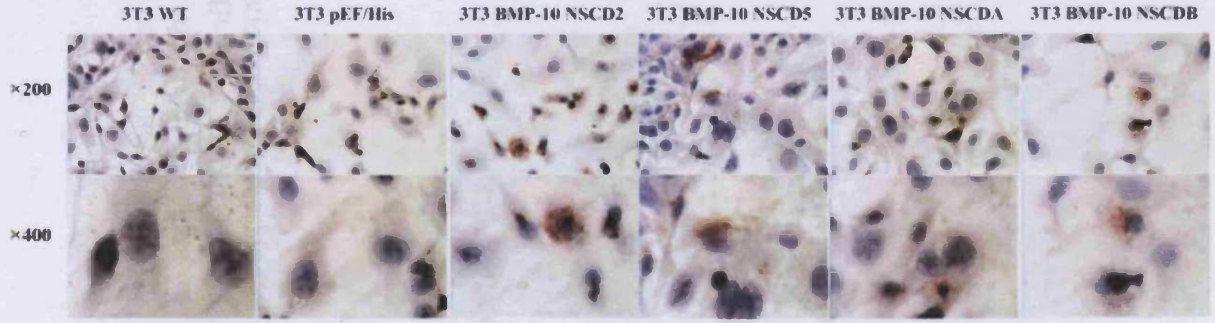

Figure 7.7 Verification of BMP-10 expression in 3T3 cells using immunochemical staining.
An intense immunostaining of BMP-10 was seen in the cytoplasm of a few cells in all the 3T3 BMP-10NSCD transfectants, in comparison with the wild type control (3T3 WT) and empty vector control (3T3 pEF/His).

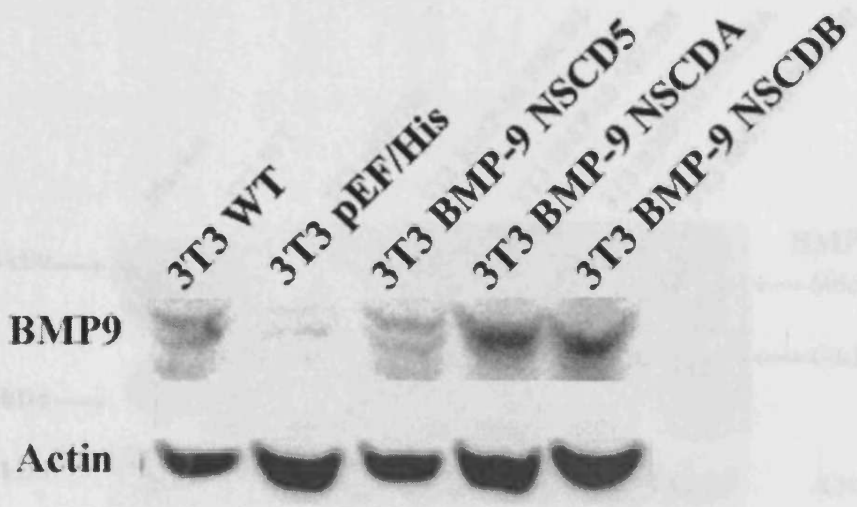

Figure 7.8 Verification of the expression of BMP-9 protein in 3T3 cells after transfection of BMP-9 NSCD transgenes using western blot analysis.
A stronger band of approximate 60kDa was seen in the cell lysates of $3T3^{BMP\text{-}9NSCDA}$ and $3T3^{BMP\text{-}9NSCDB}$ cells, which presents the monomer of unprocessed BMP-9 precursor protein.

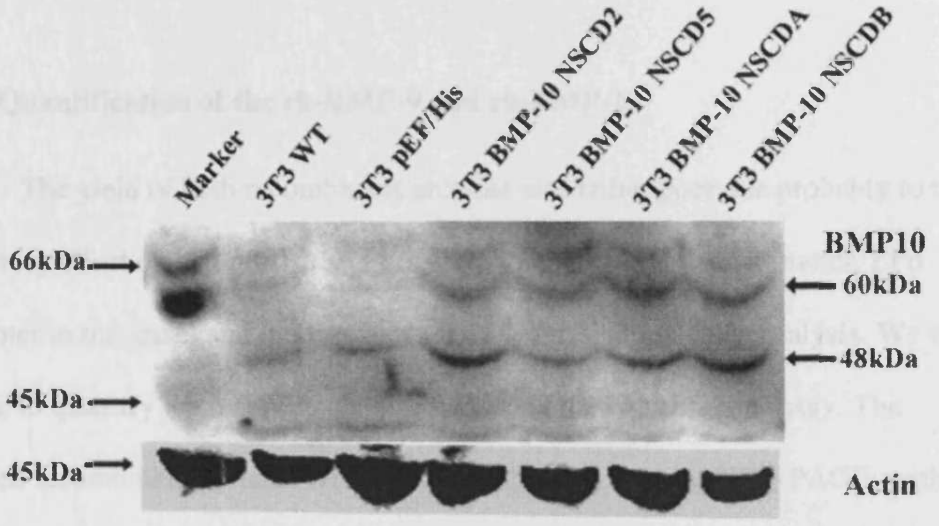

Figure 7.9 Expression of BMP-10 in 3T3 cells after transfection of BMP-10 NSCD transgenes using Western blot analysis.
Stronger bands of approximate 60kDa and 48kDa were seen in the cell lysates of 3T3 BMP-10NSCD transfectants, particularly of $3T3^{BMP\text{-}10NSCD2}$, $3T3^{BMP\text{-}10NSCDA}$ and $3T3^{BMP\text{-}10NSCDB}$ cells, which are the monomers of unprocessed BMP-10 precursor protein and the monomers of processed BMP-9 proprotein.

7.3.4 Purification of the histidine tagged recombinant proteins

We successfully purified the recombinant human BMP-9 (rh-BMP-9) from the $3T3^{BMP\text{-}9NSCDB}$ cells using metal (nickel) chelating affinity chromatography, which was demonstrated using western blot analysis (Figure 7.10). Similarly, the recombinant human BMP-10 (rh-BMP-10) was also purified as illustrated in Figure 7.11.

7.3.5 Quantification of the rh-BMP-9 and rh-BMP-10

The yield of both recombinant proteins was rather poor due probably to the inhibitory effect on cell growth and the efficiency of the vector (promoter, EF6 promoter in this case) and the loss during the desaltification using dialysis. We were unable to quantify the recombinant proteins using the colorimetric assay. The purified recombinant proteins were then quantified by running SDS-PAGE, with the BSA solutions at a series of concentrations (Figure 7.12A). The proteins on the gel were stained and photographed, the volume of the bands were then quantified. According to the standard curve of BSA, the concentration of each recombinant proteins was calculated (Figure 7.12B). The concentration of the rh-BMP-9 was 9.1μg/ml and 8.2μg/ml for the rh-BMP-10. We regarded this as disappointing, but sufficient for the planned *in vitro* use.

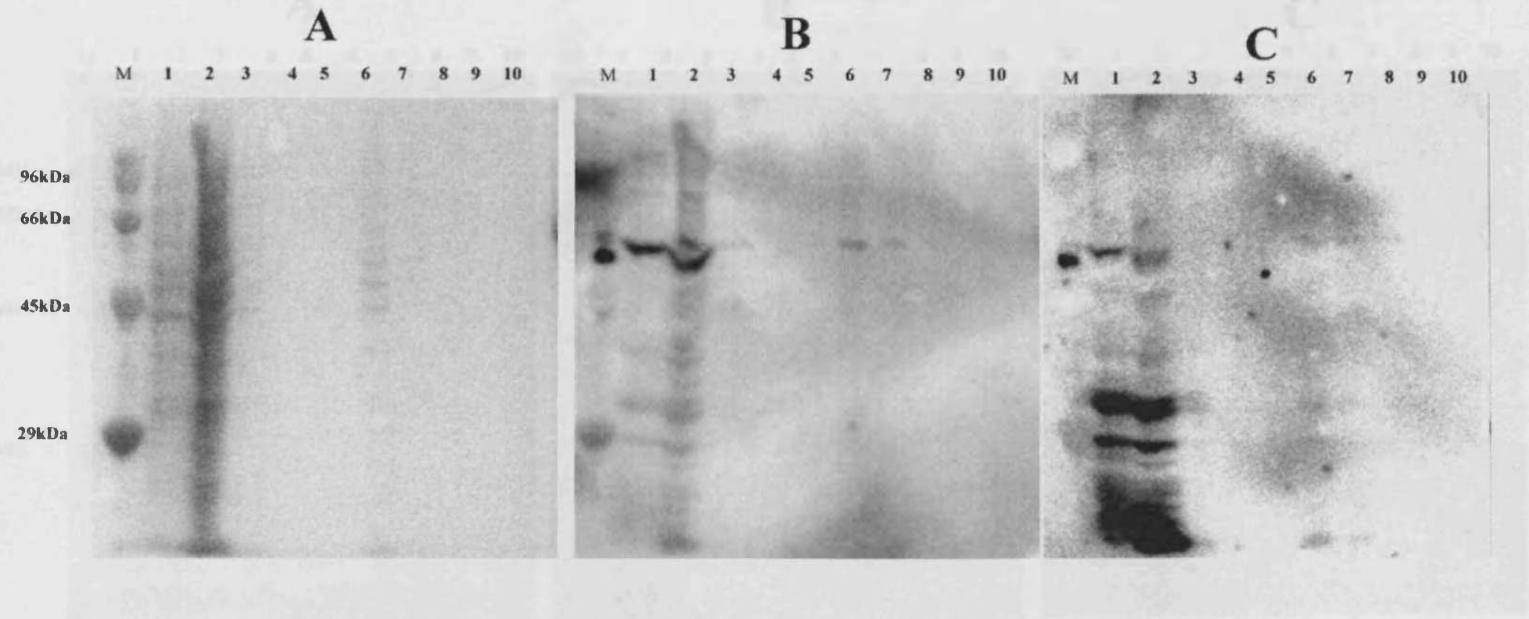

Figure 7.10 Purificaion of rhBMP9, as indicated in western blot analysis.
Lane M is molecule weight marker; 1 is cell debris after lysation; 2 is cell lysate; 3 is flowing through; 4 is washing with the binding buffer (10mM imidazole); 5 is the elution (31.25mM imidazole); 6 is the elution (62.5mM imidazole); 7 is the elution (125mM imidazole); 8 is the elution (250mM imidazole); 9 is the elution (500mM imidazole); 10 is the last elution (500mM imidazole). A is the membrane stained with Ponceau S; B is the membrane probed with the anti-His antibody; C is the membrane probed with the anti-BMP9 antibody. Proprotein of rhBMP9 (approximately 60kDa) were detected by both anti-His and the anti-BMP9 antibodies.

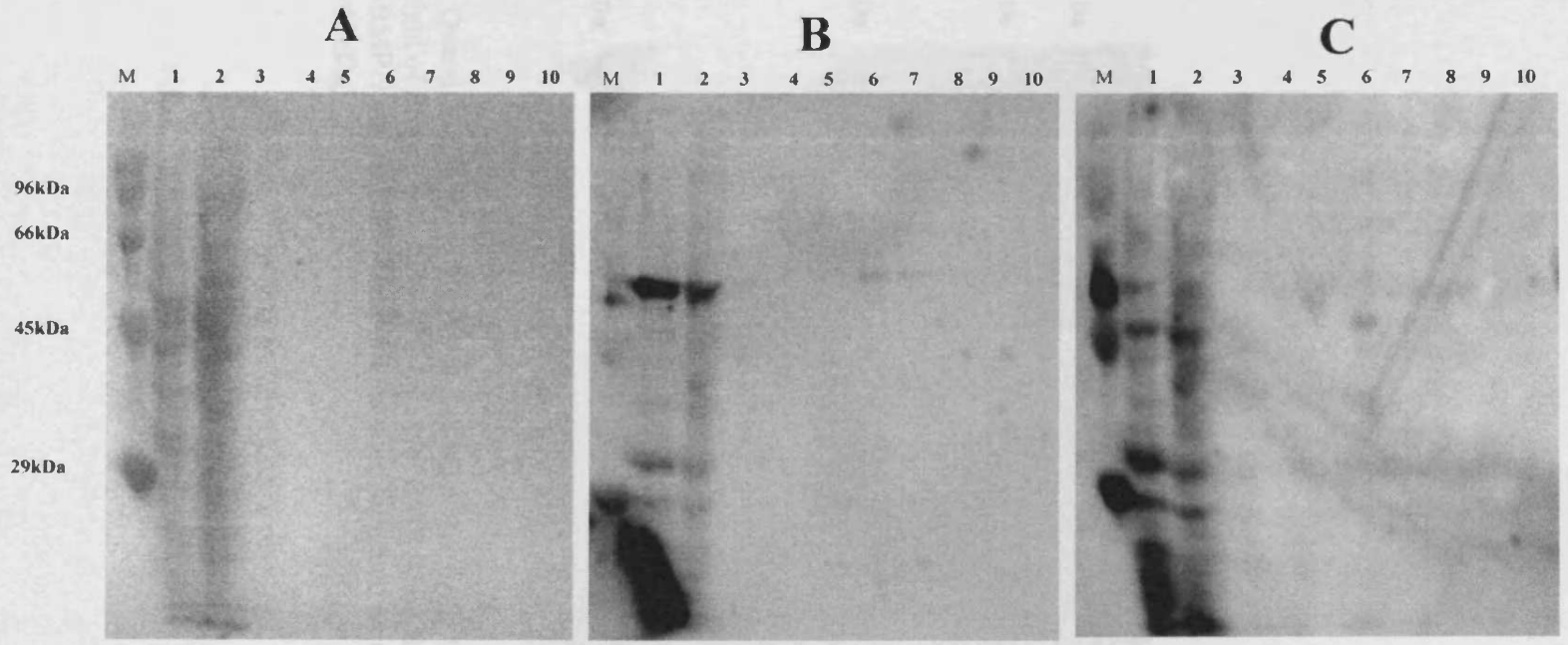

Figure 7.11 Purification of rh-BMP-10 from 3T3 transfectants, as indicated using western blot analysis.
Lane M is molecule weight marker; 1 is cell debris after lysation; 2 is cell lysate; 3 is flowing through; 4 is washing with the binding buffer (10mM imidazole); 5 is the elution (31.25mM imidazole); 6 is the elution (62.5mM imidazole); 7 is the elution (125mM imidazole); 8 is the elution (250mM imidazole); 9 is the elution (500mM imidazole); 10 is the last elution (500mM imidazole). A is the membrane stained with Ponceau S; B is the membrane probed with anti-His antibody; C is the membrane probed with anti-BMP10 antibody. Proprotein of rhBMP10 (approximately 60kDa) were detected by both anti-His and anti-BMP10 antibodies.

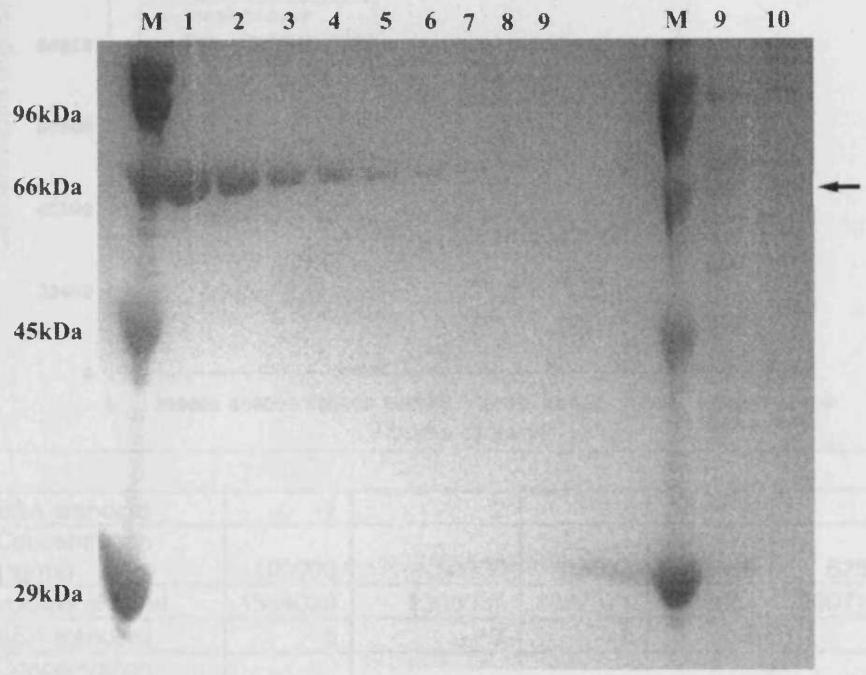

Figure 7.12A Quantification of rh-BMP-9 and rh-BMP-10, using SDS-PAGE. The molecular weight of BSA is 66.4 kDa. The bands of BMP-9 and BMP-10 in the respective rh-BMP-9 and rh-BMP-10 solutions were indicated by the arrow (approximate 60kDa).

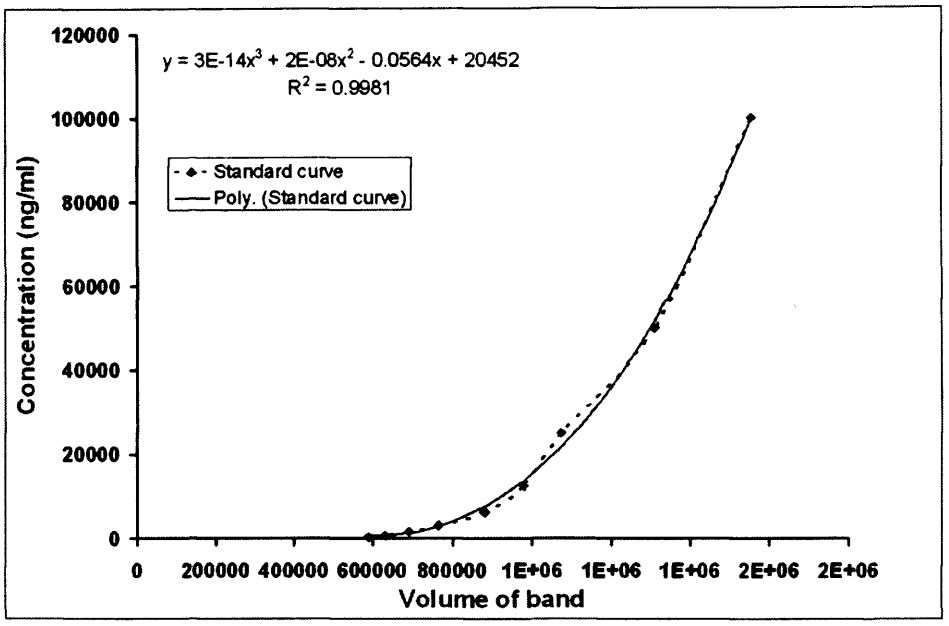

BSA standard	1	2	3	4	5
Concentration (ng/ml)	100000	50000	25000	12500	6250
volume of band	1554028	1308037	1072371	978854	880713
BSA standard	6	7	8	9	
Concentration (ng/ml)	3125	1562.5	781.25	390.625	
volume of band	764329	689746	630308	590250	

	rhBMP9	rhBMP10
Volume of Band	925069	908793
Concentration (ng/ml)	9142.06	8231.46

Figure 7.12B Quantification of rh-BMP-9 and rh-BMP-10, using SDS-PAGE.
The bands were quantified using UVIband software (UVITEC, Cambridge, UK). The concentration of rh-BMP-9 and rh-BMP-10 were subsequently calculated according the BSA standard curve.

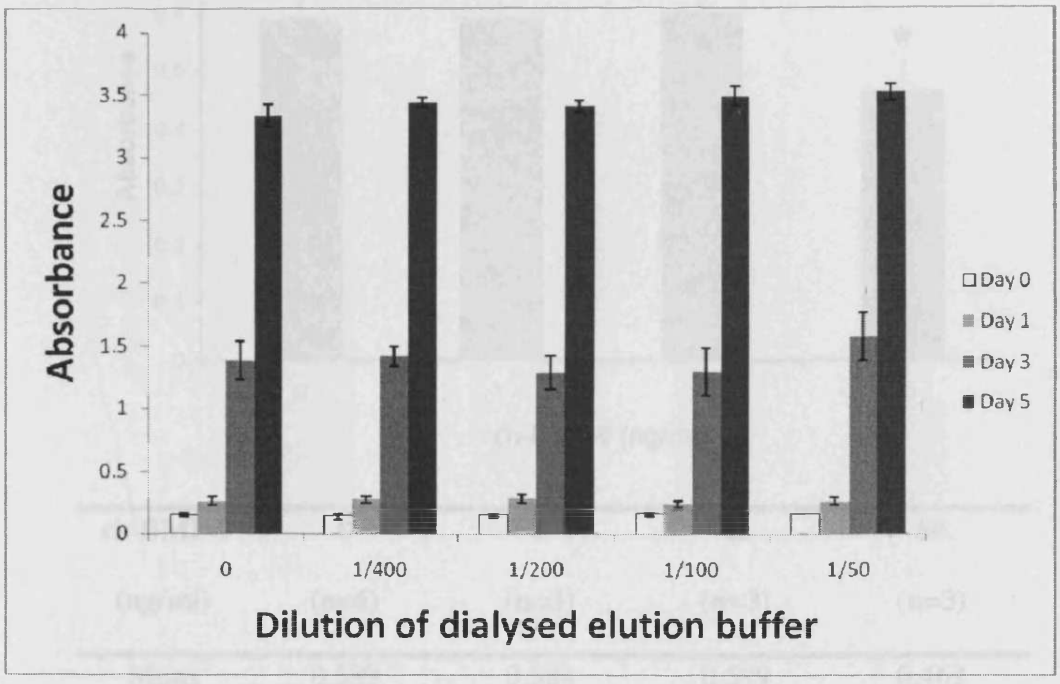

Figure 7.13 Effect of dialysed elution buffer on *in vitro* cell growth of PC-3 cells using the in vitro cell growth assay.
There is no marked influence on the in vitro growth of PC-3 cells by dialysed elution buffer which was same as used to elute recombinant proteins and then was dialysed following same dialysis procedsure for the recombinant proteins. Error bars are standard deviations. The highest dilution ratio used in this experiment is the dilution to make 40ng/ml of both BMP-9 and BMP-10.

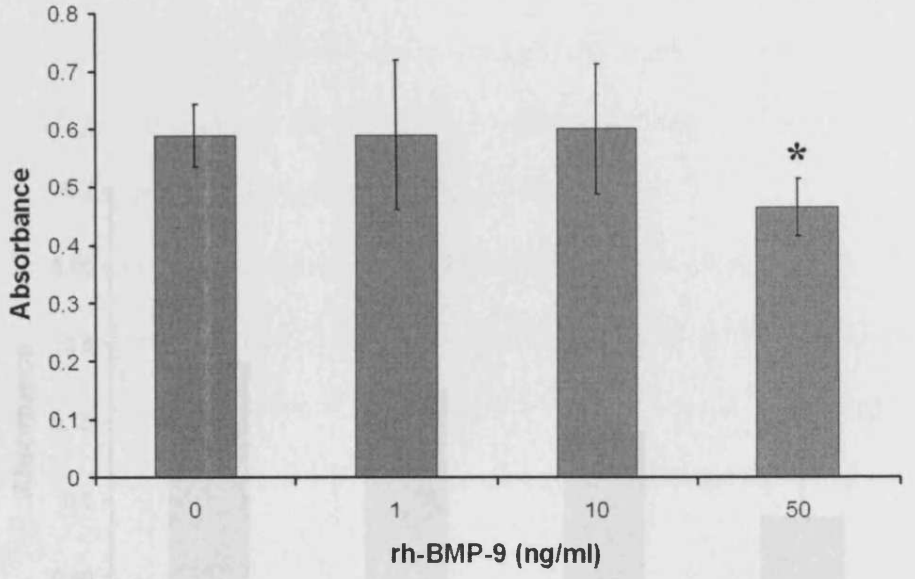

rh-BMP-9 (ng/ml)	0 (n=6)	1 (n=3)	10 (n=3)	50 (n=3)
Mean	0.589	0.588	0.599	0.462
sd	0.053	0.129	0.113	0.049

Figure 7.14 Effect of rh-BMP-9 on *in vitro* cell growth of PC-3 cells using the in vitro cell growth assay.
The cell growth of PC-3 cells were reduced by the exposure of rh-BMP-9 at 50ng/ml. Error bars are standard deviations. * $p<0.05$ vs control.

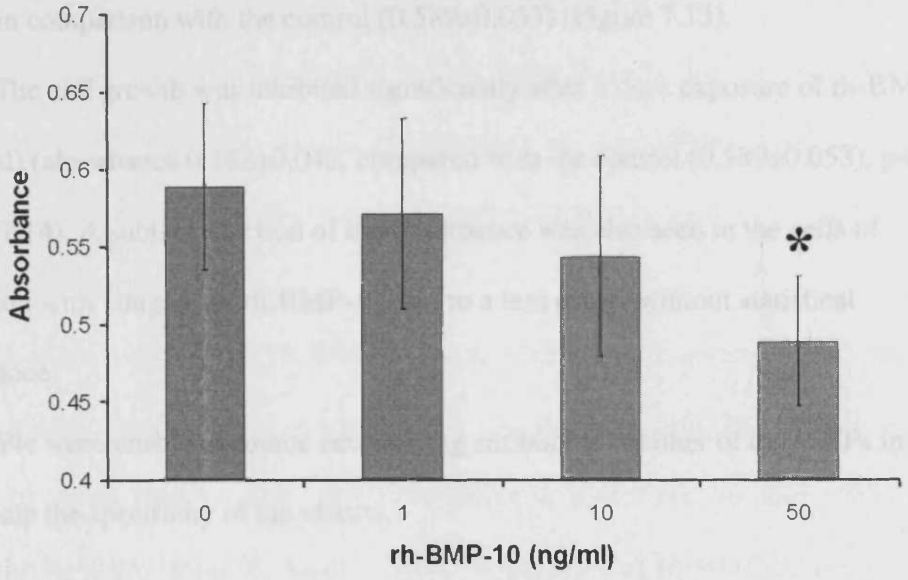

rh-BMP-10 (ng/ml)	0 (n=6)	1 (n=3)	10 (n=3)	50 (n=3)
Mean	0.589	0.571	0.543	0.488
Sd	0.0533	0.061	0.064	0.042

Figure 7.15 Effects of rh-BMP-10 on *in vitro* cell growth of PC-3 cells using the in vitro cell growth assay.
The exposure to rh-BMP-10 of 50ng/ml inhibited the *in vitro* cell growth of PC-3 cells. Error bars are standard deviations. * $p<0.05$ vs control.

7.3.6 Influence of rh-BMP-9 and rh-BMP-10 on the *in vitro* cell growth of PC-3 cells

Whether the recombinant human BMPs generated in this procedure had biological activity was first verified using the cell growth model. The cell growth was inhibited after 3 days exposure of rh-BMP-9 (50ng/ml), its absorbance is 0.462±0.049, $p<0.05$ in comparison with the control (0.589±0.053) (Figure 7.13).

The cell growth was inhibited significantly after 3 days exposure of rh-BMP-10 (50ng/ml) (absorbance 0.488±0.042, compared with the control (0.589±0.053), $p<0.05$) (Figure 7.14). A subtle reduction of the absorbance was also seen in the cells of incubation with 10ng/ml of rh-BMP-10, but to a less extent without statistical significance.

We were unable to source neutralising antibodies to either of the BMPs in order to evaluate the specificity of the effects.

7.4 Discussion

In these current experiments, a mammalian expression vector was usded to transfect a mammalian cell line, 3T3 cell. To purify the recombinant protein from the cell lysate, the mammalian expression plasmid vector which can add a histidine tag to the recombinant protein was chosen for present study. Therefore, we were able to purify the recombinant proteins using metal chelating affinity chromatography. In the *in vitro* growth assay, we have also verified that both rh-BMP-9 and rh-BMP-10 have inhibitory effects on the cell growth of PC-3 cells. This biological function is consistent with the effects of BMP-9 and BMP-10 from our previous observations in Chapter 6.

From the present study, it is clear that the yield of both recombinant proteins were low. Two possible reasons are thought to be responsible:. The first possibility is that the most productive transfectants were lost due to the inhibitory effect on cell growth. This could happen in the immediate period after transfection and the subsequent selection using blasticidin. This was the reason that we dropped CHO cell in earlier experiments (data not shown), as none of the CHO cell survive the selection and subsequent re-population, due largely to the dramatic reduction of cell growth. The second reason is the loss, during the process of desaltification, of the purified recombinant proteins, in which the recombinant protein may bind to the membrane that was used for dialysis.

In current study, both rh-BMP-9 and rh-BMP-10 were generated and used in the *in vitro* experiments. This demonstrates that this strategy could be utilised for further studies. However, improvement of this procedure or alternative methods would have to be sought for large scale production. Both rh-BMP-9 and rh-BMP-10 require further investigation, such as to elucidate the specific signal transduction of the BMPs and the implication of these molecules in prostate cancer.

One drawback of the present study was the lack of an alternative means to verify the specificity of the rhBMP9 and BMP10 in cell growth analysis, due largely to the lack of neutralising antibodies to either of the BMPs. However, two factors lead us to believe that the functional changes shown here are specific to the respective recombinant proteins. Firstly, the purification of the recombinant proteins. It is evident that the study has carried out necessary precaution when purifying the proteins (affinity column and subsequent dialysis). This has ensured maximum degree of exclusion of irrelevant

molecules (small and large) in the preparations. Secondly, subsequent reception and downstream signalling pathway investigations. It is hoped that neutralising antibodies will be generated using these recombinant protein in future studies.

Chapter 8

General Discussion

BMPs have been implicated in the development and progression of prostate cancer, particularly in the bony metastasis. However, the roles which the latest identified BMPs play in the disease development and progression, and the mechanisms underlying are still largely unknown. These are recruited in current investigations.

8.1 The main findings from this study

In the current study, we examined the expression of BMPs, BMP receptors and the molecules involved in their signal transduction in prostate cancer. The expression of some BMPs, receptors and intracellular signalling molecules in prostate cell lines has been detected using RT-PCR. These results not only give us a basic assessment of the function of these molecules in prostate cancer, but also allow us to choose suitable cell lines to manipulate the expression of BMPs and their receptors. Most interestingly, BMP-9 the most powerful osteoinductive factor up to date, and BMP-10 which is enrolled in the same subgroup, showed subtle variations in the expression of mRNA transcripts in prostate cancer cell lines. The expression of BMP-9, BMP-10, BMPR-IB and BMPR-II was further examined in prostate specimens using immunohistochemical staining. Decreasing expression of these molecules was seen in prostate cancer cells in comparison with the expression in normal prostate epithelia. This suggests that these BMPs and the receptors may play profound roles in the development and progression of prostate cancer.

Following the examination of the expression of BMPs and BMP receptors in prostate cancer, we successfully knocked down two BMP receptors, BMPR-IB and BMPR-II in prostate cancer cells (PC-3) using a respectively constructed hammer head

ribozyme transgene for each. Down-regulation of both receptors in the PC-3 cells by ribozyme transgenes resulted in an increase of cellular proliferation. This finding is consistent with previously documented biological functions of both receptors in prostate cancer. It suggests that both receptors are responsible in mediating the inhibitory effects of BMPs on cell growth in prostate cancer cells. These cell strains with reduced expression of the BMPR-IB and BMPR-II were subsequently utilized for further investigations of signal transduction of BMPs (BMP-9 and BMP-10).

A different expression pattern of BMP-7 was revealed in prostate cancer which is decreased or absent in the primary tumours but re-expressed in the bone metastases, in contrast with BMP-2, 4 and 6. Some studies have demonstrated the biological functions of BMP-7 by exposing prostate cancer cells to exogenous recombinant human BMP-7 (rh-BMP-7), which remains controversial. In current study, we further elucidated the role which BMP-7 plays in prostate cancer, through reducing the endogenous BMP-7. We constructed a ribozyme transgene targeting at human BMP-7 to knockdown the BMP7 gene transcript The ribozyme transgene reduced the expression of BMP-7, at the mRNA and protein level, in PC-3 cells. The invasive, motive and adhesive potentials were significantly increased following the loss of BMP-7 expression. The change in motility was seen together with changes in the cellular location of paxillin and focal adhesion kinase ($p125^{FAK}$). Interestingly, the reduction of endogenous BMP-7 resulted in decreased expression of both Noggin and Follistatin, which are antagonists of BMPs. This suggests that endogenous BMP-7 controls cellular motility and adhesion through regulation of the BMP antagonists.

To investigate the biological functions of BMP-9 and BMP-10 in prostate cancer cells, we constructed transgenes which carry the coding sequences of full-length human BMP-9 and BMP-10, respectively. Following the transfection of the transgenes and the selection, the over-expression of BMP-9 and BMP-10 in PC-3 transfectants was verified at both mRNA and protein level. Over-expression of BMP-9 can inhibit the cell growth, adhesion, invasion and migration of prostate cancer cells *in vitro*. Similar effects on the cellular biology of prostate cancer cells were revealed after the over-expression of BMP-10. These evidences suggest that both BMP-9 and BMP-10 have tumour-suppressor functions.

In the current study, we have also generated both recombinant human BMP-9 (rh-BMP-9) and rh-BMP-10, in order to further investigate the respective signalling, and to elucidate the mechanisms underlying. This was achieved by cloning the full length coding region of the gene products (without stop codon) into a mammalian expression vector. A murine fibroblast cell line (3T3 cell) was transfected with the transgenes. The stable transfectants produced BMP-9 or BMP-10 labelled with his-tag, and the recombinant proteins were purified using affinity chromatography.

8.2 Prospects of future study

In the current study, we have demonstrated an inhititory effect of BMP-9 and BMP-10 on the growth of prostate cancer cells. However, mechanism(s) underlying these actions remains unclear. For example what receptors and downstream cascade(s) are involved in the inhibitory effect of both BMPs. Further investigation is needed to examine the activation of some possible candidates, such as BMPR-1A, BMPR-1B,

BMPR-2 and R-Smads. If possible, the involvement of BMPR-1B and BMPR-2 in the signal transduction by BMP-9 and BMP-10 will be investigated using the PC-3 transfectants in which the receptors have been knocked down respectively. On the other hand, the influence on the cell cycle and apoptosis of prostate cancer cells is also needed to be investigated for a full understanding of the inhibitory effects on cell growth by BMP-9 and BMP-10. These work are currently undergoing in the host department.

The mechanisms underlying the effects of BMP-9 and BMP-10 on adhesion and motility of prostate cancer cells are still unclear. In current study of the endogenous BMP-7, activated Paxillin and FAK have been correlated with the facilitated adhesion and motility of PC-3. Whether these molecules or integrins are involved in these effects of BMP-9 and BMP-10 still need further exploration.

The feedback regulation of BMP antagonists (Noggin and Follistatin) by BMP-7 has been demonstrated in current study. Most recent evidence also showed these BMP antagonists were responsive genes to BMP-9 in murine basal forebrain cholinergic neurons (Lopez-Coviella *et al.*, 2005). Whether and how the BMP antagonists are involved in the biological effects of BMP-9 and BMP-10 in prostate cancer are in the plan of future study.

In prostate cancer, androgens play an important part in the carcinogenesis, progression and metastasis of the disease. The documented literature has shown that androgen can induce BMPR-IB and BMP-7 in prostate cancer cells, but not BMPR-II and BMP-6. Recent evidence shows that upon phosphorylation of the Smad-1 linker region by MAPK, Smad-1 physically interacts with androgen-activated androgen receptor (AR) and suppress its functions (Qiu *et al.*, 2007). This suggests there are some

interactions between BMPs system and androgen system. However, whether such crosstalks also exist between androgen and BMP-9 /BMP-10, is necessary to be elucidated in the further studies.

Above all as potential tumour suppressor genes, further studies using *in vivo* tumour model are necessary to elucidate the implication of both BMP-9 and BMP-10 in prevention and treatment of prostate primary tumour and corresponding secondary tumour. This may highlight the therapeutic value of BMP-9 and BMP-10, and the delivery approaches of these two BMPs may also need further study.

Bibliography

Abdelaal, M. M., S. S. Tholpady, J. D. Kessler, R. F. Morgan and R. C. Ogle (2004). BMP-9-transduced prefabricated muscular flaps for the treatment of bony defects. *J Craniofac Surg.* **15**(5):736-741; discussion 742-734.

Achbarou, A., S. Kaiser, G. Tremblay, L. G. Ste-Marie, P. Brodt, D. Goltzman and S. A. Rabbani (1994). Urokinase overproduction results in increased skeletal metastasis by prostate cancer cells in vivo. *Cancer Res.* **54**(9):2372-2377.

Affar el, B., M. P. Luke, F. Gay, D. Calvo, G. Sui, R. S. Weiss, E. Li and Y. Shi (2006). Targeted ablation of Par-4 reveals a cell type-specific susceptibility to apoptosis-inducing agents. *Cancer Res.* **66**(7):3456-3462.

Ahmed, N., J. Sammons, R. J. Carson, M. A. Khokher and H. T. Hassan (2001). Effect of bone morphogenetic protein-6 on haemopoietic stem cells and cytokine production in normal human bone marrow stroma. *Cell Biol Int.* **25**(5):429-435.

Andersson, O., E. Reissmann and C. F. Ibanez (2006). Growth differentiation factor 11 signals through the transforming growth factor-beta receptor ALK5 to regionalize the anterior-posterior axis. *EMBO Rep.* **7**(8):831-837.

Aoki, H., M. Fujii, T. Imamura, K. Yagi, K. Takehara, M. Kato and K. Miyazono (2001). Synergistic effects of different bone morphogenetic protein type I receptors on alkaline phosphatase induction. *J Cell Sci.* **114**(Pt 8):1483-1489.

Aono, A., M. Hazama, K. Notoya, S. Taketomi, H. Yamasaki, R. Tsukuda, S. Sasaki and Y. Fujisawa (1995). Potent ectopic bone-inducing activity of bone morphogenetic protein-4/7 heterodimer. *Biochem Biophys Res Commun.* **210**(3):670-677.

Arora, K. and R. Warrior (2001). A new Smurf in the village. *Dev Cell.* **1**(4):441-442.

Attisano, L., J. L. Wrana, F. Lopez-Casillas and J. Massague (1994). TGF-beta receptors and actions. *Biochim Biophys Acta.* **1222**(1):71-80.

Autzen, P., C. N. Robson, A. Bjartell, A. J. Malcolm, M. I. Johnson, D. E. Neal and F. C. Hamdy (1998). Bone morphogenetic protein 6 in skeletal metastases from prostate cancer and other common human malignancies. *Br J Cancer.* **78**(9):1219-1223.

Babitt, J. L., Y. Zhang, T. A. Samad, Y. Xia, J. Tang, J. A. Campagna, A. L. Schneyer, C. J. Woolf and H. Y. Lin (2005). Repulsive guidance molecule (RGMa), a DRAGON homologue, is a bone morphogenetic protein co-receptor. *J Biol Chem.* **280**(33):29820-29827.

Balemans, W. and W. Van Hul (2002). Extracellular regulation of BMP signaling in vertebrates: a cocktail of modulators. *Dev Biol.* **250**(2):231-250.

Barnes, J., C. T. Anthony, N. Wall and M. S. Steiner (1995). Bone morphogenetic protein-6 expression in normal and malignant prostate. *World J Urol.* **13**(6):337-343.

Batson, O. V. (1995). The function of the vertebral veins and their role in the spread of metastases. *Clin Orthop Relat Res.* 312):4-9.

BCCPSG (1994). The effect of vitamin E and beta carotene on the incidence of lung cancer and other cancers in male smokers. The Alpha-Tocopherol, Beta Carotene Cancer Prevention Study Group. *N Engl J Med.* **330**(15):1029-1035.

Beck, H. N., K. Drahushuk, D. B. Jacoby, D. Higgins and P. J. Lein (2001). Bone morphogenetic protein-5 (BMP-5) promotes dendritic growth in cultured sympathetic neurons. *BMC Neurosci.* **2**(12.

Bentley, H., F. C. Hamdy, K. A. Hart, J. M. Seid, J. L. Williams, D. Johnstone and R. G. Russell (1992). Expression of bone morphogenetic proteins in human prostatic adenocarcinoma and benign prostatic hyperplasia. *Br J Cancer.* **66**(6):1159-1163.

Beral, V., H. Inskip, P. Fraser, M. Booth, D. Coleman and G. Rose (1985). Mortality of employees of the United Kingdom Atomic Energy Authority, 1946-1979. *Br Med J (Clin Res Ed).* **291**(6493):440-447.

Bornstein, P., L. C. Armstrong, K. D. Hankenson, T. R. Kyriakides and Z. Yang (2000). Thrombospondin 2, a matricellular protein with diverse functions. *Matrix Biol.* **19**(7):557-568.

Brown, M. A., Q. Zhao, K. A. Baker, C. Naik, C. Chen, L. Pukac, M. Singh, T. Tsareva, Y. Parice, A. Mahoney, V. Roschke, I. Sanyal and S. Choe (2005). Crystal structure of BMP-9 and functional interactions with pro-region and receptors. *J Biol Chem.* **280**(26):25111-25118.

Brubaker, K. D., E. Corey, L. G. Brown and R. L. Vessella (2004). Bone morphogenetic protein signaling in prostate cancer cell lines. *J Cell Biochem.* **91**(1):151-160.

Bubendorf, L., A. Schopfer, U. Wagner, G. Sauter, H. Moch, N. Willi, T. C. Gasser and M. J. Mihatsch (2000). Metastatic patterns of prostate cancer: an autopsy study of 1,589 patients. *Hum Pathol.* **31**(5):578-583.

Buckley, S., W. Shi, B. Driscoll, A. Ferrario, K. Anderson and D. Warburton (2004). BMP4 signaling induces senescence and modulates the oncogenic phenotype of A549 lung adenocarcinoma cells. *Am J Physiol Lung Cell Mol Physiol.* **286**(1):L81-86.

Buggisch, M., B. Ateghang, C. Ruhe, C. Strobel, S. Lange, M. Wartenberg and H. Sauer (2007). Stimulation of ES-cell-derived cardiomyogenesis and neonatal cardiac cell

proliferation by reactive oxygen species and NADPH oxidase. *J Cell Sci.* **120**(Pt 5):885-894.

Burger, M. J., M. A. Tebay, P. A. Keith, H. M. Samaratunga, J. Clements, M. F. Lavin and R. A. Gardiner (2002). Expression analysis of delta-catenin and prostate-specific membrane antigen: their potential as diagnostic markers for prostate cancer. *Int J Cancer.* **100**(2):228-237.

Bussemakers, M. J., A. van Bokhoven, G. W. Verhaegh, F. P. Smit, H. F. Karthaus, J. A. Schalken, F. M. Debruyne, N. Ru and W. B. Isaacs (1999). DD3: a new prostate-specific gene, highly overexpressed in prostate cancer. *Cancer Res.* **59**(23):5975-5979.

Butler, S. J. and J. Dodd (2003). A role for BMP heterodimers in roof plate-mediated repulsion of commissural axons. *Neuron.* **38**(3):389-401.

Byrne, R. L., H. Leung and D. E. Neal (1996). Peptide growth factors in the prostate as mediators of stromal epithelial interaction. *Br J Urol.* **77**(5):627-633.

Canalis, E., A. N. Economides and E. Gazzerro (2003). Bone morphogenetic proteins, their antagonists, and the skeleton. *Endocr Rev.* **24**(2):218-235.

CancerStats (2005). CancerStats Incidence UK. *Cancer Research UK.*

Carducci, M. A., R. J. Padley, J. Breul, N. J. Vogelzang, B. A. Zonnenberg, D. D. Daliani, C. C. Schulman, A. A. Nabulsi, R. A. Humerickhouse, M. A. Weinberg, J. L. Schmitt and J. B. Nelson (2003). Effect of endothelin-A receptor blockade with atrasentan on tumor progression in men with hormone-refractory prostate cancer: a randomized, phase II, placebo-controlled trial. *J Clin Oncol.* **21**(4):679-689.

Celeste, A. J., J. A. Iannazzi, R. C. Taylor, R. M. Hewick, V. Rosen, E. A. Wang and J. M. Wozney (1990). Identification of transforming growth factor beta family members

present in bone-inductive protein purified from bovine bone. *Proc Natl Acad Sci U S A.* **87**(24):9843-9847.

Celeste, A. J., J. J. Song, K. Cox, V. Rosen and J. M. Wozney (1994a). Bone morphogenetic protein-9, a new member of the TGF-beta superfamily. *J Bone Min Res.* **Suppl 1**(9):S136.

Celeste, A. J., J. J. Song, K. Cox, V. Rosen and J. M. Wozney (1994b). Bone morphogenetic protein-9, a new member of the TGF-β superfamily. *J Bone Min Res.* **Suppl 1**(136.

Chakraborty, M., S. G. Qiu, K. M. Vasudevan and V. M. Rangnekar (2001). Par-4 drives trafficking and activation of Fas and Fasl to induce prostate cancer cell apoptosis and tumor regression. *Cancer Res.* **61**(19):7255-7263.

Chambers, A. F., A. C. Groom and I. C. MacDonald (2002). Dissemination and growth of cancer cells in metastatic sites. *Nat Rev Cancer.* **2**(8):563-572.

Chan, J. M., M. J. Stampfer, E. Giovannucci, P. H. Gann, J. Ma, P. Wilkinson, C. H. Hennekens and M. Pollak (1998). Plasma insulin-like growth factor-I and prostate cancer risk: a prospective study. *Science.* **279**(5350):563-566.

Chan, J. M., M. J. Stampfer, J. Ma, P. Gann, J. M. Gaziano, M. Pollak and E. Giovannucci (2002). Insulin-like growth factor-I (IGF-I) and IGF binding protein-3 as predictors of advanced-stage prostate cancer. *J Natl Cancer Inst.* **94**(14):1099-1106.

Chang, C. and A. Hemmati-Brivanlou (1999). Xenopus GDF6, a new antagonist of noggin and a partner of BMPs. *Development.* **126**(15):3347-3357.

Chang, C., D. A. Holtzman, S. Chau, T. Chickering, E. A. Woolf, L. M. Holmgren, J. Bodorova, D. P. Gearing, W. E. Holmes and A. H. Brivanlou (2001). Twisted gastrulation can function as a BMP antagonist. *Nature.* **410**(6827):483-487.

Chay, C. H., C. R. Cooper, J. D. Gendernalik, S. M. Dhanasekaran, A. M. Chinnaiyan, M. A. Rubin, A. H. Schmaier and K. J. Pienta (2002). A functional thrombin receptor (PAR1) is expressed on bone-derived prostate cancer cell lines. *Urology.* **60**(5):760-765.

Chen, C., K. J. Grzegorzewski, S. Barash, Q. Zhao, H. Schneider, Q. Wang, M. Singh, L. Pukac, A. C. Bell, R. Duan, T. Coleman, A. Duttaroy, S. Cheng, J. Hirsch, L. Zhang, Y. Lazard, C. Fischer, M. C. Barber, Z. D. Ma, Y. Q. Zhang, P. Reavey, L. Zhong, B. Teng, I. Sanyal, S. M. Ruben, O. Blondel and C. E. Birse (2003). An integrated functional genomics screening program reveals a role for BMP-9 in glucose homeostasis. *Nat Biotechnol.* **21**(3):294-301.

Chen, G., N. Shukeir, A. Potti, K. Sircar, A. Aprikian, D. Goltzman and S. A. Rabbani (2004a). Up-regulation of Wnt-1 and beta-catenin production in patients with advanced metastatic prostate carcinoma: potential pathogenetic and prognostic implications. *Cancer.* **101**(6):1345-1356.

Chen, H., S. Shi, L. Acosta, W. Li, J. Lu, S. Bao, Z. Chen, Z. Yang, M. D. Schneider, K. R. Chien, S. J. Conway, M. C. Yoder, L. S. Haneline, D. Franco and W. Shou (2004b). BMP10 is essential for maintaining cardiac growth during murine cardiogenesis. *Development.* **131**(9):2219-2231.

Chen, J., S. De, J. Brainard and T. V. Byzova (2004c). Metastatic properties of prostate cancer cells are controlled by VEGF. *Cell Commun Adhes.* **11**(1):1-11.

Chen, M. E., S. H. Lin, L. W. Chung and R. A. Sikes (1998). Isolation and characterization of PAGE-1 and GAGE-7. New genes expressed in the LNCaP prostate

cancer progression model that share homology with melanoma-associated antigens. *J Biol Chem.* **273**(28):17618-17625.

Chen, X., A. Zankl, F. Niroomand, Z. Liu, H. A. Katus, L. Jahn and C. Tiefenbacher (2006). Upregulation of ID protein by growth and differentiation factor 5 (GDF5) through a smad-dependent and MAPK-independent pathway in HUVSMC. *J Mol Cell Cardiol.* **41**(1):26-33.

Chen, X. D., L. W. Fisher, P. G. Robey and M. F. Young (2004d). The small leucine-rich proteoglycan biglycan modulates BMP-4-induced osteoblast differentiation. *Faseb J.* **18**(9):948-958.

Chen, Y. G. and J. Massague (1999). Smad1 recognition and activation by the ALK1 group of transforming growth factor-beta family receptors. *J Biol Chem.* **274**(6):3672-3677.

Cheng, S. K., F. Olale, J. T. Bennett, A. H. Brivanlou and A. F. Schier (2003). EGF-CFC proteins are essential coreceptors for the TGF-beta signals Vg1 and GDF1. *Genes Dev.* **17**(1):31-36.

Chiao, J. W., B. S. Moonga, Y. M. Yang, R. Kancherla, A. Mittelman, J. R. Wu-Wong and T. Ahmed (2000). Endothelin-1 from prostate cancer cells is enhanced by bone contact which blocks osteoclastic bone resorption. *Br J Cancer.* **83**(3):360-365.

Chodak, G. (2006). Prostate cancer: epidemiology, screening, and biomarkers. *Rev Urol.* **8 Suppl 2**(S3-8.

Chomczynski, P. and N. Sacchi (1987). Single-step method of RNA isolation by acid guanidinium thiocyanate-phenol-chloroform extraction. *Anal Biochem.* **162**(1):156-159.

Choueiri, M. B., S. M. Tu, L. Y. Yu-Lee and S. H. Lin (2006). The central role of osteoblasts in the metastasis of prostate cancer. *Cancer Metastasis Rev.* **25**(4):601-609.

Chung, L. W. (1995). The role of stromal-epithelial interaction in normal and malignant growth. *Cancer Surv.* **23**(33-42.

Clark, L. C., G. F. Combs, Jr., B. W. Turnbull, E. H. Slate, D. K. Chalker, J. Chow, L. S. Davis, R. A. Glover, G. F. Graham, E. G. Gross, A. Krongrad, J. L. Lesher, Jr., H. K. Park, B. B. Sanders, Jr., C. L. Smith and J. R. Taylor (1996). Effects of selenium supplementation for cancer prevention in patients with carcinoma of the skin. A randomized controlled trial. Nutritional Prevention of Cancer Study Group. *Jama.* **276**(24):1957-1963.

Clark, P. E. and F. M. Torti (2003). Prostate cancer and bone metastases: medical treatment. *Clin Orthop Relat Res.* 415 Suppl):S148-157.

Clement, J. H., N. Marr, A. Meissner, M. Schwalbe, W. Sebald, K. O. Kliche, K. Hoffken and S. Wolfl (2000). Bone morphogenetic protein 2 (BMP-2) induces sequential changes of Id gene expression in the breast cancer cell line MCF-7. *J Cancer Res Clin Oncol.* **126**(5):271-279.

Clement, J. H., M. Raida, J. Sanger, R. Bicknell, J. Liu, A. Naumann, A. Geyer, A. Waldau, P. Hortschansky, A. Schmidt, K. Hoffken, S. Wolft and A. L. Harris (2005). Bone morphogenetic protein 2 (BMP-2) induces in vitro invasion and in vivo hormone independent growth of breast carcinoma cells. *Int J Oncol.* **27**(2):401-407.

Clement, J. H., J. Sanger and K. Hoffken (1999). Expression of bone morphogenetic protein 6 in normal mammary tissue and breast cancer cell lines and its regulation by epidermal growth factor. *Int J Cancer.* **80**(2):250-256.

Clines, G. A., K. S. Mohammad, Y. Bao, O. W. Stephens, L. J. Suva, J. D. Shaughnessy, Jr., J. W. Fox, J. M. Chirgwin and T. A. Guise (2006). Dickkopf Homolog 1 Mediates Endothelin-1-Stimulated New Bone Formation*. *Mol Endocrinol.*

Cohen, P., H. C. Graves, D. M. Peehl, M. Kamarei, L. C. Giudice and R. G. Rosenfeld (1992). Prostate-specific antigen (PSA) is an insulin-like growth factor binding protein-3 protease found in seminal plasma. *J Clin Endocrinol Metab.* **75**(4):1046-1053.

Cohen, P., D. M. Peehl, H. C. Graves and R. G. Rosenfeld (1994). Biological effects of prostate specific antigen as an insulin-like growth factor binding protein-3 protease. *J Endocrinol.* **142**(3):407-415.

Condon, M. S. (2005). The role of the stromal microenvironment in prostate cancer. *Semin Cancer Biol.* **15**(2):132-137.

Constam, D. B. and E. J. Robertson (1999). Regulation of bone morphogenetic protein activity by pro domains and proprotein convertases. *J Cell Biol.* **144**(1):139-149.

Conti, G. (2005). [Zoledronic acid in the treatment of prostate cancer]. *Minerva Urol Nefrol.* **57**(4):313-317.

Cookson, M. M. (2001). Prostate cancer: screening and early detection. *Cancer Control.* **8**(2):133-140.

Cooper, C. R., C. H. Chay, J. D. Gendernalik, H. L. Lee, J. Bhatia, R. S. Taichman, L. K. McCauley, E. T. Keller and K. J. Pienta (2003). Stromal factors involved in prostate carcinoma metastasis to bone. *Cancer.* **97**(3 Suppl):739-747.

Cooper, C. R., C. H. Chay and K. J. Pienta (2002). The role of alpha(v)beta(3) in prostate cancer progression. *Neoplasia.* **4**(3):191-194.

Cramer, S. D., Z. Chen and D. M. Peehl (1996). Prostate specific antigen cleaves parathyroid hormone-related protein in the PTH-like domain: inactivation of PTHrP-stimulated cAMP accumulation in mouse osteoblasts. *J Urol.* **156**(2 Pt 1):526-531.

Cui, Y., F. Jean, G. Thomas and J. L. Christian (1998). BMP-4 is proteolytically activated by furin and/or PC6 during vertebrate embryonic development. *Embo J.* **17**(16):4735-4743.

Cunningham, N. S., N. A. Jenkins, D. J. Gilbert, N. G. Copeland, A. H. Reddi and S. J. Lee (1995). Growth/differentiation factor-10: a new member of the transforming growth factor-beta superfamily related to bone morphogenetic protein-3. *Growth Factors.* **12**(2):99-109.

Dai, J., J. Keller, J. Zhang, Y. Lu, Z. Yao and E. T. Keller (2005). Bone morphogenetic protein-6 promotes osteoblastic prostate cancer bone metastases through a dual mechanism. *Cancer Res.* **65**(18):8274-8285.

Dai, J., Y. Kitagawa, J. Zhang, Z. Yao, A. Mizokami, S. Cheng, J. Nor, L. K. McCauley, R. S. Taichman and E. T. Keller (2004). Vascular endothelial growth factor contributes to the prostate cancer-induced osteoblast differentiation mediated by bone morphogenetic protein. *Cancer Res.* **64**(3):994-999.

Dale, K., N. Sattar, J. Heemskerk, J. D. Clarke, M. Placzek and J. Dodd (1999). Differential patterning of ventral midline cells by axial mesoderm is regulated by BMP7 and chordin. *Development.* **126**(2):397-408.

Daluiski, A., T. Engstrand, M. E. Bahamonde, L. W. Gamer, E. Agius, S. L. Stevenson, K. Cox, V. Rosen and K. M. Lyons (2001). Bone morphogenetic protein-3 is a negative regulator of bone density. *Nat Genet.* **27**(1):84-88.

David, L., C. Mallet, S. Mazerbourg, J. J. Feige and S. Bailly (2007). Identification of BMP9 and BMP10 as functional activators of the orphan activin receptor-like kinase 1 (ALK1) in endothelial cells. *Blood.* **109**(5):1953-1961.

Davidson, A. J., J. H. Postlethwait, Y. L. Yan, D. R. Beier, C. van Doren, D. Foernzler, A. J. Celeste, K. E. Crosier and P. S. Crosier (1999). Isolation of zebrafish gdf7 and comparative genetic mapping of genes belonging to the growth/differentiation factor 5, 6, 7 subgroup of the TGF-beta superfamily. *Genome Res.* **9**(2):121-129.

Davies, E. L., J. M. Gee, R. A. Cochrane, W. G. Jiang, A. K. Sharma, R. I. Nicholson and R. E. Mansel (1999). The immunohistochemical expression of desmoplakin and its role in vivo in the progression and metastasis of breast cancer. *Eur J Cancer.* **35**(6):902-907.

De Pinieux, G., T. Flam, M. Zerbib, P. Taupin, A. Bellahcene, D. Waltregny, A. Vieillefond and M. F. Poupon (2001). Bone sialoprotein, bone morphogenetic protein 6 and thymidine phosphorylase expression in localized human prostatic adenocarcinoma as predictors of clinical outcome: a clinicopathological and immunohistochemical study of 43 cases. *J Urol.* **166**(5):1924-1930.

Deckers, M. M., R. L. van Bezooijen, G. van der Horst, J. Hoogendam, C. van Der Bent, S. E. Papapoulos and C. W. Lowik (2002). Bone morphogenetic proteins stimulate angiogenesis through osteoblast-derived vascular endothelial growth factor A. *Endocrinology.* **143**(4):1545-1553.

Delany, A. M., M. Amling, M. Priemel, C. Howe, R. Baron and E. Canalis (2000). Osteopenia and decreased bone formation in osteonectin-deficient mice. *J Clin Invest.* **105**(7):915-923.

Demers, L. M., L. Costa, V. M. Chinchilli, L. Gaydos, E. Curley and A. Lipton (1995). Biochemical markers of bone turnover in patients with metastatic bone disease. *Clin Chem.* **41**(10):1489-1494.

Demers, L. M., L. Costa and A. Lipton (2003). Biochemical markers and skeletal metastases. *Clin Orthop Relat Res.* 415 Suppl):S138-147.

Denhardt, D. T., C. M. Giachelli and S. R. Rittling (2001). Role of osteopontin in cellular signaling and toxicant injury. *Annu Rev Pharmacol Toxicol.* **41**(723-749.

Derynck, R., W. M. Gelbart, R. M. Harland, C. H. Heldin, S. E. Kern, J. Massague, D. A. Melton, M. Mlodzik, R. W. Padgett, A. B. Roberts, J. Smith, G. H. Thomsen, B. Vogelstein and X. F. Wang (1996). Nomenclature: vertebrate mediators of TGFbeta family signals. *Cell.* **87**(2):173.

Di Silverio, F., V. Gentile, A. De Matteis, G. Mariotti, V. Giuseppe, P. A. Luigi and A. Sciarra (2003). Distribution of inflammation, pre-malignant lesions, incidental carcinoma in histologically confirmed benign prostatic hyperplasia: a retrospective analysis. *Eur Urol.* **43**(2):164-175.

Dionne, M. S., W. C. Skarnes and R. M. Harland (2001). Mutation and analysis of Dan, the founding member of the Dan family of transforming growth factor beta antagonists. *Mol Cell Biol.* **21**(2):636-643.

Dube, J. L., P. Wang, J. Elvin, K. M. Lyons, A. J. Celeste and M. M. Matzuk (1998). The bone morphogenetic protein 15 gene is X-linked and expressed in oocytes. *Mol Endocrinol.* **12**(12):1809-1817.

Ducy, P., C. Desbois, B. Boyce, G. Pinero, B. Story, C. Dunstan, E. Smith, J. Bonadio, S. Goldstein, C. Gundberg, A. Bradley and G. Karsenty (1996). Increased bone formation in osteocalcin-deficient mice. *Nature.* **382**(6590):448-452.

Dunstan, C. R., R. Boyce, B. F. Boyce, I. R. Garrett, E. Izbicka, W. H. Burgess and G. R. Mundy (1999). Systemic administration of acidic fibroblast growth factor (FGF-1) prevents bone loss and increases new bone formation in ovariectomized rats. *J Bone Miner Res.* **14**(6):953-959.

Ebisawa, T., K. Tada, I. Kitajima, K. Tojo, T. K. Sampath, M. Kawabata, K. Miyazono and T. Imamura (1999). Characterization of bone morphogenetic protein-6 signaling pathways in osteoblast differentiation. *J Cell Sci.* **112 (Pt 20)**(3519-3527.

El-Guendy, N. and V. M. Rangnekar (2003). Apoptosis by Par-4 in cancer and neurodegenerative diseases. *Exp Cell Res.* **283**(1):51-66.

Fainsod, A., K. Deissler, R. Yelin, K. Marom, M. Epstein, G. Pillemer, H. Steinbeisser and M. Blum (1997). The dorsalizing and neural inducing gene follistatin is an antagonist of BMP-4. *Mech Dev.* **63**(1):39-50.

Feeley, B. T., S. C. Gamradt, W. K. Hsu, N. Liu, L. Krenek, P. Robbins, J. Huard and J. R. Lieberman (2005). Influence of BMPs on the formation of osteoblastic lesions in metastatic prostate cancer. *J Bone Miner Res.* **20**(12):2189-2199.

Feeley, B. T., L. Krenek, N. Liu, W. K. Hsu, S. C. Gamradt, E. M. Schwarz, J. Huard and J. R. Lieberman (2006). Overexpression of noggin inhibits BMP-mediated growth of osteolytic prostate cancer lesions. *Bone.* **38**(2):154-166.

Feeley, B. T. and J. R. Lieberman (2006). Overexpression of noggin inhibits BMP-mediated growth of osteolytic prostate cancer lesions. *Bone.*

Fizazi, K., J. Yang, S. Peleg, C. R. Sikes, E. L. Kreimann, D. Daliani, M. Olive, K. A. Raymond, T. J. Janus, C. J. Logothetis, G. Karsenty and N. M. Navone (2003). Prostate cancer cells-osteoblast interaction shifts expression of growth/survival-related genes in

prostate cancer and reduces expression of osteoprotegerin in osteoblasts. *Clin Cancer Res.* **9**(7):2587-2597.

Forster, A. C. and R. H. Symons (1987). Self-cleavage of plus and minus RNAs of a virusoid and a structural model for the active sites. *Cell.* **49**(2):211-220.

Franz-Odendaal, T. A., B. K. Hall and P. E. Witten (2006). Buried alive: how osteoblasts become osteocytes. *Dev Dyn.* **235**(1):176-190.

Gamer, L. W., N. M. Wolfman, A. J. Celeste, G. Hattersley, R. Hewick and V. Rosen (1999). A novel BMP expressed in developing mouse limb, spinal cord, and tail bud is a potent mesoderm inducer in Xenopus embryos. *Dev Biol.* **208**(1):222-232.

Ganss, B., R. H. Kim and J. Sodek (1999). Bone sialoprotein. *Crit Rev Oral Biol Med.* **10**(1):79-98.

Garnero, P., N. Buchs, J. Zekri, R. Rizzoli, R. E. Coleman and P. D. Delmas (2000). Markers of bone turnover for the management of patients with bone metastases from prostate cancer. *Br J Cancer.* **82**(4):858-864.

Gazzerro, E., V. Gangji and E. Canalis (1998). Bone morphogenetic proteins induce the expression of noggin, which limits their activity in cultured rat osteoblasts. *J Clin Invest.* **102**(12):2106-2114.

Gerber, H. P., T. H. Vu, A. M. Ryan, J. Kowalski, Z. Werb and N. Ferrara (1999). VEGF couples hypertrophic cartilage remodeling, ossification and angiogenesis during endochondral bone formation. *Nat Med.* **5**(6):623-628.

Gerlach-Bank, L. M., A. R. Cleveland and K. F. Barald (2004). DAN directs endolymphatic sac and duct outgrowth in the avian inner ear. *Dev Dyn.* **229**(2):219-230.

Giovannucci, E. and S. K. Clinton (1998). Tomatoes, lycopene, and prostate cancer. *Proc Soc Exp Biol Med.* **218**(2):129-139.

Girasole, G., G. Passeri, R. L. Jilka and S. C. Manolagas (1994). Interleukin-11: a new cytokine critical for osteoclast development. *J Clin Invest.* **93**(4):1516-1524.

Gleason, D. F. and G. T. Mellinger (1974). Prediction of prognosis for prostatic adenocarcinoma by combined histological grading and clinical staging. *J Urol.* **111**(1):58-64.

Glienke, J., A. O. Schmitt, C. Pilarsky, B. Hinzmann, B. Weiss, A. Rosenthal and K. H. Thierauch (2000). Differential gene expression by endothelial cells in distinct angiogenic states. *Eur J Biochem.* **267**(9):2820-2830.

Globus, R. K., S. B. Doty, J. C. Lull, E. Holmuhamedov, M. J. Humphries and C. H. Damsky (1998). Fibronectin is a survival factor for differentiated osteoblasts. *J Cell Sci.* **111 (Pt 10)**(1385-1393.

Granchi, S., S. Brocchi, L. Bonaccorsi, E. Baldi, M. C. Vinci, G. Forti, M. Serio and M. Maggi (2001). Endothelin-1 production by prostate cancer cell lines is up-regulated by factors involved in cancer progression and down-regulated by androgens. *Prostate.* **49**(4):267-277.

Greene FL, P. D., Fleming ID (2002). *AJCC Cancer Staging Manual.* New York, NY, Springer-Verlag.

Greenwald, J., W. H. Fischer, W. W. Vale and S. Choe (1999). Three-finger toxin fold for the extracellular ligand-binding domain of the type II activin receptor serine kinase. *Nat Struct Biol.* **6**(1):18-22.

Grotewold, L., M. Plum, R. Dildrop, T. Peters and U. Ruther (2001). Bambi is coexpressed with Bmp-4 during mouse embryogenesis. *Mech Dev.* **100**(2):327-330.

Gu, G., M. Mulari, Z. Peng, T. A. Hentunen and H. K. Vaananen (2005). Death of osteocytes turns off the inhibition of osteoclasts and triggers local bone resorption. *Biochem Biophys Res Commun.* **335**(4):1095-1101.

Guise, T. A., K. S. Mohammad, G. Clines, E. G. Stebbins, D. H. Wong, L. S. Higgins, R. Vessella, E. Corey, S. Padalecki, L. Suva and J. M. Chirgwin (2006). Basic mechanisms responsible for osteolytic and osteoblastic bone metastases. *Clin Cancer Res.* **12**(20 Pt 2):6213s-6216s.

Guo, W., R. Gorlick, M. Ladanyi, P. A. Meyers, A. G. Huvos, J. R. Bertino and J. H. Healey (1999). Expression of bone morphogenetic proteins and receptors in sarcomas. *Clin Orthop Relat Res.* 365):175-183.

Gurumurthy, S., A. Goswami, K. M. Vasudevan and V. M. Rangnekar (2005). Phosphorylation of Par-4 by protein kinase A is critical for apoptosis. *Mol Cell Biol.* **25**(3):1146-1161.

Ha, T. U., D. L. Segev, D. Barbie, P. T. Masiakos, T. T. Tran, D. Dombkowski, M. Glander, T. R. Clarke, H. K. Lorenzo, P. K. Donahoe and S. Maheswaran (2000). Mullerian inhibiting substance inhibits ovarian cell growth through an Rb-independent mechanism. *J Biol Chem.* **275**(47):37101-37109.

Hall, C. L., S. Kang, O. A. MacDougald and E. T. Keller (2006). Role of Wnts in prostate cancer bone metastases. *J Cell Biochem.* **97**(4):661-672.

Hallahan, A. R., J. I. Pritchard, R. A. Chandraratna, R. G. Ellenbogen, J. R. Geyer, R. P. Overland, A. D. Strand, S. J. Tapscott and J. M. Olson (2003). BMP-2 mediates retinoid-induced apoptosis in medulloblastoma cells through a paracrine effect. *Nat Med.* **9**(8):1033-1038.

Hamdy, F. C., P. Autzen, M. C. Robinson, C. H. Horne, D. E. Neal and C. N. Robson (1997). Immunolocalization and messenger RNA expression of bone morphogenetic protein-6 in human benign and malignant prostatic tissue. *Cancer Res.* **57**(19):4427-4431.

Hankenson, K. D. and P. Bornstein (2002). The secreted protein thrombospondin 2 is an autocrine inhibitor of marrow stromal cell proliferation. *J Bone Miner Res.* **17**(3):415-425.

Hankenson, K. D., I. E. James, S. Apone, G. B. Stroup, S. M. Blake, X. Liang, M. W. Lark and P. Bornstein (2005). Increased osteoblastogenesis and decreased bone resorption protect against ovariectomy-induced bone loss in thrombospondin-2-null mice. *Matrix Biol.* **24**(5):362-370.

Hardwick, J. C., G. R. Van Den Brink, S. A. Bleuming, I. Ballester, J. M. Van Den Brande, J. J. Keller, G. J. Offerhaus, S. J. Van Deventer and M. P. Peppelenbosch (2004). Bone morphogenetic protein 2 is expressed by, and acts upon, mature epithelial cells in the colon. *Gastroenterology.* **126**(1):111-121.

Harris, S. E., M. A. Harris, P. Mahy, J. Wozney, J. Q. Feng and G. R. Mundy (1994). Expression of bone morphogenetic protein messenger RNAs by normal rat and human prostate and prostate cancer cells. *Prostate.* **24**(4):204-211.

Haseloff, J. and W. L. Gerlach (1988). Simple RNA enzymes with new and highly specific endoribonuclease activities. *Nature.* **334**(6183):585-591.

Hashimoto, O., R. K. Moore and S. Shimasaki (2005). Posttranslational processing of mouse and human BMP-15: potential implication in the determination of ovulation quota. *Proc Natl Acad Sci U S A.* **102**(15):5426-5431.

Haudenschild, D. R., S. M. Palmer, T. A. Moseley, Z. You and A. H. Reddi (2004). Bone morphogenetic protein (BMP)-6 signaling and BMP antagonist noggin in prostate cancer. *Cancer Res.* **64**(22):8276-8284.

Hayashi, H., S. Abdollah, Y. Qiu, J. Cai, Y. Y. Xu, B. W. Grinnell, M. A. Richardson, J. N. Topper, M. A. Gimbrone, Jr., J. L. Wrana and D. Falb (1997). The MAD-related protein Smad7 associates with the TGFbeta receptor and functions as an antagonist of TGFbeta signaling. *Cell.* **89**(7):1165-1173.

Helm, G. A., T. D. Alden, E. J. Beres, S. B. Hudson, S. Das, J. A. Engh, D. D. Pittman, K. M. Kerns and D. F. Kallmes (2000). Use of bone morphogenetic protein-9 gene therapy to induce spinal arthrodesis in the rodent. *J Neurosurg.* **92**(2 Suppl):191-196.

Hirayama, T. (1979). Epidemiology of prostate cancer with special reference to the role of diet. *Natl Cancer Inst Monogr.* 53):149-155.

Hjertner, O., H. Hjorth-Hansen, M. Borset, C. Seidel, A. Waage and A. Sundan (2001). Bone morphogenetic protein-4 inhibits proliferation and induces apoptosis of multiple myeloma cells. *Blood.* **97**(2):516-522.

Hofbauer, L. C., S. Khosla, C. R. Dunstan, D. L. Lacey, W. J. Boyle and B. L. Riggs (2000). The roles of osteoprotegerin and osteoprotegerin ligand in the paracrine regulation of bone resorption. *J Bone Miner Res.* **15**(1):2-12.

Horvath, L. G., S. M. Henshall, J. G. Kench, J. J. Turner, D. Golovsky, P. C. Brenner, G. F. O'Neill, R. Kooner, P. D. Stricker, J. J. Grygiel and R. L. Sutherland (2004). Loss of BMP2, Smad8, and Smad4 expression in prostate cancer progression. *Prostate.* **59**(3):234-242.

Hoshiya, Y., V. Gupta, D. L. Segev, M. Hoshiya, J. L. Carey, L. M. Sasur, T. T. Tran, T. U. Ha and S. Maheswaran (2003). Mullerian Inhibiting Substance induces NFkB signaling in breast and prostate cancer cells. *Mol Cell Endocrinol.* **211**(1-2):43-49.

Hotten, G., H. Neidhardt, B. Jacobowsky and J. Pohl (1994). Cloning and expression of recombinant human growth/differentiation factor 5. *Biochem Biophys Res Commun.* **204**(2):646-652.

Hsieh, J. T., H. C. Wu, M. E. Gleave, A. C. von Eschenbach and L. W. Chung (1993). Autocrine regulation of prostate-specific antigen gene expression in a human prostatic cancer (LNCaP) subline. *Cancer Res.* **53**(12):2852-2857.

Hsing, A. W., L. Tsao and S. S. Devesa (2000). International trends and patterns of prostate cancer incidence and mortality. *Int J Cancer.* **85**(1):60-67.

Hsu, D. R., A. N. Economides, X. Wang, P. M. Eimon and R. M. Harland (1998). The Xenopus dorsalizing factor Gremlin identifies a novel family of secreted proteins that antagonize BMP activities. *Mol Cell.* **1**(5):673-683.

Hultenby, K., F. P. Reinholt and D. Heinegard (1993). Distribution of integrin subunits on rat metaphyseal osteoclasts and osteoblasts. *Eur J Cell Biol.* **62**(1):86-93.

Hunter, G. K. and H. A. Goldberg (1993). Nucleation of hydroxyapatite by bone sialoprotein. *Proc Natl Acad Sci U S A.* **90**(18):8562-8565.

Ide, H., M. Katoh, H. Sasaki, T. Yoshida, K. Aoki, Y. Nawa, Y. Osada, T. Sugimura and M. Terada (1997a). Cloning of human bone morphogenetic protein type IB receptor (BMPR-IB) and its expression in prostate cancer in comparison with other BMPRs. *Oncogene.* **14**(11):1377-1382.

Ide, H., T. Yoshida, N. Matsumoto, K. Aoki, Y. Osada, T. Sugimura and M. Terada (1997b). Growth regulation of human prostate cancer cells by bone morphogenetic protein-2. *Cancer Res.* **57**(22):5022-5027.

Iemura, S., T. S. Yamamoto, C. Takagi, H. Uchiyama, T. Natsume, S. Shimasaki, H. Sugino and N. Ueno (1998). Direct binding of follistatin to a complex of bone-morphogenetic protein and its receptor inhibits ventral and epidermal cell fates in early Xenopus embryo. *Proc Natl Acad Sci U S A.* **95**(16):9337-9342.

Ihara, H., D. T. Denhardt, K. Furuya, T. Yamashita, Y. Muguruma, K. Tsuji, K. A. Hruska, K. Higashio, S. Enomoto, A. Nifuji, S. R. Rittling and M. Noda (2001). Parathyroid hormone-induced bone resorption does not occur in the absence of osteopontin. *J Biol Chem.* **276**(16):13065-13071.

Imamura, T., M. Takase, A. Nishihara, E. Oeda, J. Hanai, M. Kawabata and K. Miyazono (1997). Smad6 inhibits signalling by the TGF-beta superfamily. *Nature.* **389**(6651):622-626.

Ishijima, M., K. Tsuji, S. R. Rittling, T. Yamashita, H. Kurosawa, D. T. Denhardt, A. Nifuji and M. Noda (2002). Resistance to unloading-induced three-dimensional bone loss in osteopontin-deficient mice. *J Bone Miner Res.* **17**(4):661-667.

Ishimi, Y., C. Miyaura, C. H. Jin, T. Akatsu, E. Abe, Y. Nakamura, A. Yamaguchi, S. Yoshiki, T. Matsuda, T. Hirano and et al. (1990). IL-6 is produced by osteoblasts and induces bone resorption. *J Immunol.* **145**(10):3297-3303.

Ishisaki, A., K. Yamato, S. Hashimoto, A. Nakao, K. Tamaki, K. Nonaka, P. ten Dijke, H. Sugino and T. Nishihara (1999). Differential inhibition of Smad6 and Smad7 on bone morphogenetic protein- and activin-mediated growth arrest and apoptosis in B cells. *J Biol Chem.* **274**(19):13637-13642.

Ishitani, T., J. Ninomiya-Tsuji, S. Nagai, M. Nishita, M. Meneghini, N. Barker, M. Waterman, B. Bowerman, H. Clevers, H. Shibuya and K. Matsumoto (1999). The TAK1-NLK-MAPK-related pathway antagonizes signalling between beta-catenin and transcription factor TCF. *Nature.* **399**(6738):798-802.

Israel, D. I., J. Nove, K. M. Kerns, R. J. Kaufman, V. Rosen, K. A. Cox and J. M. Wozney (1996). Heterodimeric bone morphogenetic proteins show enhanced activity in vitro and in vivo. *Growth Factors.* **13**(3-4):291-300.

Itoh, F., H. Asao, K. Sugamura, C. H. Heldin, P. ten Dijke and S. Itoh (2001). Promoting bone morphogenetic protein signaling through negative regulation of inhibitory Smads. *Embo J.* **20**(15):4132-4142.

Jacob, K., M. Webber, D. Benayahu and H. K. Kleinman (1999). Osteonectin promotes prostate cancer cell migration and invasion: a possible mechanism for metastasis to bone. *Cancer Res.* **59**(17):4453-4457.

Jemal, A., R. Siegel, E. Ward, T. Murray, J. Xu, C. Smigal and M. J. Thun (2006). Cancer statistics, 2006. *CA Cancer J Clin.* **56**(2):106-130.

Jiang, W. G., G. Davies and O. Fodstad (2005a). Com-1/P8 in oestrogen regulated growth of breast cancer cells, the ER-beta connection. *Biochem Biophys Res Commun.* **330**(1):253-262.

Jiang, W. G., G. Davies, T. A. Martin, C. Parr, G. Watkins, M. D. Mason, K. Mokbel and R. E. Mansel (2005b). Targeting matrilysin and its impact on tumor growth in vivo: the potential implications in breast cancer therapy. *Clin Cancer Res.* **11**(16):6012-6019.

Jiang, W. G., D. Grimshaw, J. Lane, T. A. Martin, R. Abounader, J. Laterra and R. E. Mansel (2001). A hammerhead ribozyme suppresses expression of hepatocyte growth

factor/scatter factor receptor c-MET and reduces migration and invasiveness of breast cancer cells. *Clin Cancer Res.* **7**(8):2555-2562.

Jiang, W. G., D. Grimshaw, T. A. Martin, G. Davies, C. Parr, G. Watkins, J. Lane, R. Abounader, J. Laterra and R. E. Mansel (2003). Reduction of stromal fibroblast-induced mammary tumor growth, by retroviral ribozyme transgenes to hepatocyte growth factor/scatter factor and its receptor, c-MET. *Clin Cancer Res.* **9**(11):4274-4281.

Jiang, W. G., S. Hiscox, M. B. Hallett, C. Scott, D. F. Horrobin and M. C. Puntis (1995a). Inhibition of hepatocyte growth factor-induced motility and in vitro invasion of human colon cancer cells by gamma-linolenic acid. *Br J Cancer.* **71**(4):744-752.

Jiang, W. G., S. Hiscox, S. K. Singhrao, T. Nakamura, M. C. Puntis and M. B. Hallett (1995b). Inhibition of HGF/SF-induced membrane ruffling and cell motility by transient elevation of cytosolic free Ca2+. *Exp Cell Res.* **220**(2):424-433.

Jiang, W. G., S. E. Hiscox, C. Parr, T. A. Martin, K. Matsumoto, T. Nakamura and R. E. Mansel (1999a). Antagonistic effect of NK4, a novel hepatocyte growth factor variant, on in vitro angiogenesis of human vascular endothelial cells. *Clin Cancer Res.* **5**(11):3695-3703.

Jiang, W. G., T. A. Martin, K. Matsumoto, T. Nakamura and R. E. Mansel (1999b). Hepatocyte growth factor/scatter factor decreases the expression of occludin and transendothelial resistance (TER) and increases paracellular permeability in human vascular endothelial cells. *J Cell Physiol.* **181**(2):319-329.

Jiang, W. G., T. A. Martin, C. Parr, G. Davies, K. Matsumoto and T. Nakamura (2005c). Hepatocyte growth factor, its receptor, and their potential value in cancer therapies. *Crit Rev Oncol Hematol.* **53**(1):35-69.

Jimi, E., I. Nakamura, L. T. Duong, T. Ikebe, N. Takahashi, G. A. Rodan and T. Suda (1999). Interleukin 1 induces multinucleation and bone-resorbing activity of osteoclasts in the absence of osteoblasts/stromal cells. *Exp Cell Res.* **247**(1):84-93.

Jornvall, H., A. Blokzijl, P. ten Dijke and C. F. Ibanez (2001). The orphan receptor serine/threonine kinase ALK7 signals arrest of proliferation and morphological differentiation in a neuronal cell line. *J Biol Chem.* **276**(7):5140-5146.

Kakehi, Y., T. Segawa, X. X. Wu, P. Kulkarni, R. Dhir and R. H. Getzenberg (2004). Down-regulation of macrophage inhibitory cytokine-1/prostate derived factor in benign prostatic hyperplasia. *Prostate.* **59**(4):351-356.

Kaneki, H., R. Guo, D. Chen, Z. Yao, E. M. Schwarz, Y. E. Zhang, B. F. Boyce and L. Xing (2006). Tumor necrosis factor promotes Runx2 degradation through up-regulation of Smurf1 and Smurf2 in osteoblasts. *J Biol Chem.* **281**(7):4326-4333.

Khodavirdi, A. C., Z. Song, S. Yang, C. Zhong, S. Wang, H. Wu, C. Pritchard, P. S. Nelson and P. Roy-Burman (2006). Increased expression of osteopontin contributes to the progression of prostate cancer. *Cancer Res.* **66**(2):883-888.

Killian, C. S., D. A. Corral, E. Kawinski and R. I. Constantine (1993). Mitogenic response of osteoblast cells to prostate-specific antigen suggests an activation of latent TGF-beta and a proteolytic modulation of cell adhesion receptors. *Biochem Biophys Res Commun.* **192**(2):940-947.

Kim, I. Y., D. H. Lee, H. J. Ahn, H. Tokunaga, W. Song, L. M. Devereaux, D. Jin, T. K. Sampath and R. A. Morton (2000). Expression of bone morphogenetic protein receptors type-IA, -IB and -II correlates with tumor grade in human prostate cancer tissues. *Cancer Res.* **60**(11):2840-2844.

Kim, I. Y., D. H. Lee, D. K. Lee, H. J. Ahn, M. M. Kim, S. J. Kim and R. A. Morton (2004). Loss of expression of bone morphogenetic protein receptor type II in human prostate cancer cells. *Oncogene.* **23**(46):7651-7659.

Kimura, N., R. Matsuo, H. Shibuya, K. Nakashima and T. Taga (2000). BMP2-induced apoptosis is mediated by activation of the TAK1-p38 kinase pathway that is negatively regulated by Smad6. *J Biol Chem.* **275**(23):17647-17652.

Kirsch, T., W. Sebald and M. K. Dreyer (2000). Crystal structure of the BMP-2-BRIA ectodomain complex. *Nat Struct Biol.* **7**(6):492-496.

Kitazawa, S., R. Kitazawa, C. Obayashi and T. Yamamoto (2005). Desmoid tumor with ossification in chest wall: possible involvement of BAMBI promoter hypermethylation in metaplastic bone formation. *J Bone Miner Res.* **20**(8):1472-1477.

Kleinberg, D. L., W. Ruan, D. Yee, K. T. Kovacs and S. Vidal (2006). Insulin-like Growth Factor-I (IGF-I) Controls Prostate Fibromuscular Development: IGF-I Inhibition Prevents Both Fibromuscular And Glandular Development In Eugonadal Mice. *Endocrinology.*

Klotz, L. (2000). Hormone therapy for patients with prostate carcinoma. *Cancer.* **88**(12 Suppl):3009-3014.

Koenig, B. B., J. S. Cook, D. H. Wolsing, J. Ting, J. P. Tiesman, P. E. Correa, C. A. Olson, A. L. Pecquet, F. Ventura, R. A. Grant and et al. (1994). Characterization and cloning of a receptor for BMP-2 and BMP-4 from NIH 3T3 cells. *Mol Cell Biol.* **14**(9):5961-5974.

Korchynskyi, O., K. J. Dechering, A. M. Sijbers, W. Olijve and P. ten Dijke (2003). Gene array analysis of bone morphogenetic protein type I receptor-induced osteoblast differentiation. *J Bone Miner Res.* **18**(7):1177-1185.

Koutsilieris, M. (1993). Osteoblastic metastasis in advanced prostate cancer. *Anticancer Res.* **13**(2):443-449.

Kowanetz, M., U. Valcourt, R. Bergstrom, C. H. Heldin and A. Moustakas (2004). Id2 and Id3 define the potency of cell proliferation and differentiation responses to transforming growth factor beta and bone morphogenetic protein. *Mol Cell Biol.* **24**(10):4241-4254.

Kraunz, K. S., H. H. Nelson, M. Liu, J. K. Wiencke and K. T. Kelsey (2005). Interaction between the bone morphogenetic proteins and Ras/MAP-kinase signalling pathways in lung cancer. *Br J Cancer.* **93**(8):949-952.

Kretzschmar, M. and J. Massague (1998). SMADs: mediators and regulators of TGF-beta signaling. *Curr Opin Genet Dev.* **8**(1):103-111.

Krupski, T., M. A. Harding, M. E. Herce, K. M. Gulding, M. H. Stoler and D. Theodorescu (2001). The role of vascular endothelial growth factor in the tissue specific in vivo growth of prostate cancer cells. *Growth Factors.* **18**(4):287-302.

Krupski, T. L., M. R. Smith, W. C. Lee, C. L. Pashos, J. Brandman, Q. Wang, M. Botteman and M. S. Litwin (2004). Natural history of bone complications in men with prostate carcinoma initiating androgen deprivation therapy. *Cancer.* **101**(3):541-549.

Kumar, C. C. (2003). Integrin alpha v beta 3 as a therapeutic target for blocking tumor-induced angiogenesis. *Curr Drug Targets.* **4**(2):123-131.

Kuratomi, G., A. Komuro, K. Goto, M. Shinozaki, K. Miyazawa, K. Miyazono and T. Imamura (2005). NEDD4-2 (neural precursor cell expressed, developmentally down-regulated 4-2) negatively regulates TGF-beta (transforming growth factor-beta) signalling by inducing ubiquitin-mediated degradation of Smad2 and TGF-beta type I receptor. *Biochem J.* **386**(Pt 3):461-470.

Kusu, N., J. Laurikkala, M. Imanishi, H. Usui, M. Konishi, A. Miyake, I. Thesleff and N. Itoh (2003). Sclerostin is a novel secreted osteoclast-derived bone morphogenetic protein antagonist with unique ligand specificity. *J Biol Chem.* **278**(26):24113-24117.

Labrie, F. (2004). Medical castration with LHRH agonists: 25 years later with major benefits achieved on survival in prostate cancer. *J Androl.* **25**(3):305-313.

Landers, K. A., M. J. Burger, M. A. Tebay, D. M. Purdie, B. Scells, H. Samaratunga, M. F. Lavin and R. A. Gardiner (2005). Use of multiple biomarkers for a molecular diagnosis of prostate cancer. *Int J Cancer.* **114**(6):950-956.

Langenfeld, E. M., S. E. Calvano, F. Abou-Nukta, S. F. Lowry, P. Amenta and J. Langenfeld (2003). The mature bone morphogenetic protein-2 is aberrantly expressed in non-small cell lung carcinomas and stimulates tumor growth of A549 cells. *Carcinogenesis.* **24**(9):1445-1454.

Langenfeld, E. M., Y. Kong and J. Langenfeld (2005). Bone morphogenetic protein-2-induced transformation involves the activation of mammalian target of rapamycin. *Mol Cancer Res.* **3**(12):679-684.

Lee, K. J., M. Mendelsohn and T. M. Jessell (1998). Neuronal patterning by BMPs: a requirement for GDF7 in the generation of a discrete class of commissural interneurons in the mouse spinal cord. *Genes Dev.* **12**(21):3394-3407.

Lee, S. J. (1990). Identification of a novel member (GDF-1) of the transforming growth factor-beta superfamily. *Mol Endocrinol.* **4**(7):1034-1040.

Lee, S. J. and A. C. McPherron (2001). Regulation of myostatin activity and muscle growth. *Proc Natl Acad Sci U S A.* **98**(16):9306-9311.

Lee, S. K. and J. Lorenzo (2006). Cytokines regulating osteoclast formation and function. *Curr Opin Rheumatol.* **18**(4):411-418.

Lee, S. W., S. I. Han, H. H. Kim and Z. H. Lee (2002). TAK1-dependent activation of AP-1 and c-Jun N-terminal kinase by receptor activator of NF-kappaB. *J Biochem Mol Biol.* **35**(4):371-376.

Lee, Y., E. Schwarz, M. Davies, M. Jo, J. Gates, J. Wu, X. Zhang and J. R. Lieberman (2003). Differences in the cytokine profiles associated with prostate cancer cell induced osteoblastic and osteolytic lesions in bone. *J Orthop Res.* **21**(1):62-72.

Lehr, J. E. and K. J. Pienta (1998). Preferential adhesion of prostate cancer cells to a human bone marrow endothelial cell line. *J Natl Cancer Inst.* **90**(2):118-123.

Lesko, S. M., L. Rosenberg and S. Shapiro (1996). Family history and prostate cancer risk. *Am J Epidemiol.* **144**(11):1041-1047.

Liang, A. K., J. Liu, S. A. Mao, V. S. Siu, Y. C. Lee and S. H. Lin (2005). Expression of recombinant MDA-BF-1 with a kinase recognition site and a 7-histidine tag for receptor binding and purification. *Protein Expr Purif.* **44**(1):58-64.

Lin, J., S. R. Patel, X. Cheng, E. A. Cho, I. Levitan, M. Ullenbruch, S. H. Phan, J. M. Park and G. R. Dressler (2005). Kielin/chordin-like protein, a novel enhancer of BMP signaling, attenuates renal fibrotic disease. *Nat Med.* **11**(4):387-393.

Lipton, A., E. Small, F. Saad, D. Gleason, D. Gordon, M. Smith, L. Rosen, M. O. Kowalski, D. Reitsma and J. Seaman (2002). The new bisphosphonate, Zometa (zoledronic acid), decreases skeletal complications in both osteolytic and osteoblastic lesions: a comparison to pamidronate. *Cancer Invest.* **20 Suppl 2**(45-54.

Liu, F., F. Ventura, J. Doody and J. Massague (1995). Human type II receptor for bone morphogenic proteins (BMPs): extension of the two-kinase receptor model to the BMPs. *Mol Cell Biol.* **15**(7):3479-3486.

Lopez-Coviella, I., B. Berse, R. Krauss, R. S. Thies and J. K. Blusztajn (2000). Induction and maintenance of the neuronal cholinergic phenotype in the central nervous system by BMP-9. *Science.* **289**(5477):313-316.

Lopez-Coviella, I., M. T. Follettie, T. J. Mellott, V. P. Kovacheva, B. E. Slack, V. Diesl, B. Berse, R. S. Thies and J. K. Blusztajn (2005). Bone morphogenetic protein 9 induces the transcriptome of basal forebrain cholinergic neurons. *Proc Natl Acad Sci U S A.* **102**(19):6984-6989.

Lopez-Coviella, I., T. M. Mellott, V. P. Kovacheva, B. Berse, B. E. Slack, V. Zemelko, A. Schnitzler and J. K. Blusztajn (2006). Developmental pattern of expression of BMP receptors and Smads and activation of Smad1 and Smad5 by BMP9 in mouse basal forebrain. *Brain Res.* **1088**(1):49-56.

Lum, L., B. R. Wong, R. Josien, J. D. Becherer, H. Erdjument-Bromage, J. Schlondorff, P. Tempst, Y. Choi and C. P. Blobel (1999). Evidence for a role of a tumor necrosis factor-alpha (TNF-alpha)-converting enzyme-like protease in shedding of TRANCE, a TNF family member involved in osteoclastogenesis and dendritic cell survival. *J Biol Chem.* **274**(19):13613-13618.

Luo, G., P. Ducy, M. D. McKee, G. J. Pinero, E. Loyer, R. R. Behringer and G. Karsenty (1997). Spontaneous calcification of arteries and cartilage in mice lacking matrix GLA protein. *Nature.* **386**(6620):78-81.

Luo, J., D. J. Duggan, Y. Chen, J. Sauvageot, C. M. Ewing, M. L. Bittner, J. M. Trent and W. B. Isaacs (2001). Human prostate cancer and benign prostatic hyperplasia: molecular dissection by gene expression profiling. *Cancer Res.* **61**(12):4683-4688.

Luo, K., S. L. Stroschein, W. Wang, D. Chen, E. Martens, S. Zhou and Q. Zhou (1999). The Ski oncoprotein interacts with the Smad proteins to repress TGFbeta signaling. *Genes Dev.* **13**(17):2196-2206.

Mansson, P. E., P. Adams, M. Kan and W. L. McKeehan (1989). Heparin-binding growth factor gene expression and receptor characteristics in normal rat prostate and two transplantable rat prostate tumors. *Cancer Res.* **49**(9):2485-2494.

Marques, S., A. C. Borges, A. C. Silva, S. Freitas, M. Cordenonsi and J. A. Belo (2004). The activity of the Nodal antagonist Cerl-2 in the mouse node is required for correct L/R body axis. *Genes Dev.* **18**(19):2342-2347.

Martin, T. A., C. Parr, G. Davies, G. Watkins, J. Lane, K. Matsumoto, T. Nakamura, R. E. Mansel and W. G. Jiang (2003). Growth and angiogenesis of human breast cancer in a nude mouse tumour model is reduced by NK4, a HGF/SF antagonist. *Carcinogenesis.* **24**(8):1317-1323.

Masuda, H., Y. Fukabori, K. Nakano, N. Shimizu and H. Yamanaka (2004). Expression of bone morphogenetic protein-7 (BMP-7) in human prostate. *Prostate.* **59**(1):101-106.

Masuda, H., Y. Fukabori, K. Nakano, Y. Takezawa, C. S. T and H. Yamanaka (2003). Increased expression of bone morphogenetic protein-7 in bone metastatic prostate cancer. *Prostate.* **54**(4):268-274.

Matsubara, A. (1995). [Studies on the mechanisms of action of fibroblast growth factors in stromal cells in hyperplastic human prostate]. *Nippon Hinyokika Gakkai Zasshi.* **86**(5):1034-1043.

Mazerbourg, S. and A. J. Hsueh (2006). Genomic analyses facilitate identification of receptors and signalling pathways for growth differentiation factor 9 and related orphan

bone morphogenetic protein/growth differentiation factor ligands. *Hum Reprod Update.* **12**(4):373-383.

Mazerbourg, S., K. Sangkuhl, C. W. Luo, S. Sudo, C. Klein and A. J. Hsueh (2005). Identification of receptors and signaling pathways for orphan bone morphogenetic protein/growth differentiation factor ligands based on genomic analyses. *J Biol Chem.* **280**(37):32122-32132.

McCarthy, T. L., C. Ji, Y. Chen, K. K. Kim, M. Imagawa, Y. Ito and M. Centrella (2000). Runt domain factor (Runx)-dependent effects on CCAAT/ enhancer-binding protein delta expression and activity in osteoblasts. *J Biol Chem.* **275**(28):21746-21753.

McNeal, J. E. (1981). The zonal anatomy of the prostate. *Prostate.* **2**(1):35-49.

McPherron, A. C., A. M. Lawler and S. J. Lee (1997). Regulation of skeletal muscle mass in mice by a new TGF-beta superfamily member. *Nature.* **387**(6628):83-90.

McPherron, A. C., A. M. Lawler and S. J. Lee (1999). Regulation of anterior/posterior patterning of the axial skeleton by growth/differentiation factor 11. *Nat Genet.* **22**(3):260-264.

McPherron, A. C. and S. J. Lee (1993). GDF-3 and GDF-9: two new members of the transforming growth factor-beta superfamily containing a novel pattern of cysteines. *J Biol Chem.* **268**(5):3444-3449.

Mehrotra, M., S. M. Krane, K. Walters and C. Pilbeam (2004). Differential regulation of platelet-derived growth factor stimulated migration and proliferation in osteoblastic cells. *J Cell Biochem.* **93**(4):741-752.

Merino, R., J. Rodriguez-Leon, D. Macias, Y. Ganan, A. N. Economides and J. M. Hurle (1999). The BMP antagonist Gremlin regulates outgrowth, chondrogenesis and programmed cell death in the developing limb. *Development.* **126**(23):5515-5522.

Midy, V. and J. Plouet (1994). Vasculotropin/vascular endothelial growth factor induces differentiation in cultured osteoblasts. *Biochem Biophys Res Commun.* **199**(1):380-386.

Miller, A. F., S. A. Harvey, R. S. Thies and M. S. Olson (2000). Bone morphogenetic protein-9. An autocrine/paracrine cytokine in the liver. *J Biol Chem.* **275**(24):17937-17945.

Miyazaki, H., T. Watabe, T. Kitamura and K. Miyazono (2004). BMP signals inhibit proliferation and in vivo tumor growth of androgen-insensitive prostate carcinoma cells. *Oncogene.* **23**(58):9326-9335.

Mochida, Y., D. Parisuthiman and M. Yamauchi (2006). Biglycan is a positive modulator of BMP-2 induced osteoblast differentiation. *Adv Exp Med Biol.* **585**(101-113.

Mohammad, K. S. and T. A. Guise (2003). Mechanisms of osteoblastic metastases: role of endothelin-1. *Clin Orthop Relat Res.* 415 Suppl):S67-74.

Moore, R. K., F. Otsuka and S. Shimasaki (2003). Molecular basis of bone morphogenetic protein-15 signaling in granulosa cells. *J Biol Chem.* **278**(1):304-310.

Mori, S., H. Yoshikawa, J. Hashimoto, T. Ueda, H. Funai, M. Kato and K. Takaoka (1998). Antiangiogenic agent (TNP-470) inhibition of ectopic bone formation induced by bone morphogenetic protein-2. *Bone.* **22**(2):99-105.

Moriguchi, T., N. Kuroyanagi, K. Yamaguchi, Y. Gotoh, K. Irie, T. Kano, K. Shirakabe, Y. Muro, H. Shibuya, K. Matsumoto, E. Nishida and M. Hagiwara (1996). A novel

kinase cascade mediated by mitogen-activated protein kinase kinase 6 and MKK3. *J Biol Chem.* **271**(23):13675-13679.

Moursi, A. M., C. H. Damsky, J. Lull, D. Zimmerman, S. B. Doty, S. Aota and R. K. Globus (1996). Fibronectin regulates calvarial osteoblast differentiation. *J Cell Sci.* **109 (Pt 6)**(1369-1380.

Moursi, A. M., R. K. Globus and C. H. Damsky (1997). Interactions between integrin receptors and fibronectin are required for calvarial osteoblast differentiation in vitro. *J Cell Sci.* **110 (Pt 18)**(2187-2196.

Moustakas, A. and C. H. Heldin (2002). From mono- to oligo-Smads: the heart of the matter in TGF-beta signal transduction. *Genes Dev.* **16**(15):1867-1871.

Mundy, G. R. (2002). Metastasis to bone: causes, consequences and therapeutic opportunities. *Nat Rev Cancer.* **2**(8):584-593.

Murakami, G., T. Watabe, K. Takaoka, K. Miyazono and T. Imamura (2003). Cooperative inhibition of bone morphogenetic protein signaling by Smurf1 and inhibitory Smads. *Mol Biol Cell.* **14**(7):2809-2817.

Nacamuli, R. P., K. D. Fong, K. A. Lenton, H. M. Song, T. D. Fang, A. Salim and M. T. Longaker (2005). Expression and possible mechanisms of regulation of BMP3 in rat cranial sutures. *Plast Reconstr Surg.* **116**(5):1353-1362.

Naitoh, J., J. B. deKernion and D. Shoskes (2000). Cancer of the prostate. *Oxford Textbook of Surgery.* P. J. Morris and W. C. Wood. New York, Oxford University Press Inc. **2:** 2110.

Nakahara, T., K. Tominaga, T. Koseki, M. Yamamoto, K. Yamato, J. Fukuda and T. Nishihara (2003). Growth/differentiation factor-5 induces growth arrest and apoptosis in mouse B lineage cells with modulation by Smad. *Cell Signal.* **15**(2):181-187.

Nakajima, Y., T. Yamagishi, S. Hokari and H. Nakamura (2000). Mechanisms involved in valvuloseptal endocardial cushion formation in early cardiogenesis: roles of transforming growth factor (TGF)-beta and bone morphogenetic protein (BMP). *Anat Rec.* **258**(2):119-127.

Nakayama, N., C. Y. Han, L. Cam, J. I. Lee, J. Pretorius, S. Fisher, R. Rosenfeld, S. Scully, R. Nishinakamura, D. Duryea, G. Van, B. Bolon, T. Yokota and K. Zhang (2004). A novel chordin-like BMP inhibitor, CHL2, expressed preferentially in chondrocytes of developing cartilage and osteoarthritic joint cartilage. *Development.* **131**(1):229-240.

Namiki, M., S. Akiyama, T. Katagiri, A. Suzuki, N. Ueno, N. Yamaji, V. Rosen, J. M. Wozney and T. Suda (1997). A kinase domain-truncated type I receptor blocks bone morphogenetic protein-2-induced signal transduction in C2C12 myoblasts. *J Biol Chem.* **272**(35):22046-22052.

Nelson, J. B., K. Chan-Tack, S. P. Hedican, S. R. Magnuson, T. J. Opgenorth, G. S. Bova and J. W. Simons (1996). Endothelin-1 production and decreased endothelin B receptor expression in advanced prostate cancer. *Cancer Res.* **56**(4):663-668.

Nelson, J. B., S. P. Hedican, D. J. George, A. H. Reddi, S. Piantadosi, M. A. Eisenberger and J. W. Simons (1995). Identification of endothelin-1 in the pathophysiology of metastatic adenocarcinoma of the prostate. *Nat Med.* **1**(9):944-949.

Neuhaus, H., V. Rosen and R. S. Thies (1999). Heart specific expression of mouse BMP-10 a novel member of the TGF-beta superfamily. *Mech Dev.* **80**(2):181-184.

Nishitoh, H., H. Ichijo, M. Kimura, T. Matsumoto, F. Makishima, A. Yamaguchi, H. Yamashita, S. Enomoto and K. Miyazono (1996). Identification of type I and type II

serine/threonine kinase receptors for growth/differentiation factor-5. *J Biol Chem.* **271**(35):21345-21352.

Nohe, A., S. Hassel, M. Ehrlich, F. Neubauer, W. Sebald, Y. I. Henis and P. Knaus (2002). The mode of bone morphogenetic protein (BMP) receptor oligomerization determines different BMP-2 signaling pathways. *J Biol Chem.* **277**(7):5330-5338.

Nohe, A., E. Keating, P. Knaus and N. O. Petersen (2004). Signal transduction of bone morphogenetic protein receptors. *Cell Signal.* **16**(3):291-299.

Nohno, T., T. Ishikawa, T. Saito, K. Hosokawa, S. Noji, D. H. Wolsing and J. S. Rosenbaum (1995). Identification of a human type II receptor for bone morphogenetic protein-4 that forms differential heteromeric complexes with bone morphogenetic protein type I receptors. *J Biol Chem.* **270**(38):22522-22526.

Oades, G. M., J. Coxon and K. W. Colston (2002). The potential role of bisphosphonates in prostate cancer. *Prostate Cancer Prostatic Dis.* **5**(4):264-272.

Ogata, T., J. M. Wozney, R. Benezra and M. Noda (1993). Bone morphogenetic protein 2 transiently enhances expression of a gene, Id (inhibitor of differentiation), encoding a helix-loop-helix molecule in osteoblast-like cells. *Proc Natl Acad Sci U S A.* **90**(19):9219-9222.

Oh, S. P., C. Y. Yeo, Y. Lee, H. Schrewe, M. Whitman and E. Li (2002). Activin type IIA and IIB receptors mediate Gdf11 signaling in axial vertebral patterning. *Genes Dev.* **16**(21):2749-2754.

Oh, W. K., M. Hurwitz, A. V. D'Amico, J. P. Richie and P. W. Kantoff (2003). Neoplasms of the Prostate. *Cancer Medicine.* D. W. Kufe, R. E. Pollock, R. R. Weichselbaum, R. C. Bast, T. S. Gansler, J. F. Holland and E. F. III. London, BC Decker Inc. **2:** 1707-1740.

Onichtchouk, D., Y. G. Chen, R. Dosch, V. Gawantka, H. Delius, J. Massague and C. Niehrs (1999). Silencing of TGF-beta signalling by the pseudoreceptor BAMBI. *Nature.* **401**(6752):480-485.

Otsuka, F., R. K. Moore, S. Iemura, N. Ueno and S. Shimasaki (2001). Follistatin inhibits the function of the oocyte-derived factor BMP-15. *Biochem Biophys Res Commun.* **289**(5):961-966.

Ozkaynak, E., D. C. Rueger, E. A. Drier, C. Corbett, R. J. Ridge, T. K. Sampath and H. Oppermann (1990). OP-1 cDNA encodes an osteogenic protein in the TGF-beta family. *Embo J.* **9**(7):2085-2093.

Ozkaynak, E., P. N. Schnegelsberg, D. F. Jin, G. M. Clifford, F. D. Warren, E. A. Drier and H. Oppermann (1992). Osteogenic protein-2. A new member of the transforming growth factor-beta superfamily expressed early in embryogenesis. *J Biol Chem.* **267**(35):25220-25227.

Paget, S. (1989). The distribution of secondary growths in cancer of the breast. 1889. *Cancer Metastasis Rev.* **8**(2):98-101.

Palumbo, C., S. Palazzini, D. Zaffe and G. Marotti (1990). Osteocyte differentiation in the tibia of newborn rabbit: an ultrastructural study of the formation of cytoplasmic processes. *Acta Anat (Basel).* **137**(4):350-358.

Parkin, D. M., F. Bray, J. Ferlay and P. Pisani (2005). Global cancer statistics, 2002. *CA Cancer J Clin.* **55**(2):74-108.

Parr, C., G. Davies, T. Nakamura, K. Matsumoto, M. D. Mason and W. G. Jiang (2001). The HGF/SF-induced phosphorylation of paxillin, matrix adhesion, and invasion of prostate cancer cells were suppressed by NK4, an HGF/SF variant. *Biochem Biophys Res Commun.* **285**(5):1330-1337.

Parr, C. and W. G. Jiang (2001). Hepatocyte growth factor activators, inhibitors and antagonists and their implication in cancer intervention. *Histol Histopathol.* **16**(1):251-268.

Paule, B. and A. Cicco (2001). [Biphosphonates in the treatment of bone metastasis of prostatic cancer]. *Prog Urol.* **11**(6):1205-1212.

Pera, M. F., J. Andrade, S. Houssami, B. Reubinoff, A. Trounson, E. G. Stanley, D. Ward-van Oostwaard and C. Mummery (2004). Regulation of human embryonic stem cell differentiation by BMP-2 and its antagonist noggin. *J Cell Sci.* **117**(Pt 7):1269-1280.

Perttu, M. C., P. M. Martikainen, H. S. Huhtala, M. Blauer, T. L. Tammela, P. J. Tuohimaa and H. Syvala (2006). Altered levels of Smad2 and Smad4 are associated with human prostate carcinogenesis. *Prostate Cancer Prostatic Dis.* **9**(2):185-189.

Piccolo, S., E. Agius, L. Leyns, S. Bhattacharyya, H. Grunz, T. Bouwmeester and E. M. De Robertis (1999). The head inducer Cerberus is a multifunctional antagonist of Nodal, BMP and Wnt signals. *Nature.* **397**(6721):707-710.

Piccolo, S., Y. Sasai, B. Lu and E. M. De Robertis (1996). Dorsoventral patterning in Xenopus: inhibition of ventral signals by direct binding of chordin to BMP-4. *Cell.* **86**(4):589-598.

Pierre, A., C. Pisselet, P. Monget, D. Monniaux and S. Fabre (2005). Testing the antagonistic effect of follistatin on BMP family members in ovine granulosa cells. *Reprod Nutr Dev.* **45**(4):419-425.

Ploemacher, R. E., L. J. Engels, A. E. Mayer, S. Thies and S. Neben (1999). Bone morphogenetic protein 9 is a potent synergistic factor for murine hemopoietic progenitor cell generation and colony formation in serum-free cultures. *Leukemia.* **13**(3):428-437.

Qiu, T., W. E. Grizzle, D. K. Oelschlager, X. Shen and X. Cao (2007). Control of prostate cell growth: BMP antagonizes androgen mitogenic activity with incorporation of MAPK signals in Smad1. *Embo J.* **26**(2):346-357.

Quinn, J. M., J. Elliott, M. T. Gillespie and T. J. Martin (1998). A combination of osteoclast differentiation factor and macrophage-colony stimulating factor is sufficient for both human and mouse osteoclast formation in vitro. *Endocrinology.* **139**(10):4424-4427.

Rabbani, S. A., J. Desjardins, A. W. Bell, D. Banville, A. Mazar, J. Henkin and D. Goltzman (1990). An amino-terminal fragment of urokinase isolated from a prostate cancer cell line (PC-3) is mitogenic for osteoblast-like cells. *Biochem Biophys Res Commun.* **173**(3):1058-1064.

Radtke, F. and H. Clevers (2005). Self-renewal and cancer of the gut: two sides of a coin. *Science.* **307**(5717):1904-1909.

Raida, M., J. H. Clement, K. Ameri, C. Han, R. D. Leek and A. L. Harris (2005). Expression of bone morphogenetic protein 2 in breast cancer cells inhibits hypoxic cell death. *Int J Oncol.* **26**(6):1465-1470.

Ramoshebi, L. N. and U. Ripamonti (2000). Osteogenic protein-1, a bone morphogenetic protein, induces angiogenesis in the chick chorioallantoic membrane and synergizes with basic fibroblast growth factor and transforming growth factor-beta1. *Anat Rec.* **259**(1):97-107.

Raubenheimer, E. J. and C. E. Noffke (2006). Pathogenesis of bone metastasis: a review. *J Oral Pathol Med.* **35**(3):129-135.

Re'em-Kalma, Y., T. Lamb and D. Frank (1995). Competition between noggin and bone morphogenetic protein 4 activities may regulate dorsalization during Xenopus development. *Proc Natl Acad Sci U S A.* **92**(26):12141-12145.

Rebbapragada, A., H. Benchabane, J. L. Wrana, A. J. Celeste and L. Attisano (2003). Myostatin signals through a transforming growth factor beta-like signaling pathway to block adipogenesis. *Mol Cell Biol.* **23**(20):7230-7242.

Reddi, A. H., D. Roodman, C. Freeman and S. Mohla (2003). Mechanisms of tumor metastasis to the bone: challenges and opportunities. *J Bone Miner Res.* **18**(2):190-194.

Reinholt, F. P., K. Hultenby, A. Oldberg and D. Heinegard (1990). Osteopontin--a possible anchor of osteoclasts to bone. *Proc Natl Acad Sci U S A.* **87**(12):4473-4475.

Richard Pazdur, L. R. C., William J. Hoskins, Lawrence D. Wagman (2005). *Cancer Management: A Multidisciplinary Approach.* Manhasset, The Oncology Group.

Ro, T. B., R. U. Holt, A. T. Brenne, H. Hjorth-Hansen, A. Waage, O. Hjertner, A. Sundan and M. Borset (2004). Bone morphogenetic protein-5, -6 and -7 inhibit growth and induce apoptosis in human myeloma cells. *Oncogene.* **23**(17):3024-3032.

Romano, L. A. and R. B. Runyan (2000). Slug is an essential target of TGFbeta2 signaling in the developing chicken heart. *Dev Biol.* **223**(1):91-102.

Roodman, G. D. (2004). Mechanisms of bone metastasis. *N Engl J Med.* **350**(16):1655-1664.

Rosen, E. M., L. Meromsky, E. Setter, D. W. Vinter and I. D. Goldberg (1990). Smooth muscle-derived factor stimulates mobility of human tumor cells. *Invasion Metastasis.* **10**(1):49-64.

Rosenzweig, B. L., T. Imamura, T. Okadome, G. N. Cox, H. Yamashita, P. ten Dijke, C. H. Heldin and K. Miyazono (1995). Cloning and characterization of a human type II receptor for bone morphogenetic proteins. *Proc Natl Acad Sci U S A.* **92**(17):7632-7636.

Rosol, T. J. (2000). Pathogenesis of bone metastases: role of tumor-related proteins. *J Bone Miner Res.* **15**(5):844-850.

Ross, J. J., O. Shimmi, P. Vilmos, A. Petryk, H. Kim, K. Gaudenz, S. Hermanson, S. C. Ekker, M. B. O'Connor and J. L. Marsh (2001). Twisted gastrulation is a conserved extracellular BMP antagonist. *Nature.* **410**(6827):479-483.

Rothhammer, T., I. Poser, F. Soncin, F. Bataille, M. Moser and A. K. Bosserhoff (2005). Bone morphogenic proteins are overexpressed in malignant melanoma and promote cell invasion and migration. *Cancer Res.* **65**(2):448-456.

Rubin, J., X. Fan, J. Rahnert, B. Sen, C. L. Hsieh, T. C. Murphy, M. S. Nanes, L. G. Horton, W. G. Beamer and C. J. Rosen (2006). IGF-I secretion by prostate carcinoma cells does not alter tumor-bone cell interactions in vitro or in vivo. *Prostate.* **66**(8):789-800.

Sakr, W. A., G. P. Haas, B. F. Cassin, J. E. Pontes and J. D. Crissman (1993). The frequency of carcinoma and intraepithelial neoplasia of the prostate in young male patients. *J Urol.* **150**(2 Pt 1):379-385.

Sakuta, H., R. Suzuki, H. Takahashi, A. Kato, T. Shintani, S. Iemura, T. S. Yamamoto, N. Ueno and M. Noda (2001). Ventroptin: a BMP-4 antagonist expressed in a double-gradient pattern in the retina. *Science.* **293**(5527):111-115.

Samad, T. A., A. Rebbapragada, E. Bell, Y. Zhang, Y. Sidis, S. J. Jeong, J. A. Campagna, S. Perusini, D. A. Fabrizio, A. L. Schneyer, H. Y. Lin, A. H. Brivanlou, L.

Attisano and C. J. Woolf (2005). DRAGON, a bone morphogenetic protein co-receptor. *J Biol Chem.* **280**(14):14122-14129.

Sammar, M., S. Stricker, G. C. Schwabe, C. Sieber, A. Hartung, M. Hanke, I. Oishi, J. Pohl, Y. Minami, W. Sebald, S. Mundlos and P. Knaus (2004). Modulation of GDF5/BRI-b signalling through interaction with the tyrosine kinase receptor Ror2. *Genes Cells.* **9**(12):1227-1238.

Sasal, Y., B. Lu, H. Steinbelsser and E. M. De Robertis (1995). Regulation of neural induction by the Chd and Bmp-4 antagonistic patterning signals in Xenopus. *Nature.* **378**(6555):419.

Scharpfenecker, M., M. van Dinther, Z. Liu, R. L. van Bezooijen, Q. Zhao, L. Pukac, C. W. Lowik and P. Ten Dijke (2007). BMP-9 signals via ALK1 and inhibits bFGF-induced endothelial cell proliferation and VEGF-stimulated angiogenesis. *J Cell Sci.* **120**(Pt 6):964-972.

Scherberich, A., R. P. Tucker, M. Degen, M. Brown-Luedi, A. C. Andres and R. Chiquet-Ehrismann (2005). Tenascin-W is found in malignant mammary tumors, promotes alpha8 integrin-dependent motility and requires p38MAPK activity for BMP-2 and TNF-alpha induced expression in vitro. *Oncogene.* **24**(9):1525-1532.

Schluter, K. D., C. Katzer and H. M. Piper (2001). A N-terminal PTHrP peptide fragment void of a PTH/PTHrP-receptor binding domain activates cardiac ET(A) receptors. *Br J Pharmacol.* **132**(2):427-432.

Scott, R., Jr., D. L. Mutchnik, T. Z. Laskowski and W. R. Schmalhorst (1969). Carcinoma of the prostate in elderly men: incidence, growth characteristics and clinical significance. *J Urol.* **101**(4):602-607.

Segev, D. L., Y. Hoshiya, M. Hoshiya, T. T. Tran, J. L. Carey, A. E. Stephen, D. T. MacLaughlin, P. K. Donahoe and S. Maheswaran (2002). Mullerian-inhibiting substance regulates NF-kappa B signaling in the prostate in vitro and in vivo. *Proc Natl Acad Sci U S A.* **99**(1):239-244.

Sells, S. F., D. P. Wood, Jr., S. S. Joshi-Barve, S. Muthukumar, R. J. Jacob, S. A. Crist, S. Humphreys and V. M. Rangnekar (1994). Commonality of the gene programs induced by effectors of apoptosis in androgen-dependent and -independent prostate cells. *Cell Growth Differ.* **5**(4):457-466.

Shaneyfelt, T., R. Husein, G. Bubley and C. S. Mantzoros (2000). Hormonal predictors of prostate cancer: a meta-analysis. *J Clin Oncol.* **18**(4):847-853.

Shariat, S. F., D. J. Lamb, M. W. Kattan, C. Nguyen, J. Kim, J. Beck, T. M. Wheeler and K. M. Slawin (2002). Association of preoperative plasma levels of insulin-like growth factor I and insulin-like growth factor binding proteins-2 and -3 with prostate cancer invasion, progression, and metastasis. *J Clin Oncol.* **20**(3):833-841.

Shariat, S. F., M. Shalev, A. Menesses-Diaz, I. Y. Kim, M. W. Kattan, T. M. Wheeler and K. M. Slawin (2001). Preoperative plasma levels of transforming growth factor beta(1) (TGF-beta(1)) strongly predict progression in patients undergoing radical prostatectomy. *J Clin Oncol.* **19**(11):2856-2864.

Shi, Y. and J. Massague (2003). Mechanisms of TGF-beta signaling from cell membrane to the nucleus. *Cell.* **113**(6):685-700.

Shibuya, H., K. Yamaguchi, K. Shirakabe, A. Tonegawa, Y. Gotoh, N. Ueno, K. Irie, E. Nishida and K. Matsumoto (1996). TAB1: an activator of the TAK1 MAPKKK in TGF-beta signal transduction. *Science.* **272**(5265):1179-1182.

Shirakabe, K., K. Yamaguchi, H. Shibuya, K. Irie, S. Matsuda, T. Moriguchi, Y. Gotoh, K. Matsumoto and E. Nishida (1997). TAK1 mediates the ceramide signaling to stress-activated protein kinase/c-Jun N-terminal kinase. *J Biol Chem.* **272**(13):8141-8144.

Siegel, P. M. and J. Massague (2003). Cytostatic and apoptotic actions of TGF-beta in homeostasis and cancer. *Nat Rev Cancer.* **3**(11):807-821.

Simonet, W. S., D. L. Lacey, C. R. Dunstan, M. Kelley, M. S. Chang, R. Luthy, H. Q. Nguyen, S. Wooden, L. Bennett, T. Boone, G. Shimamoto, M. DeRose, R. Elliott, A. Colombero, H. L. Tan, G. Trail, J. Sullivan, E. Davy, N. Bucay, L. Renshaw-Gegg, T. M. Hughes, D. Hill, W. Pattison, P. Campbell, S. Sander, G. Van, J. Tarpley, P. Derby, R. Lee and W. J. Boyle (1997). Osteoprotegerin: a novel secreted protein involved in the regulation of bone density. *Cell.* **89**(2):309-319.

Skonier, J., K. Bennett, V. Rothwell, S. Kosowski, G. Plowman, P. Wallace, S. Edelhoff, C. Disteche, M. Neubauer, H. Marquardt and et al. (1994). beta ig-h3: a transforming growth factor-beta-responsive gene encoding a secreted protein that inhibits cell attachment in vitro and suppresses the growth of CHO cells in nude mice. *DNA Cell Biol.* **13**(6):571-584.

Smith, M. R., W. C. Lee, J. Brandman, Q. Wang, M. Botteman and C. L. Pashos (2005). Gonadotropin-releasing hormone agonists and fracture risk: a claims-based cohort study of men with nonmetastatic prostate cancer. *J Clin Oncol.* **23**(31):7897-7903.

Smith, M. R., F. J. McGovern, A. L. Zietman, M. A. Fallon, D. L. Hayden, D. A. Schoenfeld, P. W. Kantoff and J. S. Finkelstein (2001). Pamidronate to prevent bone loss during androgen-deprivation therapy for prostate cancer. *N Engl J Med.* **345**(13):948-955.

Smith, R. A., V. Cokkinides and H. J. Eyre (2006). American Cancer Society guidelines for the early detection of cancer, 2006. *CA Cancer J Clin.* **56**(1):11-25; quiz 49-50.

Sommerfeldt, D. W. and C. T. Rubin (2001). Biology of bone and how it orchestrates the form and function of the skeleton. *Eur Spine J.* **10 Suppl 2**(S86-95.

Song, J. J., A. J. Celeste, F. M. Kong, R. L. Jirtle, V. Rosen and R. S. Thies (1995). Bone morphogenetic protein-9 binds to liver cells and stimulates proliferation. *Endocrinology.* **136**(10):4293-4297.

Srinivasan, S., R. S. Ranga, R. Burikhanov, S. S. Han and D. Chendil (2007). Par-4-dependent apoptosis by the dietary compound withaferin A in prostate cancer cells. *Cancer Res.* **67**(1):246-253.

Steinberg, G. D., B. S. Carter, T. H. Beaty, B. Childs and P. C. Walsh (1990). Family history and the risk of prostate cancer. *Prostate.* **17**(4):337-347.

Strausberg, R. L., E. A. Feingold, L. H. Grouse, J. G. Derge, R. D. Klausner, F. S. Collins, L. Wagner, C. M. Shenmen, G. D. Schuler, S. F. Altschul, B. Zeeberg, K. H. Buetow, C. F. Schaefer, N. K. Bhat, R. F. Hopkins, H. Jordan, T. Moore, S. I. Max, J. Wang, F. Hsieh, L. Diatchenko, K. Marusina, A. A. Farmer, G. M. Rubin, L. Hong, M. Stapleton, M. B. Soares, M. F. Bonaldo, T. L. Casavant, T. E. Scheetz, M. J. Brownstein, T. B. Usdin, S. Toshiyuki, P. Carninci, C. Prange, S. S. Raha, N. A. Loquellano, G. J. Peters, R. D. Abramson, S. J. Mullahy, S. A. Bosak, P. J. McEwan, K. J. McKernan, J. A. Malek, P. H. Gunaratne, S. Richards, K. C. Worley, S. Hale, A. M. Garcia, L. J. Gay, S. W. Hulyk, D. K. Villalon, D. M. Muzny, E. J. Sodergren, X. Lu, R. A. Gibbs, J. Fahey, E. Helton, M. Ketteman, A. Madan, S. Rodrigues, A. Sanchez, M. Whiting, A. C. Young, Y. Shevchenko, G. G. Bouffard, R. W. Blakesley, J. W. Touchman, E. D. Green, M. C. Dickson, A. C. Rodriguez, J. Grimwood, J. Schmutz, R. M. Myers, Y. S. Butterfield, M. I. Krzywinski, U. Skalska, D. E. Smailus, A. Schnerch, J. E. Schein, S. J. Jones and M. A. Marra (2002). Generation and initial analysis of more than 15,000 full-length human and mouse cDNA sequences. *Proc Natl Acad Sci U S A.* **99**(26):16899-16903.

Street, J., M. Bao, L. deGuzman, S. Bunting, F. V. Peale, Jr., N. Ferrara, H. Steinmetz, J. Hoeffel, J. L. Cleland, A. Daugherty, N. van Bruggen, H. P. Redmond, R. A. Carano and E. H. Filvaroff (2002). Vascular endothelial growth factor stimulates bone repair by promoting angiogenesis and bone turnover. *Proc Natl Acad Sci U S A.* **99**(15):9656-9661.

Stroschein, S. L., W. Wang, S. Zhou, Q. Zhou and K. Luo (1999). Negative feedback regulation of TGF-beta signaling by the SnoN oncoprotein. *Science.* **286**(5440):771-774.

Sudo, S., O. Avsian-Kretchmer, L. S. Wang and A. J. Hsueh (2004). Protein related to DAN and cerberus is a bone morphogenetic protein antagonist that participates in ovarian paracrine regulation. *J Biol Chem.* **279**(22):23134-23141.

Suttapreyasri, S., S. Koontongkaew, A. Phongdara and U. Leggat (2006). Expression of bone morphogenetic proteins in normal human intramembranous and endochondral bones. *Int J Oral Maxillofac Surg.* **35**(5):444-452.

Suzuki, A., E. Kaneko, J. Maeda and N. Ueno (1997). Mesoderm induction by BMP-4 and -7 heterodimers. *Biochem Biophys Res Commun.* **232**(1):153-156.

Takai, E., R. L. Mauck, C. T. Hung and X. E. Guo (2004). Osteocyte viability and regulation of osteoblast function in a 3D trabecular bone explant under dynamic hydrostatic pressure. *J Bone Miner Res.* **19**(9):1403-1410.

Takase, M., T. Imamura, T. K. Sampath, K. Takeda, H. Ichijo, K. Miyazono and M. Kawabata (1998). Induction of Smad6 mRNA by bone morphogenetic proteins. *Biochem Biophys Res Commun.* **244**(1):26-29.

Takuwa, Y., T. Masaki and K. Yamashita (1990). The effects of the endothelin family peptides on cultured osteoblastic cells from rat calvariae. *Biochem Biophys Res Commun.* **170**(3):998-1005.

Tamada, H., R. Kitazawa, K. Gohji and S. Kitazawa (2001). Epigenetic regulation of human bone morphogenetic protein 6 gene expression in prostate cancer. *J Bone Miner Res.* **16**(3):487-496.

ten Dijke, P., H. Yamashita, T. K. Sampath, A. H. Reddi, M. Estevez, D. L. Riddle, H. Ichijo, C. H. Heldin and K. Miyazono (1994). Identification of type I receptors for osteogenic protein-1 and bone morphogenetic protein-4. *J Biol Chem.* **269**(25):16985-16988.

Termine, J. D., H. K. Kleinman, S. W. Whitson, K. M. Conn, M. L. McGarvey and G. R. Martin (1981). Osteonectin, a bone-specific protein linking mineral to collagen. *Cell.* **26**(1 Pt 1):99-105.

Thapa, N., K. B. Kang and I. S. Kim (2005). Beta ig-h3 mediates osteoblast adhesion and inhibits differentiation. *Bone.* **36**(2):232-242.

Thomas, R., W. A. Anderson, V. Raman and A. H. Reddi (1998). Androgen-dependent gene expression of bone morphogenetic protein 7 in mouse prostate. *Prostate.* **37**(4):236-245.

Thomas, R., L. D. True, P. H. Lange and R. L. Vessella (2001). Placental bone morphogenetic protein (PLAB) gene expression in normal, pre-malignant and malignant human prostate: relation to tumor development and progression. *Int J Cancer.* **93**(1):47-52.

Tian, E., F. Zhan, R. Walker, E. Rasmussen, Y. Ma, B. Barlogie and J. D. Shaughnessy, Jr. (2003). The role of the Wnt-signaling antagonist DKK1 in the development of osteolytic lesions in multiple myeloma. *N Engl J Med.* **349**(26):2483-2494.

Tomari, K., T. Kumagai, T. Shimizu and K. Takeda (2005). Bone morphogenetic protein-2 induces hypophosphorylation of Rb protein and repression of E2F in androgen-treated LNCaP human prostate cancer cells. *Int J Mol Med.* **15**(2):253-258.

Truksa, J., H. Peng, P. Lee and E. Beutler (2006). Bone morphogenetic proteins 2, 4, and 9 stimulate murine hepcidin 1 expression independently of Hfe, transferrin receptor 2 (Tfr2), and IL-6. *Proc Natl Acad Sci U S A.* **103**(27):10289-10293.

Tsuchida, K., K. Y. Arai, Y. Kuramoto, N. Yamakawa, Y. Hasegawa and H. Sugino (2000). Identification and characterization of a novel follistatin-like protein as a binding protein for the TGF-beta family. *J Biol Chem.* **275**(52):40788-40796.

Tsuji, A., E. Hashimoto, T. Ikoma, T. Taniguchi, K. Mori, M. Nagahama and Y. Matsuda (1999). Inactivation of proprotein convertase, PACE4, by alpha1-antitrypsin Portland (alpha1-PDX), a blocker of proteolytic activation of bone morphogenetic protein during embryogenesis: evidence that PACE4 is able to form an SDS-stable acyl intermediate with alpha1-PDX. *J Biochem (Tokyo).* **126**(3):591-603.

Uhlenbeck, O. C. (1987). A small catalytic oligoribonucleotide. *Nature.* **328**(6131):596-600.

Urist, M. R. (1965). Bone: formation by autoinduction. *Science.* **150**(698):893-899.

Vakar-Lopez, F., C. J. Cheng, J. Kim, G. G. Shi, P. Troncoso, S. M. Tu, L. Y. Yu-Lee and S. H. Lin (2004). Up-regulation of MDA-BF-1, a secreted isoform of ErbB3, in metastatic prostate cancer cells and activated osteoblasts in bone marrow. *J Pathol.* **203**(2):688-695.

van der Poel, H. G., C. Hanrahan, H. Zhong and J. W. Simons (2003). Rapamycin induces Smad activity in prostate cancer cell lines. *Urol Res.* **30**(6):380-386.

Vessella, R. L. and E. Corey (2006). Targeting factors involved in bone remodeling as treatment strategies in prostate cancer bone metastasis. *Clin Cancer Res.* **12**(20 Pt 2):6285s-6290s.

Vignais, M. L. (2000). [Ski and SnoN: antagonistic proteins of TGFbeta signaling]. *Bull Cancer.* **87**(2):135-137.

Wadhwa, S., M. C. Embree, Y. Bi and M. F. Young (2004). Regulation, regulatory activities, and function of biglycan. *Crit Rev Eukaryot Gene Expr.* **14**(4):301-315.

Walsh, P. C. and A. W. Partin (1997). Family history facilitates the early diagnosis of prostate carcinoma. *Cancer.* **80**(9):1871-1874.

Walsh, P. C., A. B. Retik, E. D. Vaughan and A. J. Wein (2002a). *Cambell's Urology*, Saunders (W.B.) Co Ltd.

Walsh, P. C., A. B. Retik, E. D. Vaughan and A. J. Wein (2002b). Cambell's Urology. **4:** 3026.

Wang, W., F. V. Mariani, R. M. Harland and K. Luo (2000). Ski represses bone morphogenic protein signaling in Xenopus and mammalian cells. *Proc Natl Acad Sci U S A.* **97**(26):14394-14399.

Wen, X. Z., Y. Akiyama, S. B. Baylin and Y. Yuasa (2006). Frequent epigenetic silencing of the bone morphogenetic protein 2 gene through methylation in gastric carcinomas. *Oncogene.* **25**(18):2666-2673.

Wicks, S. J., K. Haros, M. Maillard, L. Song, R. E. Cohen, P. T. Dijke and A. Chantry (2005). The deubiquitinating enzyme UCH37 interacts with Smads and regulates TGF-beta signalling. *Oncogene.* **24**(54):8080-8084.

Wozney, J. M., V. Rosen, M. Byrne, A. J. Celeste, I. Moutsatsos and E. A. Wang (1990). Growth factors influencing bone development. *J Cell Sci Suppl.* **13**(149-156.

Wozney, J. M., V. Rosen, A. J. Celeste, L. M. Mitsock, M. J. Whitters, R. W. Kriz, R. M. Hewick and E. A. Wang (1988). Novel regulators of bone formation: molecular clones and activities. *Science.* **242**(4885):1528-1534.

Wrana, J. L., H. Tran, L. Attisano, K. Arora, S. R. Childs, J. Massague and M. B. O'Connor (1994). Two distinct transmembrane serine/threonine kinases from Drosophila melanogaster form an activin receptor complex. *Mol Cell Biol.* **14**(2):944-950.

Wu, H. C., J. T. Hsieh, M. E. Gleave, N. M. Brown, S. Pathak and L. W. Chung (1994). Derivation of androgen-independent human LNCaP prostatic cancer cell sublines: role of bone stromal cells. *Int J Cancer.* **57**(3):406-412.

Xu, J., T. R. Kimball, J. N. Lorenz, D. A. Brown, A. R. Bauskin, R. Klevitsky, T. E. Hewett, S. N. Breit and J. D. Molkentin (2006). GDF15/MIC-1 functions as a protective and antihypertrophic factor released from the myocardium in association with SMAD protein activation. *Circ Res.* **98**(3):342-350.

Xu, W., K. Angelis, D. Danielpour, M. M. Haddad, O. Bischof, J. Campisi, E. Stavnezer and E. E. Medrano (2000). Ski acts as a co-repressor with Smad2 and Smad3 to regulate the response to type beta transforming growth factor. *Proc Natl Acad Sci U S A.* **97**(11):5924-5929.

Yamaguchi, K., S. Nagai, J. Ninomiya-Tsuji, M. Nishita, K. Tamai, K. Irie, N. Ueno, E. Nishida, H. Shibuya and K. Matsumoto (1999). XIAP, a cellular member of the inhibitor

of apoptosis protein family, links the receptors to TAB1-TAK1 in the BMP signaling pathway. *Embo J.* **18**(1):179-187.

Yamaguchi, K., K. Shirakabe, H. Shibuya, K. Irie, I. Oishi, N. Ueno, T. Taniguchi, E. Nishida and K. Matsumoto (1995). Identification of a member of the MAPKKK family as a potential mediator of TGF-beta signal transduction. *Science.* **270**(5244):2008-2011.

Yamaji, N., A. J. Celeste, R. S. Thies, J. J. Song, S. M. Bernier, D. Goltzman, K. M. Lyons, J. Nove, V. Rosen and J. M. Wozney (1994). A mammalian serine/threonine kinase receptor specifically binds BMP-2 and BMP-4. *Biochem Biophys Res Commun.* **205**(3):1944-1951.

Yamashita, H., A. Shimizu, M. Kato, H. Nishitoh, H. Ichijo, A. Hanyu, I. Morita, M. Kimura, F. Makishima and K. Miyazono (1997). Growth/differentiation factor-5 induces angiogenesis in vivo. *Exp Cell Res.* **235**(1):218-226.

Yang, Q. and N. K. Tonks (1991). Isolation of a cDNA clone encoding a human protein-tyrosine phosphatase with homology to the cytoskeletal-associated proteins band 4.1, ezrin, and talin. *Proc Natl Acad Sci U S A.* **88**(14):5949-5953.

Yang, S., M. Lim, L. K. Pham, S. E. Kendall, A. H. Reddi, D. C. Altieri and P. Roy-Burman (2006). Bone morphogenetic protein 7 protects prostate cancer cells from stress-induced apoptosis via both Smad and c-Jun NH2-terminal kinase pathways. *Cancer Res.* **66**(8):4285-4290.

Yang, S., C. Zhong, B. Frenkel, A. H. Reddi and P. Roy-Burman (2005). Diverse biological effect and Smad signaling of bone morphogenetic protein 7 in prostate tumor cells. *Cancer Res.* **65**(13):5769-5777.

Yao, G. Q., B. Sun, E. E. Hammond, E. N. Spencer, M. C. Horowitz, K. L. Insogna and E. C. Weir (1998). The cell-surface form of colony-stimulating factor-1 is regulated by

osteotropic agents and supports formation of multinucleated osteoclast-like cells. *J Biol Chem.* **273**(7):4119-4128.

Ye, L., T. A. Martin, C. Parr, G. M. Harrison, R. E. Mansel and W. G. Jiang (2003). Biphasic effects of 17-beta-estradiol on expression of occludin and transendothelial resistance and paracellular permeability in human vascular endothelial cells. *J Cell Physiol.* **196**(2):362-369.

Yeh, L. C. and J. C. Lee (1999). Osteogenic protein-1 increases gene expression of vascular endothelial growth factor in primary cultures of fetal rat calvaria cells. *Mol Cell Endocrinol.* **153**(1-2):113-124.

Yi, B., P. J. Williams, M. Niewolna, Y. Wang and T. Yoneda (2002). Tumor-derived platelet-derived growth factor-BB plays a critical role in osteosclerotic bone metastasis in an animal model of human breast cancer. *Cancer Res.* **62**(3):917-923.

Yin, J. J., K. S. Mohammad, S. M. Kakonen, S. Harris, J. R. Wu-Wong, J. L. Wessale, R. J. Padley, I. R. Garrett, J. M. Chirgwin and T. A. Guise (2003). A causal role for endothelin-1 in the pathogenesis of osteoblastic bone metastases. *Proc Natl Acad Sci U S A.* **100**(19):10954-10959.

Yin, J. J., C. B. Pollock and K. Kelly (2005). Mechanisms of cancer metastasis to the bone. *Cell Res.* **15**(1):57-62.

Yip, I., D. Heber and W. Aronson (1999). Nutrition and prostate cancer. *Urol Clin North Am.* **26**(2):403-411, x.

Yokouchi, Y., K. J. Vogan, R. V. Pearse, 2nd and C. J. Tabin (1999). Antagonistic signaling by Caronte, a novel Cerberus-related gene, establishes left-right asymmetric gene expression. *Cell.* **98**(5):573-583.

Yokoyama-Kobayashi, M., M. Saeki, S. Sekine and S. Kato (1997). Human cDNA encoding a novel TGF-beta superfamily protein highly expressed in placenta. *J Biochem (Tokyo).* **122**(3):622-626.

Yoneda, T. and T. Hiraga (2005). Crosstalk between cancer cells and bone microenvironment in bone metastasis. *Biochem Biophys Res Commun.* **328**(3):679-687.

Yonou, H., A. Ochiai, M. Goya, N. Kanomata, S. Hokama, M. Morozumi, K. Sugaya, T. Hatano and Y. Ogawa (2004). Intraosseous growth of human prostate cancer in implanted adult human bone: relationship of prostate cancer cells to osteoclasts in osteoblastic metastatic lesions. *Prostate.* **58**(4):406-413.

Yoshida, Y., S. Tanaka, H. Umemori, O. Minowa, M. Usui, N. Ikematsu, E. Hosoda, T. Imamura, J. Kuno, T. Yamashita, K. Miyazono, M. Noda, T. Noda and T. Yamamoto (2000). Negative regulation of BMP/Smad signaling by Tob in osteoblasts. *Cell.* **103**(7):1085-1097.

Yoshida, Y., A. von Bubnoff, N. Ikematsu, I. L. Blitz, J. K. Tsuzuku, E. H. Yoshida, H. Umemori, K. Miyazono, T. Yamamoto and K. W. Cho (2003). Tob proteins enhance inhibitory Smad-receptor interactions to repress BMP signaling. *Mech Dev.* **120**(5):629-637.

Yoshikawa, H., W. J. Rettig, K. Takaoka, E. Alderman, B. Rup, V. Rosen, J. M. Wozney, J. M. Lane, A. G. Huvos and P. Garin-Chesa (1994). Expression of bone morphogenetic proteins in human osteosarcoma. Immunohistochemical detection with monoclonal antibody. *Cancer.* **73**(1):85-91.

Yoshizawa, K., W. C. Willett, S. J. Morris, M. J. Stampfer, D. Spiegelman, E. B. Rimm and E. Giovannucci (1998). Study of prediagnostic selenium level in toenails and the risk of advanced prostate cancer. *J Natl Cancer Inst.* **90**(16):1219-1224.

Young, M. F. (2003). Bone matrix proteins: their function, regulation, and relationship to osteoporosis. *Osteoporos Int.* **14 Suppl 3**(S35-42.

Zeisberg, M., J. Hanai, H. Sugimoto, T. Mammoto, D. Charytan, F. Strutz and R. Kalluri (2003). BMP-7 counteracts TGF-beta1-induced epithelial-to-mesenchymal transition and reverses chronic renal injury. *Nat Med.* **9**(7):964-968.

Zeisberg, M., A. A. Shah and R. Kalluri (2005). Bone morphogenic protein-7 induces mesenchymal to epithelial transition in adult renal fibroblasts and facilitates regeneration of injured kidney. *J Biol Chem.* **280**(9):8094-8100.

Zhang, J. H., J. Tang, J. Wang, W. Ma, W. Zheng, T. Yoneda and J. Chen (2003). Over-expression of bone sialoprotein enhances bone metastasis of human breast cancer cells in a mouse model. *Int J Oncol.* **23**(4):1043-1048.

Zhang, X., J. Wu, X. Li, L. Fu, D. Gao, H. Bai and X. Liu (2002). [Effects of recombinant human bone morphogenic protein-2 and hyaluronic acid on invasion of brain glioma in vivo]. *Zhonghua Yi Xue Za Zhi.* **82**(2):90-93.

Zhu, H., P. Kavsak, S. Abdollah, J. L. Wrana and G. H. Thomsen (1999). A SMAD ubiquitin ligase targets the BMP pathway and affects embryonic pattern formation. *Nature.* **400**(6745):687-693.

Zhu, W., J. Kim, C. Cheng, B. A. Rawlins, O. Boachie-Adjei, R. G. Crystal and C. Hidaka (2006). Noggin regulation of bone morphogenetic protein (BMP) 2/7 heterodimer activity in vitro. *Bone.* **39**(1):61-71.

Zou, H. and L. Niswander (1996). Requirement for BMP signaling in interdigital apoptosis and scale formation. *Science.* **272**(5262):738-741.

Zuker, M. (2003). Mfold web server for nucleic acid folding and hybridization prediction. *Nucleic Acids Res.* **31**(13):3406-3415.

Zuzarte-Luis, V., J. A. Montero, J. Rodriguez-Leon, R. Merino, J. C. Rodriguez-Rey and J. M. Hurle (2004). A new role for BMP5 during limb development acting through the synergic activation of Smad and MAPK pathways. *Dev Biol.* **272**(1):39-52.